AFAL-TR-77-75

DESIGN, DEVELOPMENT, ANALYSIS, AND LABORATORY TEST RESULTS OF A KALMAN FILTER SYSTEM-LEVEL IMU CALIBRATION TECHNIQUE

Richard A. Kitzerow
Reference Systems Branch
Reconnaissance and Weapon Delivery Division

June 1977

TECHNICAL REPORT AFAL-TR-77-75

Final Report for Period July 1973 to November 1975

Approved for Public Release; Distribution Unlimited

AIR FORCE AVIONICS LABORATORY
AIR FORCE WRIGHT AERONAUTICAL LABORATORIES
AIR FORCE SYSTEMS COMMAND
WRIGHT-PATTERSON AIR FORCE BASE, OHIO 45433

NOTICE

When Government drawings, specifications, or other data are used for any purpose other than in connection with a definitely related Government procurement operation, the United States Government thereby incurs no responsibility nor any obligation whatsoever; and the fact that the government may have formulated, furnished, or in any way supplied the said drawings, specifications, or other data, is not to be regarded by implication or otherwise as in any manner licensing the holder or any other person or corporation, or conveying any rights or permission to manufacture, use, or sell any patented invention that may in any way be related thereto.

This report has been reviewed by the Information Office (ASD/OIP) and is releasable to the National Technical Information Service (NTIS). At NTIS it will be available to the general public, including foreign nations.

This technical report has been reviewed and is approved for publication.

Richard A. Kitzerow

RICHARD A. KITZEROW
Project Engineer

FOR THE COMMANDER

Ronald L. Ringo

RONALD L. RINGO
Chief, Reference Systems Branch
Reconnaissance and Weapon Delivery Division

Copies of this report should not be returned unless return is required by security considerations, contractual obligations, or notice on a specific document.

UNCLASSIFIED

SECURITY CLASSIFICATION OF THIS PAGE *(When Data Entered)*

REPORT DOCUMENTATION PAGE

READ INSTRUCTIONS BEFORE COMPLETING FORM

1. REPORT NUMBER: AFAL-TR-77-75	2. GOVT ACCESSION NO.
3. RECIPIENT'S CATALOG NUMBER	
4. TITLE *(and Subtitle)*: Design, Development, Analysis, and Laboratory Test Results of a Kalman Filter System-Level IMU Calibration Technique	5. TYPE OF REPORT & PERIOD COVERED: Final report. July 1973 to November 1975
	6. PERFORMING ORG. REPORT NUMBER
7. AUTHOR(s): Richard A. Kitzerow	8. CONTRACT OR GRANT NUMBER(s)
9. PERFORMING ORGANIZATION NAME AND ADDRESS: Air Force Avionics Laboratory, Wright-Patterson Air Force Base, Ohio 45433	10. PROGRAM ELEMENT, PROJECT, TASK AREA & WORK UNIT NUMBERS: 60951508
11. CONTROLLING OFFICE NAME AND ADDRESS: Air Force Avionics Laboratory, Wright-Patterson Air Force Base, Ohio 45433	12. REPORT DATE: June 1977
	13. NUMBER OF PAGES: 253
14. MONITORING AGENCY NAME & ADDRESS *(if different from Controlling Office)*	15. SECURITY CLASS. *(of this report)*: UNCLASSIFIED
	15a. DECLASSIFICATION/DOWNGRADING SCHEDULE

16. DISTRIBUTION STATEMENT *(of this Report)*

Approved for Public Release; Distribution Unlimited

17. DISTRIBUTION STATEMENT *(of the abstract entered in Block 20, if different from Report)*

N/A

18. SUPPLEMENTARY NOTES

N/A

19. KEY WORDS *(Continue on reverse side if necessary and identify by block number)*

KT-73 IMU Error Model
IMU Calibation
Kalman Filter
IMU Simulation
Navigation
Error Model Development
Laboratory Test Results
Gyros, Accelerometers
IMU Maintenance and Acceptance Tests

20. ABSTRACT *(Continue on reverse side if necessary and identify by block number)*

The United States Air Force Avionics Laboratory at Wright-Patterson Air Force Base, Ohio, is presently conducting inhouse advanced aided-inertial navigation software development programs. This report describes the design, development, analysis, and laboratory test results of an IMU calibration and error model development methodology formulated to support the design and test of inertial navigation software and associated Kalman Filters. The IMU error analysis methodology incorporates a 53-state Kalman Filter and uses

DD FORM 1 JAN 73 1473 EDITION OF 1 NOV 65 IS OBSOLETE

UNCLASSIFIED

SECURITY CLASSIFICATION OF THIS PAGE *(When Data Entered)*

20. Abstract (Contd)

only system-level IMU velocity and gimbal angle measurements taken during a two and a half hour, twelve-platform attitude test to estimate IMU significant error sources relative to the inertial instrument random disturbances. The Kalman Filter incorporates a number of error model residual states which provide a measure of the degree to which the test article conforms to the assumed IMU error model. IMU error parameter estimation can be accomplished either on-line in real time or off-line using recorded IMU measurements. Results obtained from both a CDC-6600 computer simulation of the IMU calibration problem and a laboratory development program indicate that the technique is conceptually more comprehensive and accurate, and requires less specialized test equipment and test time than conventional calibration methods. The technique appears to be a likely candidate for IMU acceptance and intermediate and depot level maintenance tests.

FOREWORD

An inhouse study was initiated in March 1973 to investigate static and dynamic tests and associated data reduction and analysis computer programs that could potentially assist the Reference Systems Software Group in accomplishing its mission: development and evaluation of aided-inertial navigation software. Study emphasis has been in the areas of error modeling to support the development of the navigation Kalman Filter and the definition of tests and development of data reduction and analysis computer programs that have the capability of separating hardware and real-time software errors and isolating these errors within their respective classes.

The IMU calibration technique reported herein is the first in a series of six tests defined in the study. Development of the calibration methodology, computer simulation, and a data reduction and analysis computer program was accomplished in the June to December 1973 time period. Development of the real-time test software, integration of the test equipment, and experimental verification of the calibration technique were accomplished during the September to December 1974 time period. Several refinements to the test software, equipment, and data analysis computer program were made in 1975.

The author acknowledges the assistance of Mr. D. Kaiser who was the Task Engineer responsible for the integration of the laboratory test equipment and development of the real-time test software. Capt P. Howe and Lt H. Vassar also contributed to the development of the real-time test software. Mr. R. Clark refined and assembled the equipment associated with the IMU gimbal angle measurements. TSgt E. Edgecomb conducted many of the calibration tests.

TABLE OF CONTENTS

TABLE OF CONTENTS (Cortd)

TABLE OF CONTENTS (Contd)

TABLE OF CONTENTS (Contd)

LIST OF ILLUSTRATIONS

LIST OF ILLUSTRATIONS (Cont'd)

LIST OF ILLUSTRATIONS (Contd)

TABLES

SECTION I

INTRODUCTION

1.1 BACKGROUND AND NEED

As part of the Air Force Avionics Laboratory's Reconnaissance and Weapon Delivery Division, the Reference Systems Branch mission is concerned with conducting exploratory and advanced development of navigational reference subsystems, analyzing new concepts for reference subsystem data processing and software development, and developing new techniques for subsystem integration. The Branch's Reference Systems Software and Evaluation Groups support its mission by conducting in-house analysis and evaluation of navigation reference subsystems, with emphasis in the areas of inertial navigation software and subsystem integration via Kalman Filtering. The Evaluation Group maintains a laboratory and instrumented Greyhound bus for both static and dynamic hardware/software evaluation.

In accomplishing this mission, the Software and Evaluation Groups have and continue to encounter numerous mundane problems associated with the design, development, test, and evaluation of aided-inertial navigation software. Some of the more notable problems are: How is an inertial measurement unit (IMU) error model, suitable for Kalman Filter design and comprehensive subsystem convariance error analysis, developed and/or verified? Considering that inertial navigators are among the most precise of all electro-mechanical devices, how is it readily determined that the IMU is operating within its specification prior to conducting software evaluation tests? At the beginning of a reference subsystem test, what is the IMU platform alignment accuracy considering the wind buffet and personnel loading perturbating motion effects on the greyhound bus? How are the potential sources of aided-inertial navigation subsystem errors: hardware, alignment and software separated at the conclusion of an evaluation test? How can the various classes of software errors, coding, equations, inexact algorithms, etc., be distinguished so that software development projects can progress in

an orderly fashion? What is the best approach for establishing a position/velocity/attitude reference for the aided-inertial navigation subsystem under evaluation: by an on-line real-time or by an off-line after-the-fact data reduction/analysis computer program approach using recorded data?

1.2 OBJECTIVES OF THE STUDY

From the preceding discussion, it is clear that aided-inertial navigation software projects can require extensive analyses, test procedures, and supporting data reduction and analyses computer programs if comprehensive development and evaluation efforts are desired. Recognizing this need, the Reference Systems Software Group undertook the development of a series of tests and supporting data reduction/analyses computer programs to facilitate its software development and evaluation projects.

Table 1-1 indicates the types of tests that are currently planned and are under development. All tests have several major points in common. When a test is conducted, test data is stored on a magnetic tape for subsequent processing by a large off-line scientific computer. The concept of off-line non-real time data reduction/analyses computer programs introduces a time delay in obtaining test results but affords computer programs that are more comprehensive and easier to develop and change than those resultant from on-line real-time approaches.

The performance analysis, error diagnostic and evaluation concept for each data reduction/analysis program is a large dimensional Kalman Filter operating in parallel with deterministic logic and navigation software programs. This is a state-of-the-art approach that ensures the optimum use of the test data, minimum test time, and utmost error estimation accuracy. The extent to which Kalman Filters can be used for error source detection and isolation is a major finding to be determined by the study.

TABLE 1-1

AIDED-INERTIAL NAVIGATION SOFTWARE DEVELOPMENT AND EVALUATION TESTS

	Test	Kalman Filter States	Test Location
(1)	IMU Calibration	68	SEL
(2)	MEL Suspension	35	MEL
(3)	Scorsby Table Platform Alignment	39	SEL
(4)	Tilt Table Static Navigation	37+	SEL
(5)	MEL Perturbed Base Alignment	39+	MEL
(6)	MEL Dynamic Navigation	43+	MEL

SEL - Software Evaluation Laboratory

MEL - Mobile Evaluation Laboratory

\+ - Final Filter State Size Will Be Somewhat Larger

The major objectives of each of the tests are as follows. The IMU calibration test addresses the problems associated with: IMU error model development and validation, calibration of random bias type IMU hardware errors, estimation of time-varying error sources, and IMU hardware status assessment prior to software developmental testing.

The MEL Suspension Test utilizes three orthogonal strapdown accelerometers mounted in the greyhound bus (MEL) to obtain data relevant to the perturbed base platform alignment problem: MEL suspension physical characteristics including mass, spring and shock absorber data, IMU relative mounting data, manloading-engine-wind perturbating motion magnitudes, and statistical modeling of these disturbances.

The Scorsby Rate Table Platform Alignment Test is designed to evaluate Kalman Filter alignment software in an environment where the frequency and magnitude of base motion perturbations are accurately controlled.

The Tilt Table Static Navigation Test addresses initial Kalman Filter/inertial navigation software and IMU/computer hardware integration problems in a highly controlled environment. Emphasis is placed on the ability of the data reduction/analysis computer program to detect and isolate the potential errors. Special tests such as determining navigation performance as a function of gyro heading sensitivity can be conducted.

The MEL Perturbed Base Alignment Test assesses the ability of the alignment software to both align the platform axes and estimate gyro drifts for multi-position platform alignment schemes in the presence of real world MEL base perturbations and inertial instrument temperature transients.

The MEL Dynamic Navigation Data Reduction/Analysis Program is largely a composite of the previous programs and utilizes much of the data generated by them. The overall objective is to assess aided-inertial navigation subsystem performance and separate the associated errors into their respective classes: hardware, alignment and software. Hardware and alignment errors are separated by the inherent operation of the Kalman Filter. Software errors are further separated into: coding, equation, inexact algorithm, inertial navigation and Kalman Filtering by "ideal inertial navigation equations" operating with logic in conjunction with the large dimensional Kalman Filter of the data reduction/analysis program.

Each data reduction/analysis computer program has been developed and exercised against a computer simulation of the appropriate test subsystem in its expected environment. Simulation results have been encouraging especially in the area of error detection and isolation. The IMU calibration data reduction/analysis computer program has additionally been exercised against real world IMU test data as collected in the Evaluation Group's Software Evaluation Laboratory (SEL). The experimental results obtained clearly indicate the value of the Kalman Filter as an effective tool for detecting, isolating, and accurately estimating the error sources in complex navigation subsystems.

1.3 REPORT OVERVIEW

This report is concerned with the design, development, analysis, and laboratory test results of the IMU calibration technique. The remaining five data reduction/analysis computer programs in the aided-inertial navigation software development and evaluation test series are to be reported after they are exercised against read-world data.

In Section 2, the ground rules and versatility and accuracy goals for the IMU calibration technique are discussed. The IMU calibration methodology formulated in response to the restrictions and goals is presented.

In Section 3, an error model for the IMU is given and the error equations governing its operation during the calibration test are derived.

Section 4 contains a discussion of the conceptual approach used for separation of the IMU error sources.

Section 5 contains a description of the Kalman Filter mechanized for estimation and calibration of the IMU error sources.

Section 6 presents and discusses theoretical results obtained from a CDC-6600 computer simulation of the IMU, Kalman Filter, and calibration test.

Section 7 discusses the laboratory hardware, computer software, and the test procedure used in testing the IMU.

Section 8 contains the "lessons learned" from the initial IMU calibration tests and the subsequent IMU error model refinements.

Section 9 presents a pictorial tabulation of the results obtained from the IMU calibration tests. IMU error source calibration accuracy, as obtained from the Kalman Filter's covariance matrix, is given in addition to the recovered error source magnitudes.

Section 10 points out several applications for which the developed IMU calibration technique appears to be well suited.

Appendix A contains the CDC-6600 computer FORTRAN IV program listing to assist those attempting to develop a Kalman Filter and associated algorithms for a similar application.

SECTION II

IMU CALIBRATION METHODOLOGY

2.1 GROUND RULES

The IMU used by the Reference Systems Software and Evaluation Groups in conducting aided-inertial navigation software development and evaluation tests is a Singer-Kearfott KT-73 four-gimbal, all-attitude unit which contains gyroscope and accelerometer inertial instruments and associated electronics. This IMU is also a part of the A-7D aircraft avionics suite and is calibrated at the operational bases by the Singer-Kearfott ASM-375 testset. The IMU is maintained by the Aerospace Guidance and Metrology Center (AGMC), Heath AFB, Newark, Ohio. AGMC employs numerous digital IMU (DIMU) testsets for calibrating the units.

Initially, serious consideration was given to periodically calibrating the IMU by one of the above testsets. This approach was subsequently discarded for several reasons. Funding was not available nor was it considered cost-effective, procurement costs of the ASM-375 testset were roughly one million dollars each, to buy and maintain a testset for the periodic calibration of one IMU. Although acceptable, turnaround times for having the IMU calibrated at Heath AFB were undesirable. Finally, the sixteen parameters calibrated by the testsets were considered insufficient for comprehensive IMU error modelling studies.

The ground rules established for developing the calibration technique were necessitated by the manpower skills and equipment available in the Evaluation Group and its Software Evaluation Laboratory. The available skills and equipment precluded disassembling the IMU for special testing. "No disassembly" implies that only easily accessible system-level IMU quantized velocity pulses and gimbal synchro angle output measurements could be used. No specialized AGE was to be required other than that already available in the laboratory: digital computers, tilt and scorsby tables, a Singer-Kearfott ASN/90(V) inertial navigation system

test equipment rack, etc. A final ground rule was that the solution to the calibration problem be practically implementable on a general purpose digital computer.

2.2 PERFORMANCE AND VERSATILITY GOALS

A major limitation of contemporary IMU calibration concepts is their limited diagnostic capabilities. Present test concepts assume a priori the major sources of IMU errors, usually ten to twenty, with the test being designed to sequentially determine the magnitudes of the assumed error sources. A deficiency of this approach is that the test results cannot provide any indication as to whether or not the test article conforms to the assumed error model. It is entirely possible for an IMU to contain significant error sources other than those assumed and for them to go undetected at the conclusion of the calibration test. Adequate Kalman Filter design and comprehensive navigation subsystem covariance error analysis are dependent upon having an accurate IMU error model. One goal of the study is therefore to devise an IMU calibration concept that affords a capability for IMU error model development and/or validation. Simply stated, the calibration test results should provide some indication of the degree that the test article conforms to the assumed error model.

It is desirable that the calibration concept be versatile in regards to both IMU mechanizations and data processing approaches. The present study is largely concerned with the gimballed KT-73 IMU although future Reference Systems Branch projects may involve a strapdown IMU. A versatile methodology will permit adaption to the strapdown mechanization with a minimum of modifications to the test procedures and data reduction/analysis computer programs.

Off-line after-the-fact and on-line real-time data processing approaches are both desirable. An off-line approach to IMU calibration greatly facilitates the development of the Data Reduction/Analysis Computer Program since it can be written in a higher order language and is

not subject to the numerous real-time software development problems. Off-line data reduction/analysis programs hosted on large scientific computers can also be more sophisticated than on-line versions due to the large computer resources available. On-line real-time approaches offer the advantages of real-time IMU closed loop control and provide test results immediately upon conclusion of the test.

IMU calibration performance goals are to provide a comprehensive calibration with optimum accuracy and to minimize IMU test time. Since static IMU hardware error sources can be compensated for in the operational flight computer program, it is desirable to estimate each significant IMU error source to an accuracy such that the navigational accuracy achievable with the IMU would be limited only by uncompensatable random disturbances. Total test time of a few hours or less is desirable to allow aided-inertial navigation software tests to be conducted on the same days as the calibration tests.

2.3 FORMULATED CALIBRATION METHODOLOGY

The performance and versatility goals dictate that a generalized IMU calibration methodology be formulated which is based only on the essential functions an IMU performs. These functions are to permit the establishment and maintenance of a reference platform coordinate frame and measurement of the instantaneous specific force vector. Noting that calibration is an error estimation process, the IMU error analysis methodology formulated can be understood with the following rationale. If the orientation of the platform of an error-free IMU were initially precisely known with respect to the physical earth rate and gravity vectors, then both the orientation of the platform with respect to these vectors and the platform coordinatized specific force vector could be deterministically calculated as a function of time. Any differences between the ideal time-dependent platform orientation and accelerometer outputs and those of a real IMU must be caused by either IMU error sources or an initial platform misalignment. This fact is true regardless of initial platform orientation and can be employed for the

derivation of system-level IMU error equations relating measurable IMU performance parameters to IMU and platform misalignment angle error quantities.

Application of the generalized metnodology to a fixed-base gimballed IMU can be illustrated by the IMU line schematic of Figure 2-1. The fundamental function of the gyros, gimbals, and servo feedback control system is to maintain a reference platform coordinate frame relative to an inertial frame. If the gyro triad of an ideal IMU were commanded to precess in equality with the earth's angular rotation vector, then the angular velocity of the platform with respect to an earth fixed reference frame would be identically zero. This ideal IMU performance would result in a fixed angular orientation of the gimbals relative to each other and constant system-level synchro gimbal angle and accelerometer measurement outputs. The exact angular orientation of the platform frame with respect to the earth rate and gravity vectors must be known for a priori computation of the required gyro precession rate torquing magnitudes. In the real world, inexact initial platform attitude information and IMU error sources preclude the above ideal IMU performance and synchro gimbal angle and accelerometer measurements exhibit a time dependency.

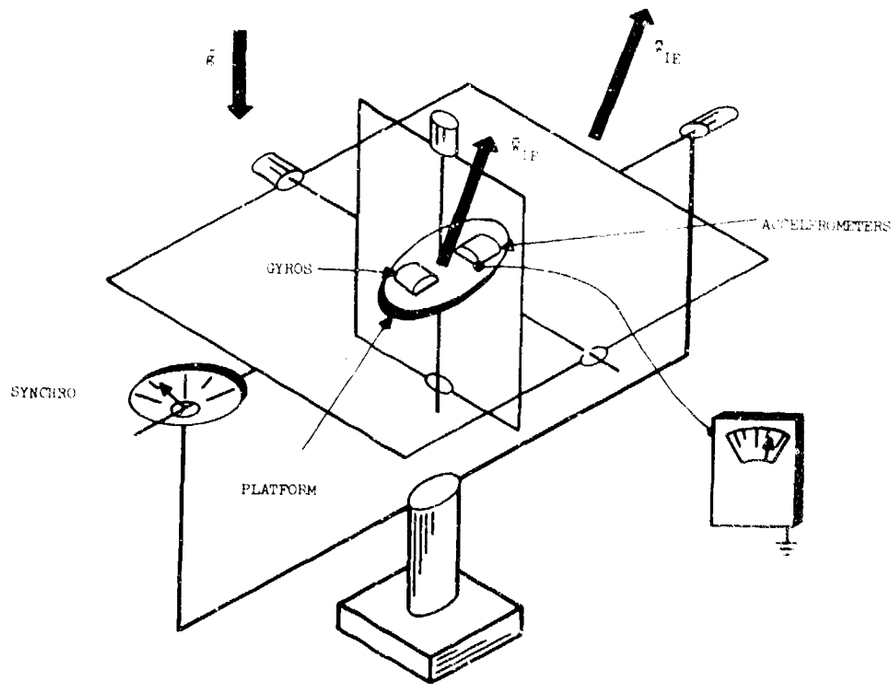

Figure 2-1. Gimballed IMU Line Schematic

SECTION III

ERROR EQUATION DEVELOPMENT

3.1 INTRODUCTION

The essential task involved in developing the error equations is the derivation of analytical expressions relating system-level IMU gimbal synchro angle and velocity measurements to IMU and platform-to-navigation frame misalignment angle error quantities. These derivations are relatively straightforward and follow directly from the physical vector equations expressing the physical relationships implicitly implied by the generalized methodology.

A prerequisite for these derivations is an IMU model explicitly containing each IMU error source's functional dependency. As stated in Section 2.1, a Singer-Kearfott KT-73 IMU was chosen for the calibration methodology application largely because it is used in the MEL as part of the Reference Navigation System and requires periodic status validation and calibration. Reference 1 contains an error model for the IMU which reportedly contains all pertinent error sources.

To achieve the stated performance goals, the "finalized IMU error model" must contain all IMU error sources that are significant relative to the gyro and accelerometer inertial instrument random disturbances. The phrase "finalized IMU error model" is used to emphasize that the error model given in Reference 1 need not be strictly accurate in the sense that it contains all error sources that are significant relative to the inertial instrument random disturbances. The error model of Reference 1 needs only to represent a good starting point since a major objective of this study is to develop a conceptual approach to IMU error model development and validation.

The conceptual approach to IMU error model development and validation that will be pursued in the study contains two basic premises: (1) Estimation of the IMU error sources in a simultaneous or parallel fashion

rather than the sequential or serial manner of contemporary techniques will permit discrepancies between the assumed and actual error model to be detected. And, (2) by adding error model residuals or additional error sources possessing very broad functional dependencies to the assumed error model, it should be possible to determine specific functional dependencies through correlation analysis. The method of implementing this conceptual approach will be described in the sequel.

3.2 GIMBAL SYNCHRO ANGLE MEASUREMENT EQUATIONS

The gimbal synchro angle measurement equations express the time rates of change of the IMU gimbals relative to each other. The key point that must be recognized in order to derive these expressions is that the gimbals rotate in such a manner as to isolate the IMU's platform angular velocity from that of its case. Before these relationships can be determined it is however necessary to define: various reference frames, the relationship between their angular velocities, gyro torquing rates, and a gyro drift model.

3.2.1 Reference Frames and Their Angular Velocities

The platform frame is defined as the innermost IMU gimbal upon which the gyro and accelerometer inertial instruments are mounted. The inertial frame is considered as a frame that is nonrotating relative to the stars and has its origin at the earth's center. The angular velocity vector of the platform frame relative to the inertial frame coordinatized in platform frame coordinates is given as:

$$\overline{W}^{P}_{I,P} = C^{P}_{g}\,\overline{W}^{g}_{I,g}$$

where

C^{P}_{g} is a small-angle nonorthogonal error transformation matrix that accounts for the physical misalignments of the gyro input axes from the platform reference frame axes. The elements of this matrix are shown in Figure 3-1.

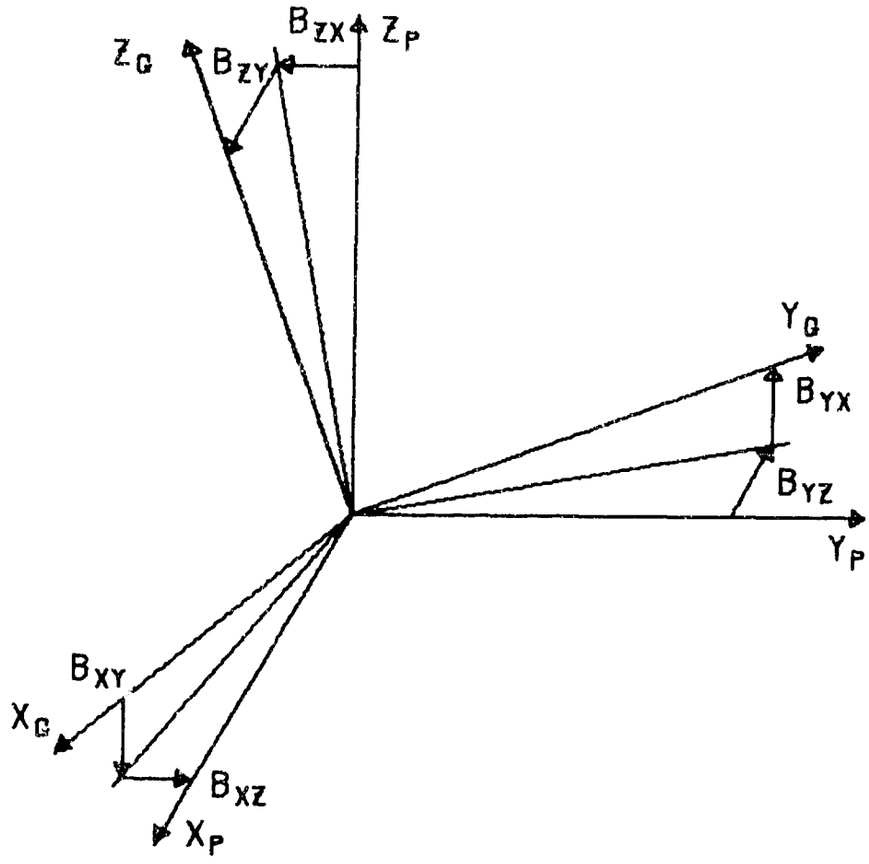

Figure 3-1. Relationship Between Gyro (G) and Platform (P) Reference Frame Axes

$$C_g^P = \begin{bmatrix} 1 & -\beta_{xz} & \beta_{xy} \\ \beta_{yz} & 1 & -\beta_{yx} \\ -\beta_{zy} & \beta_{zx} & 1 \end{bmatrix}$$

$\bar{W}^g_{I,g}$ is the angular velocity vector of the gyro frame relative to the inertial frame coordinatized in gyro frame coordinates.

$\bar{W}_{I,g}$ is composed of two basic vectors. The first represents the angular velocity at which the gyros are commanded to precess relative to inertial space $\bar{W}_{I,C}$. The second represents gyro frame angular velocity relative to inertial space due to all gyro imperfections and is commonly referred to as gyro drift $\bar{W}_{I,D}$.

$$\bar{W}^g_{I,g} = \bar{W}^g_{I,C} + \bar{W}^g_{I,D}$$

To maintain the gyro frame stabilized at approximately a constant attitude with respect to the navigation frame, it is necessary to torque the gyros corresponding to the best a priori information of the coordinization of the earth rate vector in the gyro frame.

$$\bar{W}^g_{I,C} = \left[K_F\right]\overline{PRF} = C^P_{PG}\, C^{PG}_{RG}\, C^{RG}_{CASE}\, \bar{W}^N_{I,N}$$

where

$[K_F]$ is a 3x3 diagonal matrix of the loaded gyro scale factors. The true IMU gyro scale factors $[K_{FT}]$ differ from the scale factors loaded into the digital navigation computer $[K_F]$ by an error designated as $[\Delta K_F]$.

$\overline{PRF}$ is a three-state vector of the gyro torquing pulse repetition frequencies.

$\bar{W}^N_{I,N}$ is the angular velocity vector of the navigation frame relative to inertial space coordinated in the navigation frame.

$$\tilde{W}^{N}_{I,N} = \begin{bmatrix} \Omega & C(L) \\ 0 & \\ \Omega & S(L) \end{bmatrix}$$

Ω is the magnitude of the earth rate vector.

L is the latitude.

$C(\cdot)$ and $S(\cdot)$ represent the trigonometric cosine and sine functions.

C^{RG}_{CASE} is the IMU case to roll (outer) gimbal frame coordinate transformation matrix.

$$C^{RG}_{CASE} = \begin{bmatrix} 1 & 0 & 0 \\ 0 & c(\theta_x) & s(\theta_x) \\ 0 & -s(\theta_x) & c(\theta_x) \end{bmatrix}$$

C^{PG}_{RG} is the roll gimbal to pitch (middle) gimbal frame coordinate transformation matrix.

$$C^{PG}_{RG} = \begin{bmatrix} c(\theta_y) & 0 & -s(\theta_y) \\ 0 & 1 & 0 \\ s(\theta_y) & 0 & c(\theta_y) \end{bmatrix}$$

C^{P}_{PG} is the pitch gimbal to azimuth (inner) gimbal or platform frame coordinate transformation matrix.

$$C^{P}_{PG} = \begin{bmatrix} c(\theta_z) & s(\theta_z) & 0 \\ -s(\theta_z) & c(\theta_z) & 0 \\ 0 & 0 & 1 \end{bmatrix}$$

θ_x, θ_y, and θ_z are the nominal gimbal synchro angle readings which are obtained by subsequent rotations about the roll, pitch, and azimuth gimbal axes.

The KT-73 IMU is a four-gimbal unit with an outer to inner gimbal progression of outer roll, pitch, inner roll, and azimuth. The inner roll gimbal is not instrumented with a synchro device and is slaved to coincide with the outer roll gimbal by a reluctance E-bridge. The inner roll gimbal rotates out of coincidence with the outer roll gimbal to prevent gimbal-lock when the pitch gimbal exceeds ±70 degrees from its neutral position. The inner roll gimbal is not considered in the above gimbal frame coordinate transformations because its angular orientation cannot be measured at system-level. The only penalty associated with this approach is that the IMU cannot be tested with pitch gimbal more than ±70 degrees from its neutral position.

3.2.2 Gyro Drift Model

The gyro drift vector is an error quantity composed of all gyro error sources that are significant relative to and including the random disturbances or gyro noise.

$$\bar{W}^{g}_{I,D} = \bar{W}_A + \bar{W}_B + \bar{W}_M + \bar{W}_O + \bar{W}_T + \bar{W}_{RL} + \bar{W}_{RS}$$

$\bar{W}_A$ is the platform-to-IMU case attitude dependent gyro bias drift vector. This error source is not listed in Reference 1 by the IMU manufacturer, but has, however, been added, as discussed in Section 3.1, to account for the possibility of a significant discrepancy between the Reference 1 and the true gyro error model. Note that the error source has no specific functional dependency other than attitude relative to the IMU case.

$\bar{W}_B$ is the constant gyro bias drift vector.

$\bar{W}_M$ is the gyro mass unbalance drift vector.

$$\bar{W}_M = \begin{bmatrix} -M_{Sx} & 0 & M_{Ix} \\ 0 & -M_{Sy} & M_{Iy} \\ 0 & -M_{Iz} & M_{Sz} \end{bmatrix} \bar{f}_s^g$$

M_{Sx}, M_{Sy}, and M_{Sz} are the gyro spin axes mass unbalance coefficients.

M_{Ix},M_{Iy}, and M_{Iz} are the gyro input axes mass unbalance coefficients. Gyro input, output and spin axes, and mass unbalance orientations used for deriving the mass unbalance matrix shown above are given in Figure 3-2. The vector equation equating the cross products of the mass unbalance position and specific force vectors to the gyro angular drift and angular momentum vectors establishes the sign conventions.

$\bar{f}_s^g$ is the specific force coordinatized in the gyro frame.

$$\bar{f}_s^g = C_P^g C_{PG}^P C_{RG}^{PG} C_{CASE}^{RG} C_N^{CASE} \bar{f}_s^N$$

C_N^{CASE} is an orthogonal small angle navigation to IMU case frame coordinate transformation matrix.

$$C_N^{CASE} = \begin{bmatrix} 1 & \eta_z & -\eta_y \\ -\eta_z & 1 & \eta_x \\ \eta_y & -\eta_x & 1 \end{bmatrix}$$

$\bar{f}_s^N$ is the specific force coordinated in the navigation frame.

$$\bar{f}_s^N = \begin{bmatrix} 0 \\ 0 \\ -g \end{bmatrix}$$

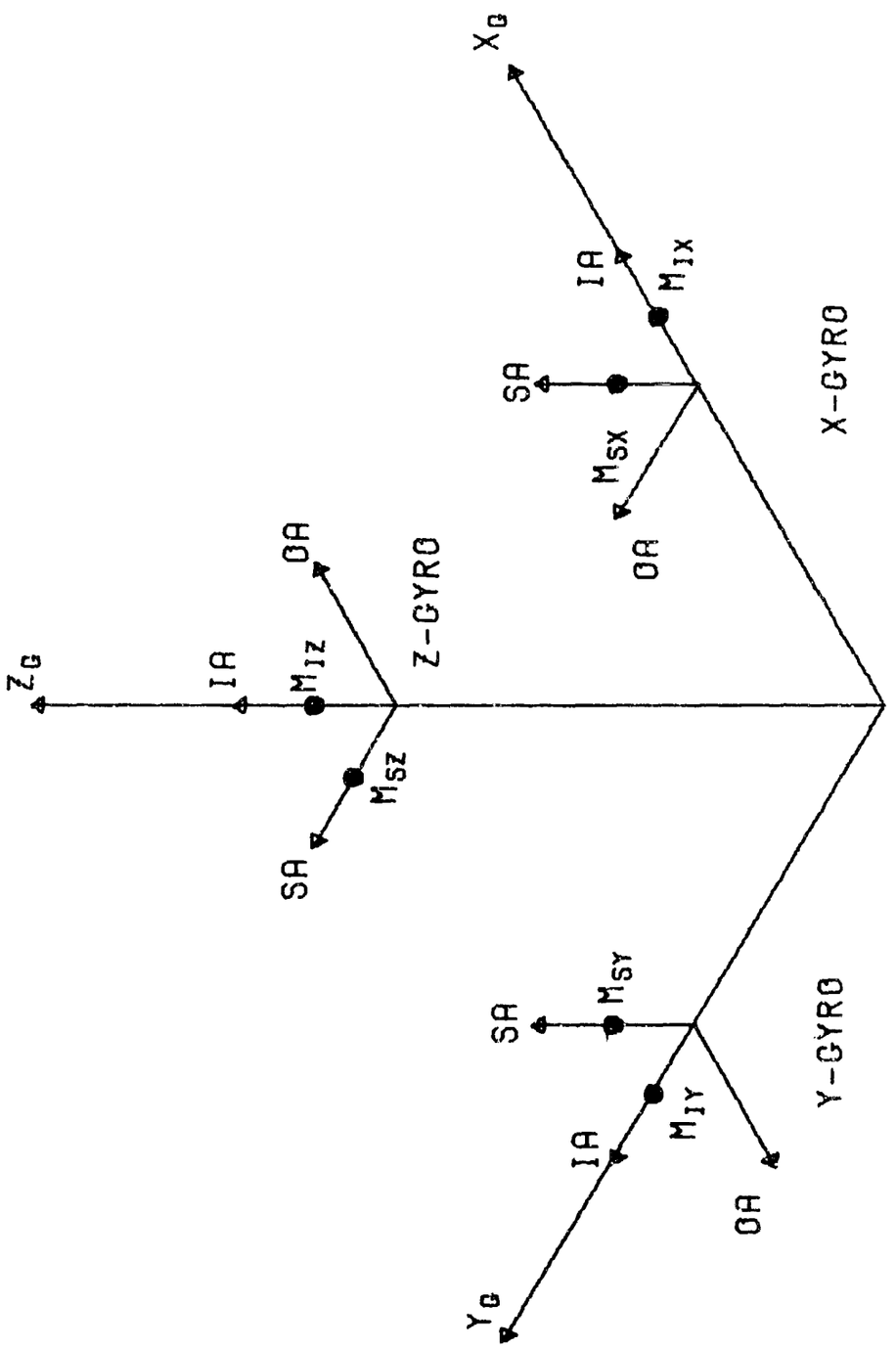

Figure 3-2. Gyro Axes and Mass Unbalance Orientations

g is the magnitude of the earth's gravity vector.

$\bar{W}_O$ is the gyro anisoelastic drift vector.

$$\bar{W}_O = \begin{bmatrix} K_{O_x} \cdot f^g_{Sy} \cdot f^g_{Sz} \\ K_{O_y} \cdot f^g_{Sx} \cdot f^g_{Sz} \\ K_{O_z} \cdot f^g_{Sx} \cdot f^g_{Sy} \end{bmatrix}$$

K_{ox}, K_{oy} and K_{oz} are the anisoelasticity coefficients for the x, y, and z gyros.

$\bar{W}_T$ is the gyro thermal transient drift vector.

$$\bar{W}_T = \bar{W}_{T_O} \cdot \frac{-(t - T_o)}{\tau_{gt}}$$

$\bar{W}_{T_O}$ is the initial gyro warm-up drift vector.

T_o is the time from power turn-on to the start of fine gyro-compass alignment.

t is the time from power turn-on.

τ_{gt} is the gyro warm-up drift time constant.

$\bar{W}_{RL}$ is the long correlation time exponentially correlated gyro random drift vector.

$\bar{W}_{RS}$ is the short correlation time exponentially correlated gyro random drift vector.

$$\dot{\bar{W}}_R(t) = -\frac{\bar{W}_R(t)}{\tau_g} + \sigma_g \sqrt{\frac{2}{\tau_g}}\, \bar{N}(t)$$

$\tau_{g\ell}$ and τ_{gs} are the long and short gyro random noise correlation times.

$\sigma_{g\ell}$ and σ_{gs} are the long and short correlation time random drift standard deviations.

N(t) is unity variance white noise.

3.2.3 Gimbal Angular Velocity Isolation

The foregoing equations for the IMU error sources, IMU case-to-navigation frame misalignment angles and gyro frame commanded angular velocity permit calculation of the angular velocity of the platform frame relative to an inertial frame. The IMU gimbals and closed-loop servo-control mechanism function so that this angular velocity is isolated from that of the IMU case. Assuming that the IMU is rigidly mounted to a static test fixture, IMU case angular velocity is simply that of the rotating earth. To achieve IMU platform-to-case angular velocity isolation, the gimbals must rotate relative to one another in a manner dictated by the following equation.

$$\bar{W}^{P}_{I,P} = \bar{W}^{P}_{PG,P} + C^{P}_{PG}\left[\bar{W}^{PG}_{RG,PG} + C^{PG}_{RG}\left(\bar{W}^{RG}_{CASE,RG} + C^{RG}_{CASE}\, C^{CASE}_{N}\bar{W}^{N}_{I,N}\right)\right]$$

where

$\bar{W}^{RG}_{CASE,RG}$ is the angular velocity vector of the roll gimbal frame relative to the IMU case coordinatized in the roll gimbal frame.

$$\bar{W}^{RG}_{CASE,RG} = \begin{bmatrix} \theta_{gx} \\ 0 \\ 0 \end{bmatrix}$$

$\bar{W}^{PG}_{RG,PG}$ is the angular velocity vector of the pitch gimbal frame relative to the roll gimbal frame coordinatized in the pitch gimbal frame.

$$W^{PG}_{RG,PG} = \begin{bmatrix} 0 \\ \dot{\theta}_{gy} \\ 0 \end{bmatrix}$$

$\bar{W}^{P}_{PG,P}$ is the angular velocity vector of the platform frame relative to the pitch gimbal frame coordinated in the platform frame.

$$\bar{W}^{P}_{PG,P} = \begin{bmatrix} 0 \\ 0 \\ \dot{\theta}_{gz} \end{bmatrix}$$

$\dot{\theta}_{gx}$, $\dot{\theta}_{gy}$, and $\dot{\theta}_{gz}$ are the time rates of change of the roll, pitch, and azimuth gimbal angles.

C^{RG}_{CASE}, C^{PG}_{RG}, and C^{P}_{PG} are the three-roll, pitch, and azimuth gimbal frame coordinate transformation matrices as defined previously except that the trigonometric function arguments are now the θ_{gx}, θ_{gy}, and θ_{gz} gimbal angles rather than the nominal gimbal synchro angle readings.

The roll, pitch, and azimuth synchros provide a measurement of the corresponding gimbal angles relative to each other or the IMU case. The absolute accuracy of the KT-73 IMU synchro devices is characterized by a 6-arc-minute standard deviation. The synchros are, however, capable of 5-arc-second precision for sufficiently small deviations about any nominal gimbal angle. To fully utilize the synchro angle measurement information, each gimbal angle is subdivided into three components.

$$\theta_g(t) = \theta + \Delta\theta + d\theta(t)$$

where

$\theta_g(t)$ is the total time-varying gimbal angle.

θ represents the nominal synchro gimbal angle used in orientating the platform relative to the IMU case. θ is considered fixed after initial platform orientation.

$\Delta\theta$ represents a six-arc-minute bias angular error inherent between θ and the actual gimbal orientation, due to synchro measurement accuracy limitations.

$d\theta(t)$ represents the differential time-varying gimbal angle component measurable to 5-arc-second accuracy by using the inherent precision of the synchros.

3.2.4 Linearized Error Equations

The foregoing system of equations given in Sections 3.2.1 through 3.2.3 can be manipulated to yield a set of three simultaneous nonlinear stochastic differential equations which relate IMU error sources and platform-to-navigation frame misalignment angles to system-level gimbal synchro angle measurable quantities. The nonlinear nature of the equations preclude a rigorous solution and for this reason a first-order linearization of the equations is assumed to be an accurate approximation. This is, of course, a major assumption that will be justified in the sequel. The manipulation and linearization of the system of equations by the use of partial derivatives is a straightforward process but is involved and tedious, and for these reasons is not illustrated here. The set of three simplified simultaneous stochastic differential equations that result from this process is given below for the differential roll, pitch, and azimuth gimbal angles.

$$\dot{d\theta}_x = C(\theta_z)\left[W_{Ax} + W_{Bx} + W_{Tx} + W_{RLx} + W_{RSx}\right] / C(\theta_y)$$

$$- S(\theta_z)\left[W_{Ay} + W_{By} + W_{Ty} + W_{RLy} + W_{RSy}\right] / C(\theta y)$$

$$+ C(\theta_z)\left[-g_x M_{S_x} + g_z M_{I_x}\right] / C(\theta y)$$

$$+ S(\theta_z)\left[g_y M_{Sy} - g_z M_{Iy}\right] / C(\theta y)$$

$$+ C(\theta_y)\, g_y g_z K_{Ox} / C(\theta_y) - S(\theta_z)\, g_x g_z K_{Oy} / C(\theta y)$$

$$+ C(\theta_z) PRF_x \Delta K_{Fx} / C(\theta_y) - S(\theta_z) PRF_y \Delta K_{Fy} / C(\theta_y)$$

$$+ C(\theta_z)\left[-W_{Cy}\beta_{xz} + W_{Cz}\beta_{xy}\right] / C(\theta_y)$$

$$+ S(\theta_z)\left[-W_{Cx}\beta_{yz} + W_{Cz}\beta_{yx}\right] / C(\theta_y)$$

$$-\Omega\, T(\theta_y) S(\theta_x)\left[S(L)(\eta_x + \Delta\theta_x + d\theta_x) - C(L)\eta_z\right]$$

$$+\Omega\left[T(\theta_y) C(\theta_x) C(L) + S(L)\right]\eta_y$$

$$+\left\{T(\theta_y)\left[C(x) W_{Cx} - S(\theta_z) W_{Cy}\right] / C(\theta_y)\right.$$

$$\left.+\Omega\, C(\theta_x) S(L) / C^2(\theta_y)\right\}\left[\Delta\theta_y + d\theta_y\right]$$

$$-\left[S(\theta_z) W_{Cx} + C(\theta_z) W_{Cy}\right]\left[\Delta\theta_z + d\theta_z\right] / C(\theta_y)$$

$$\dot{d\theta}_y = S(\theta_z)\left[W_{Ax} + W_{Bx} + W_{Tx} + W_{RLx} + W_{RSx}\right]$$

$$C(\theta_z)\left[W_{Ay} + W_{By} + W_{Tx} + W_{RLx} + W_{RSx}\right]$$

$$+ S(\theta_z)\left[-g_x M_{Sx} + g_z M_{Ix}\right]$$

$$+ C(\theta_z)\left[-g_y M_{Sy} + g_z M_{Iy}\right]$$

$$+S(\theta_z)\,g_y g_z K_{Ox} + C(\theta_z)\,g_x g_z K_{Oy}$$

$$+S(\theta_z)\,PRF_x \Delta K_{Fx} + C(\theta_z)\,PRF_y \Delta K_{Fy}$$

$$+S(\theta_z)\left[-W_{Cy}\beta_{xz} + W_{Cz}\beta_{xy}\right]$$

$$+C(\theta_z)\left[W_{Cx}\beta_{xz} - W_{Cz}\beta_{yx}\right]$$

$$-\Omega\, C(\theta_x)\left[S(L)(\eta_x + \Delta\theta_x + d\theta_x) - C(L)\,\eta_z\right]$$

$$-\Omega\, S(\theta_x)\,C(L)\,\eta_x$$

$$+\left[C(\theta_z)\,W_{Cx} - S(\theta_z)\,W_{Cy}\right]\left[\Delta\theta_z + d\theta_z\right]$$

$$\dot{d\theta_z} = -T(\theta_y)\,C(\theta_z)\left[W_{Ax} + W_{Bx} + W_{Tx} + W_{RLx} + W_{RSx}\right]$$

$$+T(\theta_y)\,S(\theta_z)\left[W_{Ay} + W_{By} + W_{Ty} + W_{RLy} + W_{RSy}\right]$$

$$+\left[W_{Az} + W_{Bz} + W_{Tz} + W_{RLz} + W_{RSz}\right] + g_z M_{Sz} - g_y M_{Iz}$$

$$+T(\theta_y)\,C(\theta_z)\left[g_x M_{Sx} - g_z M_{Ix}\right]$$

$$+T(\theta_y)\,S(\theta_z)\left[-g_y M_{Sy} + g_z M_{Iy}\right]$$

$$-T(\theta_y)\,C(\theta_z)\,g_y g_z K_{Ox} + T(\theta_y)\,S(\theta_z)\,g_x g_z K_{Oy}$$

$$+g_x g_y K_{Oz} - T(\theta_y)\,C(\theta_z)\,PRF_x \Delta K_{Fx}$$

$$+T(\theta_y)\,S(\theta_z)\,PRF_y \Delta K_{Fy} + PRF_z \Delta K_{Fz}$$

$$+T(\theta_y)\,C(\theta_z)\left[W_{Cy}\beta_{xz} - W_{Cz}\beta_{xy}\right]$$

$$+T(\theta_y)S(\theta_z)\left[W_{Cx}\beta_{yz}-W_{Cz}\beta_{yx}\right]$$

$$-W_{Cx}\beta_{zy}+W_{Cy}\beta_{zx}$$

$$+\Omega S(\theta_x)\left[S(L)(\eta_x+\Delta\theta_x+d\theta_x)-C(L)\eta_z\right]/C(\theta_y)$$

$$-\Omega C(\theta_x)C(L)\eta_y/C(\theta_y)$$

$$-\left\{\left[C(\theta_z)W_{Cx}-S(\theta_z)W_{Cy}\right]/C^2(\theta_y)\right.$$

$$\left.-\Omega T(\theta_y)C(\theta_x)S(L)/C(\theta_y)\right\}\left[\Delta\theta_y+d\theta_y\right]$$

$$+T(\theta_y)\left[S(\theta_z)W_{Cx}+C(\theta_z)W_{Cy}\right]\left[\Delta\theta_z+d\theta_z\right]$$

where $S(\cdot)$, $C(\cdot)$ and $T(\cdot)$ represent the trigonometric sine, cosine, and tangent functions.

$$g_x = g\left[C(\theta_x)S(\theta_y)C(\theta_z)-S(\theta_x)S(\theta_z)\right]$$

$$g_y = -g\left[C(\theta_x)S(\theta_y)S(\theta_z)+S(\theta_x)C(\theta_z)\right]$$

$$g_z = -gC(\theta_x)C(\theta_y)$$

$$W_{Cx} = \Omega\left\{C(L)C(\theta_z)C(\theta_y)\right.$$

$$\left.-S(L)\left[C(\theta_z)S(\theta_y)C(\theta_x)-S(\theta_z)S(\theta_x)\right]\right.$$

$$W_{Cy} = \Omega\left\{-C(L)S(\theta_z)C(\theta_y)\right.$$

$$\left.+S(L)\left[S(\theta_z)S(\theta_y)C(\theta_x)+C(\theta_z)S(\theta_x)\right]\right\}$$

$$W_{Cz} = \Omega\left[C(L)S(\theta_y)+S(L)C(\theta_x)C(\theta_y)\right]$$

Sign conventions for the error equation development assume that the navigation frame x, y, and z axes are originated north, west, and up, respectively. The IMU roll, pitch, and azimuth gimbal neutral positions are coincident with the x, y, and z navigation frame axes, respectively. All gimbal rotations have positive directions as specified by the right-hand rule.

3.3 VELOCITY MEASUREMENT EQUATIONS

3.3.1 The Specific Force Equation

Derivation of the equations relating system-level IMU velocity measurements to IMU error sources and platform-to-navigation frame misalignment angles follows directly from the specific force equation coordinatized to the accelerometer frame. Since the IMU's case will be rigidly fixed to the earth during calibration testing, the navigation frame is considered fixed to the earth and the appropriate specific force equation is given as follows.

$$\bar{f}_s^A = \bar{g}^A - \left(P_N^2 \bar{R}_{NA}\right)^A - \left(2\bar{W}_{IN} \times P_N \bar{R}_{NA}\right)^A$$

where

$\bar{R}_{NA}$ is the position vector from the navigation frame origin to the accelerometer test mass.

P_N is the derivative with respect to time taken relative to the navigation frame.

The last two terms on the right-hand side of this equation represent tangential, centripetal, and coriolis acceleration specific force components produced by a finite accelerometer test mass displacement from the origin of the accelerometer frame and both an angular acceleration and velocity of this frame relative to the earth fixed navigation frame. These components can, however, be shown to be insignificant relative to the accelerometer inertial instrument random disturbances for the KT-73 IMU.

Under these conditions, the accelerometers provide a measure of the earth's gravity vector coordinatized in the accelerometer frame.

$$\bar{f}_s^A = C_P^A C_{PG}^P C_{RG}^{PG} C_{CASE}^{RG} C_N^{CASE} \bar{g}^N$$

where

C_P^A is the platform-to-accelerometer frame non-orthogonal transformation matrix to account for physical misalignments of the accelerometer sensitive axes from the platform axes.

$$C_P^A = \begin{bmatrix} 1 & \gamma_{xz} & -\gamma_{xy} \\ -\gamma_{yz} & 1 & \gamma_{yx} \\ \gamma_{zy} & -\gamma_{zx} & 1 \end{bmatrix}$$

Definitions for the elements of this matrix are similar to those given in Figure 3-1 for the gyro-to-platform misalignment matrix. The first subscript refers to the misaligned axis and the second subscript refers to the axis about which a small angular rotation has occurred.

3.3.2 Accelerometer Error Model

In addition to ideally providing a measure of the specific force vector, the accelerometer outputs are corrupted by various hardware induced errors. The composite accelerometer output signals are not, however, measurable at system-level for the KT-73 IMU. In the hardware mechanization of this IMU, the accelerometer output signals are integrated in capacitive reset integrators which index velocity registers with delta velocity pulses. The accumulated velocity pulses are subsequently multiplied by airborne computer loaded accelerometer scale factors to obtain total velocity in the desired units.

The digitization of the accelerometer output signal into a train of pulses whose rate represents the magnitude of the acceleration introduces a velocity quantization level which represents the change in velocity per pulse. Since analog velocity data is not continuously available at any

instant of time, the quantization process introduces an error. If the quantization effects are treated as errors in the system-level IMU velocity measurements, then the accelerometer output signals can be used to define an artificial time derivative velocity vector modeled as follows.

$$\bar{\dot{V}} = \left[K_A\right]\left\{\bar{f}_s^A + \bar{A}_B + \bar{A}_R + \bar{A}_T\right\}$$

$[K_A]$ is a 3x3 diagonal matrix of the airborne computer loaded accelerometer scale factors. The true accelerometer scale factors $[K_{AT}]$ differ from the loaded ones by the sum of two errors, $[\Delta K_A]$ and $[\Delta K_{AA}]$. $[\Delta K_A]$ is considered as the nominal accelerometer scale factor error as specified in Reference 1. $[\Delta K_{AA}]$ is an additional error source showing a platform attitude dependency which has been added to the Reference 1 error model to account for potential discrepancies between the assumed and actual accelerometer error models. Since $[\Delta K_{AA}]$ can acquire new values each time the platform changes attitude with respect to the IMU case, other assumptions regarding the origin of this error model residual would be equally acceptable.

$\bar{A}_B$ is the accelerometer bias error vector.

$\bar{A}_R$ is the exponentially correlated accelerometer random noise vector.

$$\dot{\bar{A}}_R(t) = -\frac{\bar{A}_R(t)}{\tau_a} + \sigma_a\sqrt{\frac{2}{\tau_a}}\,\bar{N}(t)$$

τ_a is the random noise correlation time.

σ_a is the random noise standard deviation.

$N(t)$ is unity variance white noise.

$\bar{A}_T$ is the accelerometer thermal warm-up bias vector.

$$\bar{A}_T = \bar{A}_0 \, e^{-\frac{(t - T_0)}{\tau_{AT}}}$$

$\bar{A}_0$ is the initial accelerometer warm-up bias vector.

T_0 is the time from power turn-on to the start of fine gyro-compass alignment.

t is the time from power turn-on.

τ_{AT} is the gyro warm-up drift time constant.

A special hardware feature of the KT-73 IMU is the availability of both high and low gain accelerometer scale factors. The high gain accelerometer scale factor of 100,000 pulses-per-second per "g" (pps/g) is used for fine platform alignment to reduce velocity quantization errors and thereby shorten the necessary alignment times. The low gain scale factor of 1,000 pps/g is used for navigation since high accelerations would saturate the high gain capacitive reset integrator's maximum output of 10,000 pps. High gain scale factor modes are mechanized only as required on the two level-axis accelerometers and separate accelerometer bias errors are associated with the high and low gain scale factor modes. This IMU mechanization results in four, two bias and two scale factor, additional accelerometer errors to be calibrated.

3.3.3 Linearized Error Equations

In contrast to the gimbal angle time rates of change, the accelerometer outputs do not have an error-free value of zero. A zero mean accelerometer error vector equation can, however, be defined as follows.

$$\overline{\Delta\dot{V}} = \bar{\dot{V}} - C^{P}_{PG} \, C^{PG}_{RG} \, C^{RG}_{CASE} \, \bar{g}^{N}$$

All terms are as previously defined with the gimbal frame coordinate transformations being computed as functions of the initial θ_x, θ_y, and θ_z synchro angle settings.

The system of equations given in 3.3.1 through 3.3.3 can be solved to yield a set of three simultaneous nonlinear stochastic differential equations which relate the IMU error sources and platform-to-navigation frame misalignment angles to system-level IMU velocity measurements. These equations are manipulated and linearized, in a manner similar to that for the gimbal synchro measurement equations, such that a solution can be obtained. The resultant error equations for the x, y and z platform axes velocity measurements are given below.

$$
\begin{aligned}
\Delta\dot{v}_x \;=\; & -g\left[c(\theta_z)s(\theta_y)s(\theta_x) + s(\theta_z)c(\theta_x)\right]\eta_x \\
& + g\left[c(\theta_z)c(\theta_y)\right]\eta_y \\
& - g\left[s(\theta_z)c(\theta_x) + c(\theta_z)s(\theta_y)s(\theta_x)\right]\left[\Delta\theta_x + d\theta_x\right] \\
& + g\left[c(\theta_z)c(\theta_y)c(\theta_x)\right]\left[\Delta\theta_y + d\theta_y\right] \\
& - g\left[s(\theta_z)s(\theta_y)c(\theta_x) + c(\theta_z)s(\theta_x)\right]\left[\Delta\theta_z + d\theta_z\right] \\
& + g\left[c(\theta_z)s(\theta_y)c(\theta_x) - s(\theta_z)s(\theta_x)\right]\left[\Delta K_{Ax} + \Delta K_{AAx}\right] \\
& - g\left[s(\theta_z)s(\theta_y)c(\theta_x) + c(\theta_z)s(\theta_x)\right]\gamma_{xz} \\
& - g\left[c(\theta_y)c(\theta_x)\right]\gamma_{xy} \\
& + A_{Bx} + A_{Rx} + A_{Tx}
\end{aligned}
$$

$$
\begin{aligned}
\dot{\Delta v}_y &= g\left[s(\theta_z)\,s(\theta_y)\,s(\theta_x) - c(\theta_z)\,c(\theta_x)\right]\eta_x \\
&\quad - g\left[s(\theta_z)\,c(\theta_y)\right]\eta_y \\
&\quad + g\left[s(\theta_z)\,s(\theta_y)\,s(\theta_x) - c(\theta_z)\,c(\theta_x)\right]\left[\Delta\theta_x + d\theta_x\right] \\
&\quad - g\left[s(\theta_z)\,c(\theta_y)\,c(\theta_x)\right]\left[\Delta\theta_x + d\theta_x\right] \\
&\quad + g\left[s(\theta_z)\,s(\theta_x) - c(\theta_z)\,s(\theta_y)\,c(\theta_x)\right]\left[\Delta\theta_z + d\theta_z\right] \\
&\quad - g\left[c(\theta_z)\,s(\theta_x) + s(\theta_z)\,s(\theta_y)\,c(\theta_x)\right]\left[\Delta K_{Ay} + \Delta K_{AAy}\right] \\
&\quad + g\left[c(\theta_z)\,s(\theta_y)\,c(\theta_x) - s(\theta_z)\,s(\theta_x)\right]\gamma_{yz} \\
&\quad - g\left[c(\theta_y)\,c(\theta_x)\right]\gamma_{yx} \\
&\quad + A_{By} + A_{Ry} + A_{Ty}
\end{aligned}
$$

$$
\begin{aligned}
\dot{\Delta v}_z &= g\left[c(\theta_y)\,s(\theta_x)\right]\eta_x \\
&\quad + g\,s(\theta_y)\,\eta_y \\
&\quad + g\left[c(\theta_y)\,s(\theta_x)\right]\left[\Delta\theta_x + d\theta_x\right] \\
&\quad + g\left[s(\theta_y)\,c(\theta_x)\right]\left[\Delta\theta_y + d\theta_y\right] \\
&\quad - g\left[c(\theta_y)\,c(\theta_x)\right]\left[\Delta K_{Az} + \Delta K_{AAz}\right] \\
&\quad + g\left[c(\theta_z)\,s(\theta_y)\,c(\theta_x) - s(\theta_z)\,s(\theta_x)\right]\gamma_{zy} \\
&\quad - g\left[s(\theta_z)\,s(\theta_y)\,c(\theta_x) + c(\theta_z)\,s(\theta_x)\right]\gamma_{zx} \\
&\quad + A_{Bz} + A_{Rz} + A_{Tz}
\end{aligned}
$$

The functional dependencies for the level-axes high and low gain accelerometer scale factors and corresponding biases are, of course, the same. In the above equations, only one error source is explicitly shown but is considered to represent either the high or low gain error, depending upon which mode is being used at a particular instant during the test.

Note that while the velocity error equations appear somewhat simpler than those for the corresponding gimbal angles in the above formulation, the velocity error equations are functions of the differential gimbal angles and, therefore, functions of all the IMU and platform alignment error sources.

SECTION IV

SEPARATION OF IMU ERRORS

4.1 CONCEPTUAL APPROACH TO ERROR SEPARATION

The preceding derivations have resulted in a set of six general simultaneous equations relating the six-system-level IMU measurable quantities to roughly sixty error sources. Although a maximum of six measurements and, hence, equations are available, IMU calibration tests could be conducted where only some of the measurements were utilized. If, for example, the gimbal synchro angle measurements were not made, then only the three-velocity-measurement equations could be employed to solve for the error sources. Since a set of six or fewer specific simultaneous stochastic differential equations cannot be solved for sixty unknowns, a means functionally separating the error quantities had to be formulated. In view of the stochastic nature of the equations and IMU measurement noise, stochastic estimation of the error quantities is the best solution possible.

The conceptual approach to error source separation is to generate multiple sets of specific simultaneous differential equations from the basic set of six general ones. If not all the available IMU measurements are to be used, then the basic set of general equations would be correspondingly reduced. By generating enough multiple sets of specific equations such that the total number of equations is equal to the number of unknowns, accurate stochastic estimation of IMU error sources should be possible.

The generation of the multiple sets of specific equations is accomplished by angularly orientating the platform at various attitudes relative to the earth rate and gravity vectors. Note that a given platform attitude relative to these vectors is obtained by a specific set of gimbal angle rotations. The specific gimbal angles used, when inserted into the set of general equations, results in a set of specific equations. This approach follows directly from the observation that the

measurable IMU parameters are functions of both the IMU error sources and the coordinization of the above vectors in the platform and inertial instrument reference frame.

In developing this approach, it is convenient to group the error quantities into three groups:

(1) The first group consists of the IMU error sources which are modeled as random biases and instrument thermal transients which are commonly denoted as calibration parameters.

(2) The second group consists of those angular misalignment errors associated with platform-to-navigation frame alignment.

(3) The third group consists of the stochastic processes modeling the inertial instrument random disturbances.

4.2 IMU CALIBRATION PARAMETERS

A necessary, but not necessarily sufficient, condition for separation of the IMU error sources is that the multiple sets of system-level IMU measurement equations must be solvable for the IMU calibration parameters after the equations are simplified to contain only the calibration error sources. This simplification is accomplished by omitting the error sources associated with the above second and third groups from the general error equations. Performing this simplification reduces the set of six simultaneous stochastic differential equations to a system of six simultaneous ordinary differential equations.

This system of ordinary differential equations can be indefinitely expanded by positioning the platform at new attitudes as pointed out Section 4.1. A deterministic solution to the multiple sets of the ordinary differential equations can be attempted by application of Laplace transforms and using the initial and final IMU measurements for each attitude.

To confirm the conceptual approach to error source separation and to determine the most relevant IMU platform test attitudes for conducting the calibration tests, a solution to the simplified system of equations was attempted as described above. To facilitate the analysis, several additional error sources were omitted. The gyro and accelerometer thermal transient warm-up errors were deleted since they decay rapidly with time. Only low gain accelerometer scale factor and bias errors were considered since the errors associated with the high gain mode could be separated in a similar model. By necessity, the gyro and accelerometer error model residuals, which had been added to allow for the possibility that the actual IMU error model is significantly different from that assumed, were deleted since they assume a new value for each new platform attitude used and would thus prevent solving the system of equations.

Table 4-1 illustrates how the IMU calibration error sources become separable as a function of the cumulative number of platform test attitudes employed. Both sets of velocity and gimbal synchro angle measurements were assumed to be available. The x's indicate the earliest point at which the generated multiple sets of equations could be deterministically solved for a particular error source. All of the 33 IMU calibration errors could be determined after 7 platform attitudes times 6 specific equations per attitude or 42 equations were generated. Since only 33 equations should ideally be required, not all new equations generated are independent of previous ones. The specific attitudes shown were determined by a combination judgment and trial-and-error process.

4.2.1 Gimbal Angle Measurement Requirements

The KT-73 IMU is mechanized with synchro control transmitters and transformers having an accuracy of 6 arc minutes standard deviation. Contemporary synchro-to-digital converters have a 12 to 13 bit conversion capability which results in a precision on the order of 1 to 3 arc minutes. Since the precision of the synchro-to-digital converter is greater than the accuracy of the synchro, the equipment combination is

TABLE 1-1

SEPARATION OF IMU CALIBRATION PARAMETERS

	Cumulative Platform Attitudes						
Nominal Gimbal Angle	1	2	3	4	5	6	7
θ_x-Roll	0	π	$\pi/2$	$\pi/2$	$\pi/2$	$\pi/2$	$\pi/4$
θ_y-Pitch	0	0	0	0	0	$\pi/4$	$-\pi/4$
θ_z-Azimuth	0	0	0	π	$\pi/2$	0	0
Calibration Parameter							
A_{Bx}		X					
A_{By}		X					
A_{Bz}		X					
ΔK_{Ax}					X		
ΔK_{Ay}			X				
ΔK_{Az}		X					
γ_{xz}			X				
γ_{xy}		X					
γ_{yz}					X		
γ_{yx}		X					
γ_{zy}					X		
γ_{zx}			X				
W_{Bx}				X			
W_{By}				X			
W_{Bz}				X			
M_{Sx}					X		
M_{Ix}						X	
M_{Sy}					X		
M_{Iy}						X	
M_{Sz}						X	
M_{Iz}					X		
ΔK_{Tx}				X			
ΔK_{Ty}					X		
ΔK_{Tz}						X	
β_{xz}				X			
β_{xy}						X	
β_{yz}				X			
β_{yx}						X	
β_{zy}				X			
β_{zx}					X		
K_{Ox}							X
K_{Oy}							X
K_{Oz}							X

generally suitable for most inertial navigation applications. To accurately measure platform drift rates, however, a synchro angle measurement precision on the order of the precision of the synchro device itself of 5 arc seconds is desirable. Since a special measurement technique would have to be developed to achieve this precision, it would be desirable to calibrate the IMU by use of only the velocity measurements.

As discussed in Section 3.3.3, the velocity measurement equations contain the differential gimbal angle errors and thus all the IMU calibration error parameters. To address the question of the feasibility of calibrating the IMU by use of only the velocity measurements, the Laplace transform analysis was repeated using only these measurements. Results of this analysis showed that all calibration errors could be determined except the gyro spin axes mass unbalance errors.

The Laplace analysis results, however, raise a question as to the reason for the inseparability of the spin axes mass unbalance errors. Is the inseparability due to failure to select the required combination of platform test attitudes or is there a fundamental limitation inherent in the conceptual approach? To answer this question, the basic form of the combined velocity and gimbal synchro angle measurement equations was examined for linear independence. To facilitate the analysis, all error sources but the spin axes mass unbalance terms were omitted. One representation of the resultant set of three simultaneous equations is as follows:

$$\Delta\dot{V}_x = g^2 A C(\theta_z) C(\theta_y) \left[M_{Sy} + M_{Sz} \right]$$

$$\Delta\dot{V}_y = g^2 B C(\theta_x) C(\theta_y) \left[M_{Sx} + M_{Sz} \right]$$

$$\Delta\dot{V}_z = g^2 AB \left[M_{Sy} - M_{Sx} \right]$$

where

$$A = \left[s(\theta_z)\, s(\theta_y)\, c(\theta_x) + c(\theta_z)\, s(\theta_x) \right]$$

$$B = \left[c(\theta_z)\, s(\theta_y)\, c(\theta_x) - s(\theta_z)\, s(\theta_x) \right]$$

These equations relate the rate of change of the specific force vector, as coordinatized in the accelerometer frame, to the spin axes mass unbalance error coefficients. The equations are not independent, as can be shown by combining the first two to yield an equation directly proportional to the third.

$$B\Delta\dot{V}_x - A\Delta\dot{V}_y = 2g^2 AB \left[M_{Sy} - M_{Sx} \right]$$

Several conclusions can be reached as a result of this analysis. Without a gimbal synchro angle measurement or its equivalent, separation of the gyro spin axes mass unbalance errors is not possible. Only combinations of these errors

$$\left(M_{Sx} + M_{Sz}\right), \left(M_{Sy} + M_{Sz}\right) \text{ and } \left(M_{Sy} - M_{Sx}\right)$$

can be determined. A single piece of relevant information is required in addition to the velocity measurements to separate the spin axes mass unbalance errors. This information can, however, consist of one gimbal synchro angle measurement for a particular test attitude rather than require all three synchro gimbal angle measurements for all test attitudes.

4.3 PLATFORM ALIGNMENT ERRORS

The analyses of Section 4.2 showed that all IMU calibration parameters could be determined if the second and third groups of errors defined in Section 4.1 were omitted from the measurement equations. The first order effect of introducing the platform-to-navigation frame alignment errors of the second group into the solution for the separation of the IMU calibation parameters of the first group can be understood with reference to Figure 4-1. For a small platform-to-navigation frame misalignment, the

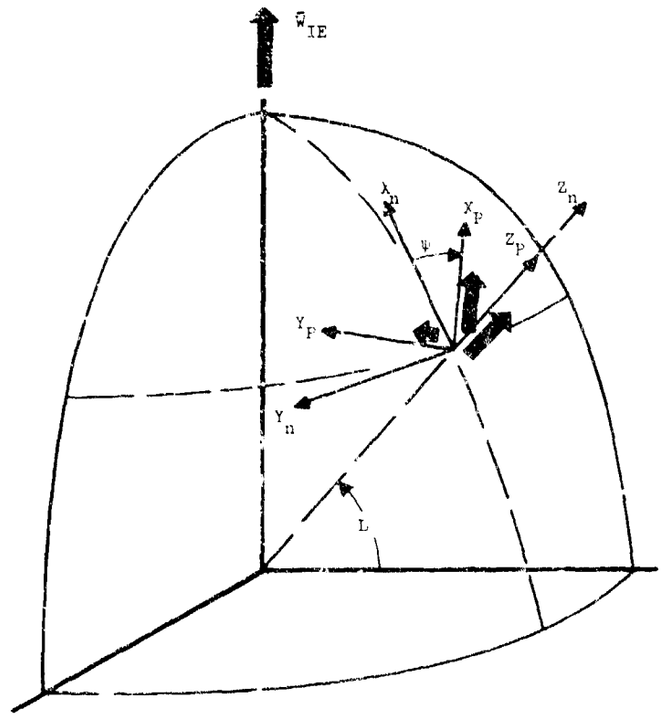

Figure 4-1. Platform Azimuth Misalignment Geometry

effect is precisely the classical problem of separating west gyro drift from the west platform axis commanded angular velocity error due to the azimuth misalignment angle ψ.

To null the angular velocity of an ideal IMU platform with respect to the navigation frame, the gyros must be commanded to precess at exactly the magnitude of the earth rate vector coordinatized in the gyro frame. Since ψ is a zero mean random variable whose magnitude is not known a priori, the west platform axis would not be commanded precess. For this condition, the angular velocity of the west platform axis with respect to the navigation axis is approximately given by:

$$W_{N,P_y} \simeq W_{I,D_y} + \Omega\, c(L)\, \psi$$

Given the standard deviation of the azimuth misalignment angle σ_ψ and a perfect measurement of $W_{N,Py}$, the standard deviation σ_W of the $W_{I,Dy}$ estimation error can be determined as:

$$\sigma_W = \sigma_\psi\, \Omega\, c(L)$$

This inability to separate the west platform commanded angular velocity error from the composite west gyro drift does not permit separation of all the IMU calibration errors as predicted in Table 4-1. The error separation problem can, however, be alleviated by realizing that the north and up platform axes do not encounter this first order limitation due to a different commanded angular velocity attitude dependency. The solution is to add additional platform test attitudes until all IMU calibration parameters become separable. It was determined by the Laplace analysis that by adding three new test attitudes, similar to the first three in Table 4-1 except that the x and y platform axes were interchanged, the calibration parameters became separable.

4.4 INERTIAL INSTRUMENT RANDOM DISTURBANCES

Incorporating the inertial instrument random disturbances of the third group of IMU error sources into the system of measurement equations

changes the problem description from one of ordinary differential equations to stochastic differential equations. The nature of the stochastic equations and the presence of IMU measurement noise precludes a deterministic solution to the separation of IMU errors and dictates the use of some form of stochastic estimation if optimal results are to be obtained.

Separation of some of the IMU calibration parameters from the inertial instrument random disturbances will have to be made on the basis of time rather than platform attitude since it is the only difference in functional dependency exhibited.

SECTION V

KALMAN FILTER

5.1 STOCHASTIC ESTIMATION

Selection of the technique for estimating the IMU errors was made in consideration of several major criteria.

(1) The technique should be optimum in the minimum variance sense.

(2) The technique should provide a statistical measure of the accuracy to which the IMU hardware errors can be calibrated.

(3) The technique should provide a convenient means of validating or justifying the first order measurement equation linearizations and other simplifying assumptions.

(4) The technique should provide a comprehensive solution by evaluating all error sources in a parallel or simultaneous manner to enhance the possibility of detecting unmodeled IMU hardware errors.

(5) The technique should be capable of being readily modified to include additional error sources or facilitate conducting correlation studies.

Although many optimal stochastic estimation techniques are available, the Kalman Filter algorithm with its associated covariance matrix was considered to be the most applicable approach. Conversely, the formulated problem satisfies the linearity, a priori system dynamics, and Gauss-Markov stochastic process modeling restrictions under which the Kalman Filter algorithm was derived.

5.2 KALMAN FILTER IMPLEMENTATION

5.2.1 Filter Equations

The error equation development results of Section 3 are consistent with state space analysis notation which is a convenient means of

mathematically representing a physical system in the time domain. The description of a continuous linear system by state variables is done by means of n first-order simultaneous differential equations. By using vectors and matrices, the IMU calibration problem can be defined by the given and derived error equations formulated in a vector differential equation.

$$\dot{x}(t) = F(t)\,x(t) + G(t)\,w(t)$$

where

$x(t)$ is the system n dimension state vector

$F(t)$ is the (nxn) dimension system dynamics matrix

$G(t)$ is the (nxp) noise distribution matrix

$w(t)$ is the p dimension disturbance vector

During the IMU calibration tests, a set of discrete measurements will be made at time t_n. The corresponding measurement process can be described as a vector algebraic equation; thus,

$$z(t_n) = H(t_n)\,x(t_n) + v(t_n)$$

where

$z(t_n)$ is the m dimension measurement vector

$H(t_n)$ is the (mxn) measurement distribution matrix

$v(t_n)$ is the m dimension measurement noise vector

The mean and covariance of the assumed white noise processes $w(t)$ and $v(t_n)$ are given as:

$$E\left[w(t)\right] = 0$$

$$E\left[w(t)\,w^T(t+\tau)\right] = Q(t)\,\delta(\tau)$$

$$E\left[v(t_n)\right] = 0$$

$$E\left[v(t_n)\,v^T(t_m)\right] = R(t_n)\,\delta(t_n - t_m)$$

where

$\delta(\tau)$ and $\delta(t_n - t_m)$ are dirac delta functions

$Q(t)$ is the (pxp) system noise matrix

$R(t_n)$ is the (mxm) measurement noise matrix

The Kalman Filter, References 2 and 3, provides an optimal (minimum variance) estimate of $x(t)$, which is denoted as $\hat{x}(t)$. The optimal estimate of the state vector $\hat{x}(t)$ and its (nxn) covariance matrix $P(t)$ are propagated between measurements by the equations.

$$\dot{\hat{x}}(t) = F(t)\,\hat{x}(t)$$

$$\dot{P}(t) = F(t)\,P(t) + P(t)F^T(t) + G(t)\,Q(t)\,G^T(t)$$

With the initial conditions at time zero t_0:

$$\hat{x}(t_0) = E\left[x(t_0)\right]$$

$$P(t_0) = E\left\{\left[x(t_0) - \hat{x}(t_0)\right]\left[x(t_0) - \hat{x}(t_0)\right]^T\right\}$$

At measurement times t_n, the Kalman Gain $K(t_n)$ is determined and the state vector optimal estimate and its covariance matrix updated according to the expressions,

$$K(t_n) = P(t_n^-)H^T(t_n)\left[H(t_n)P(t_n^-)H^T(t_n) + R(t_n)\right]^{-1}$$

$$\hat{x}(t_n^+) = \hat{x}(t_n^-) + K(t_n)\left[z(t_n) - H(t_n)\hat{x}(t_n^-)\right]$$

$$P(t_n^+) = \left[I - K(t_n)H(t_n)\right]P(t_n^-)\left[I - K(t_n)H(t_n)\right]^T + K(t_n)R(t_n)K^T(t_n)$$

5.2.2 Filter Vectors and Matrices

Formulation of the error equations, given or derived in Section 3, in state variable vector and matrix notation is a straightforward procedure. Initially, both the gyro and accelerometer short correlation

time random disturbances were included in the Kalman Filter state vector. Subsequent computer simulation studies showed, however, that the filter could neither reduce their uncertainty nor estimate their magnitudes accurately due to their relatively short correlation times as compared to the measurement time intervals. These errors were, therefore, deleted from the state vector and incorporated as disturbances on the differential gimbal angle and velocity states. The mechanized Kalman Filter 68 state vector is shown in Table 5-1. The location of individual states within the state vector has no particular significance and is partly a result of the iterative development process. The error sources associated with filter states 4 through 6 and 68 were not included in Section 3 because they were discovered during actual laboratory testing of the KT-73 IMU. These errors will be discussed further in Section 8.

The great majority of the nonzero 68 x 68 system matrix F elements are located in the F matrix rows corresponding to the system-level differential gimbal angle d0 and pseudo velocity ΔV measurement states. Due to the rather large dimensionality, this matrix is not readily pictorially illustrated. Specific F matrix elements are, however, readily identified from the linearized differential gimbal angle and velocity error equations tabulated in Sections 3.2.4 and 3.3.3.

With the exception of the three states' modeling IMU case-to-navigation frame misalignment angles, all state vector elements modeled as random constants are considered as IMU calibration parameters, and do not contribute any nonzero F matrix elements. The F matrix contains the negative reciprocals of the correlation times and time constants as diagonal elements in the rows corresponding to the states, modeled as exponentially correlated random noise and random constants with an exponential decay. The F maxtrix elements are independent of time but some do change in magnitude each time the IMU platform is re-oriented due to the nominal synchro angle dependency.

TABLE 5-1

IMU CALIBRATION KALMAN FILTER STATE VARIABLES

STATE				MODEL/ INITIAL 1σ VALUE
G-INSENSITIVE GYRO DRIFT				RANDOM CONSTANTS
1.	W_{Bx}	X	Gyro Drift Rate	0.1°/hr
2.	W_{By}	Y	Gyro Drift Rate	0.1°/hr
3.	W_{Bz}	Z	Gyro Drift Rate	0.5°/hr
G-SENSITIVE GYRO DRIFT COEFFICIENTS				RANDOM CONSTANTS
4.	W_{Qx}	X	Gyro Output Axis Quadrature G-Sensitivity	0.4°/hr/g
5.	W_{Qy}	Y	Gyro Output Axis Quadrature G-Sensitivity	0.4°/hr/g
6.	W_{Qz}	Z	Gyro Output Axis Quadrature G-Sensitivity	0.05°/hr/g
GYRO LONG CORRELATION TIME RANDOM DRIFT				EXPONENTIALLY CORRELATED
7.	W_{RLx}	X	Gyro Random Drift Rate	0.005°/hr
8.	W_{RLy}	Y	Gyro Random Drift Rate	0.005°/hr
9.	W_{RLz}	Z	Gyro Random Drift Rate	0.005°/hr
G-SENSITIVE GYRO DRIFT COEFFICIENTS				RANDOM CONSTANTS
10.	M_{Sx}	X	Gyro Spin Axis G-Sensitivity	1.0°/hr/g
11.	M_{Ix}	X	Gyro Input Axis G-Sensitivity	0.01°/hr/g
12.	M_{Sy}	Y	Gyro Spin Axis G-Sensitivity	1.0°/hr/g
13.	M_{Iy}	Y	Gyro Input Axis G-Sensitivity	0.01°/hr/g
14.	M_{Sz}	Z	Gyro Spin Axis G-Sensitivity	0.5°/hr/g
15.	M_{Iz}	Z	Gyro Input Axis G-Sensitivity	0.01°/hr/g

TABLE 5-1 (Contd)

				RANDOM CONSTANTS
G^2-SENSITIVE GYRO DRIFT COEFFICIENTS				
16.	K_{Ox}	X	Gyro Output-Spin Axes G^2 Sensitivity	$0.01°/hr/g^2$
17.	K_{Oy}	Y	Gyro Output-Spin Axes G^2 Sensitivity	$0.01°/hr/g^2$
18.	K_{Oz}	Z	Gyro Output-Spin Axes G^2 Sensitivity	$0.01°/hr/g^2$
GYRO SCALE FACTOR ERRORS				**RANDOM CONSTANTS**
19.	ΔK_{Fx}	X	Gyro Scale Factor Error	2.8×10^{-3} arc sec/pulse
20.	ΔK_{Fy}	Y	Gyro Scale Factor Error	2.8×10^{-3} arc sec/pulse
21.	ΔK_{Fz}	Z	Gyro Scale Factor Error	2.8×10^{-3} arc sec/pulse
GYRO INPUT AXES MISALIGNMENTS				**RANDOM CONSTANTS**
22.	β_{xz}	X	Gyro Input Axis Misalignment About z Axis	1.0 arc min
23.	β_{xy}	X	Gyro Input Axis Misalignment About y Axis	1.0 arc min
24.	β_{yz}	Y	Gyro Input Axis Misalignment About z Axis	1.0 arc min
25.	β_{yz}	Y	Gyro Input Axis Misalignment About x Axis	1.0 arc min
26.	β_{zy}	Z	Gyro Input Axis Misalignment About y Axis	1.0 arc min
27.	β_{zx}	Z	Gyro Input Axis Misalignment About x Axis	1.0 arch min
IMU CASE AXES MISALIGNMENTS				
28.	η_x		Case Misalignment About x Navigation Axis	4.0 arc min
29.	η_y		Case Misalignment About y Navigation Axis	4.0 arc min
30.	η_z		Case Misalignment About z Navigation Axis	4.0 arc min

TABLE 5-1 (Contd)

DIFFERENTIAL GIMBAL ANGLE ERRORS				DYNAMIC
31.	$d\theta_x$		Differential Roll Gimbal Angle Error	0.0 arc min
32.	$d\theta_y$		Differential Pitch Gimbal Angle Error	0.0 arc min
33.	$d\theta_z$		Differential Azimuth Gimbal Angle Error	0.0 arc min
ACCELEROMETER LOW GAIN MODE BIAS				RANDOM CONSTANTS
34.	A_{Bx}	X	Accelerometer Low Gain Bias	2,500 µg
35.	A_{By}	Y	Accelerometer Low Gain Bias	2,500 µg
36.	A_{Bz}	Z	Accelerometer Low Gain Bias	2,500 µg
ACCELEROMETER THERMAL WARM-UP TRANSIENTS				RANDOM CONSTANT EXPONENTIAL DECAY
37.	A_{Tx}	X	Accelerometer Thermal Warm-Up Error	5.0 µg
38.	A_{Ty}	Y	Accelerometer Thermal Warm-Up Error	5.0 µg
39.	A_{Tz}	Z	Accelerometer Thermal Warm-Up Error	200 µg
ACCELEROMETER LOW GAIN MODE SCALE FACTOR ERRORS				RANDOM CONSTANTS
40.	ΔK_{Ax}	X	Accelerometer Low Gain Scale Factor Error	0.03 numeric
41.	ΔK_{Ay}	Y	Accelerometer Low Gain Scale Factor Error	0.03 numeric
42.	ΔK_{Az}	Z	Accelerometer Low Gain Scale Factor Error	0.03 numeric
ACCELEROMETER INPUT AXES MISALIGNMENTS				RANDOM CONSTANTS
43.	γ_{xz}	X	Accelerometer Input Axis Misalignment About z	1.0 arc min
44.	γ_{xy}	X	Accelerometer Input Axis Misalignment About y	1.0 arc min
45.	γ_{yz}	Y	Accelerometer Input Axis Misalignment About z	1.0 arc min
46.	γ_{yx}	Y	Accelerometer Input Axis Misalignment About x	1.0 arc min
47.	γ_{zy}	Z	Accelerometer Input Axis Misalignment About y	1.0 arc min
48.	γ_{zx}	Z	Accelerometer Input Axis Misalignment About x	1.0 arc min

TABLE 5-1 (Contd)

PSEUDO VELOCITY ERRORS				DYNAMIC
49.	ΔV_x	x	Platform Axis Velocity Error	0.0 ft/sec
50.	ΔV_y	y	Platform Axis Velocity Error	0.0 ft/sec
51.	ΔV_z	z	Platform Axis Velocity Error	0.0 ft/sec
G-INSENSITIVE GYRO DRIFT				RANDOM CONSTANTS
52.	W_{Ax}	X	Gyro Attitude Dependent Gyro Drift Rate	0.005°/hr
53.	W_{Ay}	Y	Gyro Attitude Dependent Gyro Drift Rate	0.005°/hr
54.	W_{Az}	Z	Gyro Attitude Dependent Gyro Drift Rate	0.005°/hr
GIMBAL SYNCHRO ANGLE MEASUREMENT ERROR				RANDOM CONSTANTS
55.	$\Delta\theta_x$		Roll Synchro Measurement Bias	6.0 arc min
56.	$\Delta\theta_y$		Pitch Synchro Measurement Bias	6.0 arc min
57.	$\Delta\theta_z$		Azimuth Synchro Measurement Bias	6.0 arc min
ACCELEROMETER HIGH GAIN MODE BIAS				RANDOM CONSTANTS
58.	A_{BHx}	X	Accelerometer High Gain Bias	2,500 μg
59.	A_{BHy}	Y	Accelerometer High Gain Bias	2,500 μg
ACCELEROMETER HIGH GAIN MODE SCALE FACTOR ERRORS				
60.	ΔK_{AHx}	X	Accelerometer High Gain Scale Factor Error	0.03 numeric
61.	ΔK_{AHg}	Y	Accelerometer High Gain Scale Factor Error	0.03 numeric

TABLE 5-1 (Contd)

GYRO THERMAL WARM-UP DRIFT TRANSIENTS				RANDOM CONSTANT EXPONENTIAL DECAY
62.	W_{Tx}	X	Gyro Thermal Warm-Up Drift Rate	0.014°/hr
63.	W_{Ty}	Y	Gyro Thermal Warm-Up Drift Rate	0.014°/hr
64.	W_{Tz}	Z	Gyro Thermal Warm-Up Drift Rate	0.024°/hr
ACCELEROMETER ATTITUDE DEPENDENT SCALE FACTOR ERRORS				RANDOM CONSTANTS
65.	ΔK_{AAx}	X	Accelerometer Attitude Dependent Scale Factor Error	10 ppm
66.	ΔK_{AAy}	Y	Accelerometer Attitude Dependent Scale Factor Error	10 ppm
67.	ΔK_{AAz}	Z	Accelerometer Attitude Dependent Scale Factor Error	30 ppm
MEASUREMENT TIMING ERROR				EXPONENTIALLY CORRELATED
68.	ϕ		Measurement Timing Error	1 ppm

F matrix elements corresponding to the gyro quadrature G drift coefficients and the measurement timing error discovered during the laboratory tests are given next for completeness.

$$F(31,4) = \frac{\partial d\dot{\theta}_x}{\partial W_{Qx}} = g_y\, C(\theta_z)/C(\theta_y)$$

$$F(32,4) = \frac{\partial d\dot{\theta}_y}{\partial W_{Qx}} = g_y\, S(\theta_z)$$

$$F(33,4) = \partial\, \frac{d\dot{\theta}_z}{\partial W_{Qx}} = -\, g_y\, T(\theta_y)\, C(\theta_z)$$

$$F(31,5) = \partial\, \frac{d\dot{\theta}_x}{\partial W_{Qy}} = -\, g_x S(\theta_z)/C(\theta_y)$$

$$F(32,5) = \partial\, \frac{d\dot{\theta}_y}{\partial W_{Qy}} = g_x\, C(\theta_z)$$

$$F(33,5) = \partial\, \frac{d\dot{\theta}_z}{\partial W_{Qy}} = g_x T(\theta_y)\, S(\theta_z)$$

$$F(33,6) = \partial\, \frac{\partial\dot{\theta}_z}{\partial W_{Qz}} = g_x$$

$$F(49,68) = \frac{\partial\Delta\dot{v}_x}{\partial\phi} = g\left[C(\theta_z)\, S(\theta_y)\, C(\theta_x) - S(\theta_z)\, S(\theta_x)\right]$$

$$F(50,68) = \frac{\partial\Delta\dot{v}_y}{\partial\phi} = -g\left[C(\theta_z)\, S(\theta_x) + S(\theta_z)\, S(\theta_y)\, C(\theta_x)\right]$$

$$F(51,68) = \frac{\partial\Delta\dot{v}_z}{\partial\phi} = -g\, C(\theta_y)\, C(\theta_x)$$

The 68x10 noise distribution matrix G is illustrated in Figure 5-1. This matrix contains ten nonzero elements, four of which are located in the rows corresponding to the long correlation time exponentially correlated random noise gyro drift rate and measurement error stochastic processes. These nonzero elements are readily identified from the stochastic differential equations, modeling these noise processes, given in Section 3.2.2. The remaining six nonzero elements are located in the rows corresponding to the dynamic gimbal angle, 31 through 33, and velocity, 49 through 51, measurement states. This modeling accounts for the uncertainty of the measurement states produced by the short correlation time gyro and accelerometer random noise errors. These errors were omitted from the Kalman Filter state vector due to the filter's inability to estimate them. The magnitude of these G matrix elements was determined such that the variance of the dynamic measurements states is the same as when the short correlation time random noise errors were included as states in the filter.

The disturbance vector w(t) is a 10x1 input vector whose elements are zero mean, unity variance white noise processes. These white noise processes are assumed to be uncorrelated with each other resulting in the 10x10 system noise matrix Q being an identity matrix.

The 6x68 measurement matrix contains up to a maximum of six nonzero elements of unity magnitude in the columns corresponding to the rows of the measurement states. If all three velocity and gimbal angle measurements are utilized, the measurement matrix requires six rows. The measurements eventually decided upon consist of the three-velocity but only the azimuth gimbal synchro angle measurement, requiring only four rows for the measurement matrix.

The measurement z and measurement noise v vectors require from four to six states, depending on whether the roll and pitch gimbal synchro angle measurements are used. The first one, or three, elements of the v vector are zero mean Gaussian white random variables, with 5-arc-second standard deviations, and model the differential gimbal synchro angle measurement noise. The last three elements have similar properties and a

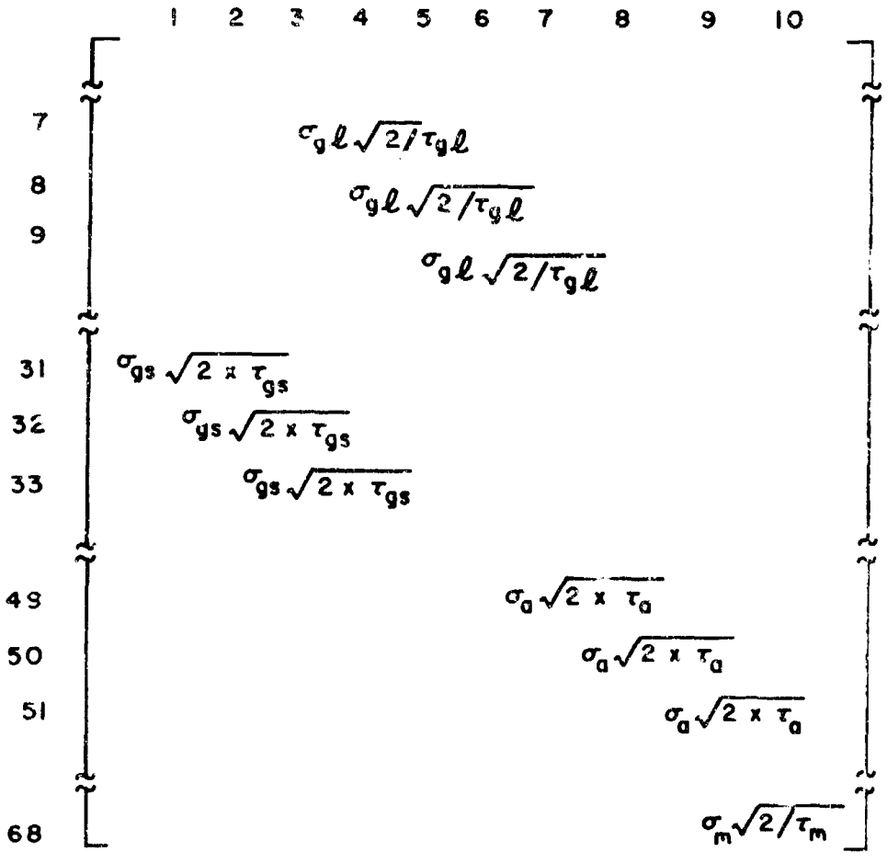

$\sigma_{g\ell}$ = 0.005 %/hr

$\tau_{g\ell}$ = 3600 sec

σ_{gs} = 0.003 %/hr

τ_{gs} = 1 sec

σ_a = 20 μg

τ_a = 0.0016 sec

σ_m = 1 ppm

τ_m = 250 sec

Figure 5-1. Noise Distribution Matrix Q

standard deviation representative of the accelerometer quantization process (quantization level/3.46) and model the artificial velocity measurement noise. The assumption that elements of the measurement noise vector are statistically independent of each other results in the 6x6 measurement noise matrix R being a diagonal matrix. Diagonal elements of the R matrix are variances of the corresponding measurement noise vector elements.

The 68x68 covariance matrix P is initially a diagonal matrix composed largely of the IMU error source variances. The initial uncertainty of all the 68 Kalman Filter states, in terms of their standard deviations as determined by taking the square root of the corresponding initial covariance matrix diagonal elements, is given in Table 5-1. The initial uncertainty of many of these error states is given in Reference 1. Since Reference 1 values correspond to inertial instrument biases and scale factors which have been trimmed for navigation, while the Kalman Filter mechanization does not, these instrument errors were increased to their untrimmed values. In those instances, gyro spin axis mass unbalance coefficients, where IMU laboratory calibration test results showed that the actual errors were significantly larger than those given in Reference 1 the initial uncertainties were increased to reflect the test results. The initial variances of the velocity and differential gimbal angle measurement states are identically zero due to the manner in which these states were defined. The initial variances of the IMU case-to-navigation frame misalignment angles depend on the laboratory test table or mounting fixture used and the manner in which the IMU case is aligned to the navigation frames. This topic is further discussed in Section 7.

A partial covariance matrix re-initialization is required each time the platform frame is re-oriented, for several reasons. The variances of the velocity and differential gimbal angle measurement states, having increased during testing at a given platform attitude, must be reset to zero. The gimbal synchro angle bias variances, having decreased over the previous test attitude, must be increased to the

nominal 6-arc-minute uncertainty to reflect that new biases are being encountered. Covariance matrix elements associated with the gyro bias and accelerometer scale factor platform attitude dependent error model residual states are reset to reflect the attitude dependency. In addition to resetting the variances of these states, any covariances that have built up between other error states must be re-initialized to zero.

In addition to those error sources included in the Kalman Filter state vector, it is desirable to computer optimal estimates and estimation errors for several composite error quantities. Inertial navigation system parameters, such as total gyro and platform drift and platform and accelerometer-to-navigation frame misalignment angles, provide additional insight to the Kalman Filter's capability to separate the IMU calibration parameters and estimate them accurately. Optimal estimates for these composite parameters are computed as functions of the sum of appropriate state vector element's optimal estimates. Optimal estimation errors for these composite error quantities are computed by use of the expectation operator and corresponding elements of the covariance matrix.

5.2.3 Integration Algorithms

The majority of the storage and computational time computer resources required to implement and exercise the Kalman Filter algorithm on a digital computer are associated with propagating the Kalman Filter state vector and covariance matrix. Computational time requirements can easily become burdensome, when we consider that the state vector and covariance matrix are propagated for time periods of one to two hours. The necessary computer resources can, however, be kept within reasonable limits by carefully selecting the integration algorithms required to propagate these quantities.

The final version of the IMU calibration Kalman Filter was hosted on a CDC-6600 digital computer having a word length of 60 bits. The state vector was propagated with laboratory test data stored on a magnetic

tape corresponding to off-line non-real-time operation. Total IMU test time was 69 minutes with measurements being nominally taken every 30 seconds. CDC-6600 computer resources required to execute the job were 900 seconds for compilation and execution time and 221,000 octal words for memory.

In developing the CDC-6600 Kalman Filter computer program, it was found that the most efficient operation of acceptable accuracy was accomplished by using relatively large integration step sizes accompanied by sophisticated integration algorithms. The covariance matrix is propagated in one step between the measurements, integration step size of 30 seconds, according to the fifth order Kutta-Mersion integration algorithm.

$$y_0 = P(t)$$

$$y_1 = y_0 + \frac{\Delta T}{3}\dot{P}(y_0)$$

$$y_2 = y_0 + \frac{\Delta T}{6}\left[\dot{P}(y_0) + \dot{P}(y_1)\right]$$

$$y_3 = y_0 + \frac{\Delta T}{8}\left[\dot{P}(y_0) + 3\dot{P}(y_2)\right]$$

$$y_4 = y_0 + \frac{\Delta T}{2}\dot{P}(y_0) - \frac{3\Delta T}{2}\dot{P}(y_2) + 2\Delta T\,\dot{P}(y_3)$$

$$P(t + \Delta T) = y_0 + \frac{\Delta T}{6}\left[\dot{P}(y_0) + \dot{P}(y_4)\right] + \frac{2\Delta T}{3}\dot{P}(y_3)$$

where ΔT is the integration step size

$$\dot{P}(t) = F(t)P(t) + \left[F(t)P(t)\right]^T + G(t)Q(t)G^T(t)$$

The covariance matrix derivative $\dot{P}(t)$ is determined using the above expression. Due to the sparse nature of the system dynamics matrix $F(t)$, the $\dot{P}(t)$ algorithm was coded in a manner that eliminated the bulk of the zero multiples.

Propagation of the Kalman Filter state vector $\hat{x}(t)$ requires substantially less computer resources than those necessary for propagation of the covariance matrix. Modified Euler integration is used to propagate the state vector with an integration step size of one second.

$$\hat{x}(t + \Delta t) = \hat{x}(t) + \frac{\Delta T}{2}\left[\dot{\hat{x}}(t) + \dot{\hat{x}}(t + \Delta t)\right]$$

where

$$\dot{\hat{x}}(t) = F(t)\,\hat{x}(t)$$

SECTION VI

THEORETICAL COMPUTER SIMULATION RESULTS

6.1 SIMULATION OBJECTIVES

A CDC-6600 computer simulation of the KT-73 IMU, Kalman Filter and laboratory calibration test was developed in consideration of several major objectives.

(1) To validate the concept of the premise postulated for separation of the IMU calibration parameters.

(2) To determine the accuracy to which the Kalman Filter can estimate the IMU calibration parameters, considering the effects of inertial instrument random disturbances, measurement noise, and limited test time.

(3) To perform limited analysis in regard to the power of the IMU calibration methodology and the usefulness of the Kalman Filter as a tool for conducting IMU error model development and validation studies.

(4) To justify the first-order equation linearizations made for facilitating a solution to the calibration equations.

(5) To assist in the preparation of a computer software specification and test procedure for the ensuing IMU calibration laboratory development program.

6.2 VALIDATION OF CALIBRATION METHODOLOGY AND ASSUMPTIONS

To obtain the highest level of confidence possible by the use of computer simulations, the concept validation philosophy of demonstrating strict convergence of the Kalman Filter optimal estimates to the error sources of a simulated KT-73 IMU was adopted. Strict sense convergence implies that the ensemble average of the simulated estimation errors conform to the zero mean gaussian processes having time-dependent variances given by the filter's covariance matrix.

In keeping with the concept validation philosophy, the developed KT-73 IMU simulation contains all the error sources given in Reference 1. The IMU simulation is based on the whole number, nonlinear equations developed above, and utilizes random number generators to simulate the random bias and stochastic process error sources. Digital gyro torquing and accelerometer quantization effects are included. The adequacy to which the Reference 1 error sources model the real KT-73 IMU will be addressed in the laboratory development program and also in conducting the aided-inertial navigation software development and evaluation tests in Table 1-1.

Figure 6-1 illustrates the Kalman Filter's ability to accurately estimate IMU platform drift rate and pseudo velocity errors in terms of the standard deviation of the estimation error. Platform drift rate is a composite error source containing up to eighteen error sources per axis for the platform and navigation frames approximately aligned situation shown in the figure. Similar remarks also apply to the pseudo velocity errors. Estimation error standard deviations for the psuedo velocity errors are obtained by taking the square root of the appropriate diagonal element of the filter's covariance matrix. Since total platform drift rate error is not a state variable in the Kalman Filter, corresponding estimation accuracies had to be obtained by utilizing the expectation operator in conjunction with on and off diagonal elements of the covariance matrix.

Each graph in Figure 6-1 contains two sets of data, corresponding to whether or not the system-level IMU velocity and gimbal angle measurements are taken. Velocity measurement errors corresponding to the low-gain accelerometer mode quantization levels were assumed. The x, y, and z platform axes symbols indicate the time instants the six simultaneous IMU measurements were taken and are uniformly spaced at thirty second intervals. The line segments between measurement points indicate how the estimation uncertainty propagates in time. The primary information conveyed by these graphs is that the Kalman Filter is capable of estimating composite system-level IMU errors to an accuracy essentially

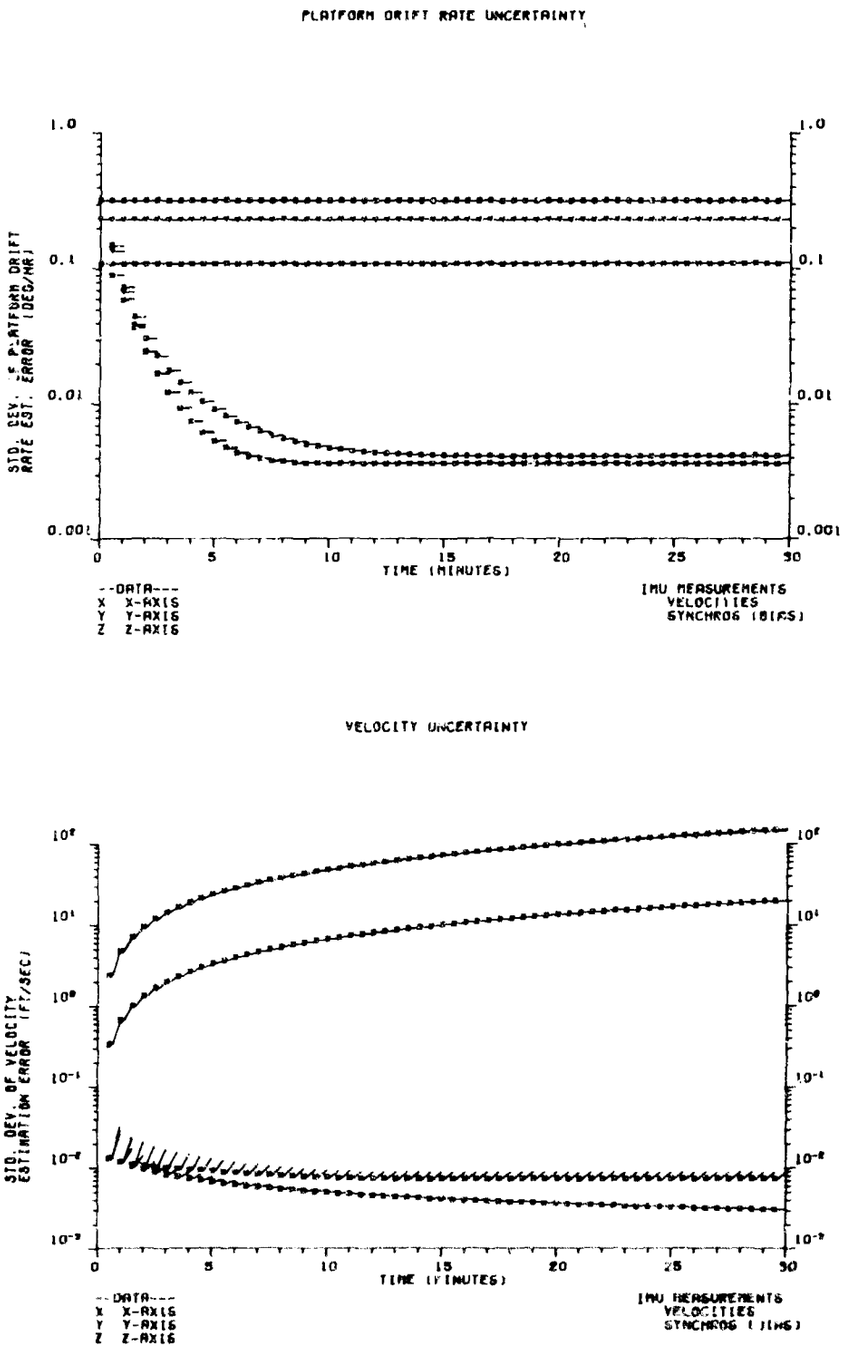

Figure 6-1. Platform Drift and Velocity Uncertainty

limited by the inertial instrument random disturbances in a five to ten minute IMU test. The length of time required to achieve this level of accuracy is heavily influenced by the magnitude of the measurement errors.

Although the Kalman Filter can accurately estimate the composite error quantities during a single platform orientation test, it cannot separate or accurately observe the individual IMU calibration parameters. The filter can, however, during the single platform orientation test, heavily correlate certain groups of error sources from an initially uncorrelated condition. To calibrate the IMU, the error sources must be decorrelated and accurately observed. The means by which this is accomplished is by testing the IMU with its platform at numerous orientations with respect to the earth rate and gravity vectors as discussed in Section IV.

Figure 6-2 is a graphic illustration of the error separation process. This figure shows an increasing Kalman Filter capability to estimate the y-gyro bias drift rate error component as additional platform test attitudes are introduced. Platform attitudes No. 1 through 5, 10, and 11 correspond to those of Table 4-1. Platform attitudes-No. 7 through 9 are the additional attitudes introduced to permit error source separation in the presence of the west-gyro-commanded angular velocity error due to the azimuth platform-to-navigation frame misalignment. Attitudes No. 6 and 12 are identical to No. 1 and illustrate that repeated use of the same test attitude does not significantly improve error source observation accuracy. These attitudes are synonomous with the navigation frame axes of north, west, and up.

The IMU is tested for five minutes per attitude as suggested by the estimation accuracy versus measurement time characteristic of Figure 6-1. Total IMU test time would, however, be somewhat longer than the one hour measurement time shown due to the several minutes' platform slew time required to periodically re-orient the platform. The sequence of platform test attitudes shown was selected such that the most significant IMU error sources are calibrated first and allow the option of omitting latter test attitudes in favor of reducing test time.

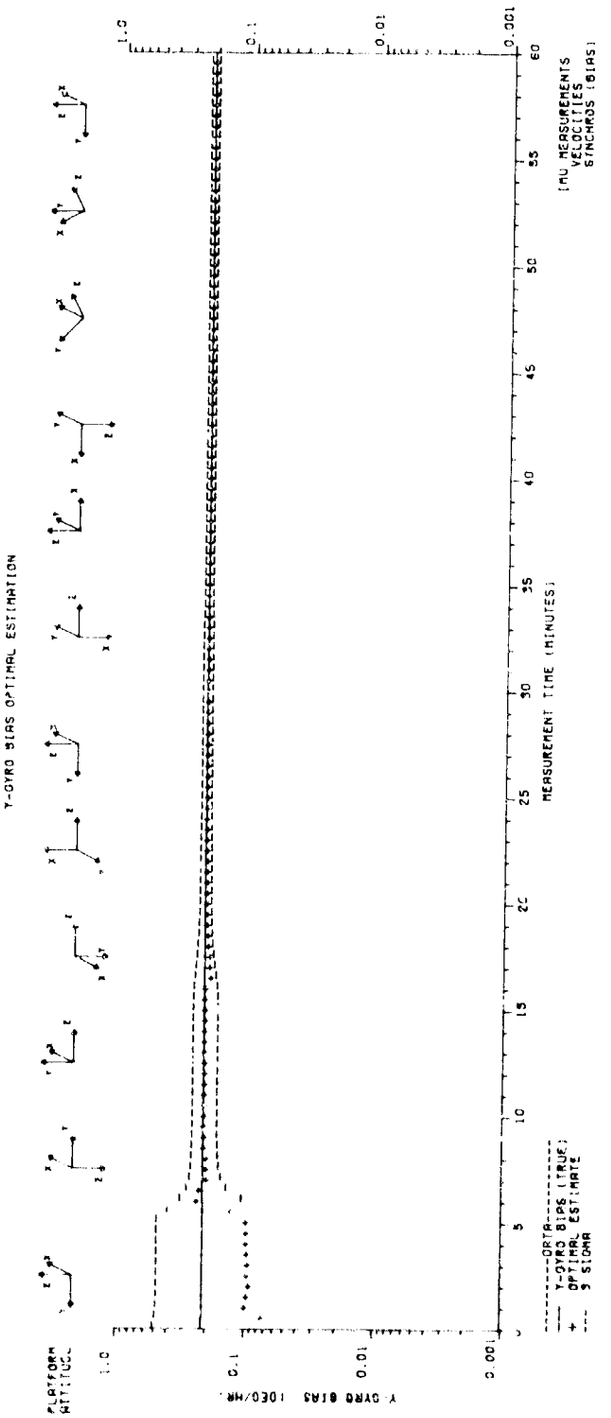

Figure 6-2. Gyro Bias Calibration

The upper and lower bounds superimposed about the simulated y-gyro bias error represent three standard deviations of the optimal estimation error stochastic process. The standard deviations used in determining these bounds were obtained by taking the square root of covariance matrix diagonal element corresponding to the y-gyro bias error as a function of time. Optimal estimation theory predicts that the Kalman Filter's optimal estimates should converge to the simulated y-gyro bias error to within these bounds a certain percentage of the time on an ensemble average basis. For Gaussian processes and three standard deviation bounds, this percentage is 99.5% of the time. Inspection of Figure 6-2 shows that all 120 or 100% of the filter's optimal estimates fall within the three standard deviation bounds, thus satisfying the criterion. Examination of the computer simulation results for convergence of the filter's optimal estimates to the other simulated IMU error sources showed that the criterion was met also.

Several conclusions can be reached as a result of the filter's optimal estimates converging to the simulated IMU error sources to within the accuracy predicted by optimal estimation theory. The major conclusion is that the gimballed IMU calibration problem, as formulated, can be adequately represented by a system of first-order linear equations. A second conclusion is that treatment of velocity quantization errors as measurement noise, omission of digital gyro pulse torquing effects, and other simplifying assumptions are justifiable. A final conclusion is that the Kalman Filter is a suitable analytical technique for calibrating IMUs.

6.3 IMU CALIBRATION ACCURACY LIMITATIONS

Examination of the estimation accuracy bounds depicted in Figure 6-2 shows that the estimation accuracy increases rapidly for the first four or five platform test attitudes. A slight increase in estimation accuracy occurs during the latter platform test attitudes due to the further separation of the y-gyro bias error from the other IMU calibration parameters modeled as random biases. The y-gyro bias estimation error does not, however, approach zero at the conclusion of the platform test attitude sequence.

To determine the reasons for the limitation in IMU calibration accuracy, the analytical results shown in Figure 6-3 were computed by use of the Kalman Filter simulations. The upper graph shows the optimal estimation errors for all three gyro bias drift rate components. This representation contains the same estimation accuracy information as Figure 6-2 but is plotted as one standard deviation on an absolute scale. This data is obtained by taking the square root of the appropriate diagonal element of the updated covariance matrix.

The lower graph in Figure 6-3 shows the estimation accuracy for the random variables defined as the sum of the gyro bias and long correlation time random gyro drift rate error components. Comparison of the upper and lower graphs illustrate the gyro bias calibration accuracy limitations imposed by the gyro random noise components. Each gyro is modeled with two exponentially correlated disturbances having 1 and 3600 second correlation times and 0.003 and 0.005 degree per hour drift rates, respectively. Reference to the upper graph shows that the long correlation time disturbance imposes itself as an approximate lower bound on gyro bias calibration accuracy. The reason that the long correlation time random gyro disturbance acts as lower bound for the gyro bias error estimation accuracy is that time is the only difference in the functional dependency of these two error sources. Accurate measurements taken frequently over an approximate correlation time period are required to separate them. This condition is not satisfied during the calibration test due to those platform test attitudes where platform drift can only be inaccurately inferred from the differential gimbal angle measurements. This limitation is illustrated in the lower graph in Figure 6-3 by the filter's ability to estimate the sum of these two error sources to an accuracy now limited by the short correlation time disturbance.

Estimation of the IMU calibration parameters to an accuracy limited by the inertial instrument random disturbances is the desired result from the navigational accuracy standpoint. Conceptually, this result implies that the IMU calibration error sources could be software compensated for with the pure inertial navigation accuracy achievable with the IMU being essentially limited by the inertial instrument random disturbances.

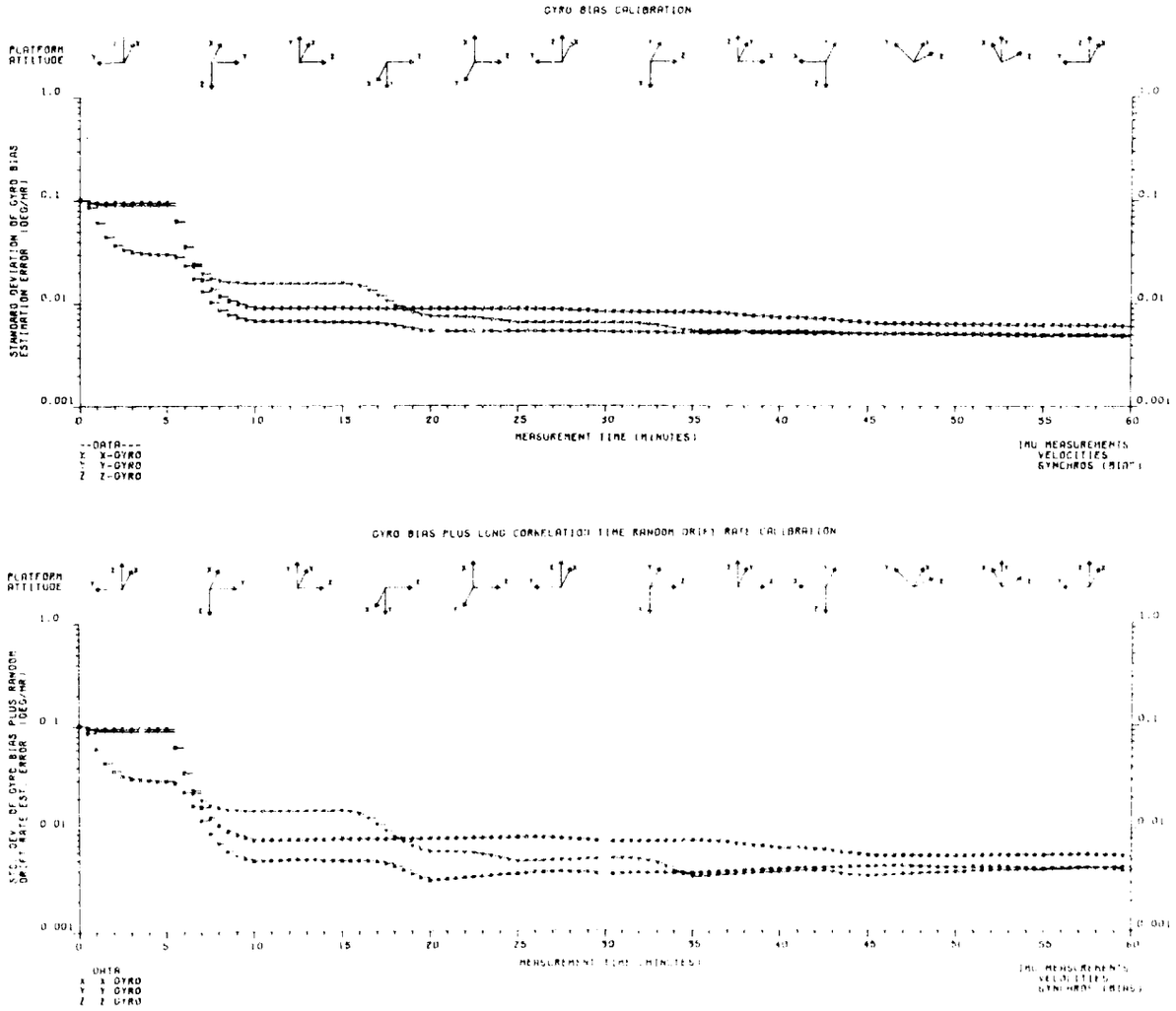

Figure 6-3. Gyro Bias and Gyro Bias Plus Random Noise Calibration Accuracy

6.4 DYNAMIC ERROR ESTIMATION

The Kalman Filter's ability to estimate a dynamic composite IMU error as opposed to the static IMU calibration parameters is illustrated by the total gyro drift rate characteristic shown in Figure 6-4. Total gyro drift is defined as a random variable composed of the sum of the long and short correlation time disturbances, thermal warm-up, constant and attitude-dependent biases, input and spin axis mass unbalance, and anisoelastic drift rate error components. Total platform drift would additionally contain the gyro scale factor, gyro-to-platform misalignment angle, and commanded angular velocity error sources.

The simulated x-gyro drift rate is plotted with straight line segments connecting the 30-second measurement intervals and does not show the fine grain structure due to the random disturbances. Convergence of the Kalman Filter's optimal estimates to the simulated gyro drift rate error is illustrated along with the one standard deviation estimation error upper and lower bounds. Assuming gaussian statistics, 68% of the filter's optimal estimates should fall within these boundaries. Optimal estimation errors appear consistent with this criterion.

6.5 IMU ERROR MODEL REFINEMENTS

A major objective of the IMU calibration study is to develop a methodology and companion analytical tool that affords some capability for conducting IMU error model development and validation efforts. An essential feature on any such approach is the ability to start with a functionally correct IMU error model, but with incorrect statistical information regarding the magnitudes of the individual error sources, and through iterative testing determine the correct error source magnitudes. The problem of refining a functionally incorrect IMU error model is addressed in Section 8.

To address the problem of refining the a priori IMU-error-model statistical magnitude data, the analysis depicted in Figure 6-5 was conducted. The upper graph shows that the nominal computer loaded

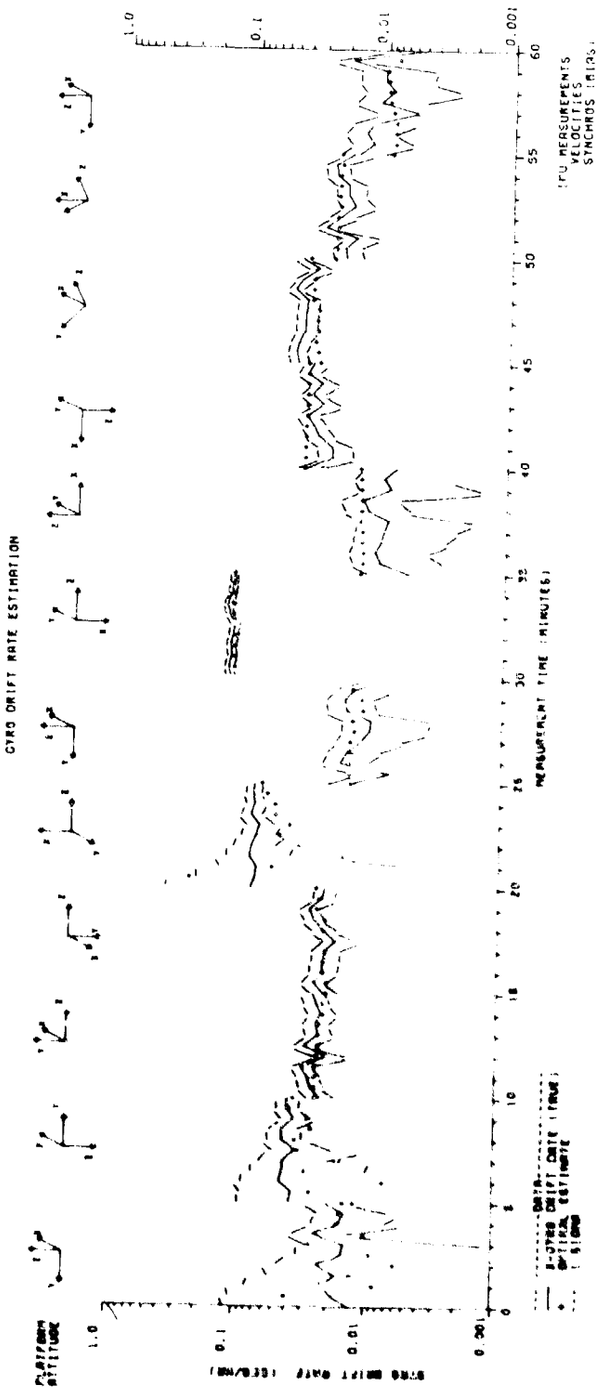

Figure 6-4. Gyro Drift Rate Estimation

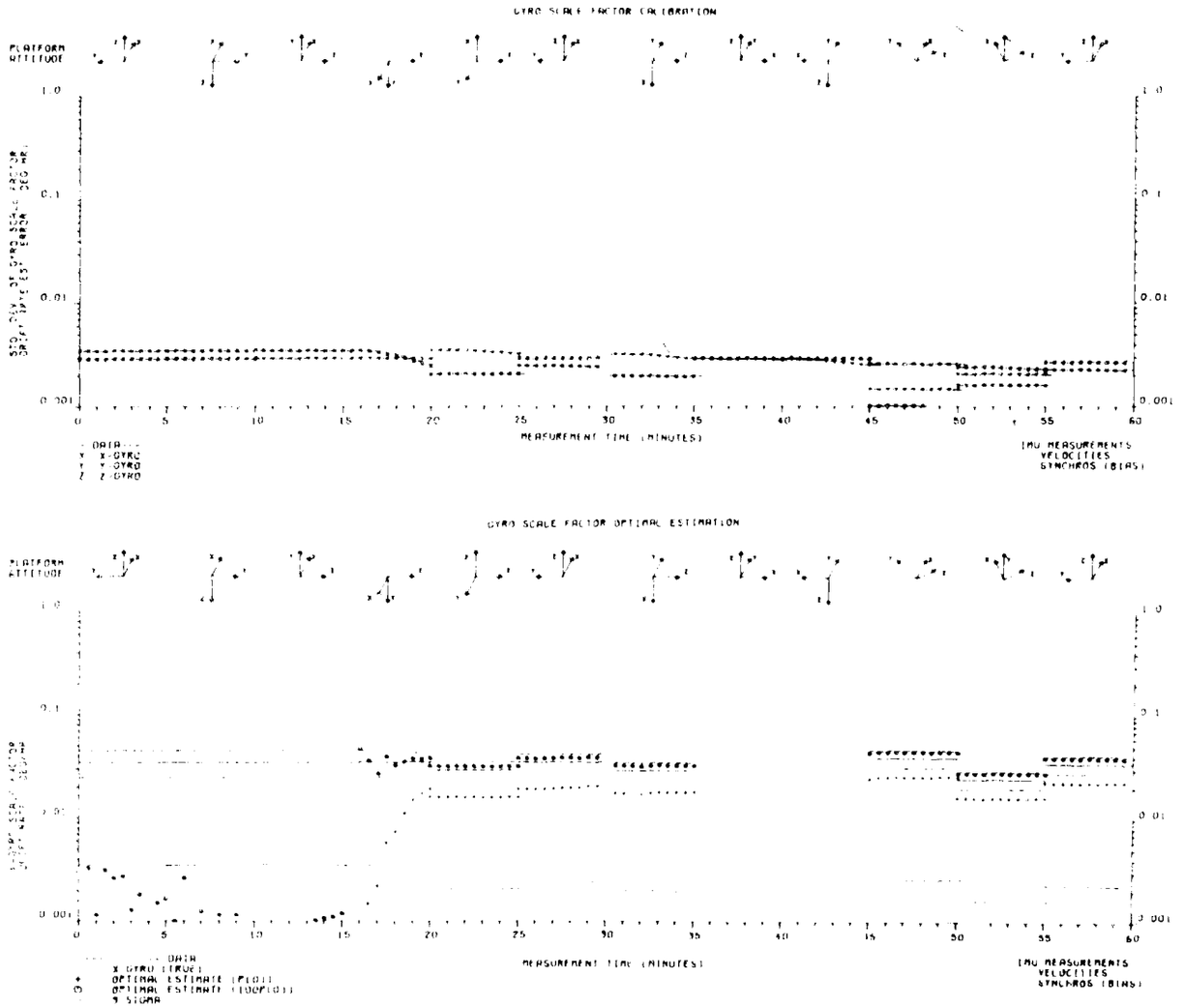

Figure 6-5. Gyro Scale Factor Estimation

gyro scale factor errors do not contribute significant platform drift rate components. Since these error sources do not contribute significant platform drift rate components relative to the gyro disturbances, the filter is precluded from reducing the uncertainty associated with them. Gyro scale factor errors are shown in terms of the platform drift rate error components they produce to emphasize the calibration accuracy limitations imposed by the gyro random noise errors. The lower graph shows the filter's performance against a simulated IMU containing a x-gyro scale factor error an order-of-magnitude larger than assumed in the initial covariance matrix.

The optimal estimates for two simulation runs are plotted in the lower graph. The plus symbols correspond to the first run and an initial covariance matrix based on the nominal a priori error model data. The nominal x-gyro scale factor error assumed for the initial covariance matrix is a factor of ten less than that simulated in the IMU. The filter begins to estimate an abnormally large error, optimal estimates compared with the estimation error standard deviation, during the fourth platform attitude test. It is interesting to note that the Kalman Filter begins to estimate the abnormally large scale factor error during the same platform test attitude that the error source separation data of Table 4-1 predicts. The filter's optimal estimates do not, however, strictly converge to the simulated error in accordance with the three sigma bounds. This failure of the filter's optimal estimates to converge to the simulated error is due to the non-conformance of the initial covariance matrix with the simulated error.

A major consideration at the end of the first simulation run is the behavior of the Kalman Filter's estimates for all the other IMU calibration parameters. If the filter estimates abnormally large errors for some of the other calibration parameters, this might preclude isolation of the problem to its true source. Examination of filter's estimates for all other error sources indicates, however, that these estimates converge to the simulated errors to within the accuracy predicted by the filter's convariance matrix.

The second simulation run was made to verify that filter convergence could be obtained by increasing the initial covariance matrix in accordance with the x-gyro scale factor optimal estimates obtained from the first run. Specifically, the initial x-gyro scale factor variance was increased from that corresponding to a platform drift rate component of 0.0035 to 0.024 degrees per hour as indicated by the filter's final first run estimate. The small circle symbols represent the second run optimal estimates and show a convergence which is consistent with the estimation uncertainty obtained from the first run. This result indicates that calibration accuracy is essentially determined by the inertial instrument random disturbances and is relatively insensitive to the initial covariance matrix.

SECTION VII

IMU LABORATORY TEST REQUIREMENTS

7.1 SOFTWARE ALTERNATIVES

Digital computer computational, storage, and associated programming requirements for implementing the IMU calibration tests and estimating the error sources can vary greatly in accordance with the specific application and software approach. All software approaches must, however, satisfy three functional requirements.

(1) The platform must be commanded to precess at earth rate during each IMU test sequence.

(2) System level IMU pseudo velocity and gimbal angle measurements must be taken and recorded.

(3) IMU error source estimates must be computed.

The first two requirements involve on-line in real-time software and can be met in a similar manner for various approaches with software complexity being a function of the desired automation. The manner of accomplishing the third function can be either on-line in real-time or off-line after-the-fact and greatly distinguishes the software approaches.

7.1.1 Kalman Filter Software Approach

Two approaches to the Kalman Filter error source estimation software were considered for implementation of the laboratory IMU tests. The first approach consisted of an off-line parameter estimation scheme in which the error source estimates were computed after the IMU test was completed. The Kalman Filter mechanization and IMU test procedure formulated purposely omitted real-time closed-loop platform control in favor of the off-line software flexibility. In this approach, the IMU test would be conducted with use of a small general purpose digital computer(s) with the IMU measurements being recorded on a magnetic tape.

The recorded IMU measurements would serve as input data to the Kalman Filter software program hosted on a large scientific digital computer. This approach permits use of the Kalman Filter software program developed for the CDC-6600 computer simulation studies.

The second Kalman Filter software approach considered utilized a small general purpose digital computer and stored Kalman gain matrices to estimate the error sources on-line in real-time. This technique is possible because the filter's covariance matrix can be propagated and updated independently of the IMU measurements. This allows prior computation of the covariance and related Kalman gain matrices on a large digital computer. The precomputed Kalman gain matrices, corresponding to specified IMU measurement times, would be stored on a magnetic tape and read by the small test computer as required during the test. Estimation of the error sources is well within a small digital computer's capabilities and is accomplished by multiplying the measurement vector by the Kalman gain matrix after each IMU measurement and propagating the optimal estimates between measurements. The software program could be written in assembly or a higher order language depending on the support software available for the small digital computer.

The first approach of off-line error sources estimation was selected for the initial IMU calibration tests for several reasons. Real-time software development was required only for recording data and not additionally for error source estimation as in the second approach. The ease of modifying the CDC-6600 Fortran IV Kalman Filter computer program and the ability to exercise the modified versions against the mag tape stored IMU measurement data without continuously repeating the IMU tests was expected to greatly facilitate the development effort. This consideration was especially important in view of the IMU error model development and validation objective of the study.

The major disadvantage of the selected approach is the turn-around time associated with the CDC-6600 computer system. It was thought that if aided-inertial navigation software development efforts demonstrated

a need for having IMU calibration test results prior to conducting the software development tests, the real-time error estimation scheme could be implemented for the production calibration tests. This need has not, however, materialized.

7.1.2 Real Time Test Software Approach

To keep the real-time software development effort to a minimum, maximum utilization was made of the Singer-Kearfott AN/ASN-90 Inertial Measurement Set and associated equipment, including the SKC-2000 digital computer and the operational computer program (OCP) documented in Reference 4. A functional block diagram of the hardware used in conducting the IMU calibration tests is given in Figure 7-1. The Singer equipment constitutes a self-contained inertial navigation capability including IMU ground alignment and a two-position north and west gyro auto-calibration.

The philosophy for obtaining the necessary real-time test software was to utilize applicable portions of the Singer OCP with minor software modifications being made as required. References to Singer's OCP development specification indicated that this approach was feasible and would entail a modification of the ground align and gyro auto-calibration software routines.

Two versions of the OCP real-time test software were developed. The first version retained the 15 sequence ground align and gyro auto-cal software routines so that: (1) The IMU case could be properly aligned to the navigation frame, and (2) The gyro turn-on biases recovered by the OCP could be compared to those estimated by the Kalman Filter. Compatibility between the OCP and Kalman Filter gyro turn-on bias estimates was ensured by conducting the 12 IMU calibration platform attitude test sequences immediately after the 15 OCP ground align and gyro auto-cal test sequences. Comparison of the OCP-recovered gyro biases, as well as the high and low gain accelerometer bias and scale factor and gyro scale factor ASM-375-test-set calibrated errors, with those recovered by the Kalman Filter, was considered essential in the development of the calibration technique.

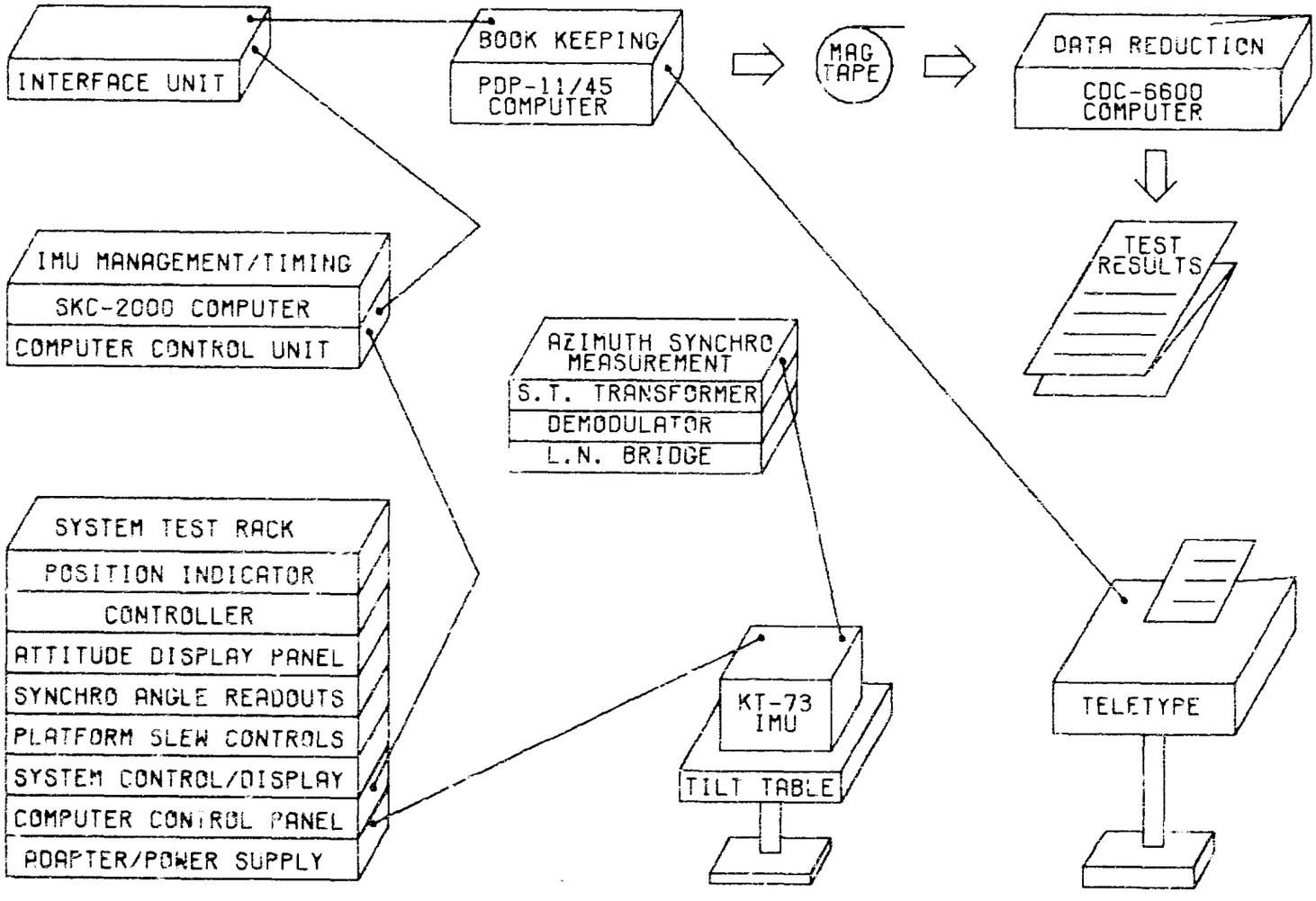

Figure 7-1. IMU Calibration Test Equipment Configuration

After the development of the calibration technique was well underway, the second version of the real-time test software was developed to eliminate a scheduling problem inherent in the above versions. The 15-sequence ground align and gyro auto-cal routines required 24 minutes to execute and thus prohibited obtaining the IMU measurements necessary to estimate the inertial instrument warm-up transients corresponding to the A-7D aircraft fine ground alignment time interval of 7 to 10 minutes after power turn-on. The second version was similar to the first, except that the 15-sequence ground align and gyro auto-cal routines were omitted. Proper IMU case alignment to the navigation frame was obtained by use of the original OCP if realignment was made necessary due to dismounting and remounting the IMU on the tilt table, as discussed in Section 7.2.1.

Initiating and terminating the different IMU platform test sequences and recording the IMU measurements on a magnetic tape could not readily be accomplished with the Singer AN/ASN-90 and associated equipment. Referring to Figure 7-1, the teletype and PDP-11/45 computers were added for these purposes. The PDP-11/45 computer and its peripheral equipment is used largely for bookkeeping purposes. Nominal earth rate torquing values are stored and sent to the SKC-2000 computer at the start of each new platform test sequence. IMU measurements are transferred from the SKC-2000 computer and recorded on magnetic tape. Although the initiation of new platform test sequences is controlled from the teletype, the exact instants of time the IMU measurements are taken is determined by the SKC-2000 computer's internal clock and associated real-time software.

Input/output data precision and IMU measurement timing accuracy requirements were determined such that errors in these quantities do not contribute any significant IMU calibration errors. This criterion implies that the errors are on the same order as the accelerometer and gyro random disturbances. For gyro torquing, the net gyro torquing PRF required to command the platform at earth rate must be entered into the SKC-2000 computer with an accuracy of 50 ppm. The magnitude of the time

interval between IMU pseudo velocity measurements is not critical; nominally, both 10 and 30 seconds are used. This time interval must be constant to simplify execution of the Kalman Filter algorithm and precisely known to 0.1 msec. The total number of pseudo velocity pulses generated each measurement time interval are recorded with the least significant bit representing 0.0322 and 0.000322 ft/sec for the low and high gain accelerometer scale factor modes, respectively. Gimbal angle measurements are discussed in Section 7.2.2, but are not automatically recorded via the real-time software.

7.1.3 Recorded Pseudo Velocity Pulses

The finalized IMU platform test attitudes used in conjunction with the second version of the OCP real-time software are shown in Figure 7-2. A sample of the total IMU pseudo velocity pulses recorded by the real-time software during a calibration test is illustrated in Figure 7-3. In this figure, the left hand column represents time in seconds and from left to right the three columns per test attitude represent the total number of accelerometer pulses generated per measurement time interval.

Data recording for IMU platform test attitude No. 1 begins seven minutes after power turn-on and continues for ten minutes, with velocity pulses being recorded every 10 seconds. The x and y level axis accelerometers are employed in the high gain mode (the z accelerometer does not have a high gain mode), in an attempt to accurately estimate the gyro and accelerometer warm-up transients.

Data recording periods are nominally five minutes long for platform test attitudes No. 2 through 12, with measurements being recorded every 30 seconds. The low gain navigation accelerometer scale factor mode is used for the first five minutes of testing for each of these test sequences. Accelerometer scale factors are switched from the low to the high gain mode at the end of the five minutes for test sequences No. 3 and 10, with testing being continued for an additional one and a half minutes. This approach permits the Kalman Filter to accurately observe the high gain accelerometer scale factor and bias errors without adding two

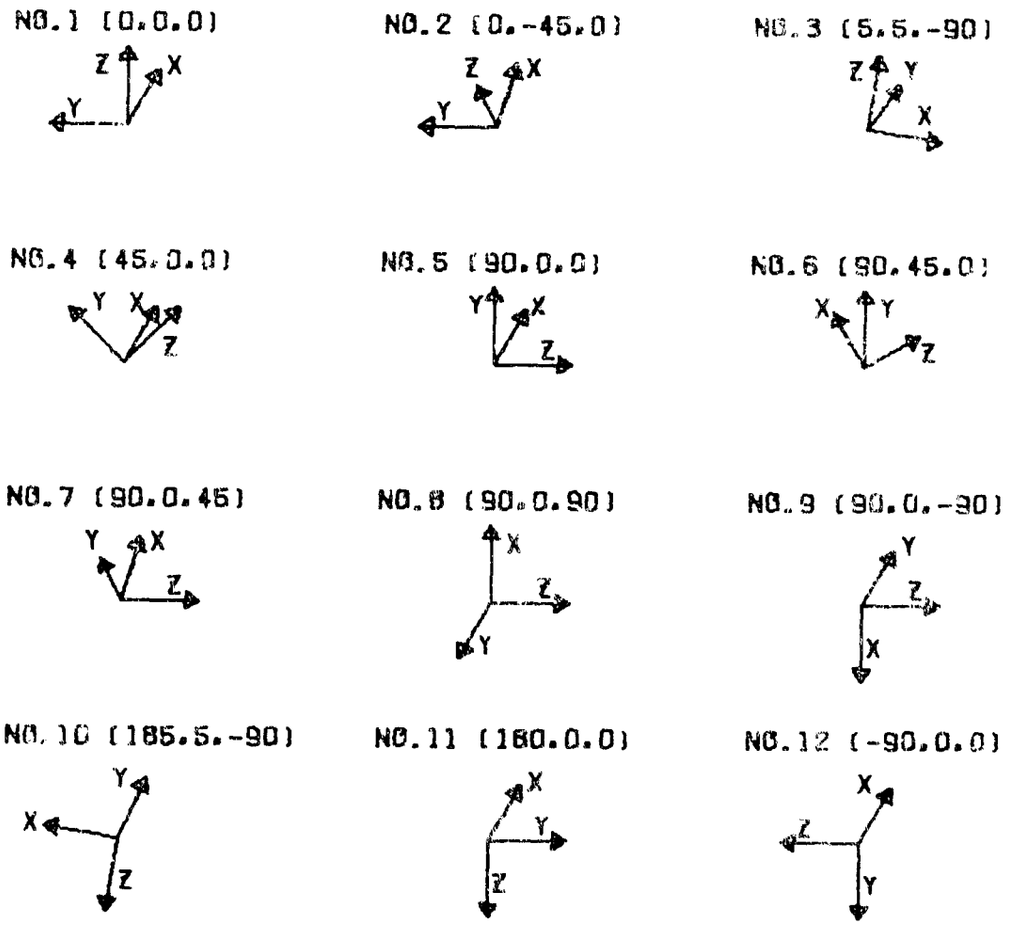

Figure 7-2. IMU Platform Test Attitudes and Corresponding Gimbal Angle Rotations

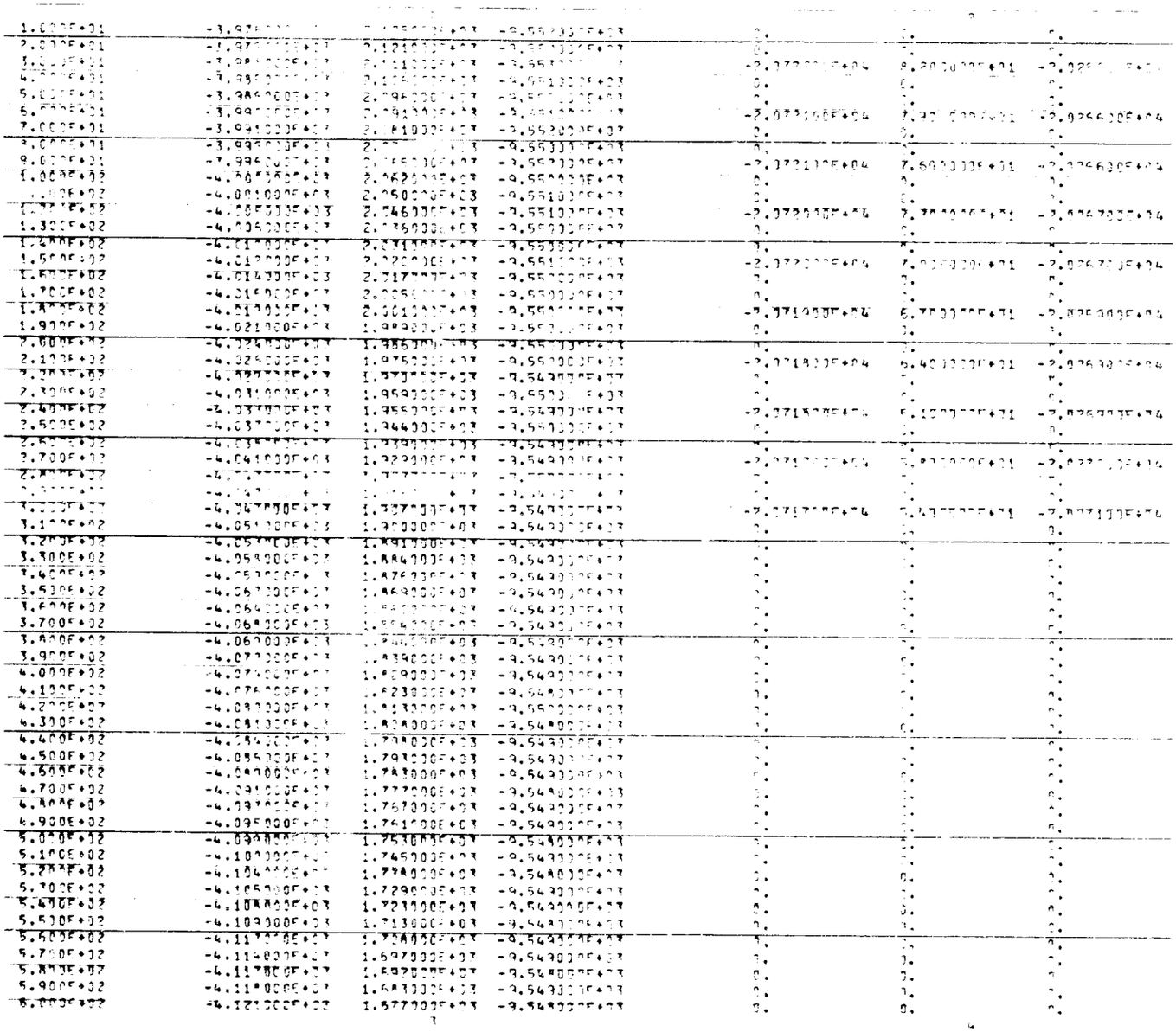

Figure 7-3. Recorded IMU Pseudo Velocity Pulses

	3			4		
3.000E+01	2.417[illegible]	2.626000E+03	-2.843900E+04	-1.333000E+02	-2.078800E+04	-2.026700E+04
6.000E+01	2.417[illegible]	2.622[illegible]	-2.843[illegible]E+04	-1.340[illegible]	-2.078800E+04	-2.026700E+04
9.0[illegible]	[illegible]	[illegible]	[illegible]	[illegible]	[illegible]	[illegible]
[illegible]	[illegible]	[illegible]	[illegible]	[illegible]	-2.0759[illegible]	[illegible]E+04
[illegible]	2.417[illegible]	2.621[illegible]	-2.843[illegible]	-1.283000E+02	-2.078700E+04	-2.026900E+04
1.800E+02	2.4[illegible]E+03	2.622000E+03	-2.843000E+04	-1.271000E+02	-2.078300E+04	-2.025900E+04
2.100E+02	[illegible]	2.621000E+03	-2.843[illegible]E+04	-1.245000E+02	-2.077[illegible]E+04	-2.026900E+04
2.400E+02	2.41[illegible]	2.622000E+03	-2.844[illegible]E+04	-1.220000E+02	-2.078700E+04	-2.026900E+04
2.700E+02	[illegible]	2.622000E+03	-2.847[illegible]E+04	-1.2[illegible]E+02	-2.0775[illegible]E+04	-2.026900E+04
3.000E+02	2.4[illegible]E+03	2.6[illegible]E+03	-2.443[illegible]E+04	-1.190000E+02	-2.078700E+04	-2.027000E+04
3.300E+02	0.	0.	0.	0.	0.	0.
3.600E+02	2.411592E+05	2.624710E+05	-2.847100E+04	0.	0.	0.
3.900E+02	2.41[illegible]E+05	2.625[illegible]E+05	-2.843100E+04	0.	0.	0.
	5			6		
3.000E+01	-1.350000E+02	-2.944100E+04	-4.000000E+01	-1.220000E+02	-2.944100E+04	-5.400000E+01
6.000E+01	-1.330000E+02	-2.944100E+04	-4.200000E+01	-1.190000E+02	-2.944200E+04	-5.500000E+01
9.000E+01	-1.300000E+02	-2.944100E+04	-4.300000E+01	-1.170000E+02	-2.944100E+04	-5.600000E+01
1.200E+02	-1.280000E+02	-2.944100E+04	-4.400000E+01	-1.150000E+02	-2.944200E+04	-5.800000E+01
1.500E+02	-1.260000E+02	-2.944200E+04	-4.500000E+01	-1.120000E+02	-2.944100E+04	-5.800000E+01
1.800E+02	-1.230000E+02	-2.944100E+04	-4.500000E+01	-1.110000E+02	-2.944200E+04	-6.000000E+01
2.100E+02	-1.210000E+02	-2.944100E+04	-4.600000E+01	-1.080000E+02	-2.944100E+04	-6.100000E+01
2.400E+02	-1.180000E+02	-2.944100E+04	-4.800000E+01	-1.060000E+02	-2.944200E+04	-6.100000E+01
2.700E+02	-1.150000E+02	-2.944100E+04	-4.700000E+01	-1.050000E+02	-2.944100E+04	-6.300000E+01
3.000E+02	-1.140000E+02	-2.944100E+04	-4.900000E+01	-1.020000E+02	-2.944200E+04	-6.400000E+01
3.300E+02	0.	0.	0.	0.	0.	0.
3.600E+02	0.	0.	0.	0.	0.	0.
3.900E+02	0.	0.	0.	0.	0.	0.
	7			8		
3.000E+01	-2.075500E+04	-2.076900E+04	-4.300000E+01	-2.327100E+04	4.800000E+01	-5.700000E+01
6.000E+01	-2.075200E+04	-2.077700E+04	-4.800000E+01	-2.327100E+04	4.700000E+01	-5.800000E+01
9.000E+01	-2.07[illegible]E+04	-2.077700E+04	-5.000000E+01	-2.327200E+04	4.400000E+01	-5.900000E+01
1.200E+02	-2.075000E+04	-2.077500E+04	-5.000000E+01	-2.327100E+04	4.200000E+01	-6.100000E+01
1.500E+02	-2.075[illegible]E+04	-2.077600E+04	-5.200000E+01	-2.327100E+04	4.000000E+01	-6.300000E+01
1.800E+02	-2.075[illegible]E+04	-2.077700E+04	-5.200000E+01	-2.327100E+04	3.800000E+01	-6.400000E+01
2.100E+02	-2.074500E+04	-2.077900E+04	-5.300000E+01	-2.327000E+04	3.500000E+01	-6.500000E+01
2.400E+02	-2.074700E+04	-2.078000E+04	-5.400000E+01	-2.327100E+04	3.400000E+01	-6.700000E+01
2.700E+02	-2.074100E+04	-2.078300E+04	-5.400000E+01	-2.327100E+04	3.100000E+01	-6.800000E+01
3.000E+02	-2.074[illegible]E+04	-2.078400E+04	-5.500000E+01	-2.327100E+04	3.030000E+01	-7.000000E+01
3.300E+02	0.	0.	0.	0.	0.	0.
3.600E+02	0.	0.	0.	0.	0.	0.
3.900E+02	0.	0.	0.	0.	0.	0.
	[illegible]			10		
3.000E+01	2.90[illegible]E+04	8.[illegible]E+01	-4.700000E+01	-2.5[illegible]E+03	-2.488000E+03	2.842800E+04
6.000E+01	2.906700E+04	8.600000E+01	-5.000000E+01	-2.58[illegible]E+03	-2.488000E+03	2.842800E+04
9.000E+01	2.905400E+04	8.800000E+01	-5.300000E+01	-2.588000E+03	-2.488000E+03	2.842800E+04
1.200E+02	2.905800E+04	9.000000E+01	-5.500000E+01	-2.58[illegible]E+03	-2.488000E+03	2.842800E+04
1.500E+02	2.905[illegible]E+04	9.[illegible]E+01	-5.600000E+01	-2.58[illegible]E+03	-2.489000E+03	2.842800E+04
1.800E+02	2.905400E+04	9.600000E+01	-5.800000E+01	-2.586000E+03	-2.489000E+03	2.842800E+04
2.100E+02	2.905[illegible]E+04	9.800000E+01	-6.000000E+01	-2.585000E+03	-2.489000E+03	2.842900E+04
2.400E+02	2.905400E+04	1.010000E+02	-6.200000E+01	-2.585000E+03	-2.490000E+03	2.842900E+04
2.700E+02	2.905300E+04	1.030000E+02	-6.500000E+01	-2.584000E+03	-2.490000E+03	2.842900E+04
3.000E+02	2.905400E+04	1.060000E+02	-6.700000E+01	-2.584000E+03	-2.490000E+03	2.842800E+04
3.300E+02	0.	0.	0.	0.	0.	0.
3.600E+02	0.	0.	0.	-2.587480E+05	-2.484860E+05	2.842950E+04
3.900E+02	0.	0.	0.	-2.586800E+05	-2.485010E+05	2.842800E+04
	11			12		
3.000E+01	-1.3[illegible]E+02	3.4[illegible]E+01	2.863[illegible]E+04	-9.400000E+01	2.958500E+04	1.500000E+01
6.000E+01	-1.31[illegible]E+02	3.300000E+01	2.863400E+04	-9.600000E+01	2.958500E+04	1.200000E+01
9.000E+01	-1.30[illegible]E+02	3.[illegible]E+01	2.863500E+04	-9.800000E+01	2.958500E+04	1.100000E+01
1.200E+02	-1.31[illegible]E+02	4.[illegible]E+01	2.863[illegible]E+04	-1.0[illegible]E+02	2.958600E+04	9.000000E+00
1.500E+02	-1.3[illegible]E+02	4.[illegible]E+01	2.863500E+04	-1.0[illegible]E+02	2.958500E+04	6.000000E+00
1.800E+02	-1.3[illegible]E+02	4.[illegible]E+01	2.863[illegible]E+04	-1.0[illegible]E+02	2.958600E+04	3.000000E+00
2.100E+02	-1.3[illegible]E+02	4.[illegible]E+01	2.863500E+04	-1.0[illegible]E+02	2.958500E+04	2.000000E+00
2.400E+02	-1.3[illegible]E+02	4.4[illegible]E+01	2.863[illegible]E+04	-1.0[illegible]E+02	2.958500E+04	0.
2.700E+02	-1.3[illegible]E+02	4.[illegible]E+01	2.863500E+04	-1.0[illegible]E+02	2.958600E+04	-3.000000E+00
3.000E+02	-1.3[illegible]E+02	4.[illegible]E+01	2.863[illegible]E+04	-1.0[illegible]E+02	2.958500E+04	-5.000000E+00
3.300E+02	0.	0.	0.	0.	0.	0.
3.600E+02	0.	0.	0.	0.	0.	0.
3.900E+02	0.	0.	0.	0.	0.	0.

Figure [illegible]. Recorded [illegible] Pseudo [illegible] Unity Pulses (Concluded)

additional test sequences specifically for this purpose. Platform tilts are limited to approximately six degrees to prevent saturation of the capacitive reset integrators (10,000 pulses per second maximum) when in the high gain mode. As can be seen from Figure 7-3, IMU calibration does not require an abnormally large quantity of measurements to be taken.

7.1.4 Data Recording Problems

Two data recording problems were encountered during the IMU calibration testing. Eventually one problem was attributed to the IMU hardware and the other to the OCP r 1-time test software. both of these problems caused improper operation of the Kalman Filter and were only correctly isolated as data recording problems after scanning the raw data lists as depicted by Figure 7-3. The recorded velocity pulse raw data computer printouts proved to be extremely valuable during the development cycle, particularly when the data was massaged to show the number of accelerometer pulses generated in each measurement interval, as in Figure 7-3, rather than the cumulative time total which constitutes the Kalman Filter measurements.

The data recording anomaly attributed to the IMU hardware was termed an accelerometer dropout problem. Anomalous data was found to exist on 2 of the total 24 IMU calibration tests conducted and took the form of a zero accelerometer pulse count for one to two minutes of the total 68 minutes IMU measurement time. Only one dropout time interval was found to occur for each of the two calibration tests that the problem manifested itself. Although this anomalous behavior was never verified as being caused by the IMU hardware, discussions with personnel at the Aerospace Guidance and Metrology Center (AGMC) indicated they had observed similar problems with the KT-73 IMUs. AGMC personnel thought the problem was due to burnt or corroded slip rings. Valid Kalman Filter estimates for the IMU calibration parameters could still be obtained by smoothing over the zero pulse count anomalous recordings with interpolated data.

The second data recording problem was traced to a timing instability in the real-time OCP software. Instead of timing the pulses generating pseudo velocity pulses to the required accuracy of 0.1 msec, errors as large as 15 msec were found to exist. The effect of these timing errors on IMU calibration accuracy is discussed in Section M.

The timing instability problem was also isolated by scanning the raw velocity pulse data as depicted in Figure 7-3. For the accelerometer random noise magnitude given by the IMU error model of Reference 1 and a timing accuracy of 0.1 msec, the difference in the number of velocity pulses generated over a measurement interval should never exceed one when an accelerometer is oriented parallel to the gravity vector. The difference in velocity pulse counts was found to be as high as 15 pulses for adjacent measurement intervals. For a low gain accelerometer scale factor of 1,000 pulses per second per g, 15 pulses implies a 15 msec measurement timing error. Longer term timing variations of greater than 15 msec were also found to exist over the entire 5-minute test interval.

The cause of the timing errors was traced to the "interrupt" priorities of, and the failure to remove all unnecessary software routines from, the OCP real-time software program. The timing instability problem was never completely solved but the instabilities were reduced to roughly one msec in magnitude. Since a timing error of this magnitude is not negligible relative to the inertial instrument random disturbances, modifications of the Kalman filter had to be made to account for its presence. The short term uncorrelated timing instability was accounted for by adding a disturbance to the affected or pseudo velocity error states. The longer term correlated timing instability was accounted for in a first order manner by adding an additional clock (pseudo accelerometer scale factor) error to the Kalman filter state vector. Error modeling of the clock error state is characterized by a standard deviation of one ppm and a correlation time of 250 seconds. The net result of these timing errors is a very slight decrease in the accuracy to which accelerometer errors can be calibrated. Gyro calibration accuracy is virtually unaffected.

7.2 TEST HARDWARE CONSIDERATIONS

In addition to the general hardware capabilities provided by the Singer AN/ASN-90 inertial measurement set and associated system test rack equipment, two additional hardware capabilities are required to conduct the IMU calibration tests. These hardware considerations involve accurately aligning the IMU case to the navigation frame and precisely measuring gimbal angle movements.

7.2.1 IMU Case Alignment

The methodology developed for IMU calibration assumes that the attitude of the platform relative to the navigation frame is accurately known. The IMU case frame was defined synonymous with the gimbal neutral frame defined by coincidence of the neutral IMU roll, pitch, and azimuth gimbal axes with the x (north), y (west), and z (up) navigation frame axes. Rotating the navigation frame through the [η] coordinate transformation produces the IMU case, and gimbal neutral frames and rotating the gimbal neutral frame through the gimbal angle [θ] coordinates transformation produces the platform frame.

If given that the IMU case is aligned to the navigation frame, the twelve relative platform-to-navigation frame angular orientations required for separation of the IMU error sources shown in Figure 7-2 can be obtained by gimbal angle rotations, thus obviating any need to rotate the IMU case. There are, however, several advantages to mounting the IMU on a rotating tilting precision table. (1) It assists in aligning the case to the navigation frame. (2) It allows for an independent calibration of the gimbal synchro angle measuring devices for comparison with the Kalman Filter estimates. And (3) additional special testing including heading sensitivity can readily be conducted. For these reasons, an IMTCO rotary tilting table was used throughout all IMU calibration testing.

Aligning the IMU case to the navigation frame is a straightforward procedure. The IMU case is mounted on the tilt table with use of the Singer mounting bracket. The necessary three angular degrees of freedom are provided by this arrangement, about the gimbal neutral IMU pitch and azimuth axes by the tilt table and about the gimbal neutral roll axis by the mounting bracket. The IMU is brought up and Singer's OCP software routines are executed through ground alignment. This aligns the x, y, and z platform frame with the north, west, and up navigation frame. The gimbal neutral and hence IMU case frame is then aligned to the navigation frame by nulling the synchro angle readouts using tilt table and mounting bracket angular rotations. The IMU case alignment accuracy is essentially the accuracy of the synchro measuring devices or 6 arc minutes. Assuming that tilt table and mounting brackets are unperturbed or can be accurately returned to their original position, the IMU can be installed for additional testing without repeating the alignment process.

7.2.2 Gimbal Angle Measurements

As discussed in Section 4.2.1, a gimbal angle measurement or its equivalent is required for separation of the gyro spin axes mass unbalance error sources. Although the gimbal synchro angle measuring devices are capable of measuring small differential gimbal angular positions to 5 arc seconds, no hardware capability existed in the Singer AN/ASN-90 IMS or system test rack equipment to obtain measurements to this precision. Initially, low precision manual gimbal angle measurements were taken with the visual readout indicators in the Singer test rack equipment to support the IMU calibration development. Two high precision synchro measurement technique developments were undertaken that would have afforded the capability of automatic data recording. These developments were never completed. A high precision, manual synchro measurement technique was eventually perfected for use in the final calibration tests. These topics are discussed in the sequel.

The Singer system test rack equipment contains roll, pitch, and azimuth gimbal synchro angle readouts having 1 arc minute graduations. These meters can be read to roughly 0.2 arc minute precision. Repeated IMU testing showed that the azimuth gimbal angle drifted about 0.3 arc minutes in ten minutes when torqued at earth rate in test attitude No. 1. This data implies a vertical or z-axis platform drift rate angular velocity of 0.03 degrees per hour.

Knowledge of the actual z-axis platform drift rate error is sufficient additional information to enable the Kalman Filter to separate the gyro mass unbalance error sources. To utilize this data in the Kalman Filter, it must be recognized that z-gyro bias and spin axis mass unbalance error sources completely dominate z-axis platform drift rate error when the axis is oriented vertically. This fact implies that these two error sources are statistically correlated such that the sum of the platform drift rates they produce has an initial uncertainty equal to that determined by the above measurements. This information is utilized by the Kalman Filter in the form of an initial covariance between the error sources having a magnitude given by:

$$P\left(W_{Bz}, M_{Sz}\right) = \left[P\left(W_{Bz}, W_{Bz}\right) + g^2 P\left(M_{Sz}, M_{Sz}\right) - (0.03)^2\right]/2g$$

$$P\left(M_{Sz}, W_{Bz}\right) = P\left(W_{Bz}, M_{Sz}\right)$$

Entering these off-diagonal covariances into the Kalman Filter's initial covariance matrix permits the filter to estimate each of the three gyro spin axes mass unbalance errors to an accuracy determined by the z-axis platform drift rate magnitude or roughly 0.03 degrees per hour per g. This technique of separating the gyro spin axes mass unbalance errors worked quite well resulting in a reduction of 30 of the initial uncertainty of 1.0 degrees per hour per g. Since this technique does, however, have the disadvantages of the estimation accuracy being limited by z-axis platform drift rate and the measurements not being automatically recorded via the real-time software, additional gimbal angle measurement techniques were investigated.

The first attempt at achieving high precision automatic gimbal angle measurements involved a modification of the Singer-Kearfott synchro-to-digital converter obtained from the TRW INI program. This converter contained three synchro channels with a 12 bit plus sign conversion capability resulting in a measurement precision of 50 arc seconds. The philosophy for upgrading this converter to a measurement precision of approximately one arc second was to increase the precision of the device at the expense of dynamic range. This was achieved by inserting a variable voltage source in series with the synchro demodulator's output to define a nominal operating point of zero volts. Amplification of this voltage by a factor of 50 immediately prior to analog-to-digital conversion increased the precision to the desired one arc second. The dynamic range of the gimbal angle measurements about the nominal operating point was, however, reduced from 180 degrees to 69 arc minutes. This dynamic range is about an order of magnitude larger than required for the calibration tests.

The Singer synchro-to-digital converter was modified to include the required electronic circuitry. Laboratory tests were conducted with a synchro standard which verified the one arc second measurement precision. Integration testing with the IMU was being conducted to determine the magnitude of potential noise problems when the converter failed. The Singer converter was a specialty item employing non-standard parts which required redesigning a failed printed circuit board and fabricating a new one to keep the device in service. After a second failure, a management decision was made that the converter could not be practically maintained and the measurement scheme abandoned.

The second attempt at achieving high precision automatic gimbal angle measurements involved the use of a production Burr-Brown analog-to-frequency electronic converter. The operation of this circuitry is analogous to those used to quantize analog accelerometer outputs into velocity pulses. A second synchro was used in conjunction with the IMU's synchro to complete the control transmitter and transformer pair.

Unfortunately, this measurement scheme was also abandoned when it became obvious that the I/O interface electronics and real-time data collection software could not be completed in accordance with the management schedule for completing the IMU calibration development effort.

The final attempt at obtaining high precision gimbal angle measurements was successful and is depicted in Figure 7-1. The measurements were manually recorded with synchronization between the measurements and the velocity pulses being accomplished with a buzzer tied into the teletype. The measurement scheme consisted of a serial arrangement of the IMU synchro control transmitter, scott tee transformer, electronic demodulator, and a Leeds and Northrop bridge.

A parametric covariance analysis study conducted with use of the IMU calibration Kalman Filter showed that only the azimuth gimbal angle measurement was required during the first platform test attitude for accurate estimation of the gyro spin axes mass unbalance error coefficients. Employment of the roll and pitch and even the azimuth gimbal angle measurements during platform test attitudes 2 through 12 did not significantly increase the filter's estimation accuracy. Actual gimbal angle measurements taken during the IMU calibration tests were consistent with these findings.

Calibration of the azimuth gimbal angle measurement equipment's scale factor and verification of its high resolution capability was accomplished with the IMU calibration Kalman Filter. Referring to Figure 7-2, the platform orientation in test attitudes No. 5 and No. 12 is such that the Kalman Filter is capable of accurately estimating the differential azimuth gimbal angle about the same operating point as test attitude No. 1 (zero degrees) by virture of the measurements obtained from the level accelerometers. By normalizing the manually recorded Leeds and Northrup data to the corresponding Kalman Filter estimates for the differential azimuth gimbal angles, a scale factor calibration is obtained from the same data used for calibrating the IMU.

Calibration data for the azimuth gimbal angle measurement technique's scale factor covering the last eight IMU calibration tests is shown in Figure 7-4. The tests were conducted by positioning the azimuth gimbal synchro readout indicator located in the system test rack slightly below the nominal setting used in test attitude No. 1 and then allowing the platform to drift through this nominal setting. This technique ensures that the scale factor derived from the No. 5 or No. 12 platform test attitude corresponds to the nominal operating point used in test attitude No. 1. Scale factor determination accuracy is a function of both the Kalman Filter differential azimuth gimbal angle estimation accuracy and the angular excursion of the azimuth gimbal during the test sequence. Nominal estimation accuracies of 1.4 arc seconds' one sigma and azimuth gimbal angle excursions of 3 arc minutes results in a scale factor calibration error of roughly one percent.

The calibration data of Figure 7-4 shows that the scale factor differs somewhat from day-to-day tests and also slightly during the nominal one hour time period between the No. 5 and No. 12 platform test attitude calibrations. The causes for these scale factor variations are not completely understood. Replacement of 400 Hz demodulator line voltage reference by a precision Hewlett Packard oscillator, component electrostatic shielding and circuit filtering were found to be helpful in reducing the scale factor variations from those initially encountered. Scale factor variations for the No. 5 and No. 12 test attitudes are seen to vary only a few percent for the same IMU calibration test over the last six tests conducted. The average of the No. 5 and No. 12 test sequence scale factors is used in conjunction with the No. 1 test sequence azimuth gimbal angle measurement for the formal Kalman Filter measurement. Assuming that this average scale factor differs from the true one for test attitude No. 1 by this same small percentage, the scale-factor-induced measurement error is on the order of two arc seconds and well within the 5 arc second noise assumed for this measurement.

The precision of the azimuth gimbal angle measurement scheme around the zero degree operating point is shown in Figure 7-5. This data was

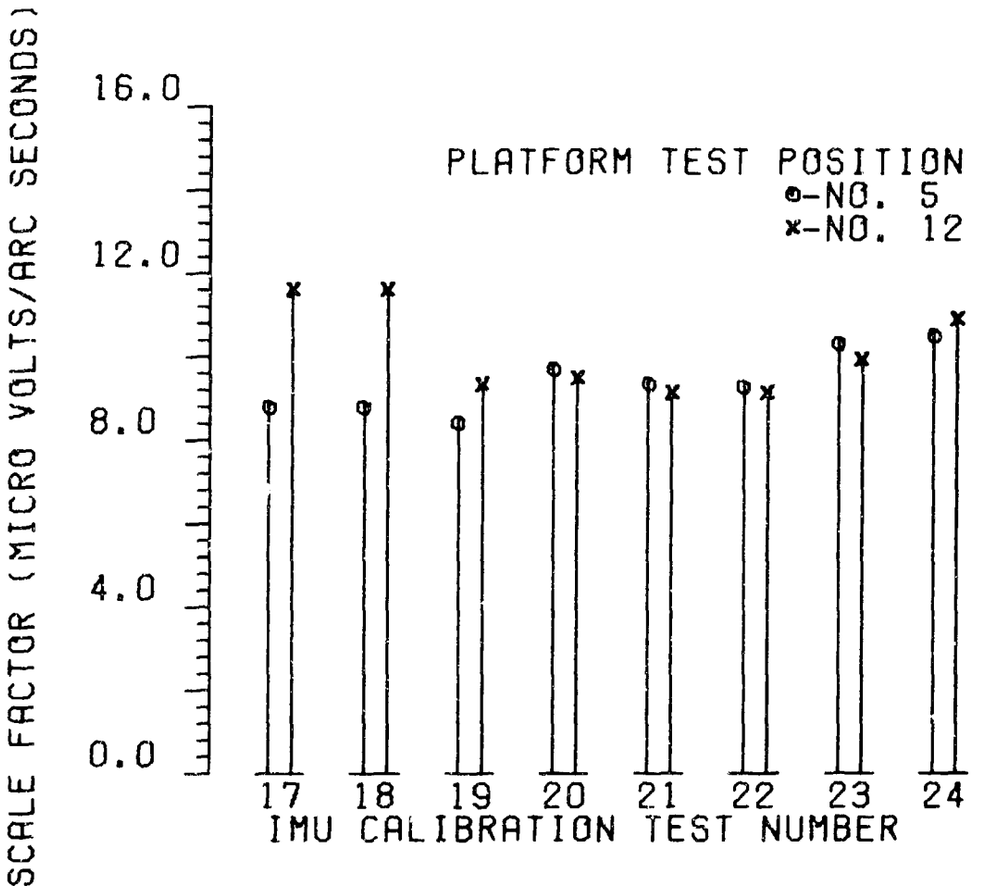

Figure 7-4. Azimuth Synchro Scale Factor Calibration Results

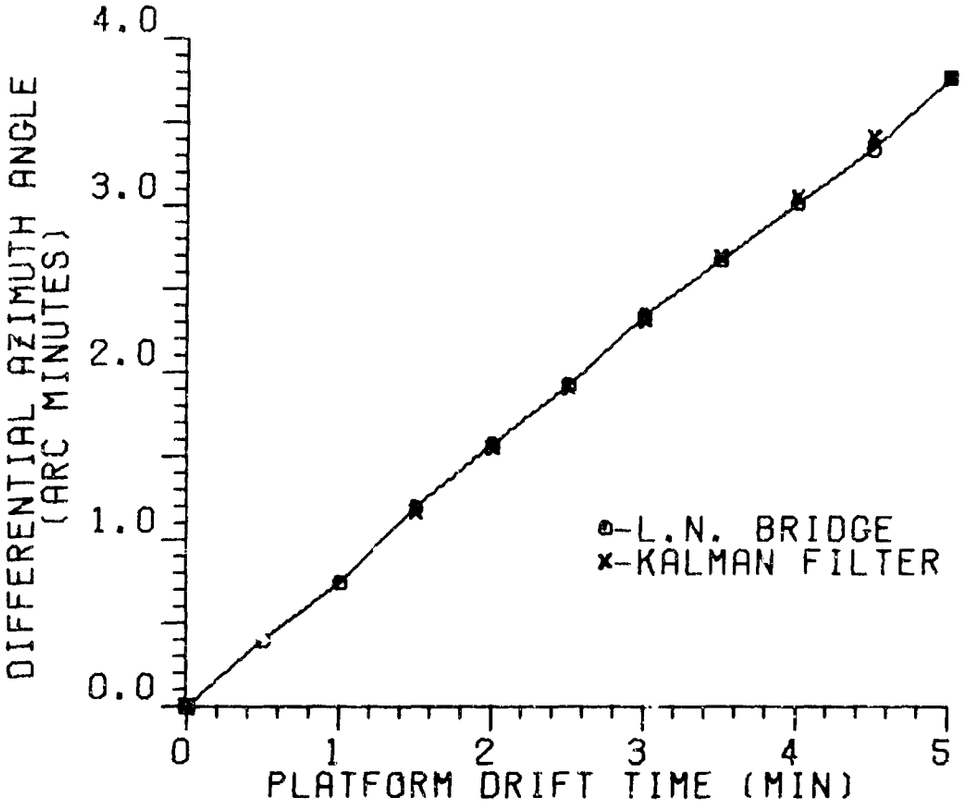

Figure 7-5. Azimuth Synchro Differential Precision About Zero Degrees

plotted by normalizing the Leeds and Northrup bridge data to the first and last Kalman Filter differential azimuth gimbal angle estimates. The Kalman Filter estimates at the interior data points serve as a reference with an accuracy of 1.4 arc seconds one sigma. This data shows that the precision of measurement technique is consistent with the assumed 5-arc-second-measurement noise.

SECTION VIII

IMU ERROR MODEL REFINEMENTS

As stated in Section 2.2, a major goal of this study is to devise and demonstrate an IMU calibration methodology that affords a significant capability for conducting IMU error model development and validation efforts. The approach taken to achieve this goal has been to formulate a methodology employing an optimal estimation technique that estimates all IMU error sources in a simultaneous rather than the sequential manner used in contemporary IMU calibration methods. It is anticipated that simultaneous estimation of all IMU errors sources will permit IMU error model inadequacies to be readily detected. Correlation analyses conducted in conjunction with IMU error model residual Kalman Filter states, added to the assumed IMU error model to account for potential error model omissions, should permit determining the functional dependency of detected unmodeled IMU errors. By adding the detected and modeled error source to the initial IMU error model and iterating the process, development of a complete and functionally correct error model appears feasible.

Kalman Filter processing of the system level IMU measurement data generated during the laboratory calibration tests resulted in the detection of both an unmodeled gyro quadrature gee and accelerometer attitude dependent scale factor error. Neither of these error sources had been included in the Reference 1 error model developed by the IMU manufacturer. The detection and modeling of these error sources was accomplished as indicated above and is the subject of this section.

8.1 INITIAL KALMAN FILTER ESTIMATION RESULTS

Examination of the initial Kalman Filter IMU error estimation results requires a judgment in regard to the adequacy of the IMU error model incorporated by the Kalman Filter. Two approaches were found useful in arriving at this judgment. The first approach involved processing the IMU measurements with the Kalman Filter, embodying only those IMU error

sources thought to exist The degree of inconsistency between the Kalman Filter estimates and known hardware manufacturing tolerances for the IMU error sources comprised the criterion for the judgment. The second approach involves iterative use of the assumed IMU error model residual states to determine the magnitude of the discrepancies. This approach is well suited to both detecting and isolating unmodeled errors and is the topic of Section 8.2.

Two examples of the inconsistencies obtained between the Kalman Filter estimates and the known manufacturing tolerances for the KT-73 IMU error sources are shown in Figure 8-1. The left and right-hand portions of this figure contrast the Kalman Filter estimates against the β_{yz} gyro frame misalignment angle and gyro long time constant correlated random drift rate manufacturing tolerances. Manufacturing tolerances are indicated by the dashed horizontal lines. In addition to those shown, many other similar inconsistencies were observed.

KT-73 IMU manufacturing methods are such that the alignment errors for the six gyro-to-platform misalignment angles are nominally held to one arc minute. Figure 8-1 illustrates, however, that as soon as the IMU has been tested with its platform oriented at enough different attitudes to permit the Kalman Filter to separate the misalignment angles from the other error sources, recovered estimates for these angular errors are a factor of twenty times the manufacturing tolerances. Similar results were obtained for the correlated gyro random drift rate error with recovered values exceeding production tolerances by an order of magnitude.

The conclusion to be drawn as a result of the Kalman Filter estimates for many of the IMU errors exceeding their manufacturing tolerances by an order of magnitude or more is that the IMU contains significant errors other than those modeled in the filter. This judgment was particularly easy to make since many different IMU errors exhibiting different functional dependencies were estimated as being abnormally large. As discussed in Section 6.5, had only one error source been recovered as abnormally large, there would be a strong likelihood that a hardware anomaly existed.

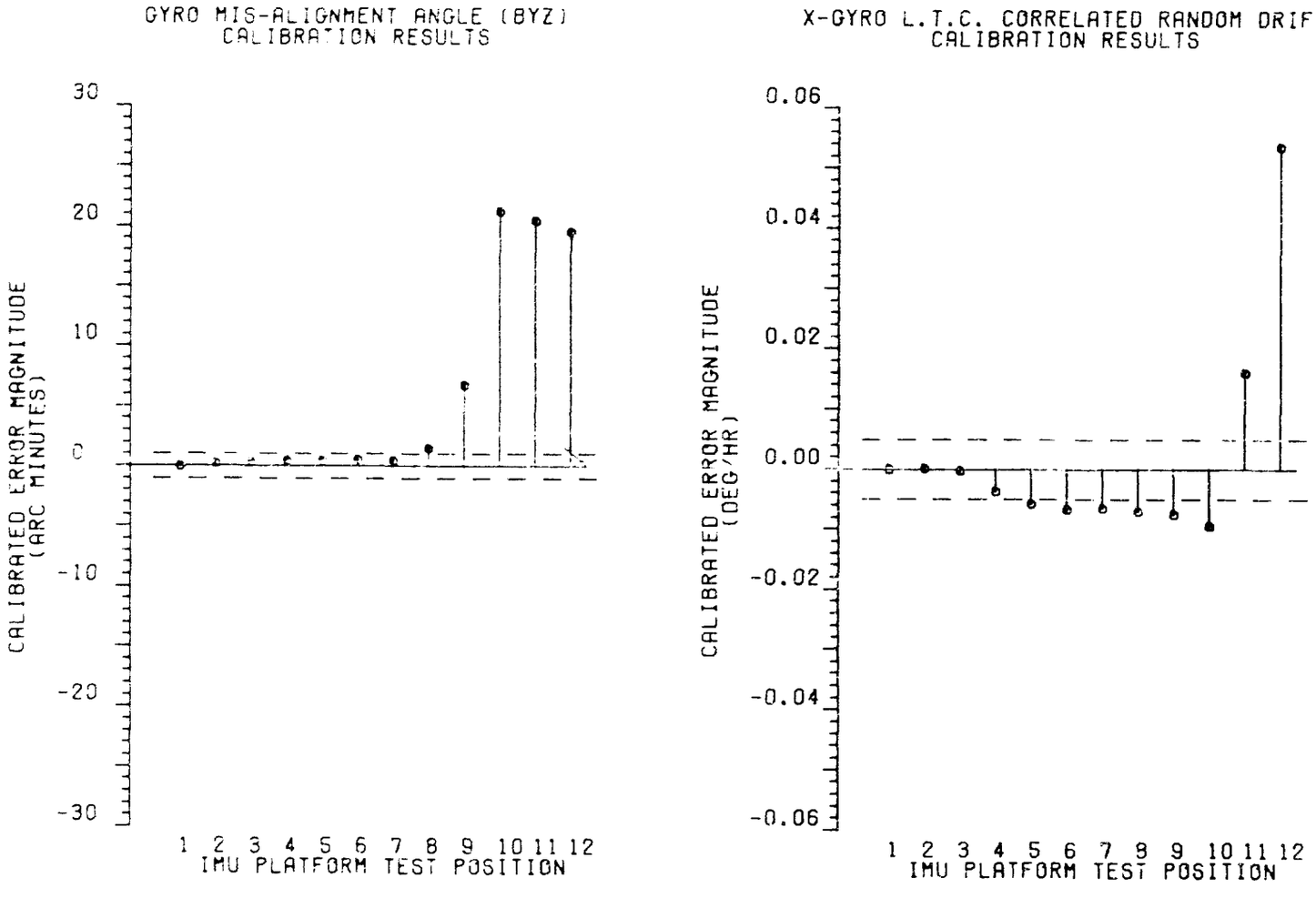

Figure 5-11. Kalman Filter Estimates Contrasted Against KT-73 IMU Manufacturing Tolerances

[illegible] GYRO MODELING REFINEMENTS

[illegible].1 Gyro Quadrature Error

Having made the judgment that a significant IMU error model discrepancy(s) existed, it becomes necessary to determine both the magnitude of the omitted error source and its functional dependency. Successfully accomplishing this task will, of course, confirm the initial IMU error model deficiency judgment. The manner of accomplishing this task is by the employment of IMU error model residual Kalman Filter states in conjunction with iterative processing of the same recorded IMU measurement data.

The initial objective of iterative Kalman Filter processing of the IMU measurement data is to obtain consistency between the initial uncertainties assumed for the filter's initial covariance matrix and the filter's estimates of the corresponding error source. Consistency implies that the Kalman Filter estimates for the random bias error states are within three standard deviations of the uncertainties assumed for the initial covariance matrix. Three standard deviations is a rule-of-thumb used in conjunction with the Gaussian distribution and includes roughly 99.5% of all experiment trials. Consistency is sought for filter estimates corresponding to each platform test attitude as well as final filter estimates corresponding to the final test sequence.

Obtaining consistency between the Kalman Filter's estimates and its initial covariance matrix is required for proper or accurate estimation by the Kalman Filter algorithm. Without consistency, the filter's estimation accuracy is not given by its covariance matrix and estimation errors are unknown. By adding the IMU error model residual states to the Kalman Filter state vector and determining, by iteration, their uncertainties for insertion in the initial covariance matrix, consistency can be obtained. Having obtained consistency, Kalman Filter error source estimation errors are now accurately known and given by the filter's covariance matrix. Consistency permits the Kalman Filter estimation results to be used with a high degree of confidence in conjunction with correlation studies to determine the magnitude and functional dependency of unmodeled IMU errors.

An illustration of obtaining Kalman Filter optimal estimate consistency through the use of error model residual states is shown in Figure 8-2. The left and right-hand portions of this figure contain similar data for the x and y-gyros, respectively. Three gyro error model residual states were included in the Kalman Filter state vector, a drift rate error for each gyro. These drift rate errors were modeled as random biases and were reset to their assumed initial uncertainty at the start of each platform test sequence. In effect, this resulted in a 3 errors per test sequence times 12 test sequences or 36 additional error sources for the Kalman Filter to estimate. These additional 36 error sources do not, of course, permit the Kalman Filter to separate and accurately estimate the other IMU error sources when the assumed initial uncertainties of the residual states are large compared with the other errors.

The error model residual states depicted in Figure 8-2 could also be termed as gyro-attitude-dependent bias errors, since they are modeled as being constant for a given platform attitude relative to the IMU case but assume a new value anytime the platform's orientation is changed. The Kalman Filter's estimates for these attitude-dependent biases is shown for each of the twelve platform test orientations. The upper and lower brackets about each estimate represent the standard deviation of the filter's estimation error as obtained from the covariance matrix at the end of each platform test sequence. Since filter consistency or proper convergence has been obtained, these estimation errors are accurate.

Filter consistency was obtained by iteratively increasing the initial uncertainty of the attitude-dependent bias error states in conjunction with reprocessing of the same recorded IMU measurement data until the filter's estimates for these errors were within three standard deviations of their initial uncertainty. Initial trial values were chosen to be the same as the correlated gyro random noise of 0.005 degree per hour with about two iterations being required to reach the consistency value of 0.2 degree per hour shown in Figure 8-2. New trial values were taken to be the maximum of the Kalman Filter's estimates for the attitude-dependent biases on the previous trial. Figure 8-2 shows that maximum

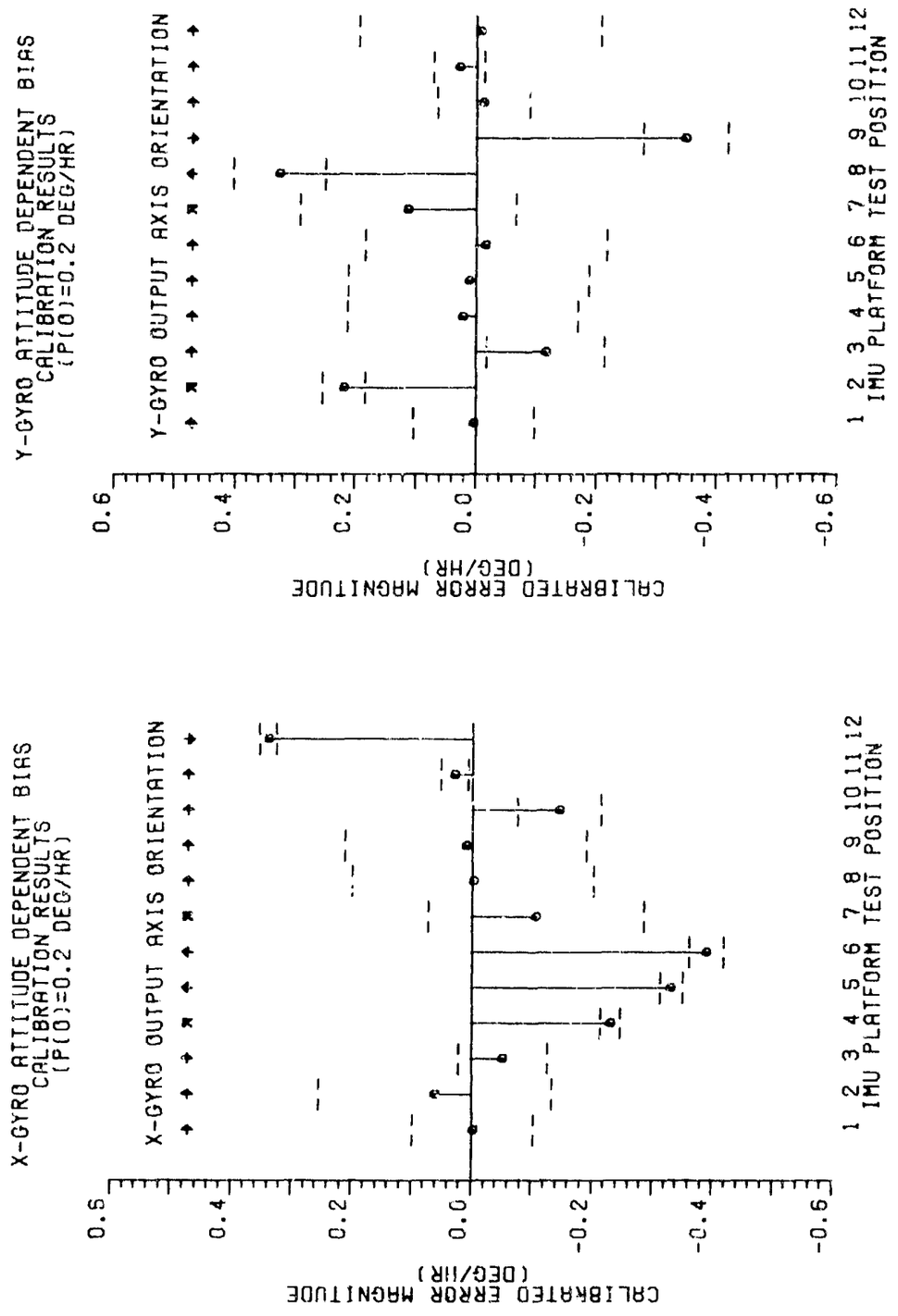

Figure 8-2. Gyro Error Model Residual Estimation Results
($P(0) = 0.2°/Hr$)

Kalman Filter estimates for the x and y-gyro attitude-dependent biases are roughly 0.4 degree per hour, which is within two standard deviations of the initial uncertainty of 0.2 degree per hour. Two standard deviations include about 95% of the trial outcomes for Gaussian statistics.

Examination of the Kalman Filter's estimation errors for the other IMU error sources at the end of the twelfth platform test sequence indicates that the filter is unable to accurately calibrate all of them due to the presence of the attitude-dependent biases with large initial uncertainties. In effect, a solution is precluded because, although each platform test sequence results in three additional equations for separation of the IMU calibration parameters, three additional unknowns are added also. The filter's estimates for all IMU error sources are, however, within three standard deviations of their initial uncertainties. This consistency is obtainable only through the use of error model residual states.

In addition to a desire to upgrade the KT-73 IMU error model, the exact functional dependency of the errors producing the 0.4 degree per hour gyro drift rate for some platform attitudes must be determined so that it can be explicitly included in the Kalman Filter system dynamics matrix to enable the filter to accurately calibrate the other IMU errors. Determining the exact functional dependency of error model residual states amounts to performing a trial and error analysis to determine the parameter, if any, which varies in magnitude or vector direction with changing platform attitude with which the gyro drift rate error is correlated. The results of this analysis are shown in Figure 8-2 and indicate a high degree of correlation between gyro drift rate magnitude and the orientation of the gyro output axis relative to the specific force vector. The specific force vector is essentially the gravity vector for the fixed IMU base situation and has been assumed to be oriented parallel with the y-axis of the graph in Figure 8-2. Note in this figure that the correlation appears to be especially high for those platform test sequences where estimation accuracy is high, as indicated by closely spaced brackets.

To confirm the apparent error model residual gyro output axis specific force dependency, three additional states were added to the Kalman Filter explicitly containing this functional dependency and an initial uncertainty of 0.4 degree per hour per g. The initial uncertainty of the error model residual states was reduced to the gyro random noise level of 0.005 degree per hour and the recorded IMU measurement data reprocessed by the modified Kalman Filter. Kalman Filter estimation results for the error model residual or gyro attitude-dependent bias states are shown in Figure 8.3. Brackets about the filter's estimates indicate the initial uncertainty of 0.005 degrees per hour and illustrates that no estimates were obtained greater than this value. These results confirm the existence of a gyro output axis specific force dependent error source. The results of Figure 8-3 along with the now obtained accurate calibration of the other gyro and related error sources showing consistency with their initial uncertainties also indicate the absences of any additional gyro-related errors of magnitude appreciably larger than the 0.005 degree per hour error model residuals.

The physics of why a specific force acting along the output axis of the KT-73 gyroflex gyros produced a drift rate error were initially perplexing. It is well known that a mass unbalance in conjunction with a specific force acting along a gyro input or spin axis can produce a drift rate error. However, the vector relationships are such that it is impossible for this to occur when it concerns the output axis. Mr. Bud Bleichroth of AGMC eventually isolated the cause. The gyroflex gyro is a two-degree-of-freedom, dry flexure joint suspended, free rotor gyro. Its unique feature is a special rotating flexure suspension on one end of a shaft, supporting and pivoting the wheel. The other shaft end is driven by a synchronous hysteresis motor. If the flexure suspension joint is not machined in a completely symmetrical manner, then a specific force acting along the output axis acts in conjunction with the flexure asymmetry to yield a torque which produces the drift rate error. This error source has been termed a gyro quadrature g error by the Singer engineers and has been specified at 1.0 degree per hour per g for the SRAM KT-76 IMU.

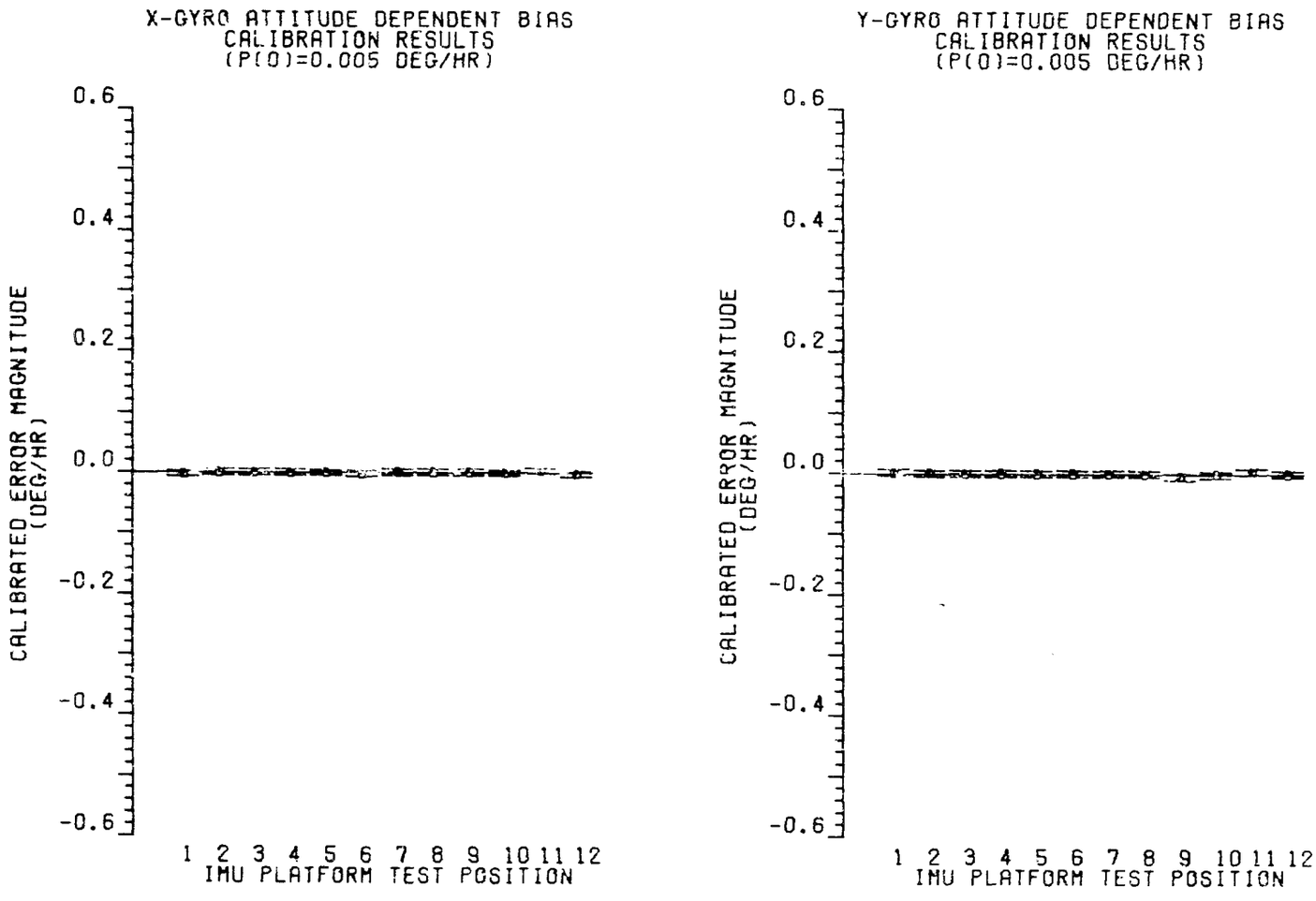

Figure 8-3. Gyro Error Model Residual Estimation Results
(P(0) = 0.005°/Hr)

8.2.2 Gyro G-Squared Error Correlation Studies

Having found a rather major omission in the Reference 1 IMU error model raises the question as to the possible omission of additional gyro error sources that are not strictly negligible relative to the inertial instrument random disturbances. This concern seems particularly justified for specific force related gyro errors since the Reference 1 IMU error model was formulated for navigational error analyses where accelerations are generally of short time durations. Since the IMU calibration tests are conducted with the platform at numerous attitudes relative to the specific force vector for extended periods of time, gyro error sources insignificant for navigational accuracy computations may not be negligible in consideration of Kalman Filter IMU calibration accuracy constraints. For these reasons, it was decided to conduct correlation studies on the next most logical gyro specific force related errors omitted from the Reference 1 IMU error model which are additional g-squared gyro errors.

The Reference 1 gyro error model contains an anisoelastic drift rate error having a magnitude proportional to the product of specific forces acting along the output and spin axes of the gyro. Taking possible combinations of three things, input-spin-output axes specific forces, taken two at a time, leaves five additional g-squared gyro error sources to be evaluated.

The philosophy for evaluating the magnitude of the gyro g-squared error sources can be understood with the aid of Figure 8-4. The recorded IMU measurement data is processed by two versions of the IMU calibration Kalman Filter. The first is the nominal or baseline version while the second version has been modified to include three additional g-squared gyro drift rate error states. There is one error state per gyro with each g-squared error having the same gyro axes specific force dependency. The initial uncertainty of these error sources is found by iteration such that the final Kalman Filter g-squared error estimate is within one to two standard deviations of the initial uncertainty. Generally, only one iteration was required and all initial uncertainties were found to be between 0.003 and 0.005 degrees per hour per g-squared.

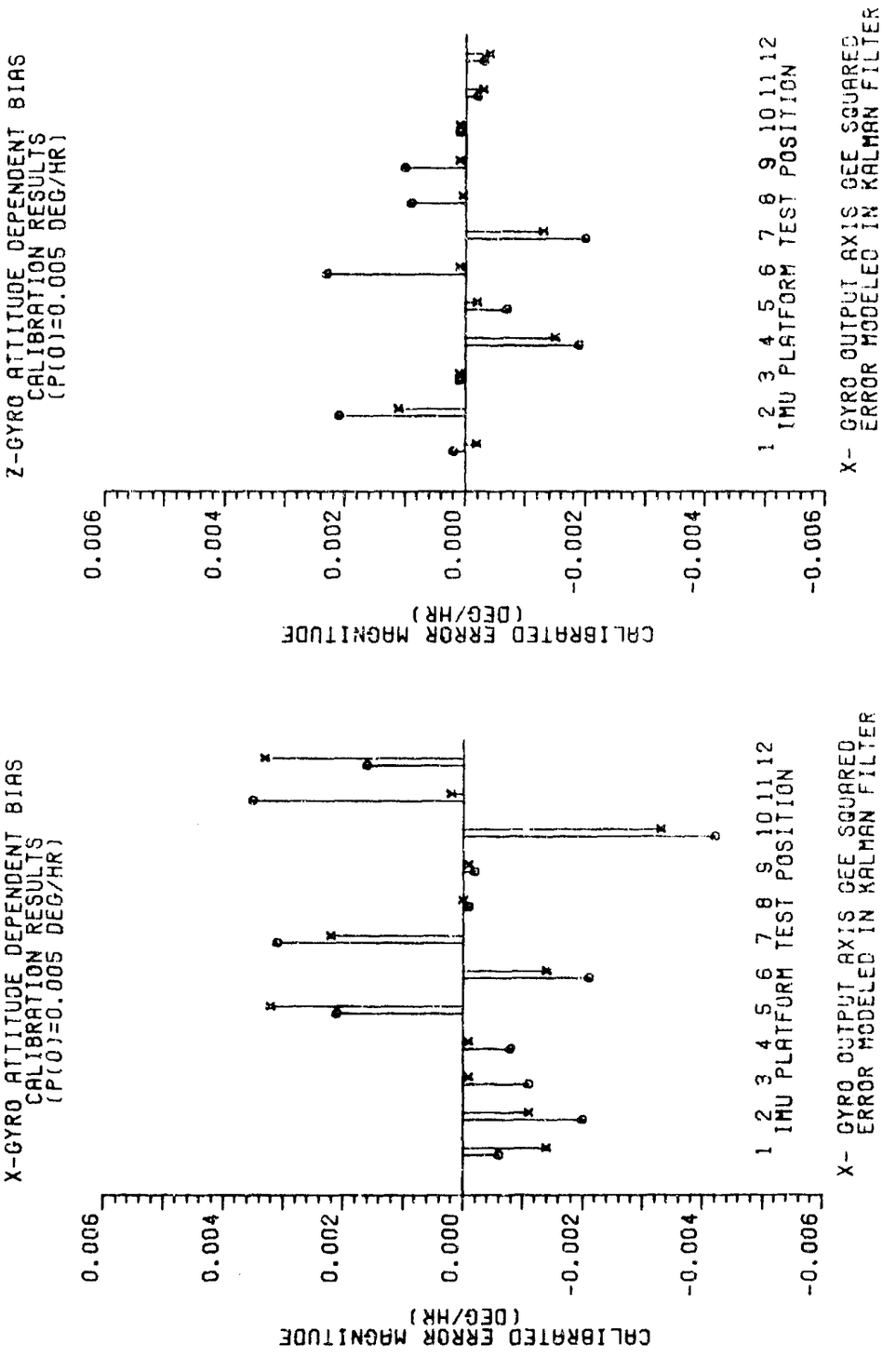

Figure 6-4. Gyro Attitude Dependent Bias Estimation Results

The evaluation criteria were both the Kalman Filter's estimate of the g-squared error source and the degree to which the addition of this error source to the IMU error model reduced the filter's estimate for the error model residual or gyro attitude-dependent bias states. The relative reduction in gyro attitude dependent bias filter estimates is shown in Figure 8-4 for the addition of gyro output axis g-squared error states to the Kalman Filter state vector. The Kalman Filter's estimate for these g-squared errors were 0.004 and 0.003 degree per hour per g-squared for the x and z-gyros, respectively. Initial uncertainties were 0.003 and 0.004 degrees per hour per g-squared. Substantial reductions in the z-gyro attitude-dependent biases are seen to occur while little improvement is obtained by adding an output axis g-squared error source to the x-gyro error model.

Of the five sets of three g-squared error sources evaluated, those showing an output axis g-squared functional dependency rated highest in terms of the above criteria. Since: (1) the filter's estimates for all the g-squared error sources were less than the correlated gyro random drift rate magnitudes, (2) only a marginal reduction in the error model residual states was obtained, and (3) inclusion of the g-squared errors in the Kalman Filter state vector did not significantly affect the filter's estimates for the IMU error sources, it was concluded that the g-squared errors could be neglected.

8.2.3 Heading Sensitivity Tests

Prior to actually trying the IMU calibration technique in the laboratory and demonstrating its feasibility, there was a high degree of concern that potential inertial instrument heating and magnetic errors induced by gyro slewing, and variations in cooling air and magnetic fields with relative platform-to-IMU case orientations, might mask or induce significant errors in the determination of the IMU calibration parameters. Several special tests were conducted to confirm or negate this hypothesis. The first series of tests were modifications of the basic IMU calibration test and the second series constituted heading sensitivity tests.

In the first series, a test was conducted to determine if rapidly torquing the platform from one test sequence to another would result in significant gyro heating and an associated thermal drift rate error. Usually, a calibration test was conducted by slewing the platform to new test attitudes, using the analog torquing mode with a 30 (x, y-gyro) and 90 (z-gyro) degree per minute slew rate, and immediately recording the IMU measurement data. A special test was conducted by allowing the gyros a fifteen minute cooling down period between their time of arrival at a new test attitude and the time data recording commenced. Two tests were conducted, one using five and the other using ten minute measurement time intervals per test sequence. Kalman Filter IMU error source estimates obtained from these tests agreed with those obtained for the nominal tests to within the accuracy predicted by the filter's covariance matrix. These results indicate that gyro heating due to rapid torquing is not a significant source of error for the KT-73 IMU gyros.

In another special test, some of the platform test attitudes were changed to alternate ones to determine if the different magnetic fields encountered by the inertial instruments were sufficient to cause a shift in the recovered IMU calibration parameters. The results of this test were negative.

Another special test was conducted to demonstrate that the gyro drift rate errors could be software compensated. Test results showed a reduction in platform total drift rate from about 1.0 to 0.01 degree per hour for many of the test attitudes. Gyro spin and input axes mass unbalan e, quadrature g, scale factor, misalignment angles, anisoelastic and bias error sources were compensated for by modification of the gyro earth rate torquing magnitudes. IMU calibration parameter values recovered from this test were also consistent with those obtained from the baseline calibration tests.

The second series of special tests were conducted to determine heading sensitivities. The term heading sensitivity is used to denote gyro drift rate errors produced by cooling air, temperature, and magnetic field variations associated with changes in platform-to-IMU case azimuth

orientations for the situation of both platform and IMU case being approximately level. To conduct the heading sensitivity test in the laboratory, the IMU case was maintained in alignment with the navigation frame while the platform was indexed one complete revolution in azimuth in 30-degree increments. The platform was stabilized relative to the navigation frame by application of earth rate torquing. IMU measurements were recorded at 30-second intervals for a duration of ten minutes at each test attitude.

Kalman Filter heading sensitivity estimation results are shown in Figure 8-5. Four drift rate errors are depicted to illustrate the filter's ability to separate the various error sources. Gyro attitude-dependent drift rate error was modeled as a random bias and reset to its initial uncertainty of 0.005 degree per hour at the start of each new platform test sequence. These three Kalman Filter error states are the same as those discussed in previous sections and reflect the gyro heading sensitive drift rate errors at each platform orientation. Gyro total drift rate error is a composite error composed of all gyro errors considered internal to the instrument. Platform gyro-dependent drift rate error is a composite error composed of gyro total drift rate plus gyro scale factor and gyro-to-platform misalignment angle errors. Platform total drift rate is a composite error composed of platform gyro-dependent drift rate plus IMU case-to-navigation frame misalignment angle, gimbal synchro bias, and differential angle errors.

The estimates for the composite errors were computed by summing the appropriate Kalman Filter estimates for the individual component error states. Estimation errors for these composite errors were computed by using the expectation operator and appropriate on and off diagonal covariance matrix elements. Estimation error standard deviations for all x-gyro and x-axis platform error quantities plotted in Figure 8-5 fall between 0.003 and 0.006 degrees per hour.

Platform total and gyro-dependent drift rate error estimates show similar characteristics. The seemingly abnormal -0.01 degree per hour platform total drift rate error at a 90 degree platform heading was

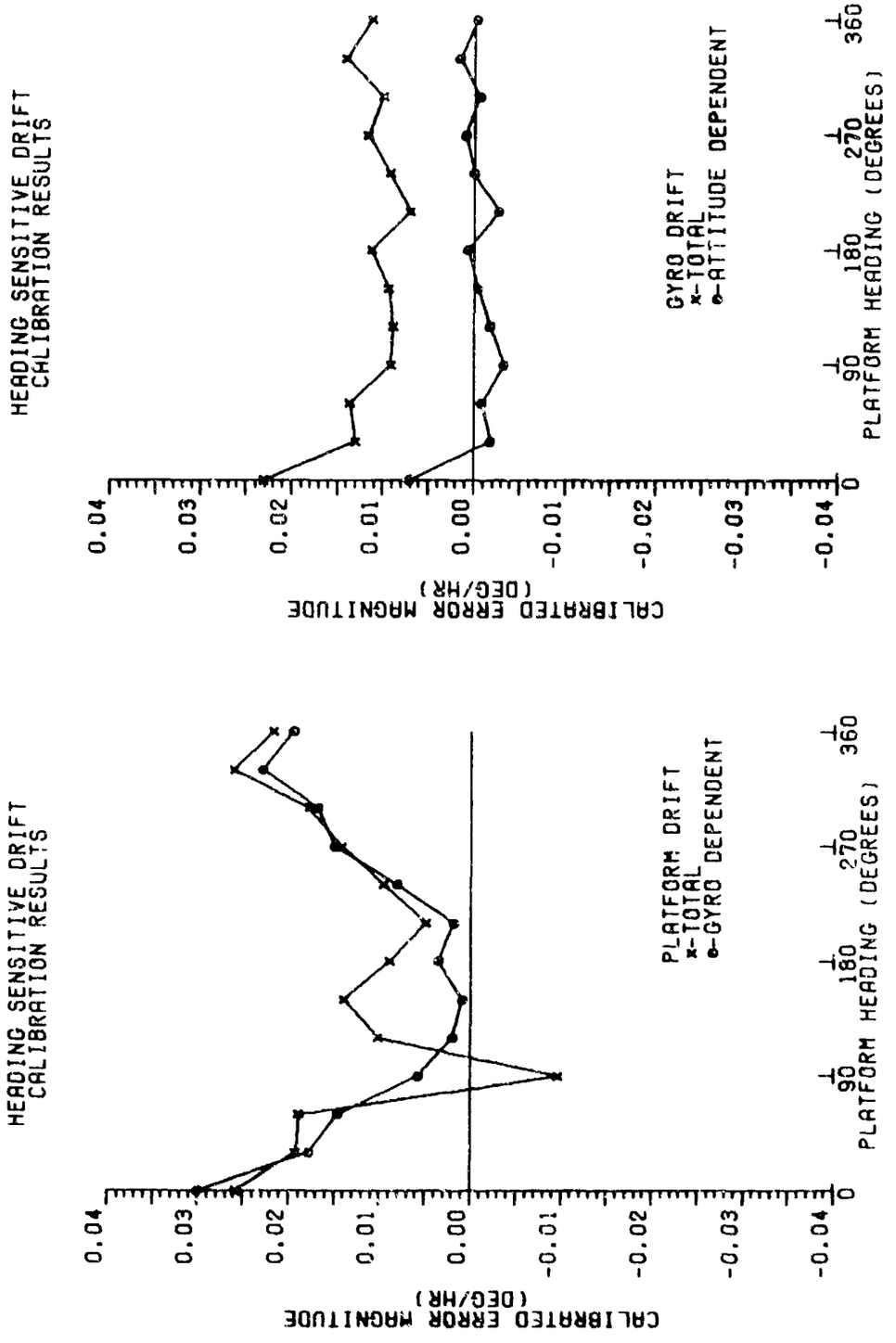

Figure 8-5. Heading Sensitive Drift Calibration Results

produced by an unusually large error in positioning the platform via the synchro angle readouts at this particular attitude. Both composite platform drift rate error characteristics tend to indicate a heading sensitivity; however, comparison of these characteristics to that for total gyro drift rate error and examination of other Kalman Filter estimation results shows the apparent heading sensitivity to be due to an x-gyro scale factor error. Except for one point, all x-gyro attitude-dependent bias estimates are less than the KT-73 IMU heading sensitive drift rate error specification of 0.004 degree per hour.

The conclusion to be drawn from these special and heading sensitive test results is that thermal and magnetic field variations over the different platform-to-IMU case test orientations used are on the order of the gyro random disturbances and do not significantly affect gyro error source calibration accuracy.

8.3 ACCELEROMETER MODELING REFINEMENTS

Initial Kalman Filter estimation results for the accelerometer error sources were reasonably consistent with those expected. Three error model residual states, modeled as accelerometer attitude-dependent scale factor errors, had been included in the accelerometer error model to account or allow for possible error model discrepancies. Functional modeling of the residual states is not critical and attitude-dependent bias errors would have served equally well. With the initial variances of these error model residual states set at relatively small values, the only detected inconsistency of the estimation results was a non-repeatibility of the accelerometer bias and scale factor error estimates to within the accuracy predicted by the filter's covariance matrix. This problem could be ameliorated, however, by sufficiently increasing the initial variance of the error model residual states. Increasing the initial uncertainty of the error model residual states results in corresponding increases in estimation error, as predicted by the filter's covariance matrix, but does not substantially affect the error state estimates.

The above procedure of adjusting the error model residual state initial uncertainties to obtain error state estimate test-to-test repeatibility to within the filter's predicted calibration error was considered unsatisfactory because it did not answer the basic questions. Are there thermal and/or magnetic field variations present at the various platform test attitudes that perturb the nominal accelerometer scale factor and bias errors? How accurately should test-to-test calibration results repeat, considering normal IMU hardware turn-on variations? In an attempt to answer these questions, it was decided to examine in detail the repeatibility of the accelerometer misalignment angle errors, since these error sources are essentially static and not subject to hardware turn-on variations.

8.3.1 Accelerometer Non-Orthogonality Angles

An examination of the filter's covariance matrix elements corresponding to the platform-to-accelerometer frame misalignment angle errors indicates that the filter is capable of reducing the initial manufacturing tolerance uncertainty of 1.0 arc minutes to only 0.7 arc minutes. In contrast to the accelerometer bias and scale factor error estimates, the platform-to-accelerometer misalignment angle error estimates did repeat to within the accuracy predicted by the filter's covariance matrix. As such, the error state estimates and estimation errors for the accelerometer misalignment angles as defined in Section 3.3.2 are unsuitable for a detailed study of the accelerometer error model as envisioned in the previous section. A reformulation of the platform-to-accelerometer misalignment angles, that results in estimation accuracies limited largely by the accelerometer random disturbances, is necessary to conduct this study.

The limitation encountered by the Kalman Filter in attempting to accurately estimate the angular misalignments of the accelerometers from the platform frame by use of only the accelerometers measurements is that these measurements indicate a misalignment of the accelerometer's electrical null axis from an assumed orientation relative to the gravity vector. The misalignment of the accelerometer's electrical null axis from the

gravity vector is a composite error having accelerometer bias, scale factor, random noise, accelerometer to-platform and synchro gimbal bias angular misalignment error components. Introduction of new synchro gimbal angle bias errors each time the platform is re-oriented precludes the filter from accurately separating the accelerometer-to-platform frame misalignment angle errors from the composite accelerometer electrical null axis tilt errors. Separation of this error from the composite tilt error requires an accurate measure of the platform's angular attitude which is not available. Note that the KT-73 IMU synchros are precise to 5 arc seconds but accurate to only 6 arc minutes and, therefore, too inaccurate for this measurement.

From the above discussion, it can be concluded that accurate estimation of some type of accelerometer misalignment angles can only be achieved by eliminating to first order the gimbal synchro angle bias errors from the determination process. This will require, however, that a measurement reference or its equivalent other than the gravity vector be used. The most logical choice for an accelerometer measurement reference other than the gravity vector is another accelerometer measurement and this leads to that accelerometer misalignments from an orthogonal set is the quantity to be estimated. To illustrate the concept, consider the No. 4 platform test sequence shown in Figure 7-2. Assume that the y and z-accelerometer time varying outputs are given to first order by:

$$a_y(t) = -gK_{Ay}\cos(\theta_{gx}(t)) + A_{By} + A_{Ry}(t)$$

$$a_z(t) = -gK_{Az}\cos\left[90^\circ - (\theta_{gx}(t) + \alpha_{zx})\right] + A_{Bz} + A_{Rz}(t)$$

where

α_{zx} is the non-orthogonality error angle of the z-accelerometer input axis with respect to the y-accelerometer input axis. α_{zx} is produced by rotating the z-accelerometer about the x-axis.

These expressions can be solved for α_{zx} by using a trigonometric formula and a small angle approximation to yield:

$$\alpha_{zx} = \frac{K_{Ay}}{K_{Az}} \left[\frac{a_z(t) - A_{Bz} - A_{Rz}(t)}{a_y(t) - A_{By} - A_{Ry}(t)} \right] - \left[\frac{g^2 K_{Ay}^2}{\left[a_y(t) - A_{By} - A_{Ry}(t) \right]^2} - 1 \right]^{\frac{1}{2}}$$

This expression demonstrates that accelerometer non-orthogonality error angles can be determined by simultaneously taking pairs of accelerometer measurements and to first order, the solution is independent of the gimbal synchro angle bias errors, which is the desired result. Estimation of the non-orthogonality error angles by the Kalman Filter requires that these errors be expressed in terms of the platform-to-accelerometer misalignment angle error states. These expressions can be derived by use of coordinate transformations that "square up" the accelerometer frame and then rotate it into the platform frame.

An orthogonal accelerometer frame can be defined in the following manner. Rotate the y-accelerometer, in the plane defined by the x and y-accelerometer input axes, by the small angle α_{yz} into orthogonality with the x-accelerometer. Rotate the z-accelerometer by the small angle α_{zx} about the x-accelerometer axis into orthogonality with the y-accelerometer. And finally, rotate the z-accelerometer by the small angle α_{zy} about the y-accelerometer axis into orthogonality with the x-accelerometer. All rotations are done in accordance with the right-hand rule. The coordinate transformation rotating the orthogonal accelerometer frame into the frame defined by the physical orientation of the accelerometer input axes is given by C_{OA}^{A}.

$$C_{OA}^{A} = \begin{bmatrix} 1 & 0 & 0 \\ -\alpha_{yz} & 1 & 0 \\ \alpha_{zy} & -\alpha_{zx} & 1 \end{bmatrix}$$

To relate these non-orthogonality error angles to the platform-to-accelerometer misalignment angles defined in Section 3.3.2 requires definition of a platform-to-orthogonal accelerometer frame orthogonal small angle coordinate transformation matrix C_P^{OA}

$$C_P^{OA} = \begin{bmatrix} 1 & \epsilon_z & -\epsilon_y \\ -\epsilon_z & 1 & \epsilon_x \\ \epsilon_y & -\epsilon_x & 1 \end{bmatrix}$$

Equating the platform-to-accelerometer frame coordinate transformations yields:

$$C_P^A = C_{OA}^A \; C_P^{OA}$$

$$\begin{bmatrix} 1 & \gamma_{xz} & \gamma_{xy} \\ -\gamma_{yz} & 1 & \gamma_{yx} \\ \gamma_{zy} & \gamma_{zx} & 1 \end{bmatrix} = \begin{bmatrix} 1 & 0 & 0 \\ -\alpha_{yz} & 1 & 0 \\ \alpha_{zy} & -\alpha_{zx} & 1 \end{bmatrix} \begin{bmatrix} 1 & \epsilon_z & -\epsilon_y \\ -\epsilon_z & 1 & \epsilon_x \\ \epsilon_y & -\epsilon_x & 1 \end{bmatrix}$$

The matrix equation can be solved for the expressions relating the three accelerometer non-orthogonality to the six platform-to-accelerometer misalignment angle errors.

$$\alpha_{yz} = \gamma_{yz} - \gamma_{xz}$$

$$\alpha_{zy} = \gamma_{zy} - \gamma_{xy}$$

$$\alpha_{zx} = \gamma_{zx} - \gamma_{yx}$$

8.3.2 Accelerometer Attitude Dependent Errors

Kalman Filter estimation results for the α_{yz} accelerometer non-orthogonality error angle are shown in Figure 8-6. Calibration results are depicted in three sets of five IMU tests and illustrate the history of improvements made in estimating this error source by refining the IMU error model. For each series of five IMU tests, the brackets or

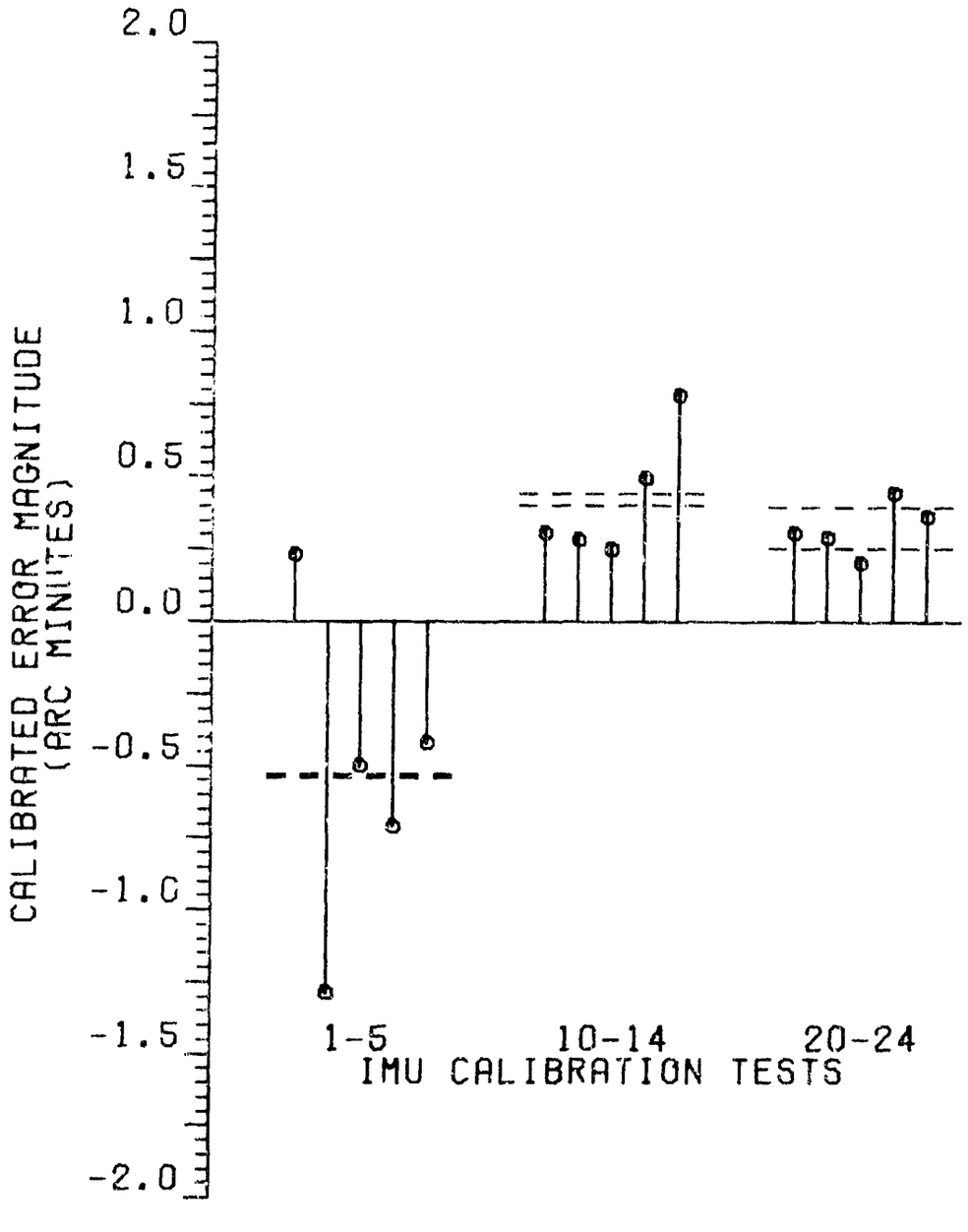

Figure 8-6. Accelerometer Non-Orthogonality Angle Calibration Results

boundaries superimposed about either side of the calibrated average estimate (average estimate not shown) represent a standard deviation of the estimation error. Total spacing between the boundaries is, therefore, two standard deviations. This data was computed using Kalman Filter estimation results.

Optimal Estimate:

$$\hat{\alpha}_{yz} = \hat{\gamma}_{yz} - \hat{\gamma}_{xz}$$

Estimation Error:

$$P(\alpha_{yz}, \alpha_{yz}) = E\left[(\gamma_{yz} - \gamma_{xz})(\gamma_{yz} - \gamma_{xz})\right]$$

$$= P(\gamma_{yz}, \gamma_{yz}) + P(\gamma_{xz}, \gamma_{xz}) - 2P(\gamma_{yz}, \gamma_{xz})$$

The estimation error shown for the first five calibration tests was computed using the accelerometer error modeling given in Reference 1. This error modeling resulted in an estimation error standard deviation of 0.7 arc seconds and was essentially determined by the accelerometer random disturbances. Gaussian statistics imply that 68% of the estimates should fall between the estimation error bounds on an ensemble average basis with virtually all estimates falling within three standard deviations of the five test estimation average. Figure 8-6 clearly shows that the estimation results obtained for the first five tests are grossly inconsistent with these statistical averages and suggests the presence of unmodeled error sources.

As discussed in Section 7.1.4, the real-time data recording software suffered from a measurement timing instability of 15.0 msec. This instability was eventually reduced to around 1.0 msec by the fifteenth calibration test. It was necessary to modify the Kalman Filter by adding one error state to the state vector and three disturbances to the velocity error states to account for this error since it was somewhat larger than the permissible 0.1 msec timing error. The longer term correlated timing error was modeled as a pseudo accelerometer scale factor error, one error affecting all three accelerometer outputs, having an initial uncertainty of one ppm and a 250 second correlation time.

The shorter term disturbances on the velocity error states was modeled as being proportional to the amount of gravity measured by an accelerometer. Disturbance modeling is such that it produced a velocity uncertainty corresponding to one CAPRI pulse in a measurement interval when an accelerometer experiences full gravity along its input axis.

The estimation results shown in Figure 8-6 for the second series of IMU calibration tests illustrate, tests 10-14 compared with 1-5, how a reduction in timing instability from 15.0 to 1.0 msec and a modification of the Kalman Filter to account for the residual timing errors improves the non-orthogonality error angle estimates. Figure 8-7 shows the filter's estimates for the clock error state at the end of each platform test sequence for IMU calibration Test No. 24. This error state is reset to its initial uncertainty at the beginning of each test sequence.

Figure 8-6 also shows, however, that the spread in accelerometer non-orthogonality error angle estimates is still inconsistent with Gaussian distribution ensemble averages for IMU calibration Tests 10-14. This inconsistency again indicates the presence of unmodeled accelerometer errors and a special test was designed to determine the presence of accelerometer attitude dependent errors due to thermal and magnetic field variations with changes in platform-to-IMU case orientations. Test philosophy was to monitor the number of velocity pulses generated by an accelerometer when its input axis was parallel to the gravity vector and its case axis was at different azimuth attitudes relative to the IMU case. Accelerometer error modeling of Reference 1 and the alignment accuracy of the accelerometer input axis to the gravity vector by use of the gimbal synchro angle devices predict no more than one velocity pulse variation over a 30 second measurement interval. To eliminate the possibility of the real-time software timing errors affecting the data, velocity pulses were accurately summed by Aztec electronic counters via Singer system test rack connectors.

Tests were conducted for accelerometer-to-IMU case orientations similar to those used during the IMU calibration tests. Referring to Figure 7-2, platform test sequences No. 1 with No. 3 and No. 10 with No. 11 were used for collecting z-axis velocity pulse data in both the

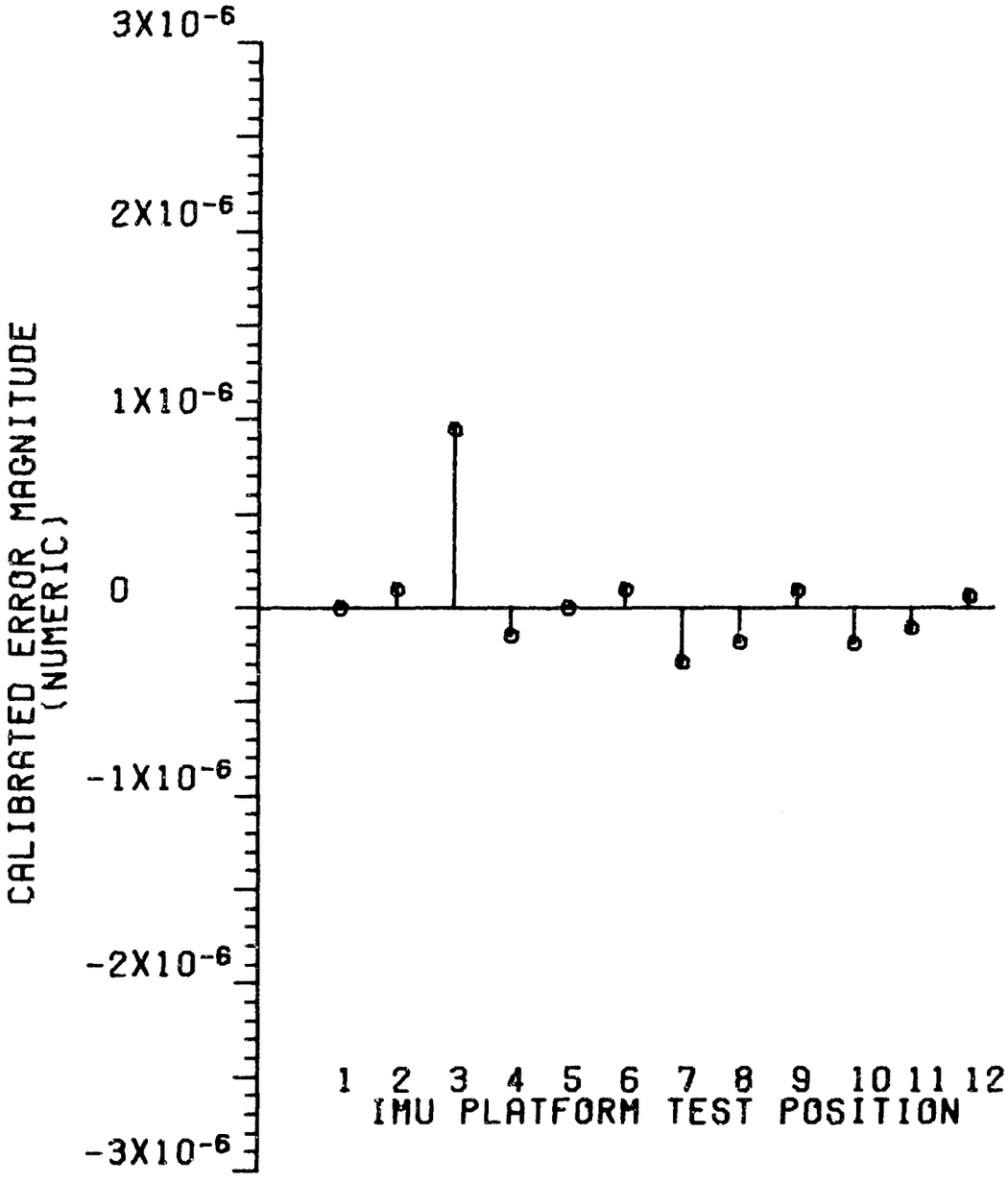

Figure 8-7. Measurement Timing Error Calibration Results

up and down orientations after leveling the x and y-accelerometers in the No. 3 and No. 10 sequences. Test sequences No. 5 and 6 were used to collect data for the y-accelerometer in the up orientation. The y-accelerometer data similar to that collected by the Aztec electronic counters is shown in Figure 7-3 for test sequences No. 5 and 6.

The x and y-platform axes of the KT-73 IMU are instrumented by a two-axis horizontal accelerometer employing a force rebalance design. Test results indicated that the number of velocity pulses generated by this accelerometer changed by only a fraction of a pulse, out of a nominal thirty thousand pulses generated in a thirty second measurement interval, for the various platform attitudes. The z-axis accelerometer is a single axis device also of the force rebalance type. Test results showed, however, that the total velocity pulse count varied between one and four pulses out of a total of thirty thousand for the various test attitudes. Test results were consistent on a day-to-day basis for specific test attitudes. Test results also appeared independent of test time with the total number of pulses generated being identical for the first and last measurement intervals of a particular test sequence. This last test result rules out a thermal sensitivity problem.

Three accelerometer error model residual states had previously been included in the Kalman Filter state vector to account for a potential attitude dependency. These states had been modeled as random bias accelerometer scale factor errors which were reset to their initial uncertainty at the beginning of each platform test sequence. These assumptions are consistent with the above test results and the only modification being required is an increase in the initial uncertainty. The above data suggests attitude-dependent scale factor errors of 10 and 30 ppm for the horizontal and vertical accelerometers, respectively.

Increasing the initial uncertainty of accelerometer attitude-dependent scale factor error states to the above values resulted in the non-orthogonality error angle estimates depicted by IMU calibration tests 20-24 shown in Figure 8-6. These estimation results are totally consistent with ensemble averages predicted by a Gaussian distribution. The standard

deviation of the estimation error for the α_{yz} non-orthogonality error angle predicted by the filter's covariance matrix is 4.3 arc seconds. Accelerometer attitude-dependent scale factor estimates are shown in Figure 8-8. This data depicts the maximum of the x, y, or z-accelerometer error for each platform test attitude.

Modifying the Kalman Filter to account for both the measurement timing and accelerometer attitude-dependent scale factor errors also improved the repeatability of the accelerometer high and low gain mode bias and scale factor error estimates. The Kalman Filter estimates of these error sources were found to be consistent with those determined via the ASM-375 test set. The repeatability of the estimates was also found to be consistent with those predicted by the Singer error model.

8.4 FUTURE ERROR MODEL DEVELOPMENT EFFORTS

The rationale used for validating both the IMU calibration Kalman Filter and error model has largely been to obtain consistency of the estimation results with the known KT-73 IMU manufacturing tolerances and the estimation error ensemble averages predicted by a Gaussian distribution. Additional confidence has been obtained by cross-checking the filter's optimal estimates for certain IMU error sources with the calibration results obtained via Singer's OCP Auto-Cal software routines and the ASM-375 test set. The IMU error source software compensation, heading sensitivity, and thermal and magnetic field variation special tests have provided justification for some of the major assumptions made while cross-checking baseline IMU calibration test results.

The present status of the IMU calibration Kalman Filter and error model is such that there is no known deficiency or inconsistency in the calibration results presently being obtained. This does not imply that undetected IMU error sources cannot exist or might not become evident under more exhaustive validation testing. There are a number of error model assumptions (inertial instrument random disturbances modeling is a prime example) of fundamental importance in the IMU calibration methodology that have not been adequately verified. Although additional studies and

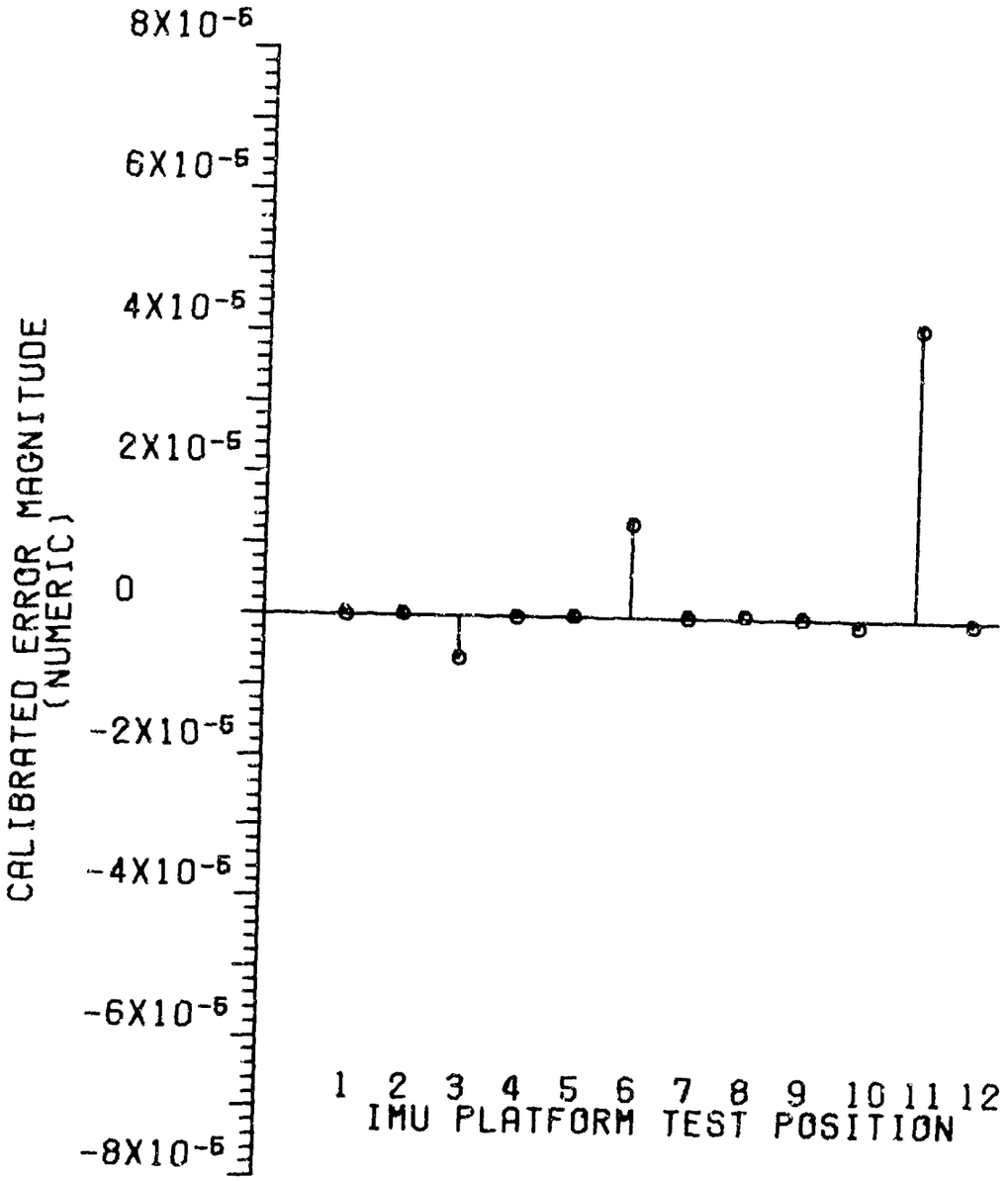

Figure 8-8. Accelerometer Attitude Dependent Scale Factor Estimation Results

tests are considered necessary for a more complete validation and refinement of the IMU calibration technique, to date they have not been conducted largely because they are more logically and conveniently performed in conjunction with the aided-inertial navigation software development and evaluation tests discussed in Section 1.2.

The aided-inertial navigation software development and evaluation tests 4, 5, and 6 shown in Table 1-1, are expected to provide a cross-check of many of the IMU error source magnitudes while providing a basis for conducting various special tests. Gyro scale factor and misalignment angle error sources can be accurately estimated by the Kalman Filter formulated for the tilt table static navigation tests. This test and associated filter also provide a good vehicle for studying the inertial instrument random disturbances since their effects can be continuously observed over several hours. The MEL perturbed base alignment test and associated Kalman Filter will provide an alternate evaluation of the inertial instrument thermal warm-up transients. Finally, the MEL dynamic navigation tests and associated real-time navigation software can be used to demonstrate the software compensation of calibrated IMU hardware errors and achievement of navigational accuracy which will be limited only by alignment and system random disturbance errors. The data reduction/reference system Kalman Filter formulated for the MEL navigation tests will be capable of cross-checking some of the specific force dependent gyro errors.

SECTION IX

IMU CALIBRATION RESULTS

This section presents the major IMU calibration results obtained during the study. These results are twofold: the theoretical estimation errors as obtained from the Kalman Filter's covariance matrix, and the filter's estimates for the magnitudes of the IMU and associated error sources. These results are conveyed in a pictorial rather than tabular or summary manner for three basic reasons:

(1) This type of presentation greatly enhances one's understanding of the calibration methodology and associated Kalman Filter's operation. It also brings out many subtle points not discussed in the text.

(2) It gives the reader an opportunity to view the consistency obtained between the Kalman Filter's estimates and their predicted uncertainty thus giving credence to large dimensional Kalman Filters as viable mathematical tools.

(3) It can be a valuable basis for debugging and validating a Kalman Filter computer program for a similar application, in spite of its characteristic of seeming to be repetitious

Estimation accuracies obtained from the filter's updated covariance matrix are shown for each IMU measurement taken and plotted as a function of time. Platform test orientations are superimposed on these plots to facilitate one's understanding of the error source separation process. Kalman Filter estimates of the same error source are plotted in groups of five and correspond to the last five (20 through 24) IMU calibration tests conducted. Five data points were selected as a compromise between sufficient data demonstrating estimation consistency and data reduction complexity.

9.1 SYSTEM-LEVEL IMU MEASUREMENTS

Estimation accuracy for the system-level IMU differential gimbal angle and pseudo velocity error measurement states is shown in Figure 9-1. A typical record of recorded pseudo velocity pulses was shown in Figure 7-3. Platform test sequences and data recording timing instances and intervals are the same in both figures. Total measurement time during a calibration test is 68 minutes. The platform test sequences have been arranged to minimize the time required to manually torque the platform from one test orientation to another. Depending on the test sequence number, the 30 and 90 degree per minute x-y and z-gyro slew rates result in up to several minutes being required to re-orientate the platform. Total time required to conduct the IMU calibration test, including a seven minute warm-up period before any measurements are taken, is nominally two to two and a half hours. The platform test attitudes shown across the top of these figures are the same as those depicted in Figure 7-2 with the first attitude representing the north, west, and up navigation frame.

The initial uncertainty of both the differential gimbal angle and pseudo velocity error is zero at the start of each test sequence due to the manner in which these error states were defined. The Calcomp plotter logic used in generating the semi-log graphs was to omit plotting a 30 second propagated uncertainty segment when its initial value was less than the minimum value indicated on the ordinate axis. This logic, necessitated by the semi-log plots, prevented plotting the initial steep rise from the zero initial uncertainty.

To distinguish the different sets of data in these figures, alphabetic characters are plotted in the center of the dead time between the platform test sequences. The vertical positioning of these characters is determined by the final value of the updated covariance matrix for the particular test sequences. Referrring to the differential gimbal angle plot in Figure 9-1, only one differential synchro angle measurement is taken during the entire test. This measurement corresponds to the azimuth gimbal axis at the end of the first test sequence. Estimation

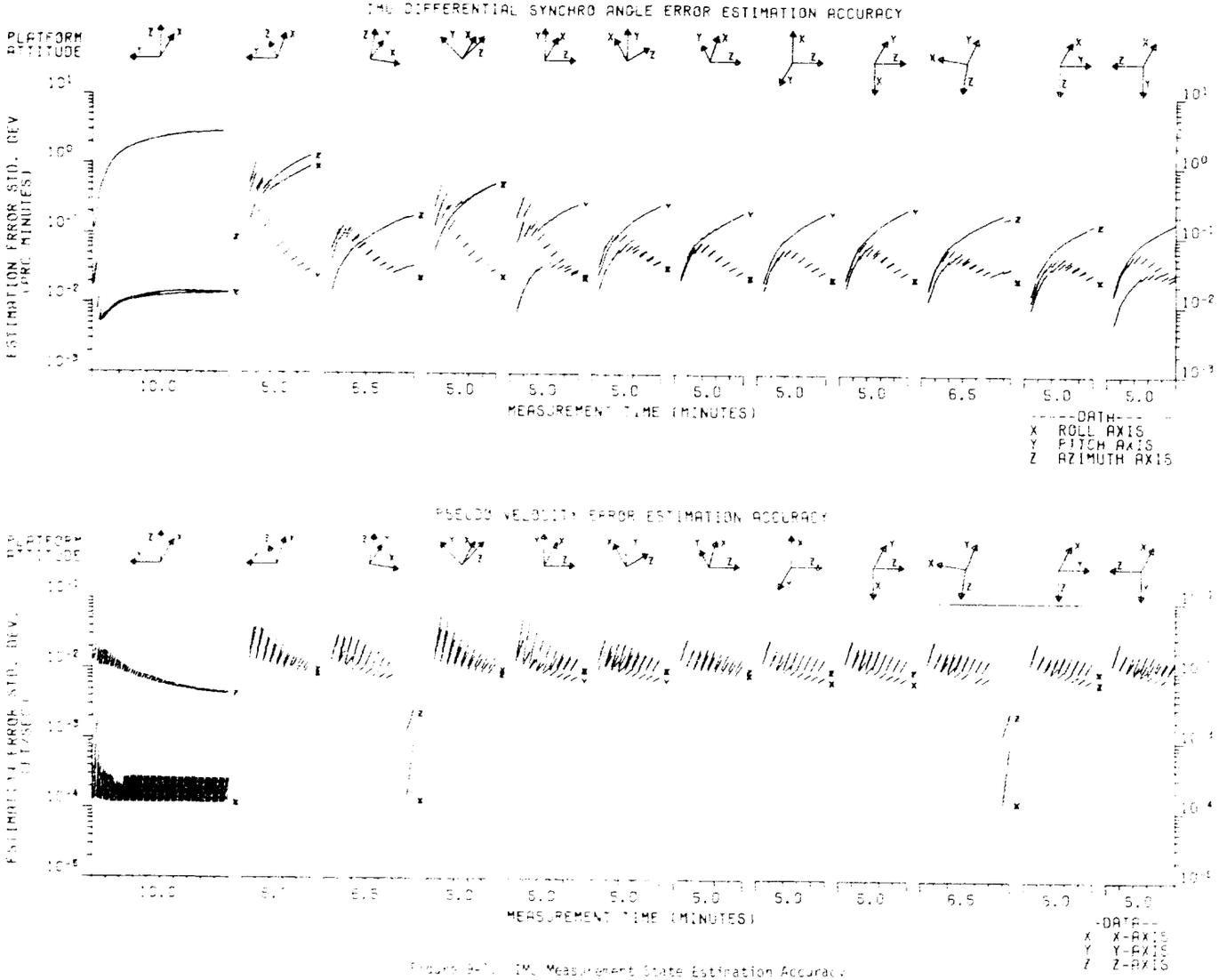

Figure B-1. IML Measurement State Estimation Accuracy

accuracy for the differential azimuth gimbal angle immediately after the measurement is taken is essentially that of the synchro device's precision of 5 arc seconds as indicated in the figure. Estimation of the differential gimbal angles for all instances other than the above measurement is accomplished by the Kalman Filter on the basis of the pseudo velocity measurements.

In contrast to the gimbal angle measurements, three axis pseudo velocity measurements are utilized by the Kalman Filter at each measurement interval. The accuracy of these measurements is determined by the velocity pulse quantization level which is governed by the accelerometers scale factor. The accelerometer low gain navigation scale factor is nominally used throughout the test. The high gain alignment scale factor is, however, used by the x and y-axis accelerometers for the entire first and last minute and a half of the third and tenth test sequence. Pseudo velocity measurement accuracy is two orders of magnitude greater for the high gain rather than the low gain mode. A thirty second measurement interval is used throughout the test except during the first test sequence where it is ten seconds.

Differential roll gimbal angle magnitude estimation results are shown in Figure 9-2. This data corresponds to the total roll gimbal angular excursion occurring during each of the twelve platform test sequences and was obtained as the final Kalman Filter estimate or this error state for each test sequence. Superimposed about the average estimate for each test sequence, not shown, are one standard deviation estimation error brackets for a total bracket separation of two standard deviations. These estimation error standard deviations are the same as those corresponding to the end of a test sequence shown in Figure 9-1. Figure 9-2 shows that the roll gimbal angle excursions for the last five calibration tests conducted are highly consistent, repeating to almost the accuracy of the estimate. Note that test-to-test variations are due largely to gyro bias, spin axis mass unbalance and quadrature g turn-on and platform positioning variations and are not required to obey the ensemble averages predicted by the Gaussian distribution for the estimation error.

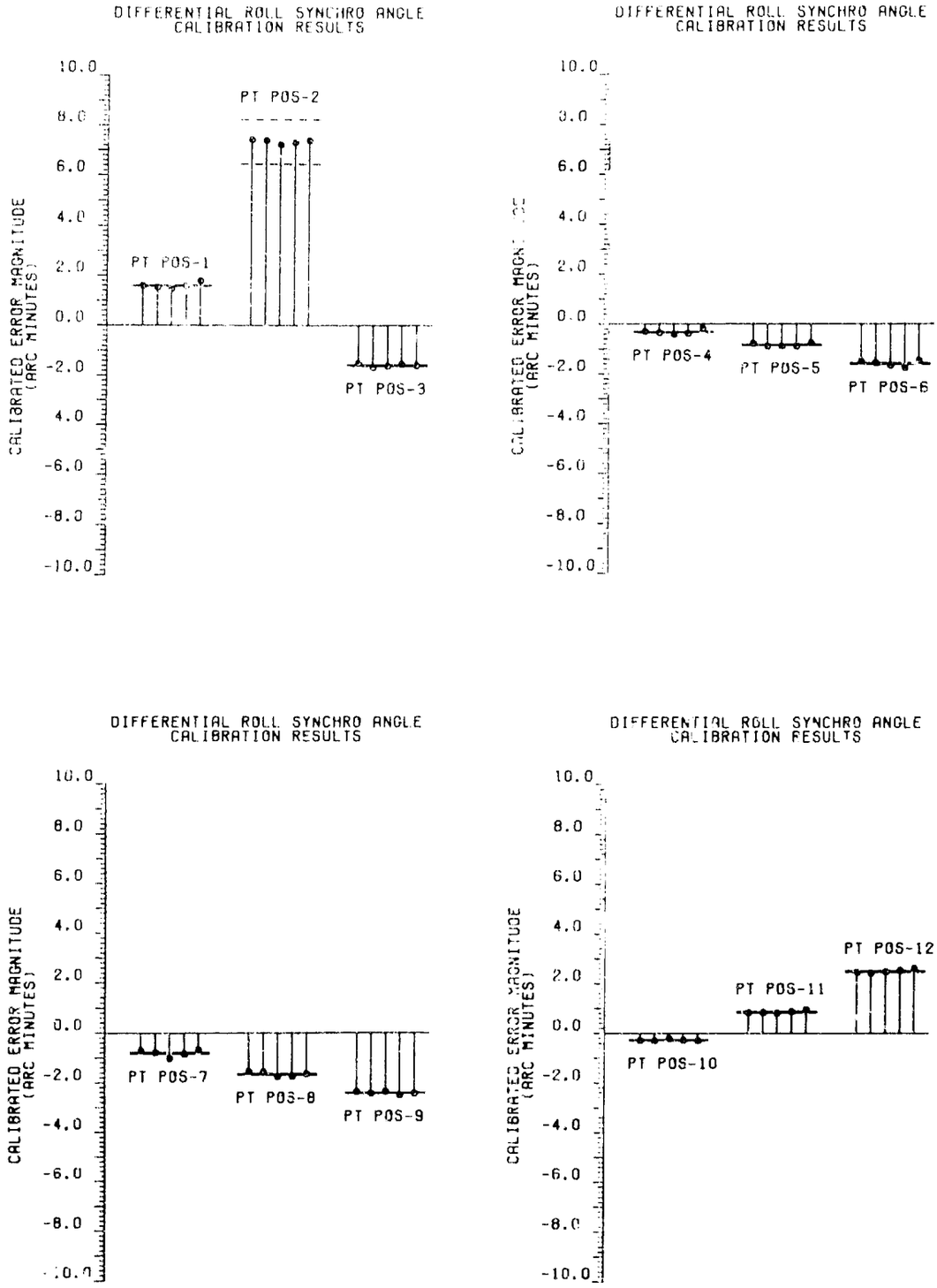

Figure 9-2. Differential Roll Gimbal Angle Estimation Results

9.2 COMPOSITE DRIFT RATE ERRORS

Platform and gyro total drift rate error estimation accuracy is shown in Figure 9-3 and the corresponding estimated magnitudes are shown in Figures 9-4 and 9-5, respectively. These quantities are composite error sources and are estimated, and the estimation uncertainty is determined as described in Section 8.2.3. Gyro total drift rate error contains all the error sources composing the platform total drift rate error except the gyro scale factor and misalignment angle, IMU case-to-navigation frame misalignment angle and the gimbal differential and synchro angle bias errors. Both the absolute value and estimation accuracy of these composite error sources are of general interest in the development of Kalman Filter IMU calibration computer programs.

Estimation of platform drift rate can be inferred directly from the accelerometer measurements, except when an axis is orientated near vertical, resulting in the relatively high estimation accuracy shown at the completion of a test sequence. Final test sequence estimation accuracy is roughly 0.006 degrees per hour and could be increased to the limiting short correlation time gyro random disturbance magnitude of 0.003 degree per hour by doubling the measurement time to ten minutes per test sequence. Gyro total drift rate estimation accuracy is somewhat less than that for the platform due to the incomplete separation of this composite error source from some of the total platform drift rate related error sources. Examination of the estimated magnitudes for these composite errors depicted in Figures 9-4 and 9-5 shows that they are repeatable to roughly the estimation error.

9.3 INERTIAL INSTRUMENT WARM-UP TRANSIENTS

Inertial instrument warm-up transients are not generally considered as calibration parameters and were not included in the first version of the Kalman Filter. During the course of the development effort, excessive navigational errors encountered with the inertial navigation systems on the A-7D aircraft were postulated as caused by an incomplete alignment due to instrument thermal warm-up transients. For this reason

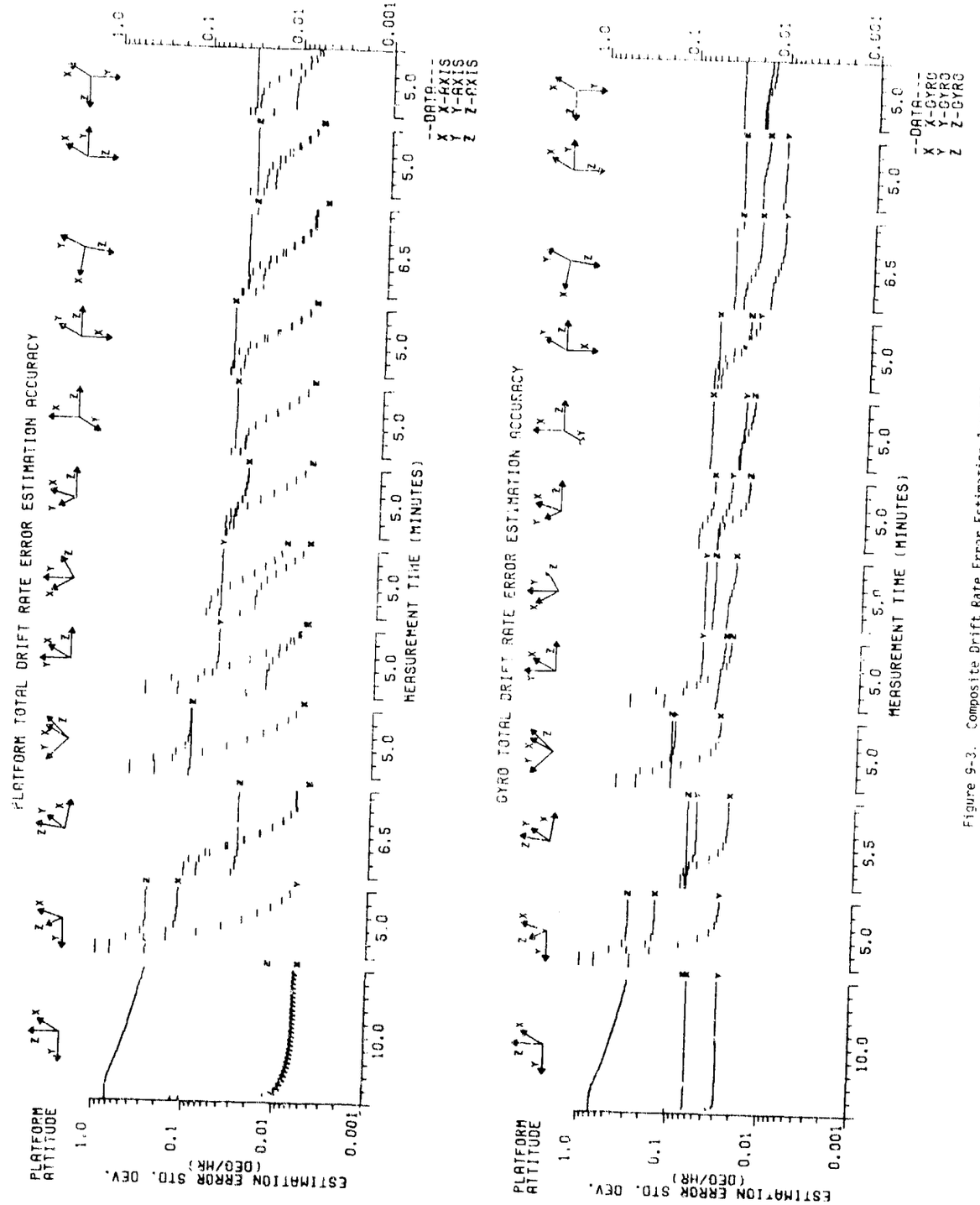

Figure 9-3. Composite Drift Rate Error Estimation Accuracy

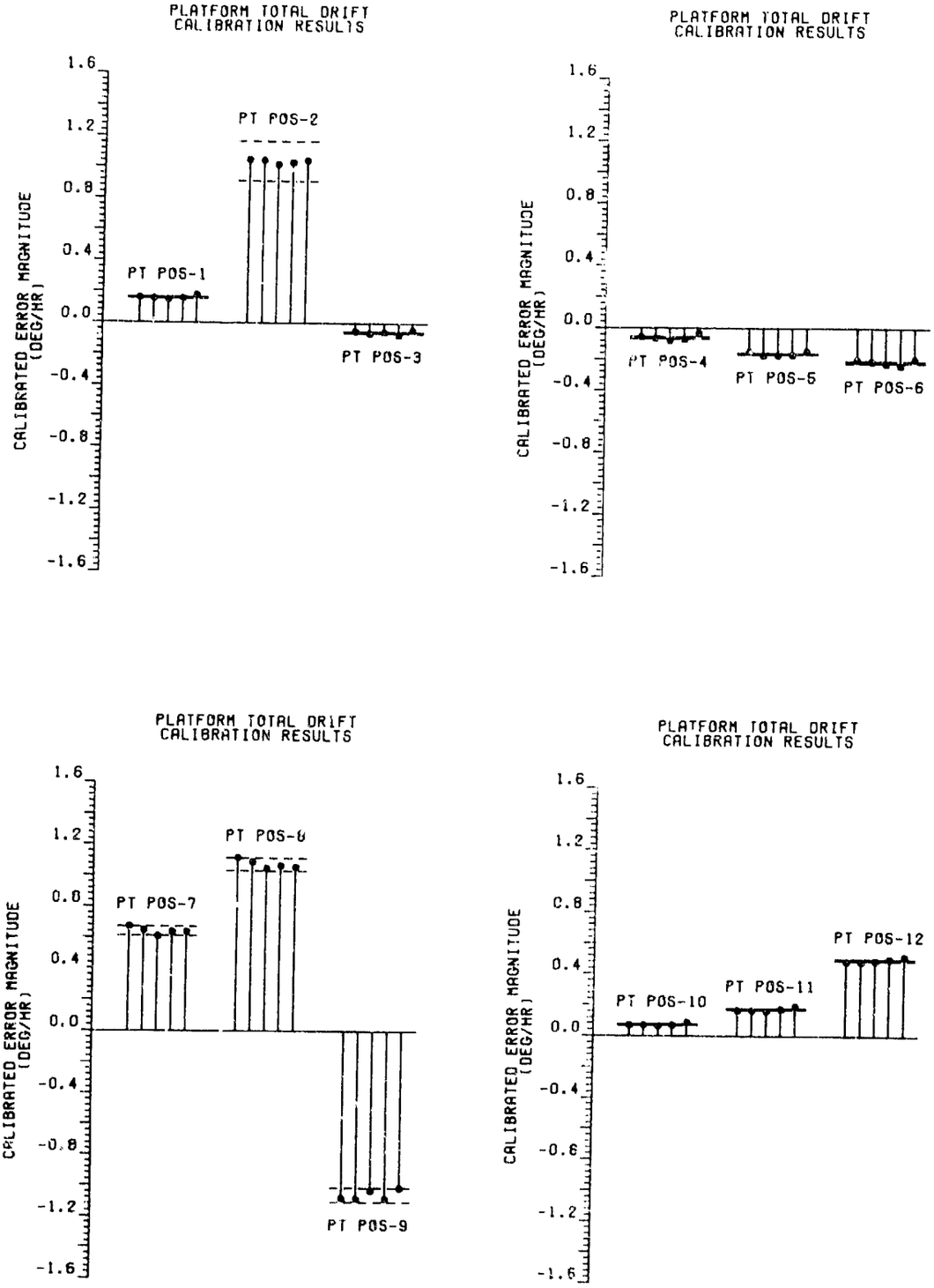

Figure 9-4. Platform Total Drift Rate Estimation Results

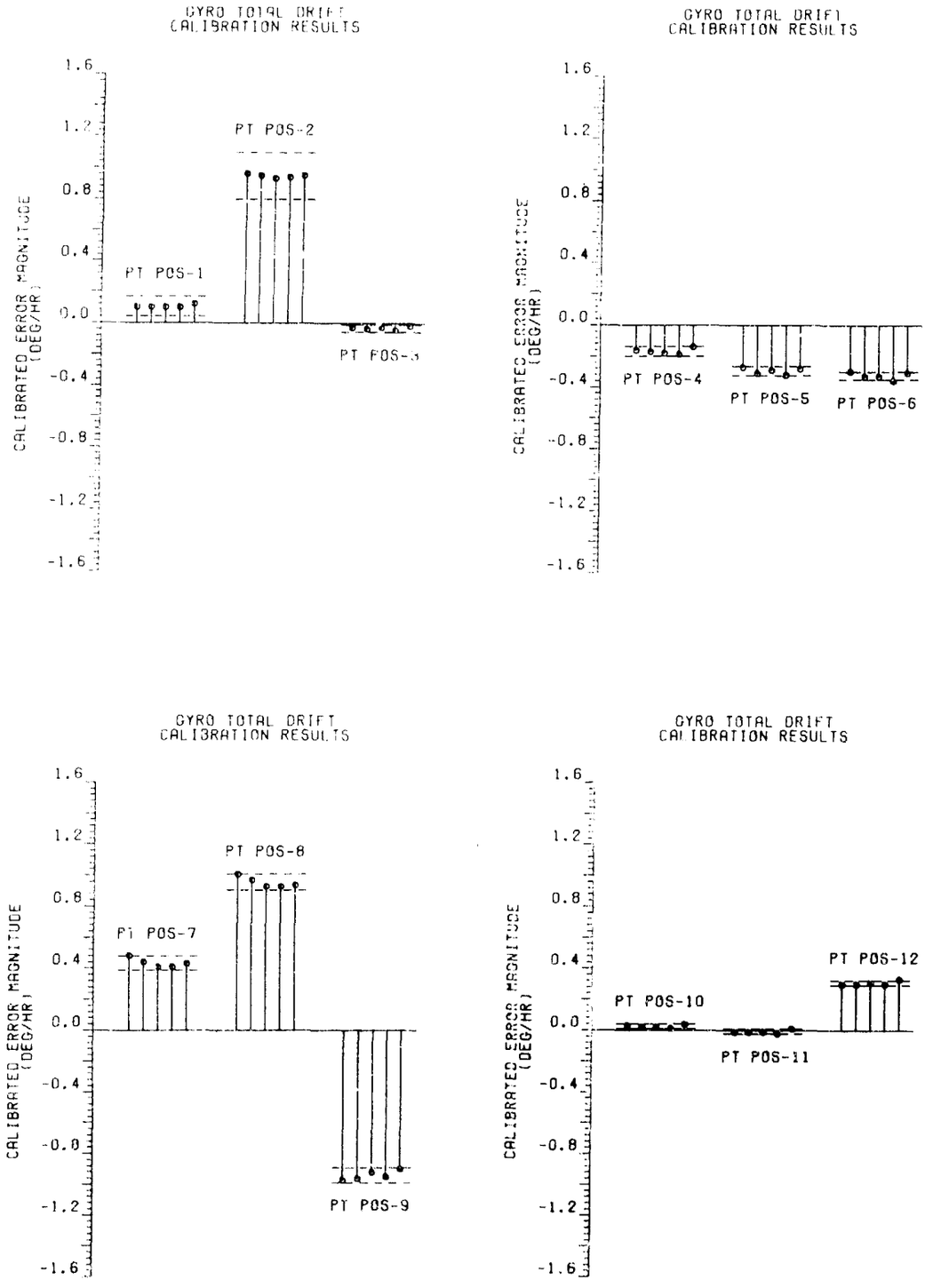

Figure 9-5. Gyro Total Drift Rate Estimation Results

and in preparation for a demonstration program with AGMC, instrument warm-up error states were included in the second version of the Kalman Filter.

Gyro thermal drift rate error modeling and fine gyro-compass alignment timing considerations are shown in Figure 9-6. The gyro warm-up characteristic consists of an exponentially decaying bias term which can be assumed to be the envelope of a complicated transient function of the ambient temperature during the rapid warm-up period. The nominal data depicted in Figure 9-6 corresponds to a 0° C ambient temperature. A similar characteristic is obtained for a 35° C ambient temperature except that the transient magnitude over the fine alignment time interval is greatly reduced. To have a negligible effect on navigation accuracy, instrument thermal transients must die out by the end of the fine alignment time interval.

The inertial instrument exponentially decaying bias modeling has been described in Section 3. It was also necessary to model the fine grain structure of the thermal transient to ensure proper filter performance. It was assumed that the fine grain component of the thermal transient could be modeled as a random bias error over two short ten second measurement intervals. The gyro error model residual states were used to implement this modeling and their uncertainty reset to its initial value every twenty seconds.

Inertial instrument exponentially decaying bias thermal transient estimation accuracy is shown in Figure 9-7. These transient errors decay rapidly to insignificant levels and need not be considered after the first test sequence. The uncertainty of these error states decreases by virtue of both the measurements made and the exponential time decay of their magnitudes. The decrease in the x, y-gyro drift rate error uncertainty is a factor 3.04 and 1.7 as a result of the exponential decay and measurements taken respectively at the end of the ten minute test sequence. Corresponding data for the accelerometers are exponential decay and measurement factors of 54.5 and only 1.24 for the x,y-accelerometers.

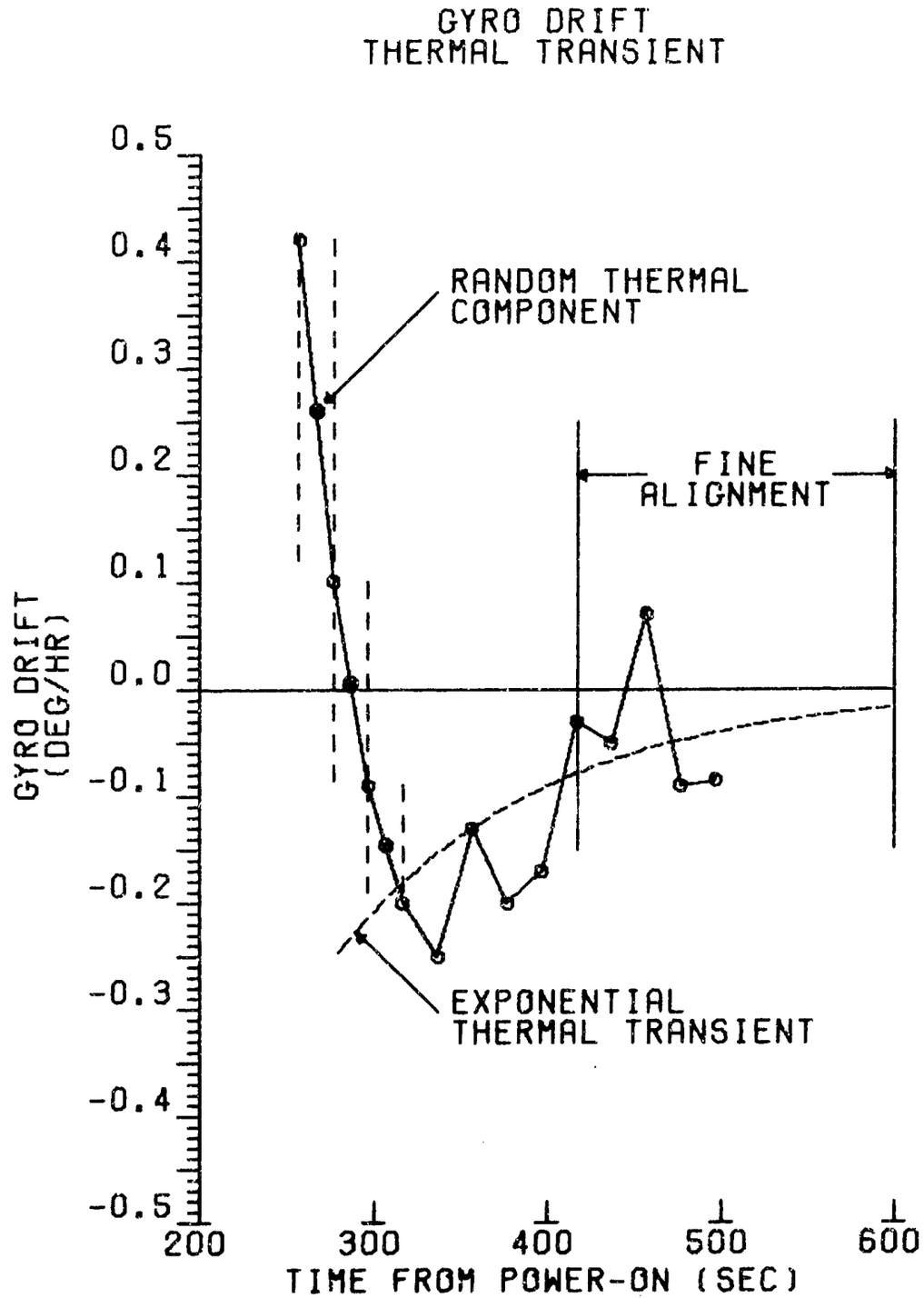

Figure 9-6. Gyro Warm-Up Drift Rate Error

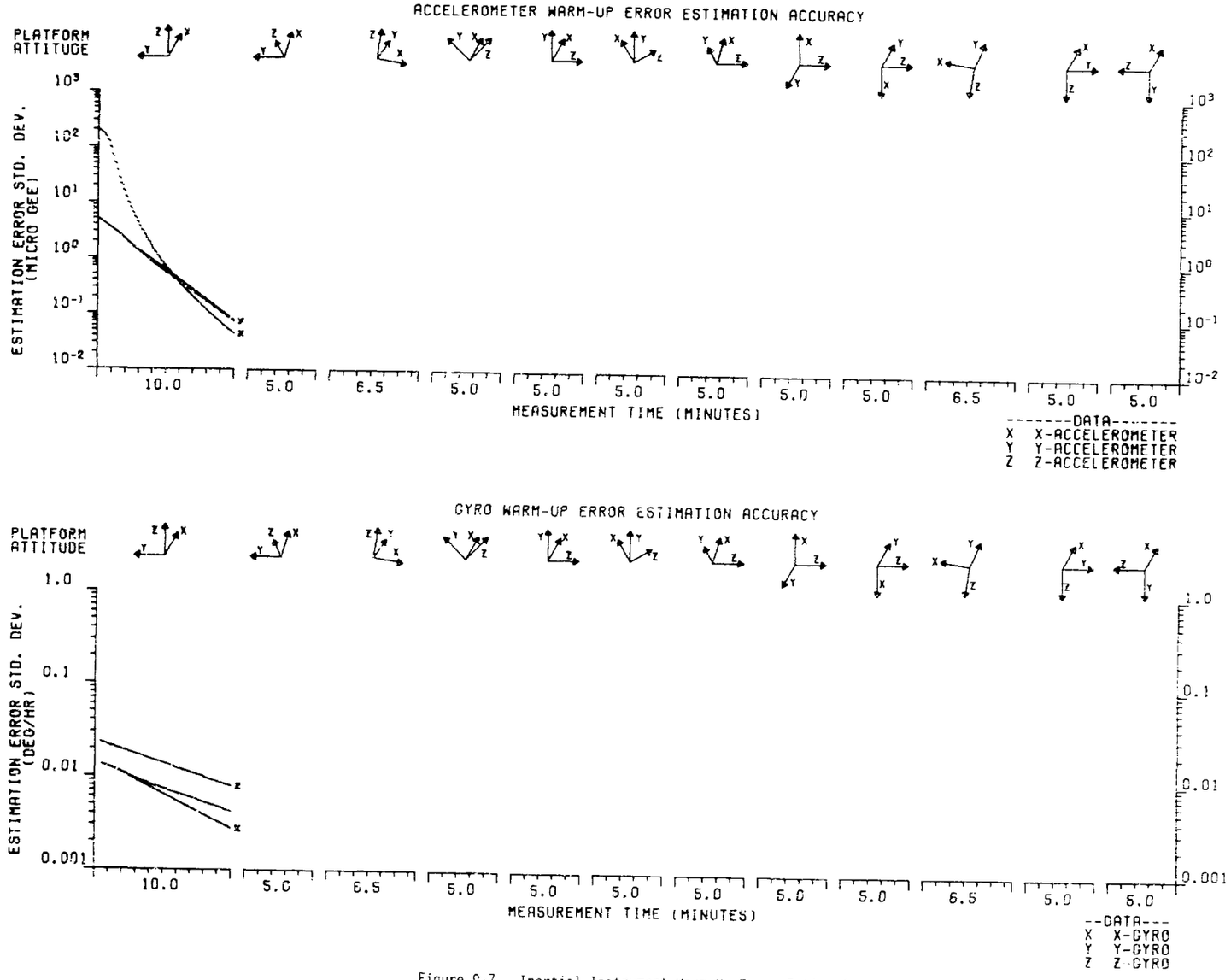

Figure 9-7. Inertial Instrument Warm-Up Error Estimation Accuracy

Inertial instrument estimated thermal transient magnitudes are shown in Figure 9-8. This data corresponds to a time instant seven minutes after power turn-on which is the start of the fine gyro-compass alignment time interval. This data was obtained by referring the Kalman Filter estimates obtained at seventeen minutes after power turn-on, seven minutes warm-up plus ten minutes measurement time, backwards in time ten minutes. The brackets superimposed about the average estimates correspond to warm-up transient uncertainty at seven minutes after power turn-on. These uncertainties were obtained by referring the seventeen minutes after power turn-on Kalman Filter estimation errors backwards in time. Table 9-1 lists the seven-minute after-power turn-on thermal warm-up transient-uncertainty reduction attributable to the Kalman Filter.

TABLE 9-1

INERTIAL INSTRUMENT THERMAL TRANSIENT
UNCERTAINTY AT SEVEN MINUTES AFTER POWER TURN ON

Inertial Instrument	Standard Deviation of Thermal Transient Uncertainty	
	Initial	After Kalman Filtering
x, y-Gyro	0.014°/hr	0.0084°/hr
z-Gyro	0.024°/hr	0.024°/hr
x, y-Accelerometer	5.0 μg	4.0 μg
z-Accelerometer	200.0 μg	2.4 μg

Table 9-1 shows that the Kalman Filter is capable of making a dramatic initial uncertainty reduction for only the z-accelerometer inertial instrument. This is possible because the warm-up transient is the only error source that gives rise to the z-accelerometer's output showing a time dependency when oriented vertically. Recovered transient magnitudes of -114, -42, -339, -414, and -42 μg indicate a rather large turn-on variation for this instrument.

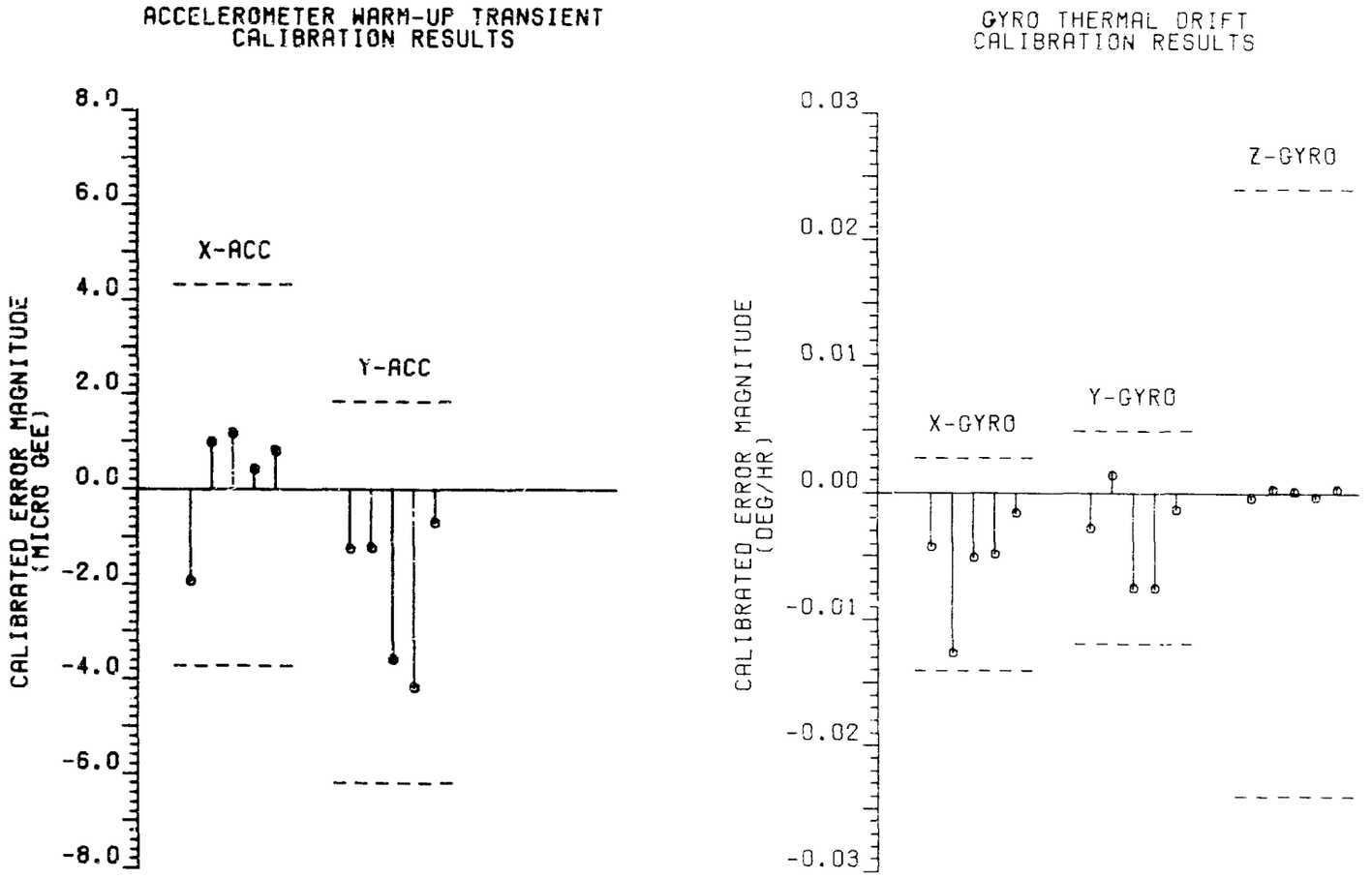

Figure 9-8. Inertial Instrument Estimated Thermal Transient Magnitudes

A conclusion drawn from the inertial instrument warm-up transient estimation results is that the magnitudes of these errors decay to roughly the instrument noise level at the end of the fine gyro-compass alignment time interval and should not, therefore, have a significant effect on alignment accuracy. This conclusion applies only to the particular KT-73 IMU tested and an ambient temperature of 23°C. While of general interest, no tests were conducted at other than with a 23°C ambient temperature.

9.4 GYRO ERROR SOURCES

Gyro error sources are considered in two groups: (1) the random disturbance errors which ultimately limit achievable navigation accuracy, and (2) the errors commonly termed calibration parameters whose effects can be software compensated for in the operational flight computer program. Gyro instrument angular alignment errors are discussed in Section 9.6.1.

9.4.1 Random Errors

Gyro random error estimation accuracy is shown in Figure 9-9. The platform test orientations and measurement times have been formulated so that the Kalman Filter estimates the gyro calibration parameters to an accuracy approaching the limit imposed by these random errors. No attempt is made to estimate these random errors by increasing the IMU measurement time. Although the filter does not significantly reduce the uncertainty of these random errors, inclusion of them in the filter is required for accurate magnitude estimation and estimation accuracy results.

Gyro attitude dependent bias drift rate error magnitude estimates are shown in Figure 9-10 for each of the platform test orientations. The estimates for these error model residual states are similar to those shown in Figure 8-3 except for being plotted to a different scale. Modeling of the discovered quadrature g error source in the Kalman Filter state vector resulted in a reduction of the magnitude estimates for these errors to the heading sensitive drift rate error hardware specification of 0.004 degree per hour.

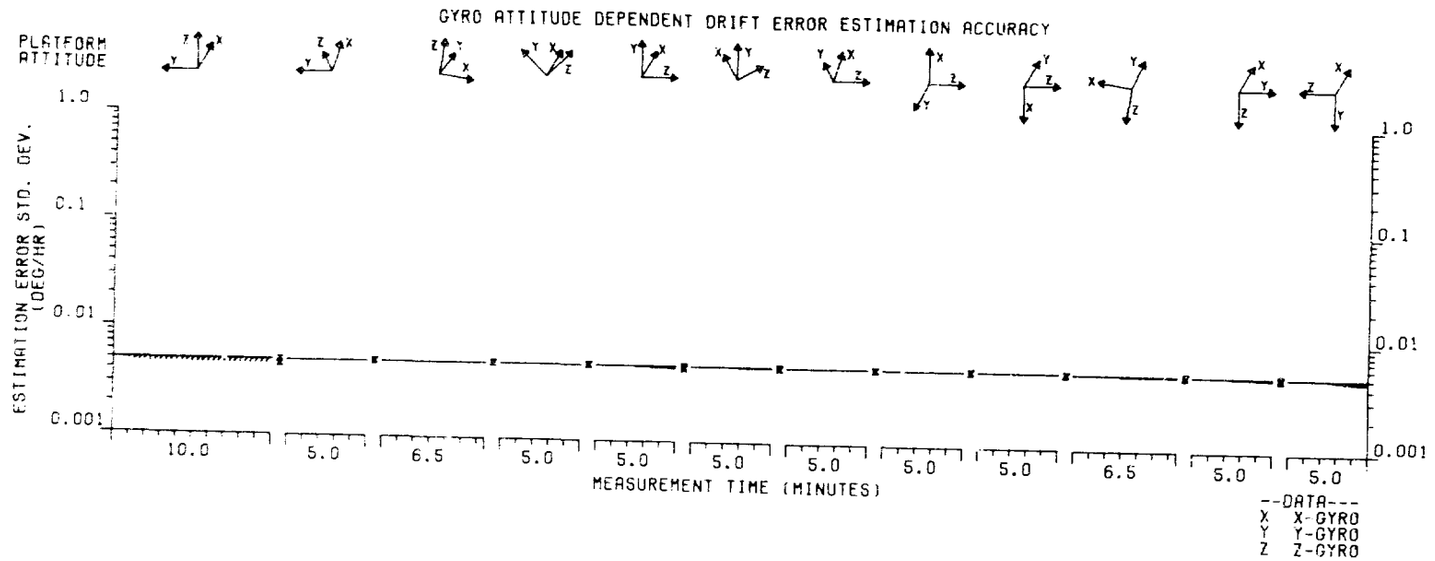

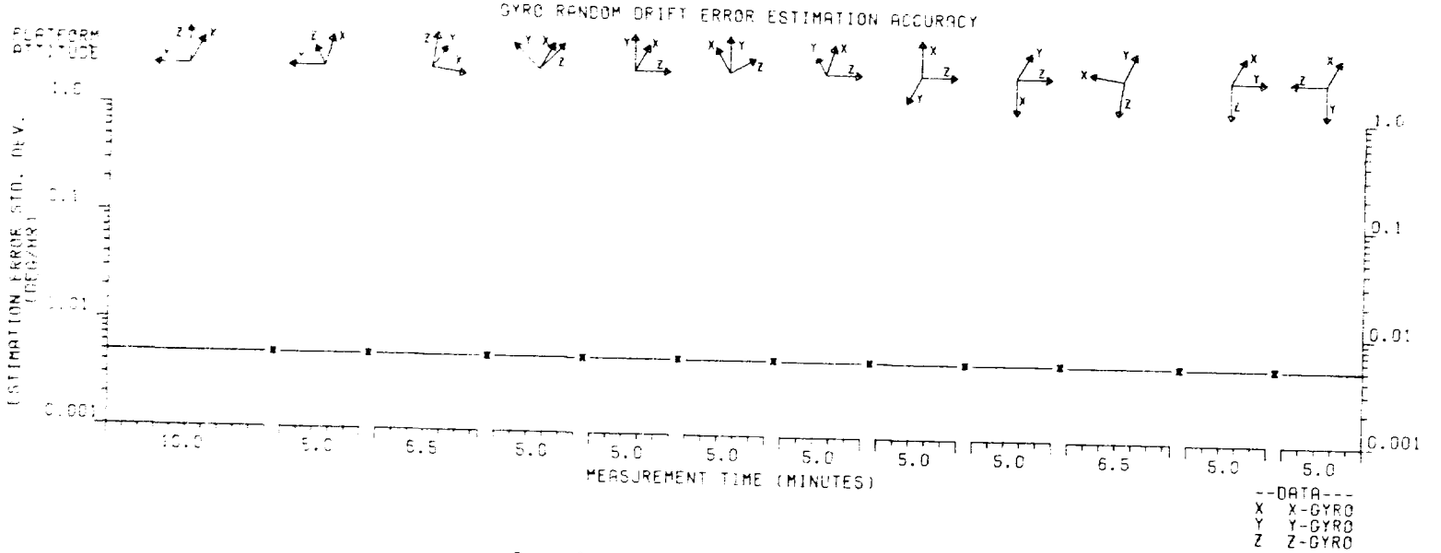

Figure 9-5. Gyro Random Error Estimation Accuracy

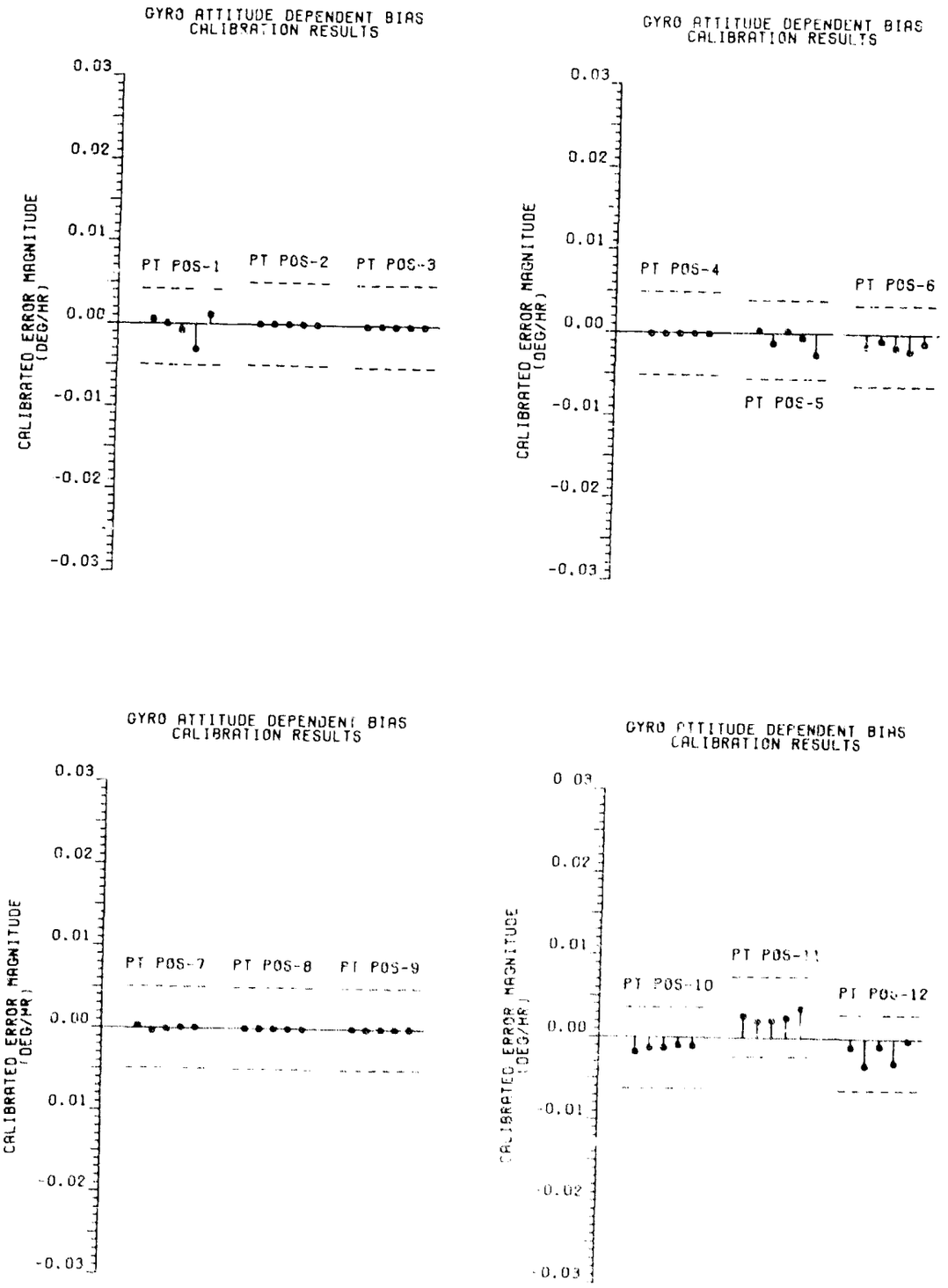

Figure [illegible] Gyro Attitude-Dependent Drift Rate Error Estimation Results

9.4.2 Calibration Parameters

Gyro bias drift rate and scale factor error estimation accuracies are shown in Figure 9-11 and corresponding magnitude estimates are given in Figure 9-12. The initial uncertainty of the error sources given in Reference 1 were not always found to be consistent with those recovered from the IMU tests. In some instances, these inconsistencies were due to discrepancies in the definition of the error sources. A good example of this is z-gyro bias, to which Reference 1 assigns an uncertainty of 0.02 degrees per hour, implying a turn-on variation. The actual hardware configuration is such that the z-gyro bias is adjusted to offset the drift rate error produced by the spin axis mass unbalance when the z-gyro input axis is oriented vertically. This procedure requires that the bias error magnitude be approximately that of the spin axis mass imbalance drift rate error in a one g field or 0.5 degree per hour.

Regardless of the reason for the discrepancies between the initial uncertainties given by Reference 1 and those implied by the Kalman Filter error magnitude estimates, the initial covariance matrix was adjusted so that its initial variances were consistent with the end-of-test Kalman Filter magnitude estimates. This procedure worked well with no apparent pitfalls; however, it should be understood that the initial IMU error source uncertainties shown by the estimation accuracy plots of this section correspond to the particular KT-73 IMU tested and do not represent an IMU error model derived by ensemble IMU testing.

Reference to the trends of and final estimation accuracies shown in Figure 9-11 indicates that estimation accuracies could be further reduced by increasing the length of the test. A covariance analysis showed that the gyro bias drift rate estimation errors could be further reduced to the limiting 0.005 degree per hour by adding a couple of additional platform test attitudes and doubling the measurement time. This was felt to be unnecessary since the calibration accuracy obtained by the present test schedule is consistent with the one to three NM inertial navigation performance of the KT-73 IMU. Note that the turn-on

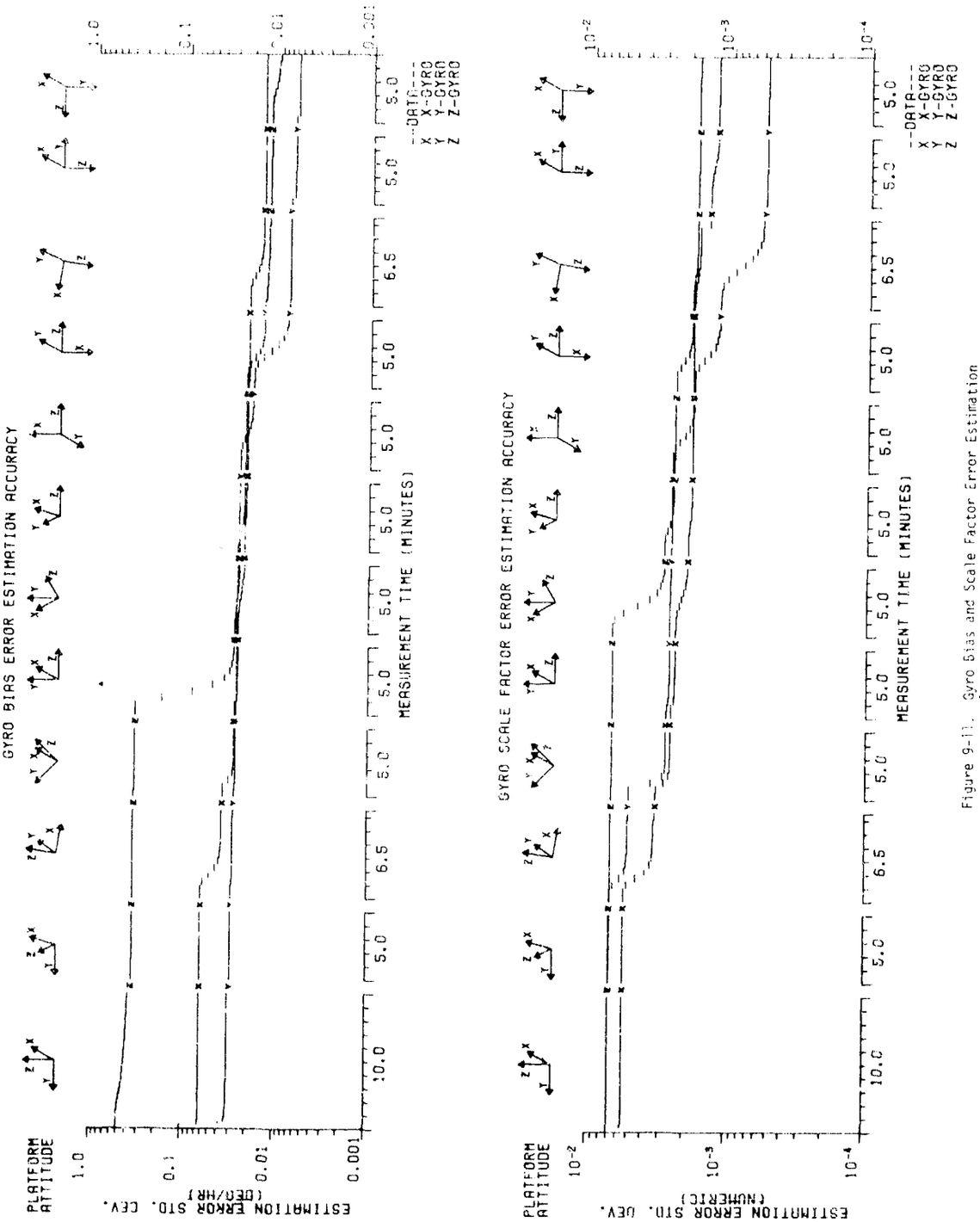

Figure 9-11. Gyro Bias and Scale Factor Error Estimation Accuracy

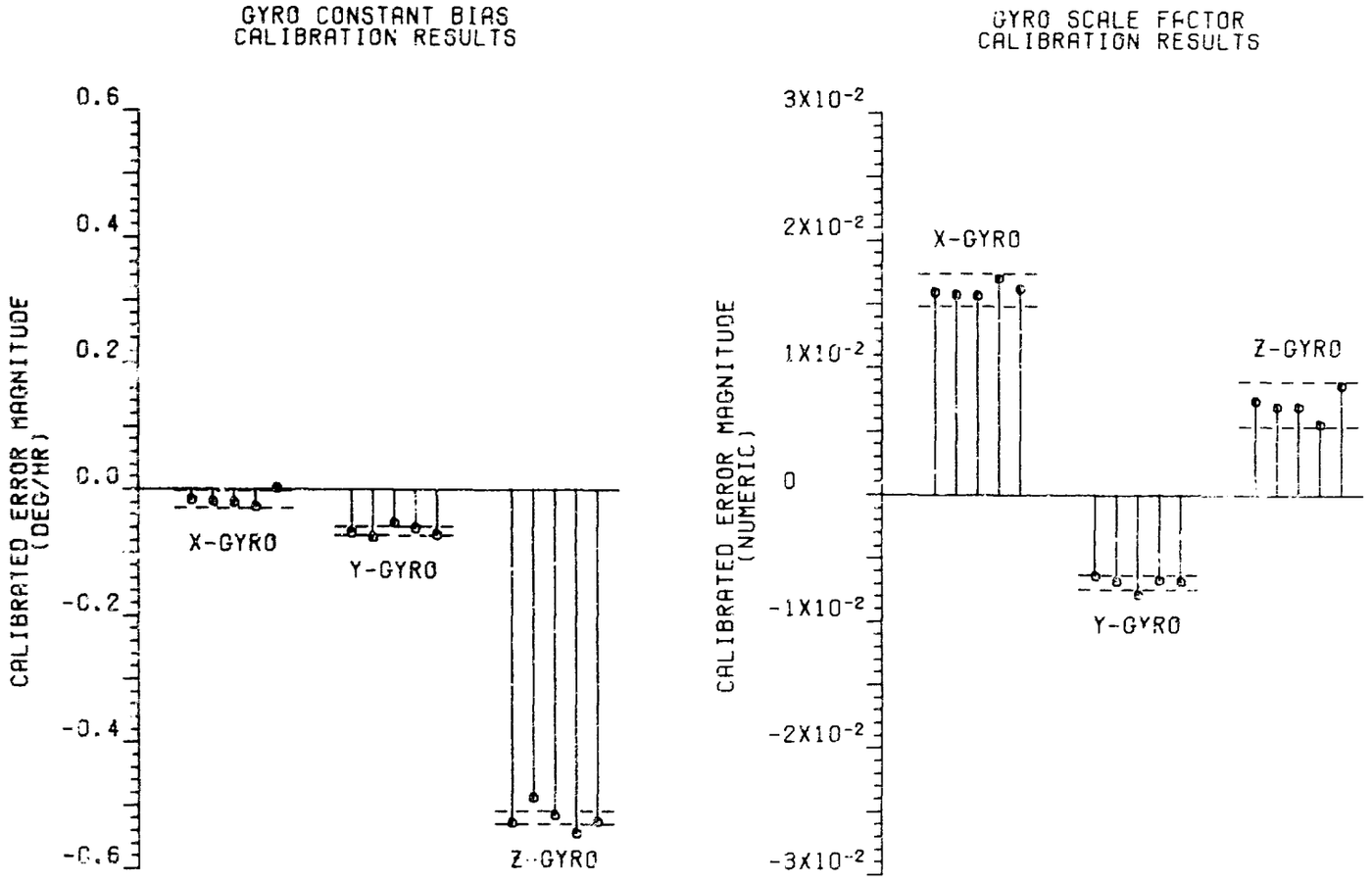

Figure 9-12. Gyro Bias and Scale Factor Error Magnitude Estimates

gyro bias drift rate error variations shown in Figure 9-12 are consistent with the 0.01 degree per hour gyro performance claimed for the system.

Specific force dependent gyro drift rate error estimation accuracies are shown in Figures 9-13 and 9-15 and corresponding magnitude estimates shown in Figures 9-14 and 9-16. The input axis mass unbalance errors appears to be insignificant error sources for the IMU while the recovered spin axis mass unbalance errors were found to be a factor of three larger than given in Reference 1. The g-squared gyro anisoelastic error also appears to be insignificant while the discovered quadrature g errors can be significant for high velocity and dynamic flight profiles. Note that all the specific force-dependent gyro drift rate errors are repeatable to within the estimation accuracy of the Kalman Filter. No significant shift in any of these errors was observed in over 400 hours of IMU operation accumulated in a year's time. Software compensation for these error sources would be a straightforward procedure.

The symmetry of construction between the x and y axes of the two-degree-of-freedom x, y-gyro provides a ready means for cross checking some of the Kalman Filter estimates. Since the x and y channels of this gyro share the same spin axis, mass unbalance of this axis should produce identical mass unbalance drift rate error coefficients for these channels. Unsymmetrical machining of the rotating flexure suspension joint should also give rise to equal quadrature g drift rate error coefficients for these channels. Reference to Figures 9-14 and 9-16 shows that the filter has estimated these error sources to be of the same magnitude for each channel to within the estimation accuracy. Inclusion of the high degree of correlation in the initial covariance matrix does not, however, substantially increase the estimation accuracy for these error states.

9.5 ACCELEROMETER ERROR SOURCES

The accelerometer error sources are covered in a similar manner to those for the gyro. They are grouped into random disturbances and the

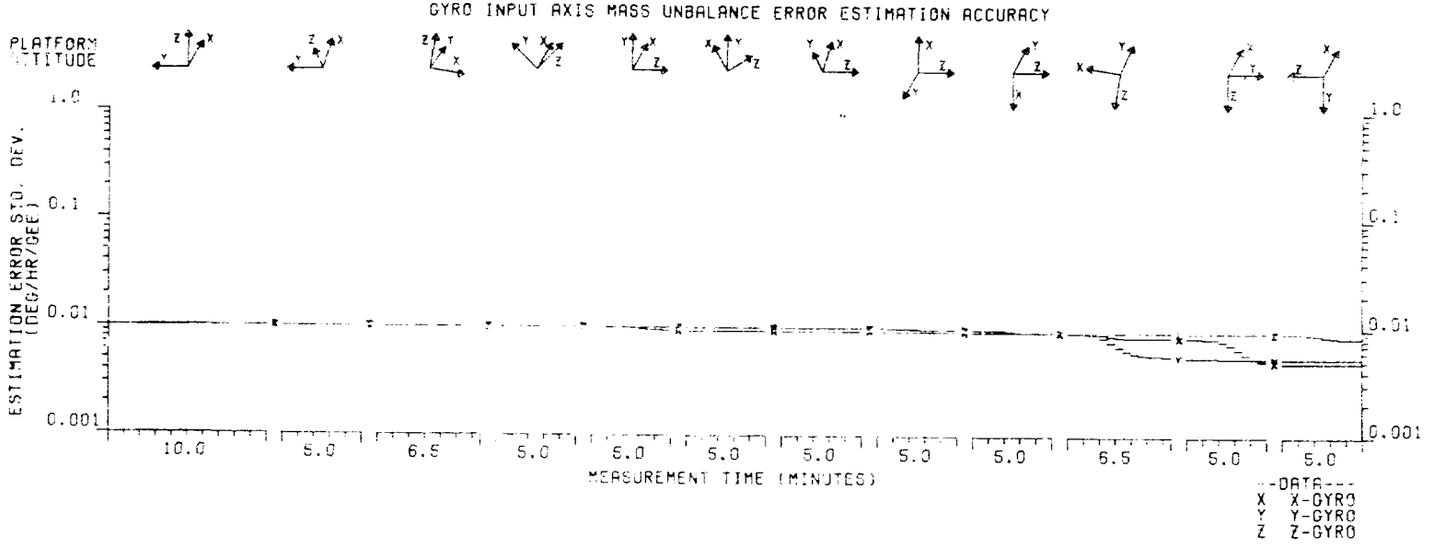

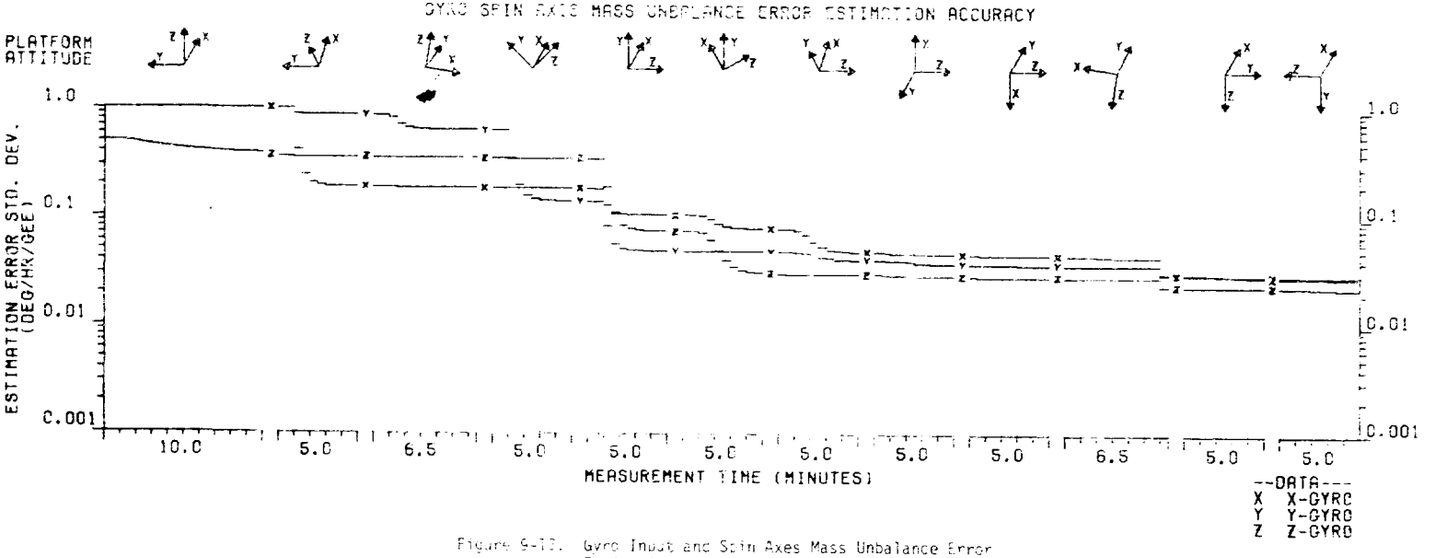

Figure 9-12. Gyro Input and Spin Axes Mass Unbalance Error Estimation Accuracy

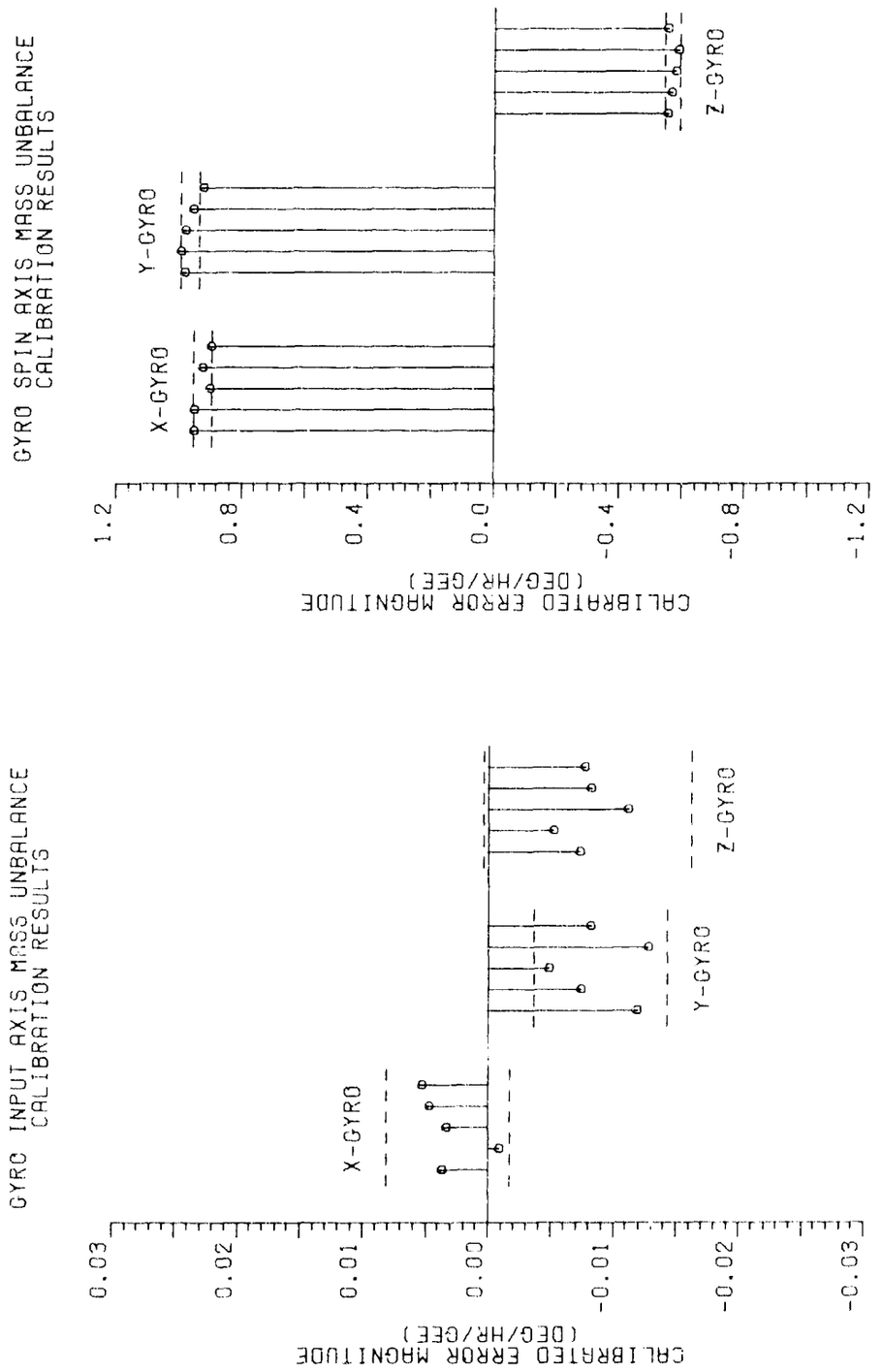

Figure 9-14. Gyro Input and Spin Axes Mass Unbalance Coefficient Magnitude Estimates

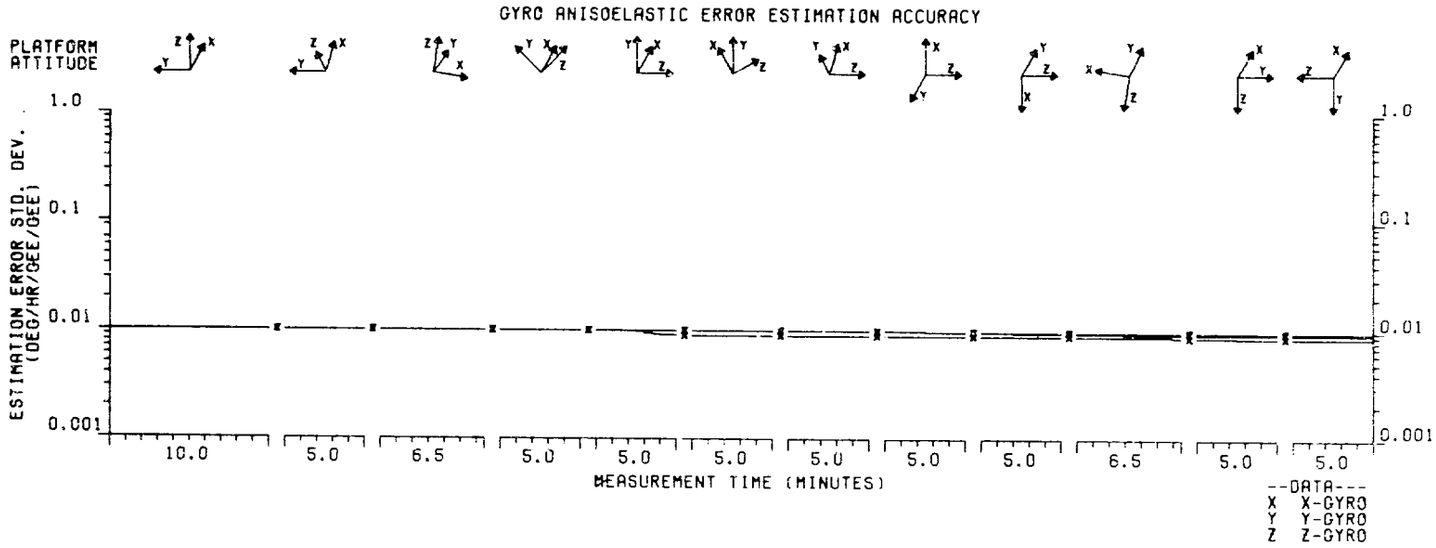

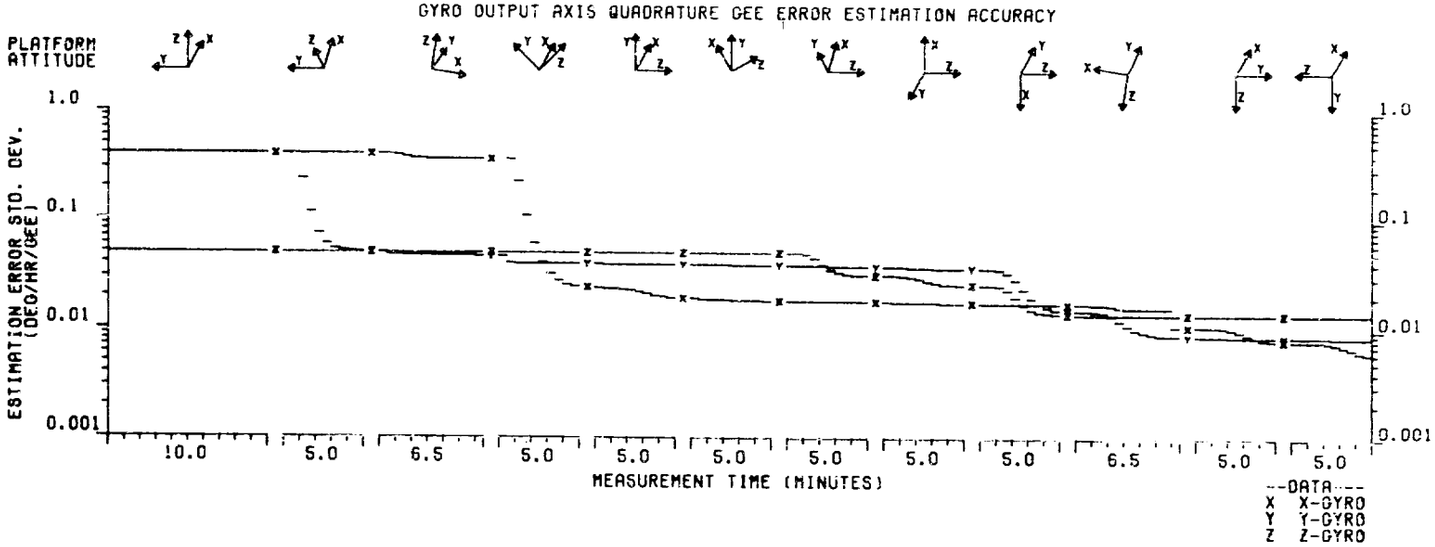

Figure 9-15. Gyro Anisoelastic and Quadrature Gee Error Estimation Accuracy

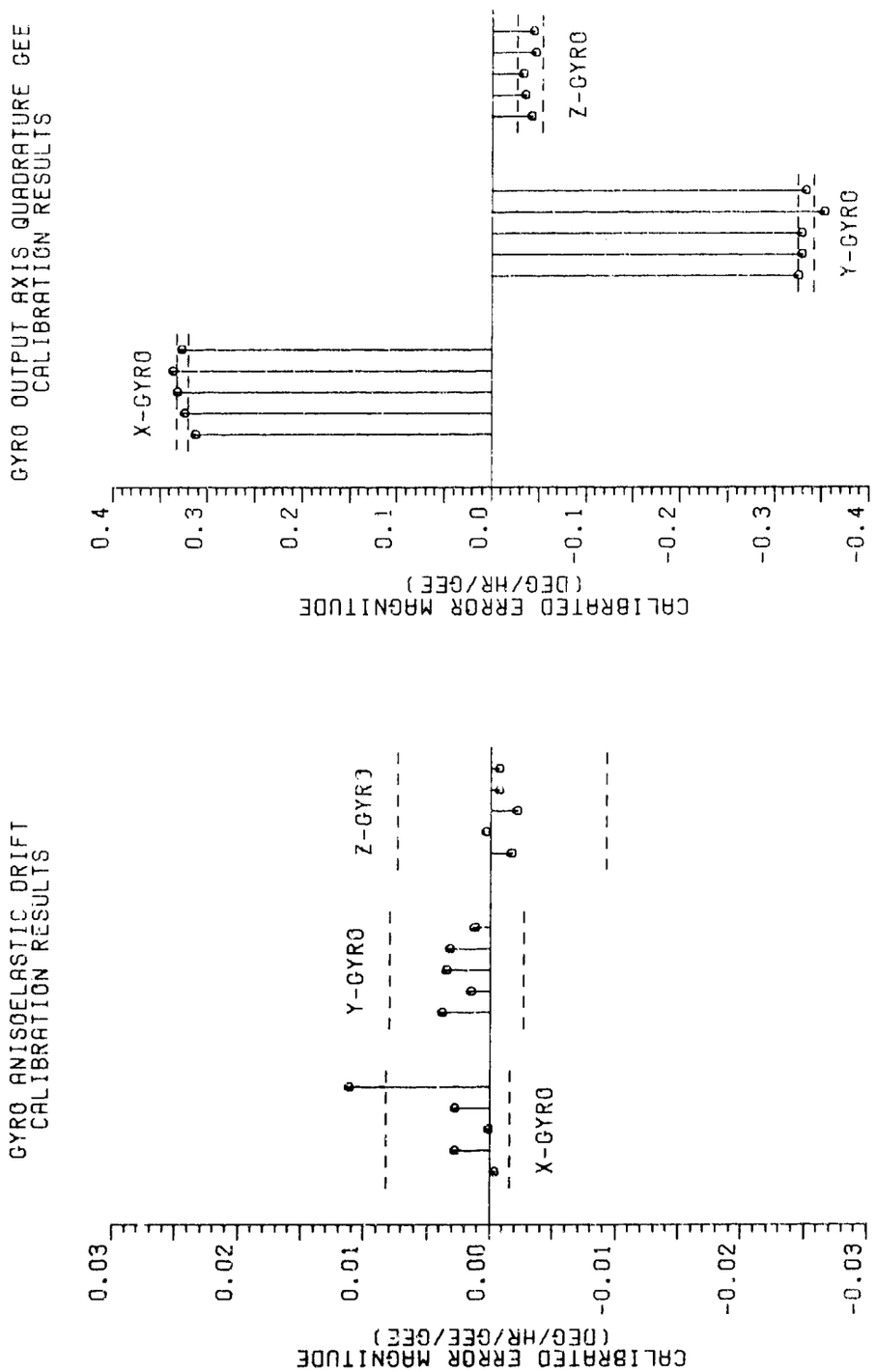

Figure 9-16. Gyro Anisoelastic and Quadrature Gee Error Coefficient Magnitude Estimates

commonly denoted calibration parameters with the accelerometer instrument angular misalignments being treated in Section 9.6.1.

9.5.1 Random Errors

Accelerometer random error estimation accuracy is shown in Figure 9-17 and the corresponding magnitude estimates depicted in Figures 9-18 and 9-19. The attitude-dependent scale factor errors represent the accelerometer error model residual states and are the major random errors limiting accelerometer parameter calibration accuracy. These errors are thought to be related to magnetic field variations with platform-to-IMU case attitude changes, since they do not show a time dependency as would be the case if they were temperature related. The clock stability error refers to the real-time software measurement timing error and is modeled as a scale factor error which affects all three accelerometers. Although the filter is unable to significantly reduce the uncertainty of these errors, inclusion of their effects in the filter algorithm is essential to obtaining proper estimation results.

The attitude-dependent scale factor error magnitude estimates shown in Figure 9-18 represent that set having the largest recovered value for a particular test attitude. Comparing these estimates with the platform test attitudes shown in Figure 7-2 shows that discrepancies appear only after a particular accelerometer's input axis has been oriented at or near vertical for the second time, orientations both up or down, as would be expected. Comparing the measurement timing with the attitude-dependent scale factor error magnitude estimates shows them to be of generally reduced magnitudes. Since the real-time software timing errors do not appreciably affect IMU calibration accuracy, as compared to the attitude-dependent scale factor errors, efforts to improve the real-time data collection software were suspended.

9.5.2 Calibration Parameters

Accelerometer low and high gain mode bias and scale factor error estimation accuracies are shown in Figure 9-20 and 9-22 and the corresponding magnitude estimates shown in Figures 9-21 and 9-23.

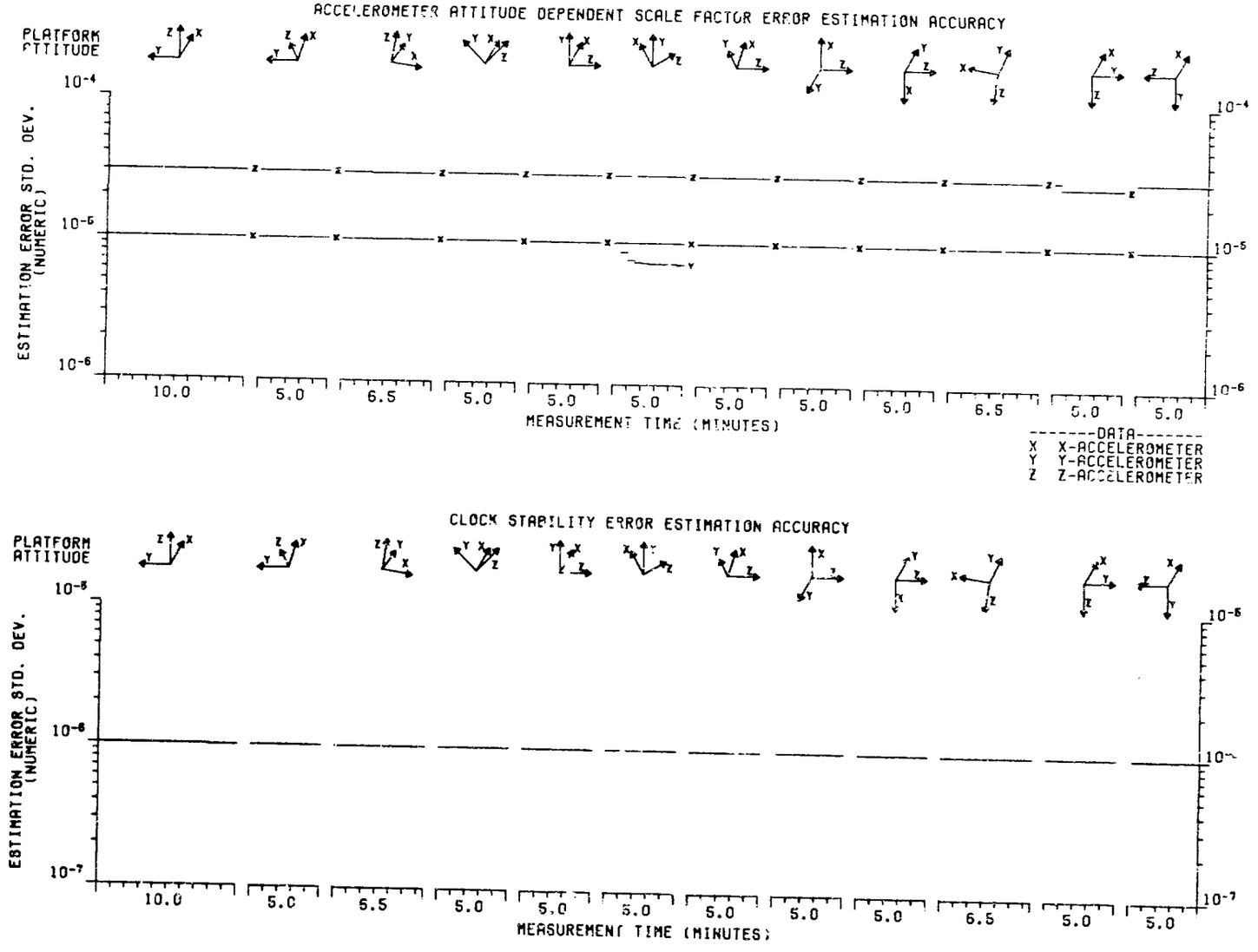

Figure 9-17. Accelerometer Random Error Estimation Accuracy

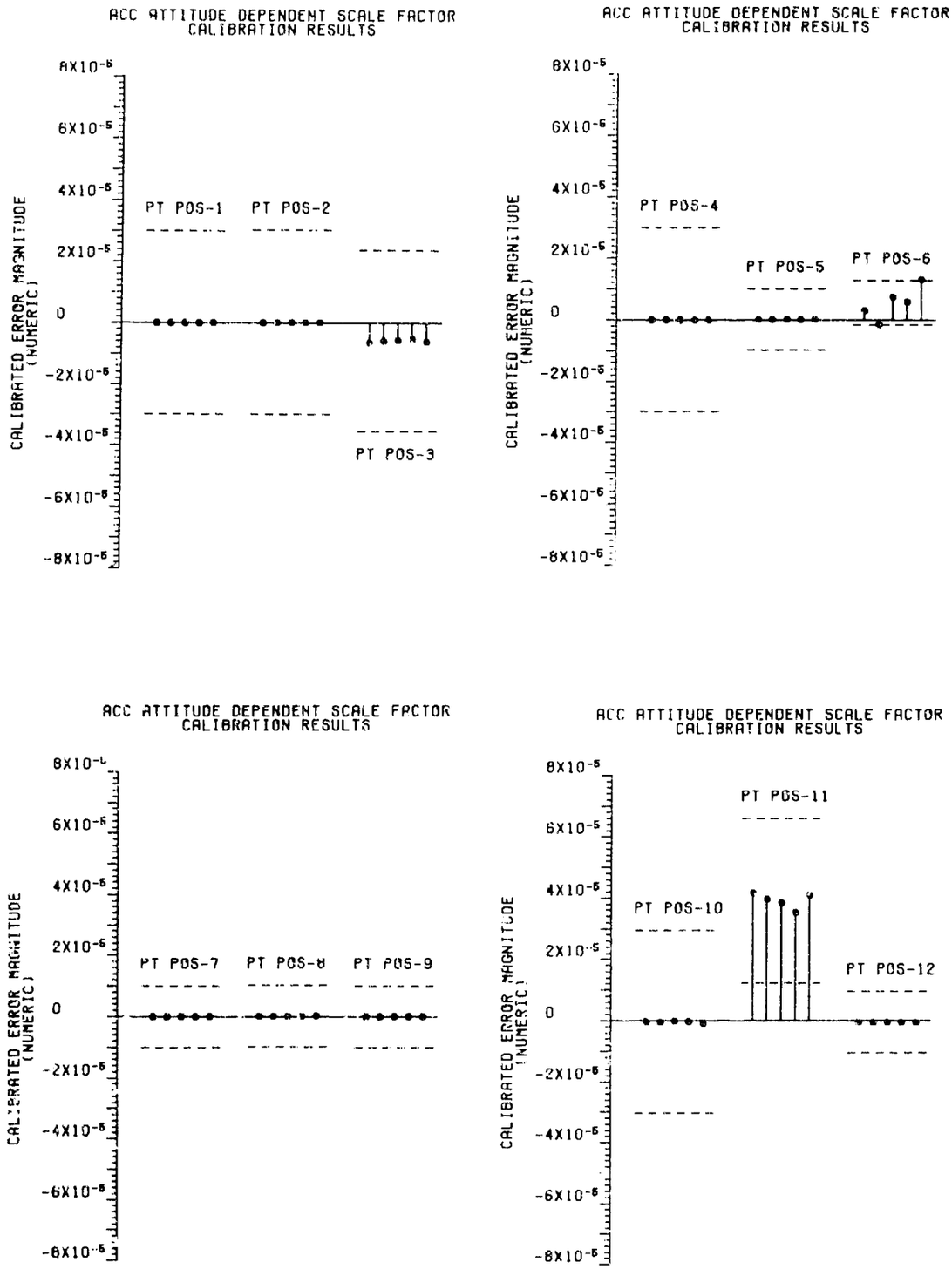

Figure 9-18. Accelerometer Attitude Dependent Scale Factor Error Magnitude Estimates

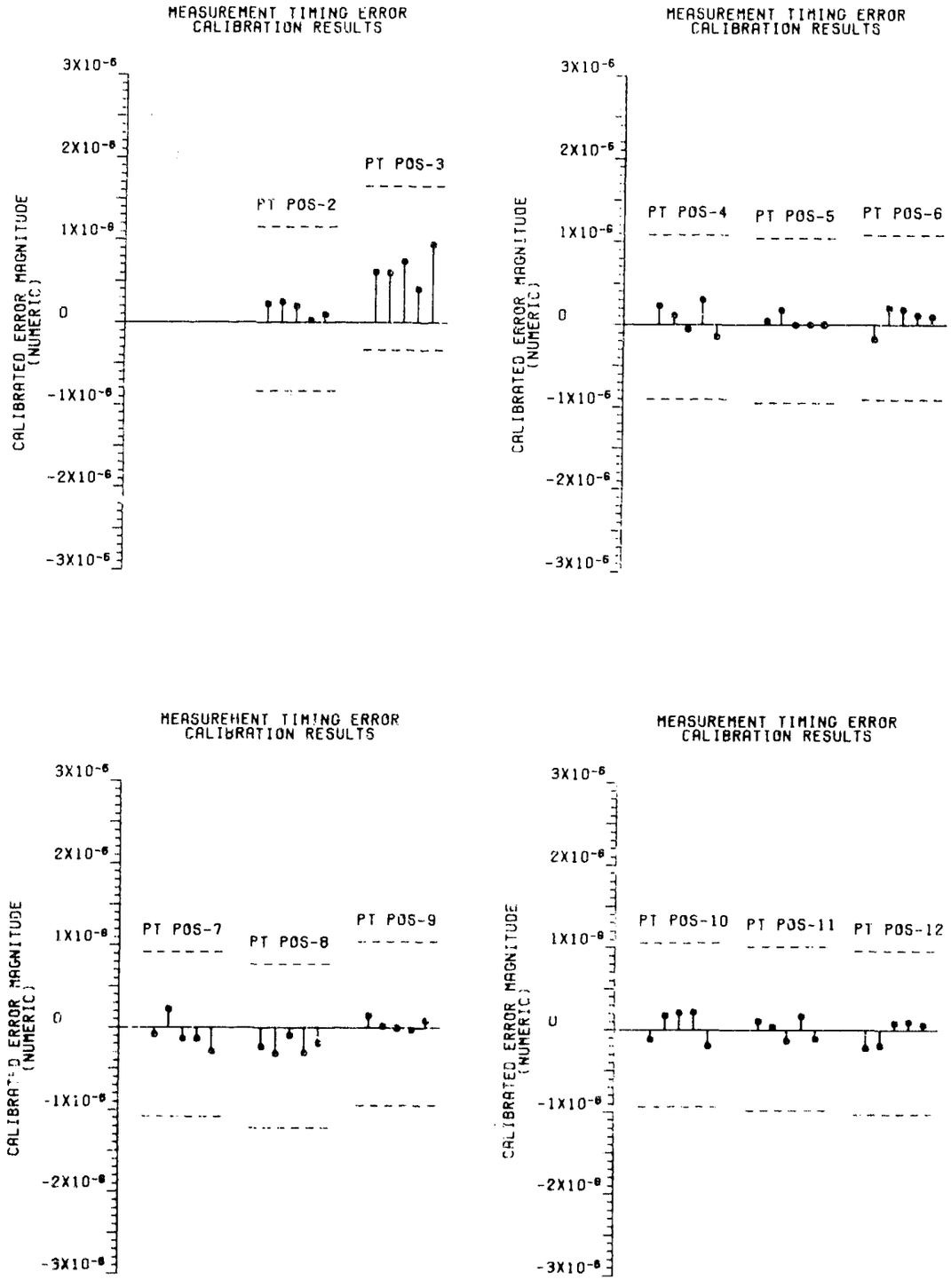

Figure 9-19. Measurement Timing Error Magnitude Estimates

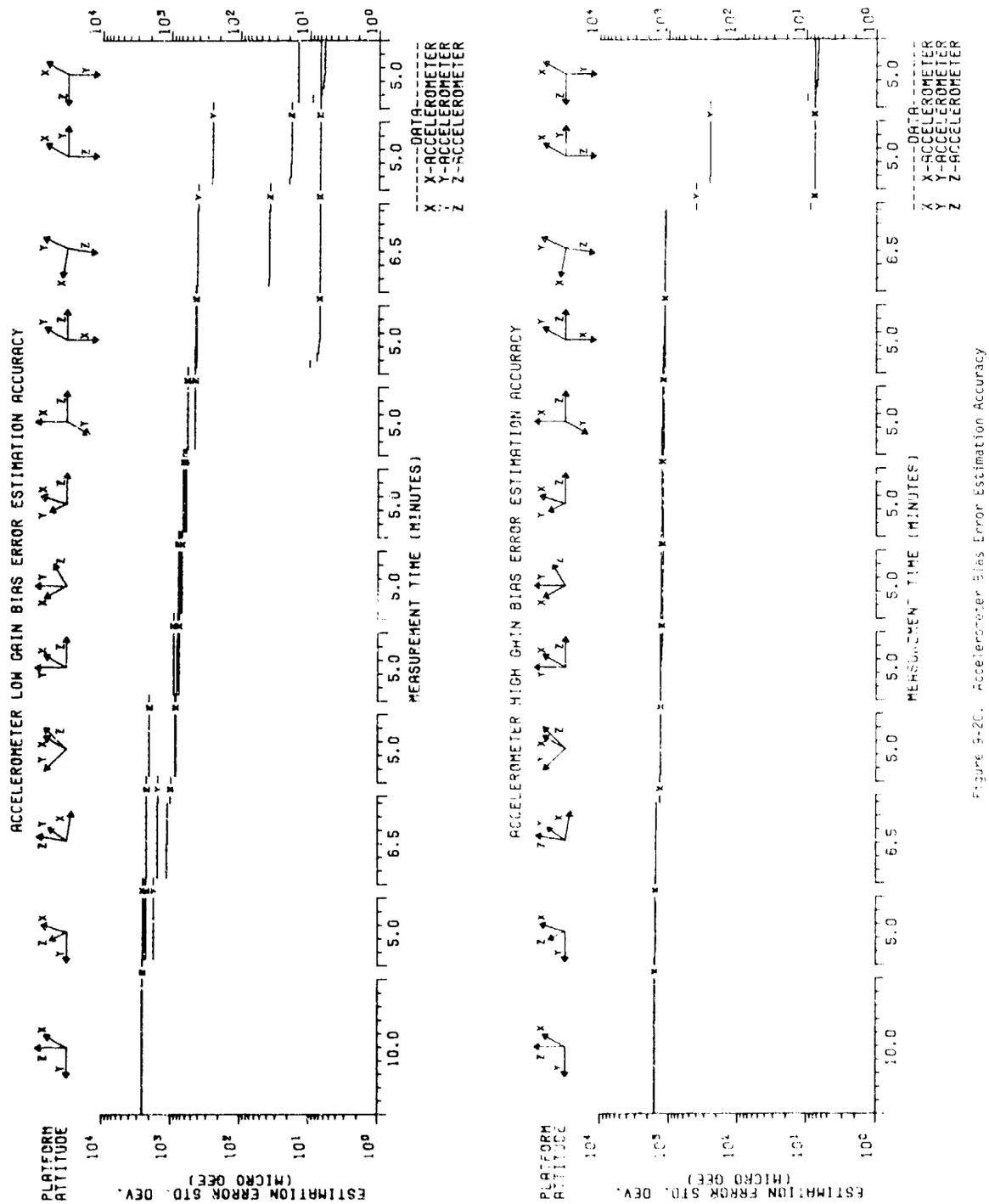

Figure 5-20. Accelerometer Bias Error Estimation Accuracy

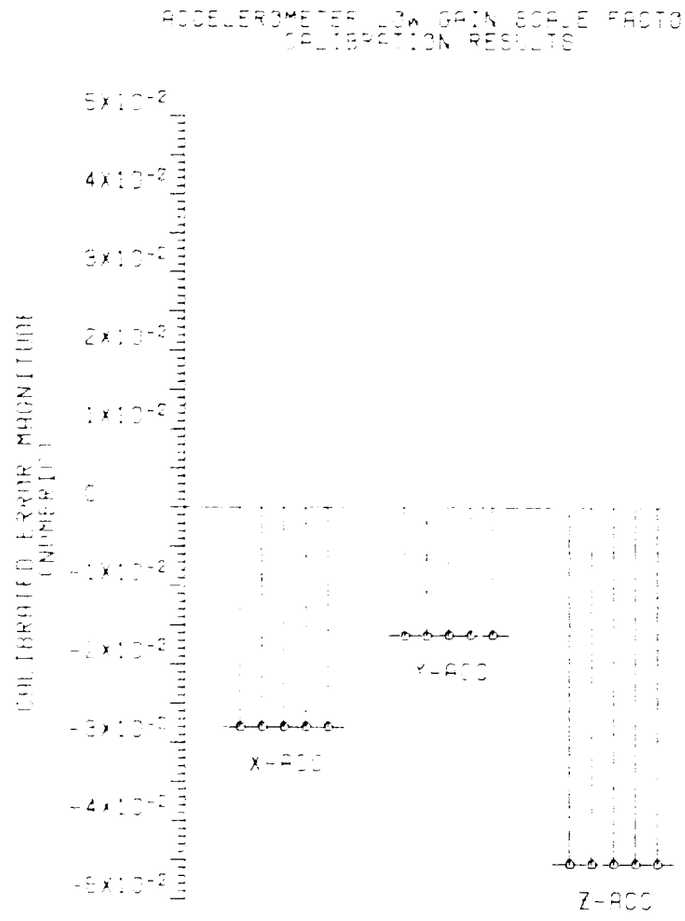

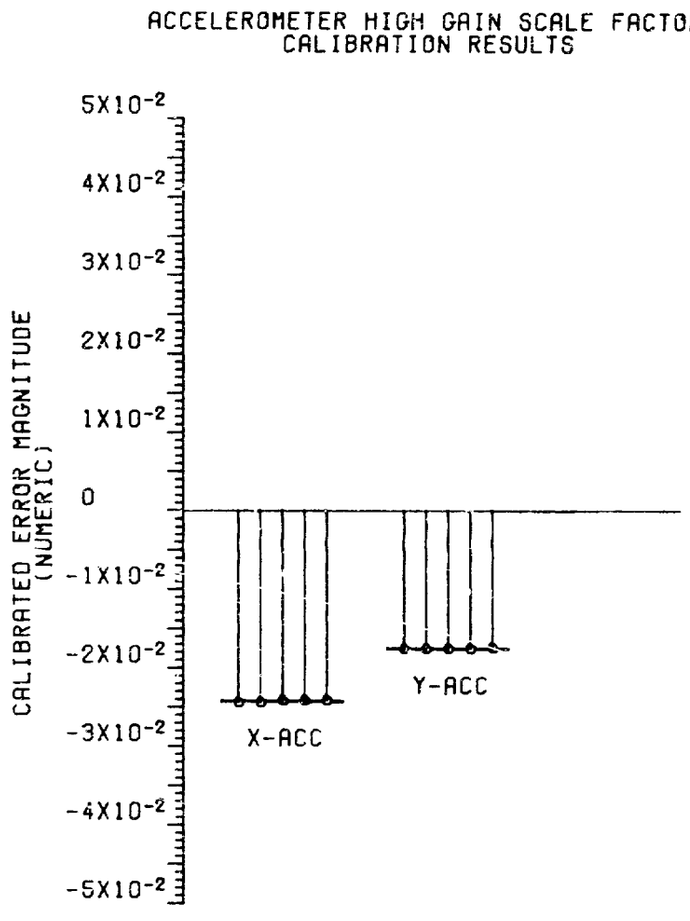

Figure 9-21. Accelerometer Bias Error Magnitude Estimates

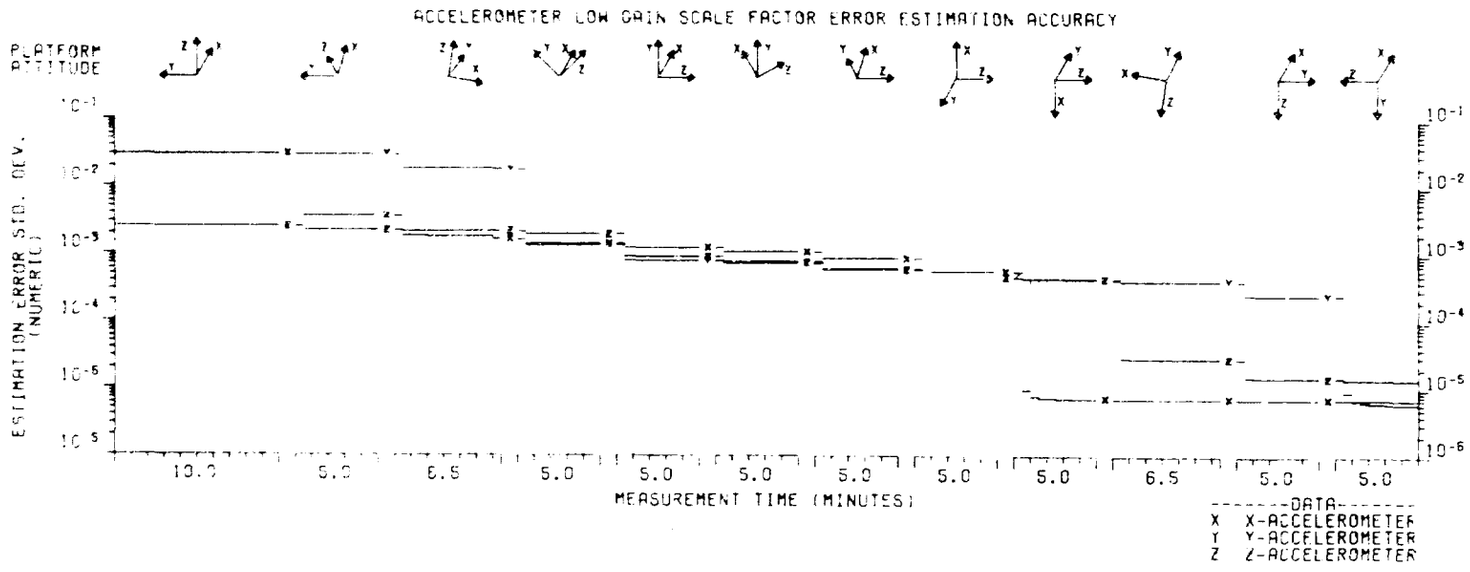

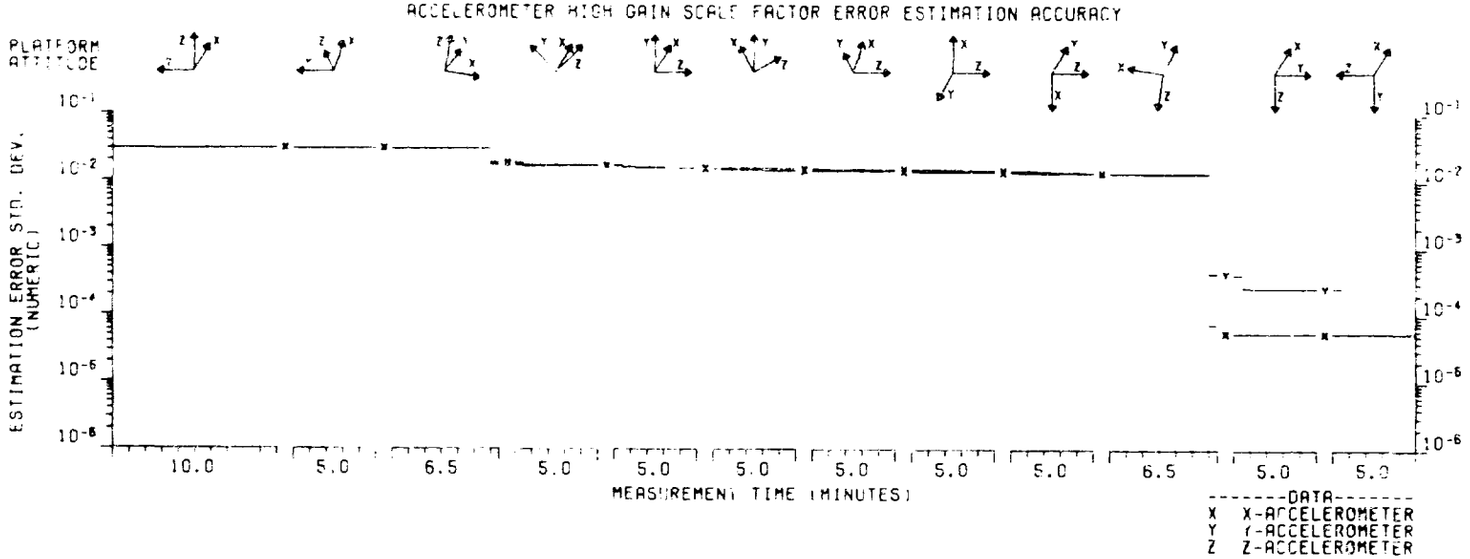

Figure 4-2. Accelerometer Scale Factor Error Estimation Accuracy

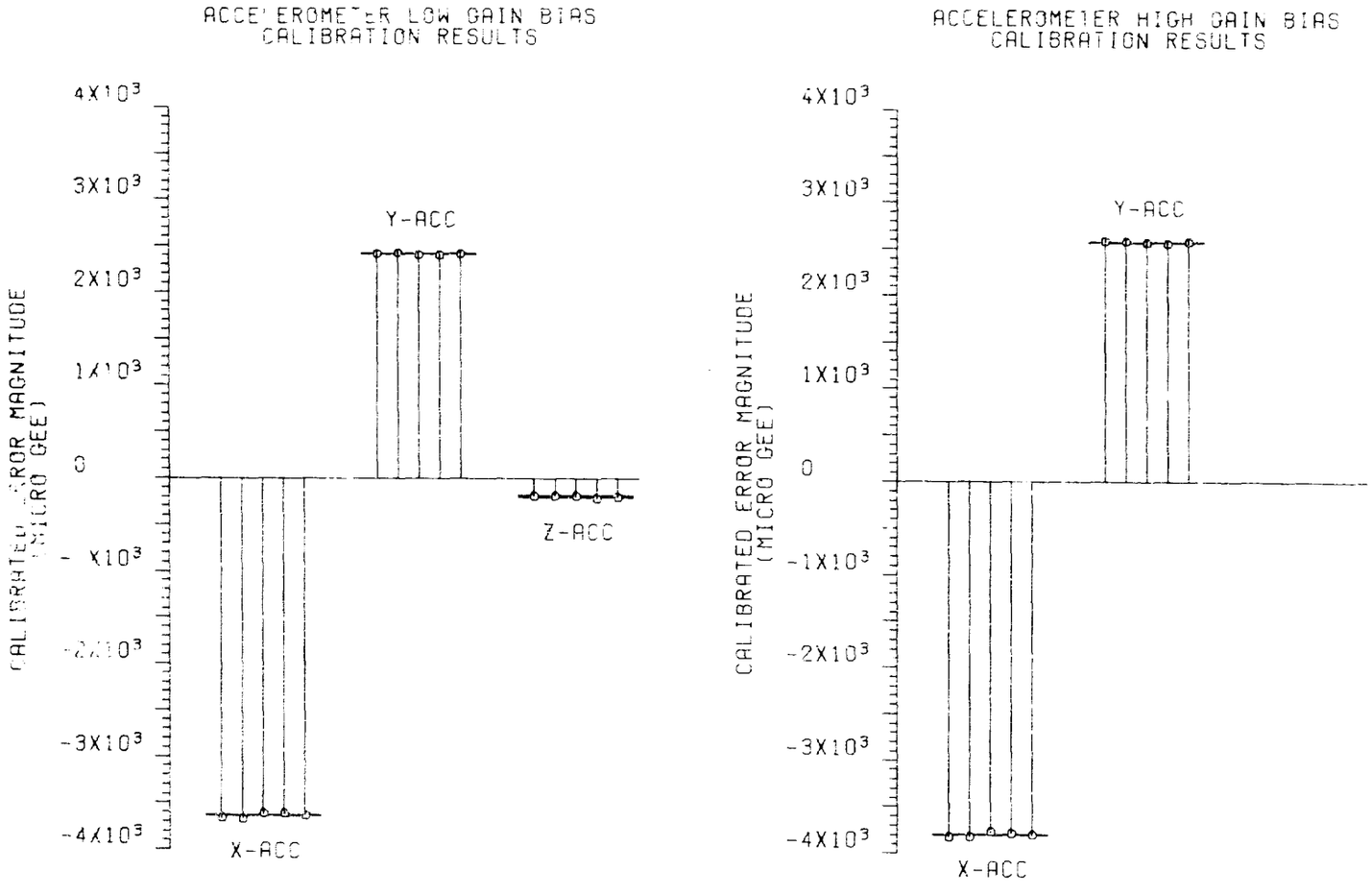

Figure 9-23. Accelerometer Scale Factor Error Magnitude Estimates

Low gain mode bias and scale factor errors can be separated and accurately observed by the Kalman Filter after an accelerometer's input axis has been oriented up and down in the gravity field. Error source separation is possible using these attitudes because no other IMU errors, except the low level random disturbances, have a first-order effect on the accelerometer's output when its input axis is parallel to the gravity vector.

The above technique cannot be used to separate the alignment high gain mode bias and scale factor errors because the capacitive reset integrators (CAPRIS) saturate at a pulse repetition frequency of ten thousand pulses per second, which occurs when an accelerometer's input axis is tilted about six degrees off horizontal. Calibration of the high gain mode bias and scale factor errors, therefore, requires extremely accurate accelerometer attitude information, including the angular drift over the measurement interval. The philosophy used in calibrating the high gain mode errors is to use two platform test attitudes where the accelerometer's input axes are oriented both up and down roughly five degrees off horizontal. To allow both an accurate accelerometer attitude and attitude rate determination, the Kalman Filter employs low gain accelerometer measurements over the first five minutes of the platform test sequences, which are No. 3 and No. 10. The accelerometer mode is then switched from low to high gain and high gain measurements made for an additional minute after a thirty second switching delay. Complete separation of the high gain errors must, however, wait until the filter is able to separate the low gain errors during test sequence No. 12. This is an efficient procedure for estimating the high gain errors because the two test attitudes used were perturbations of existing ones and not additionally added.

Examination of the bias and scale factor error magnitude estimates shown in Figures 9-21 and 9-23 indicates that the repeatability of the estimate is on the order of the estimation error. For example, x-accelerometer low gain bias estimates fluctuate about 20 to 25 μg about the average estimate, which is a factor of 3 to 4 times the estimation

error standard deviation. The y-accelerometer estimate variations are somewhat less, being only 1 to 2 times the estimation error standard deviation. Both variations are well within the manufacturer's Reference 1 value of 67 μg. Whether these variations are due to instrument turn-on fluctuations or measurement error or combinations of both is not known. Estimation repeatability on the order of 10 μg was only obtained after adding the random errors of Section 9.5.1 to the Kalman Filter state vector.

9.6 ANGULAR ERROR SOURCES

Angular error sources estimated by the Kalman Filter fall into two classes: inertial instrument-to-platform frame misalignment errors, and angular errors associated with orienting the platform relative to the navigation frame.

9.6.1 Inertial Instruments

Accelerometer and gyro-to-platform frame misalignment angle estimation accuracy is shown in Figure 9-24 and the corresponding magnitude estimates given in Figure 9-25. As discussed in Section 8.3, inertial instrument misalignment angle errors relative to the navigation frame are the quantities of fundamental importance in the calibration methodology. The inertial instrument-to-navigation frame misalignment angles are composite error sources composed of inertial instrument-to-platform, synchro differential and bias and IMU case-to-navigation frame angle errors. The Kalman Filter is precluded from accurately estimating the inertial instrument-to-platform misalignment angle errors because it cannot separate them from the synchro angle bias errors which assume new values each time the platform is reoriented.

In an attempt to overcome this estimation accuracy limitation, gyro and accelerometer misalignment angle errors have been reformulated to represent instrument misalignments from orthogonal sets and the misalignment of the orthogonal instrument sets from each other rather than

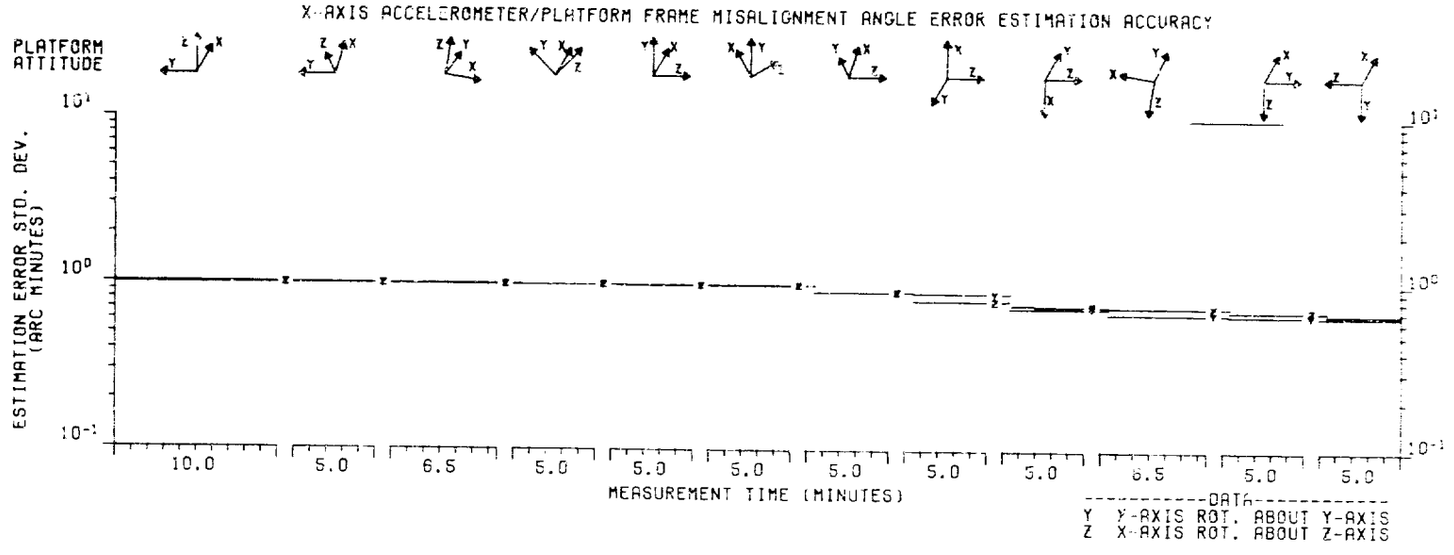

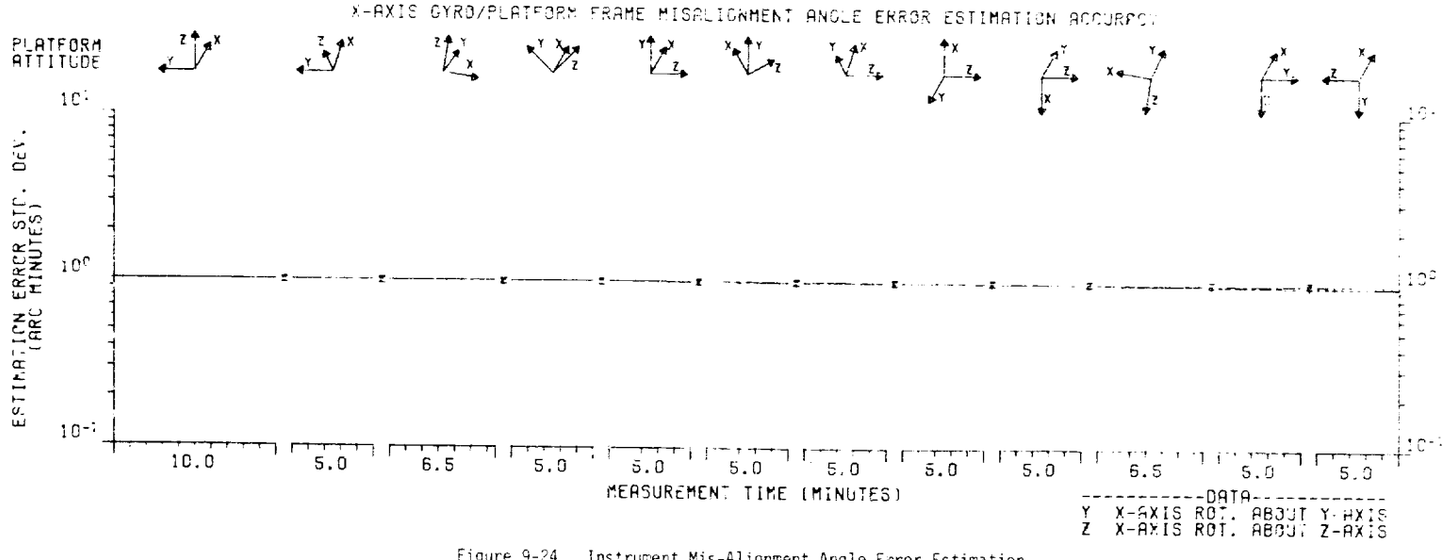

Figure 9-24. Instrument Mis-Alignment Angle Error Estimation Accuracy

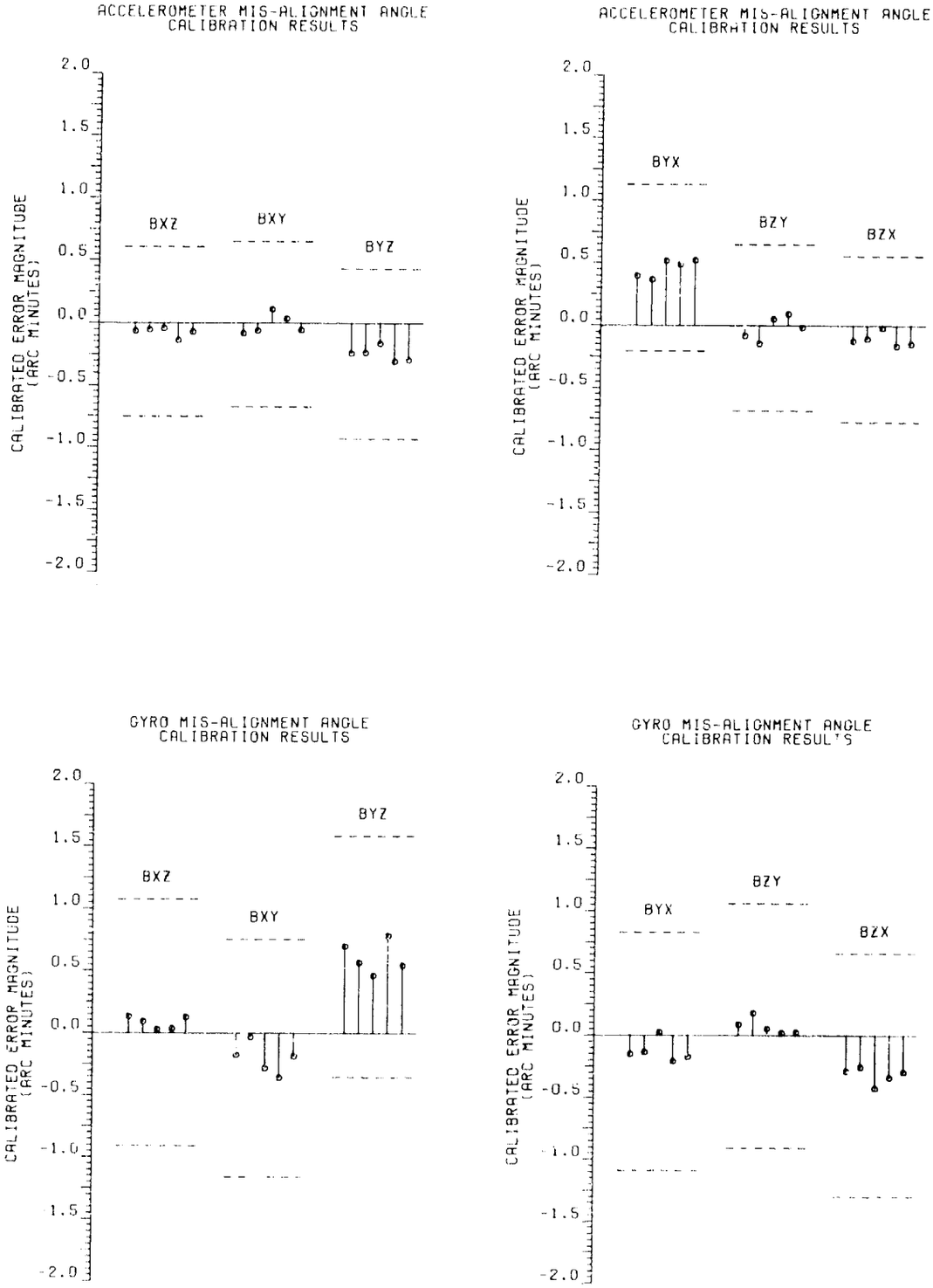

Figure 9-25. Instrument Mis-Alignment Angle Error Magnitude Estimates

the platform. The motivation for this approach is to let the inertial instruments serve as relative references rather than to use the gravity vector as an absolute reference.

Accelerometer and gyro instrument set non-orthogonality angle error estimation accuracies are shown in Figure 9-26 and the corresponding magnitude estimates given in Figure 9-27. The estimation accuracy of the misalignment between the "squared-up" accelerometer and gyro instrument sets is shown in Figure 9-28 and the corresponding magnitude estimates given in Figure 9-29. The misalignment of the instrument sets from each other is approximated by a small angle orthogonal coordinate transformation matrix.

Figure 9-26 shows that the Kalman Filter is capable of calibrating the accelerometer non-orthogonality error angles with an error of only a few arc seconds by comparing accelerometer outputs against each other. Since the gyros do not have an output analogous to the accelerometers, the filter has to relay on the equivalent platform drift rate errors produced by the non-orthogonality angle errors to separate these angular errors from the other gyro error sources. The equivalent drift rate errors produced by the one arc minute instrument misalignments are, however, only on the order of the short and long time constant gyro random disturbance of 0.003 and 0.005 degree per hour, which prevents the filter from reducing the uncertainties associated with these misalignments. This is an acceptable filter performance, since the one arc minute gyro misalignments do not contribute significantly to KT-73 IMU navigational errors.

Figure 9-27 illustrates that the accelerometer non-orthogonality angle error magnitude estimates are consistent with Gaussian distribution ensemble averages. The estimation accuracy for the β_{yz} angle error component is somewhat greater than the other two because it is not affected by the larger attitude-dependent scale factor errors associated with the vertical accelerometer. Accurate calibration of this error

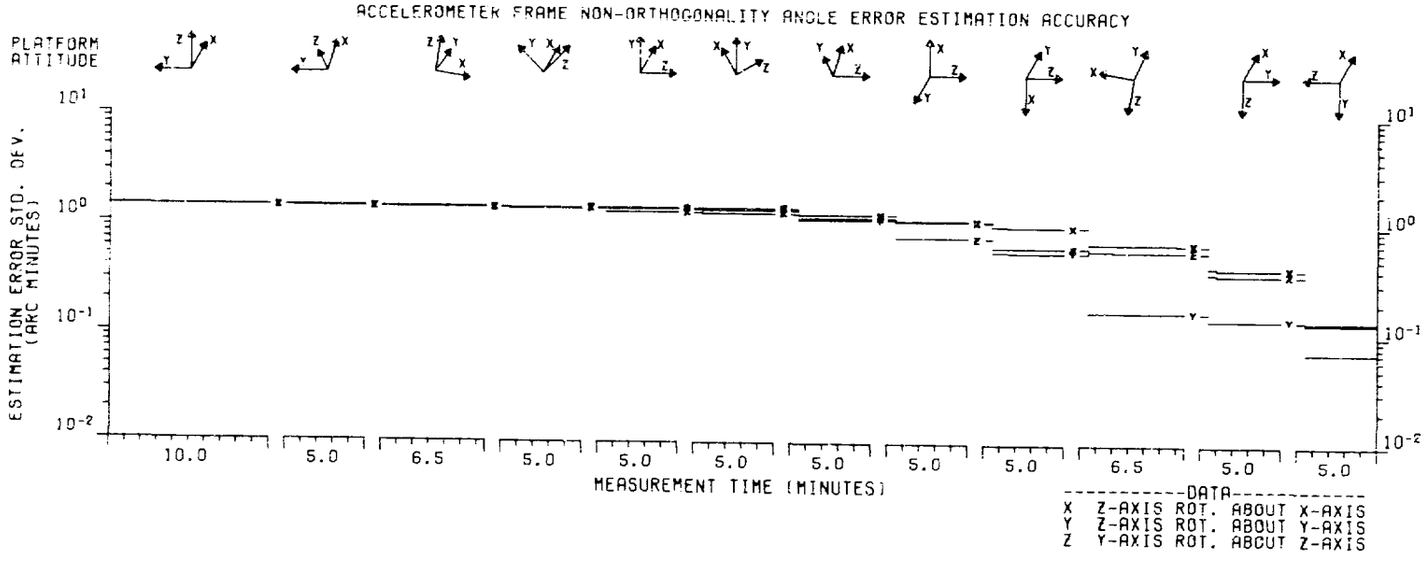

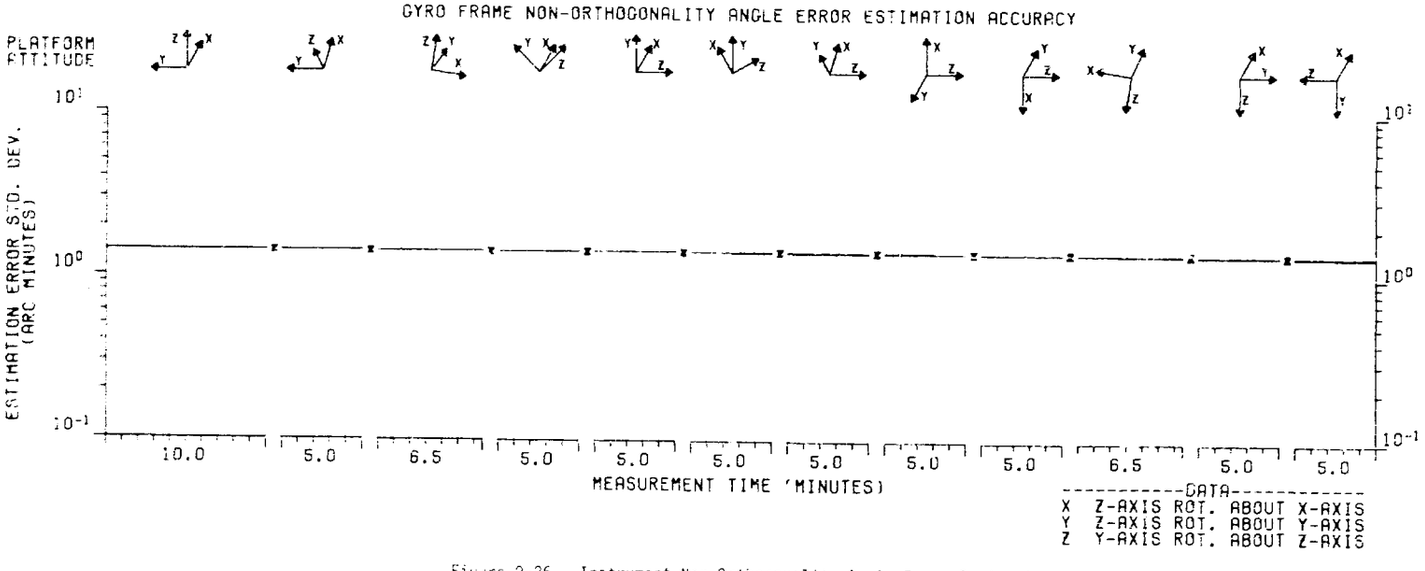

Figure 9-26. Instrument Non-Orthogonality Angle Error Estimation Accuracy

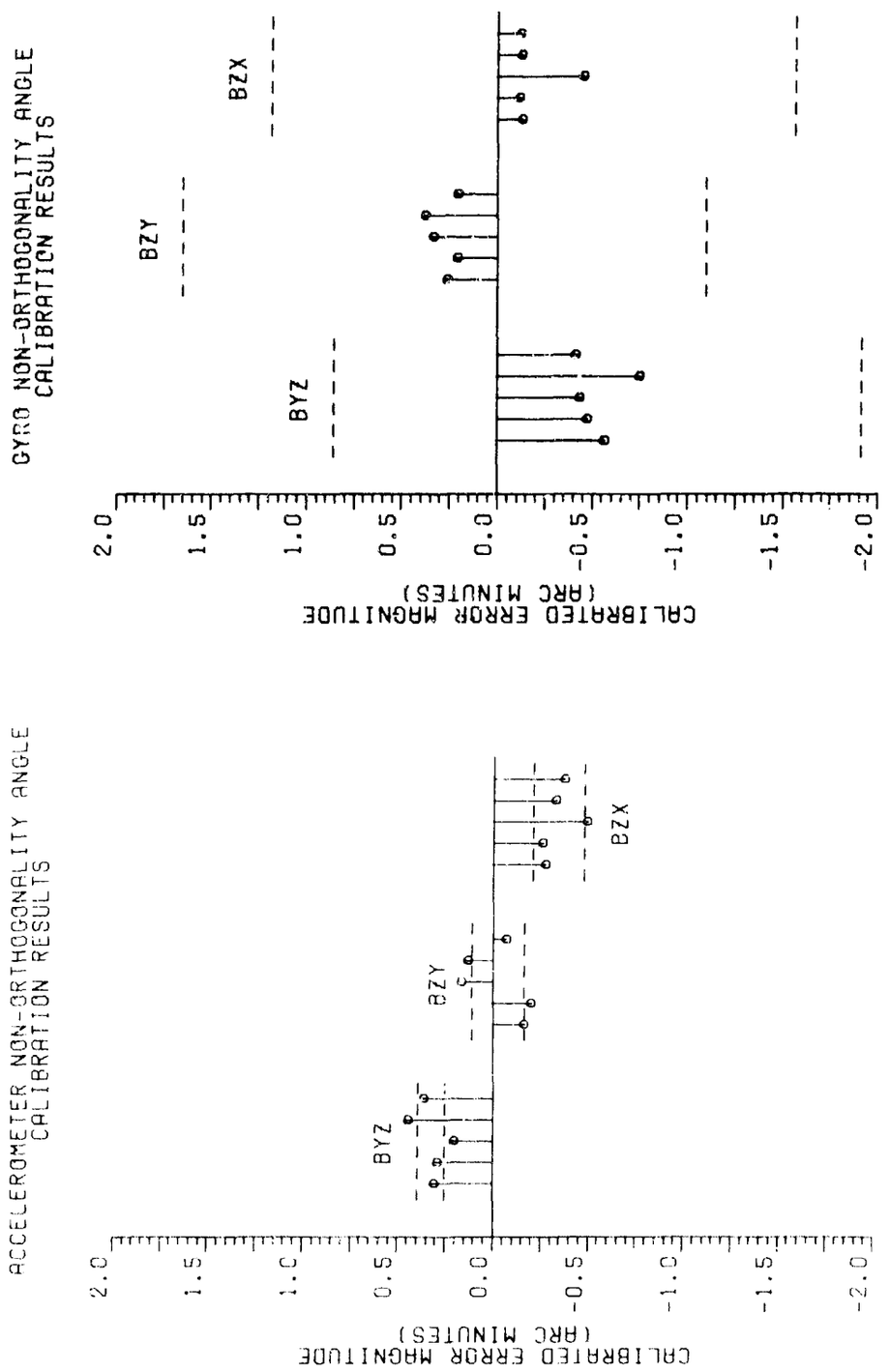

Figure 9-27. Instrument Non-Orthogonality Angle Error Magnitude Estimates

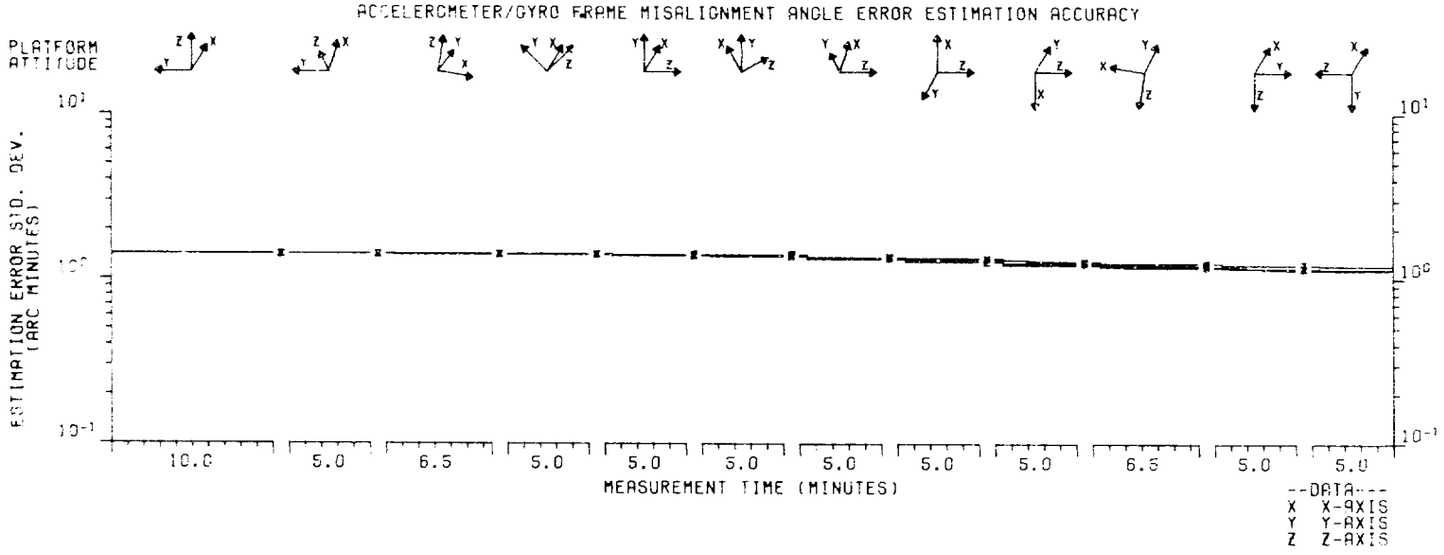

Figure 9-28. Accelerometer-to-Gyro Frame Mis-alignment Angle Error Estimation Accuracy

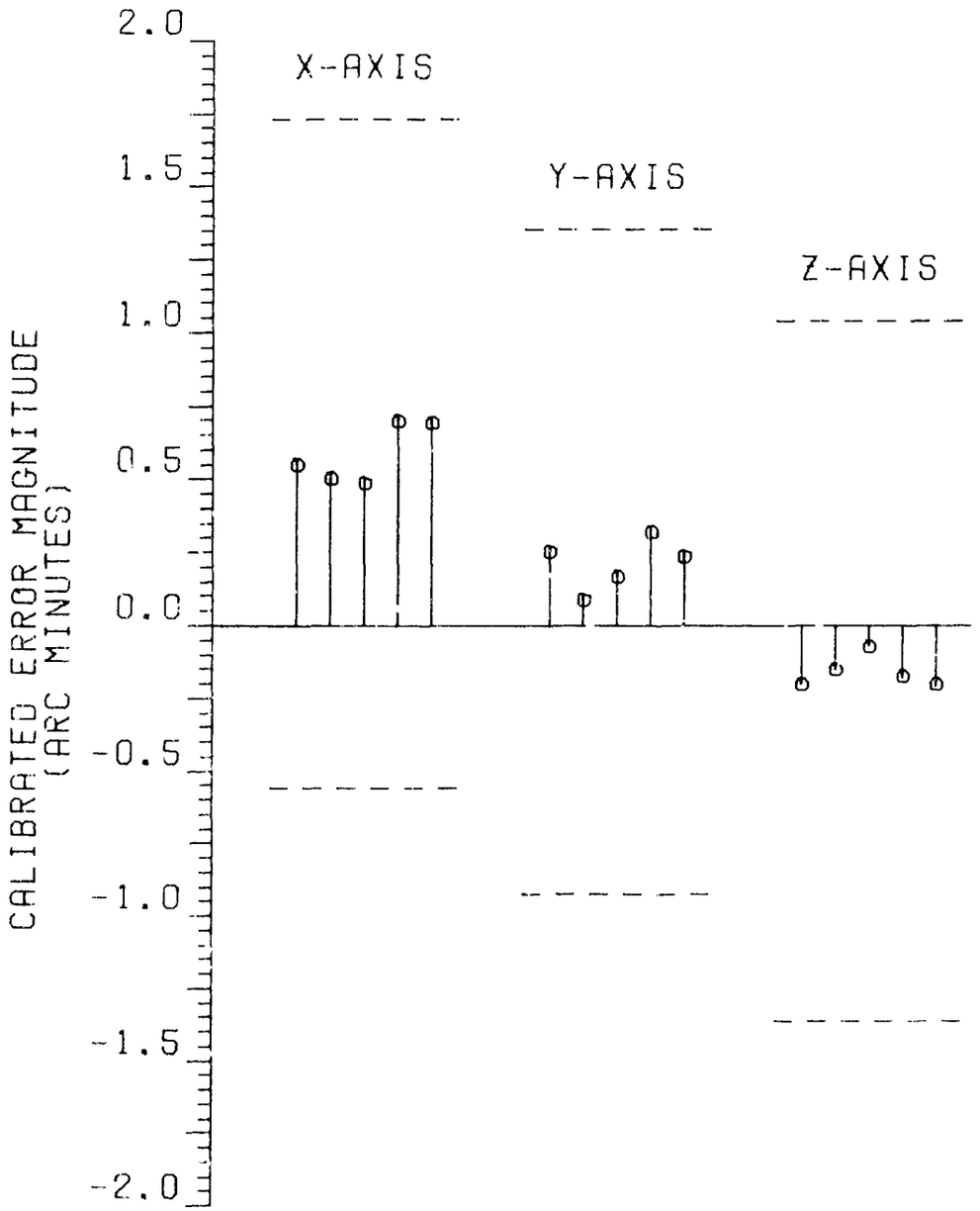

Figure 9-29. Accelerometer-to-Gyro Frame Mis-Alignment Angle Error Magnitude Estimates

angle can be important to navigation accuracy since, if software compensated for, it can ensure that the x and y-accelerometers are orthogonal in the horizontal plane.

9.6.2 Platform Attitude Related

The accuracy with which the platform can be oriented at the start of each test sequence is determined by two major error sources: the misalignment errors of the IMU case relative to the navigation frame, and the errors in positioning the gimbals (termed the synchro angle bias errors). The estimation accuracy for these angular errors is given in Figure 9-30 and the corresponding magnitude estimates shown in Figures 9-31 and 9-32.

The initial uncertainty of the roll, pitch, and azimuth control transmitter and transformer synchro devices is six arc minutes and is reset to this value in the covariance matrix at the start of each platform test sequence. Figure 9-30 shows that the filter can reduce this uncertainty to about one arc minute with the first pseudo velocity error measurement for the latter test sequences. End-of-test one arc minute estimation accuracy is also obtained for the IMU case-to-navigation frame misalignment angle errors. The Kalman Filter reduces the uncertainty associated with these error sources and the inertial instrument-to-platform misalignment angle errors by statistical averaging rather than by separating and accurately observing them. The separation process is, as previously discussed, precluded by the introduction of new synchro angle bias errors each time the platform is reoriented.

Recovered roll synchro angle bias magnitude estimates shown in Figure 9-31 conform to Gaussian distribution ensemble averages. To cross-check the Kalman Filter's estimates of these errors, the synchro devices were calibrated by making large angle IMU case rotations relative to the navigation frame and using the rotary tilt table with the IMU in the inertial navigational mode. Calibration results for the rotary

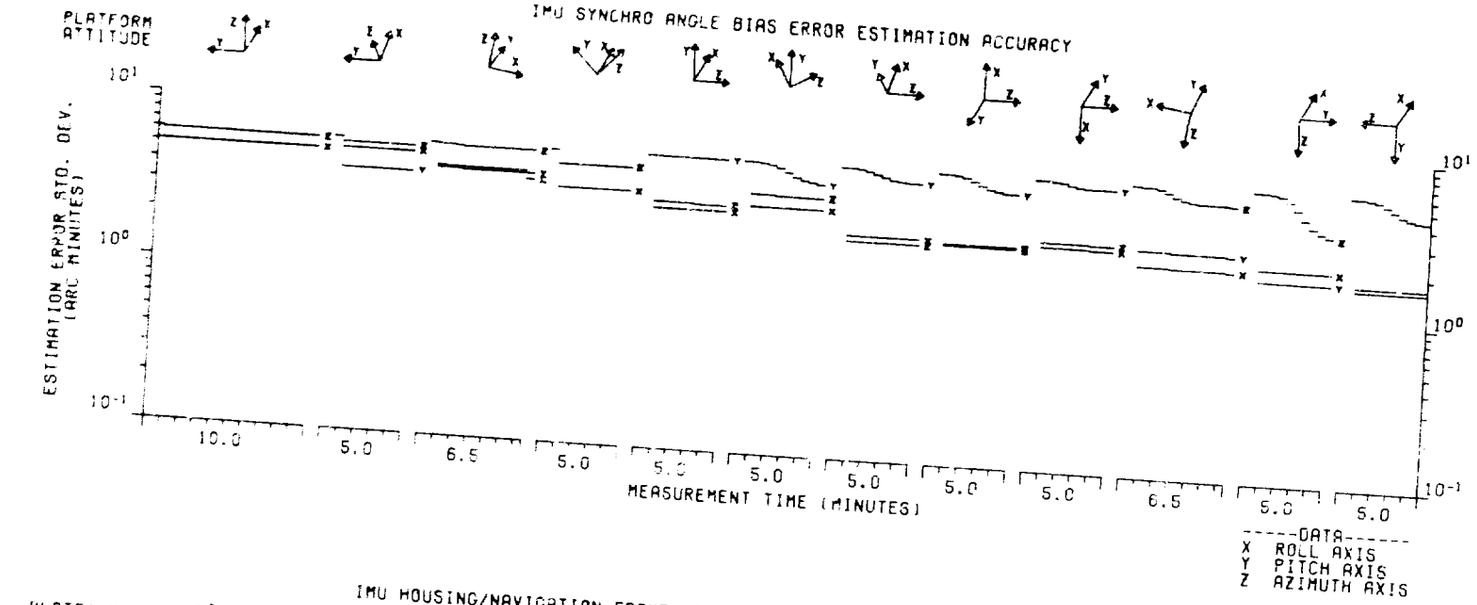

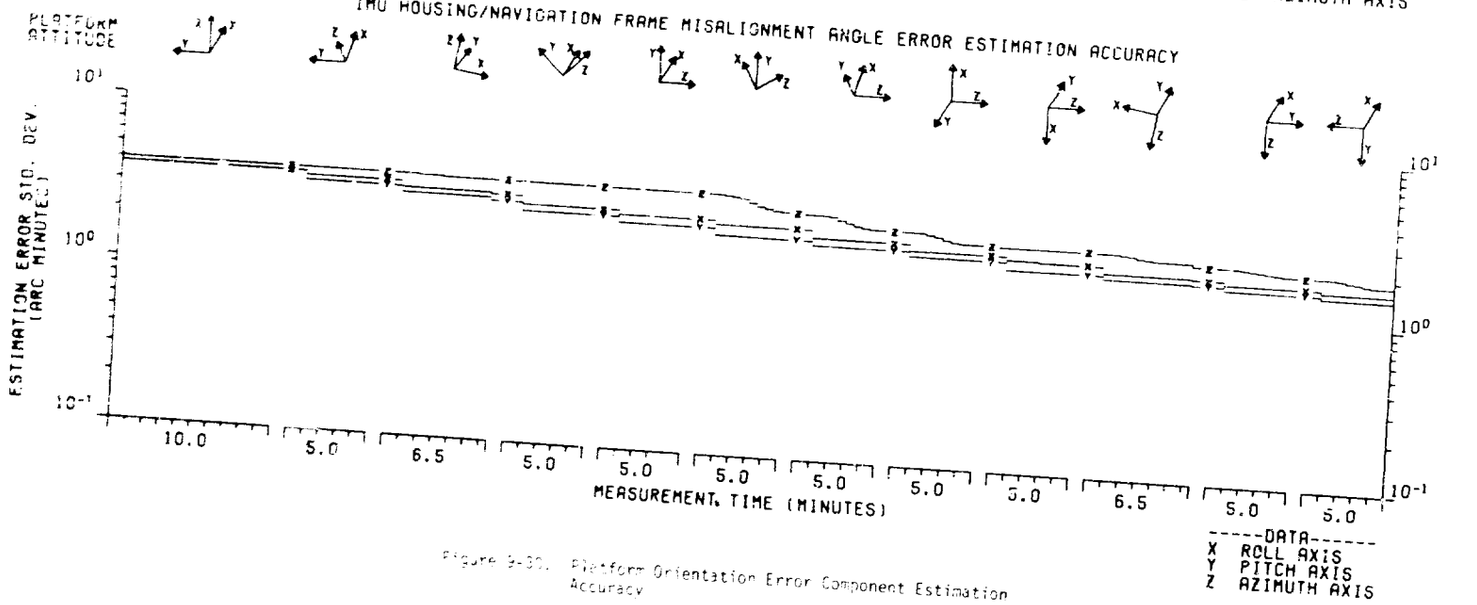

Figure 3-30. Platform Orientation Error Component Estimation Accuracy

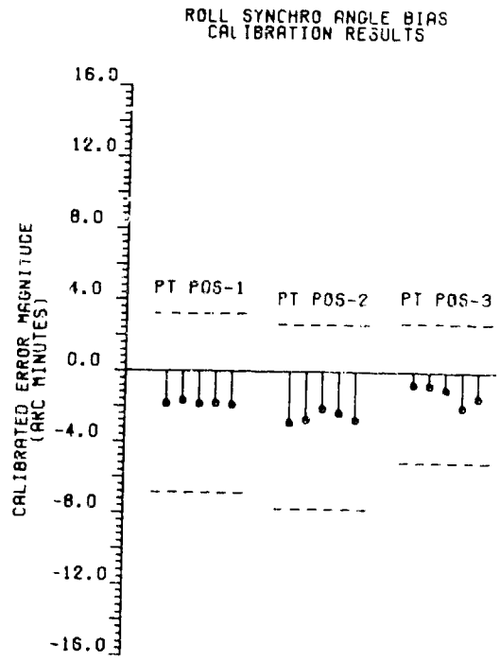

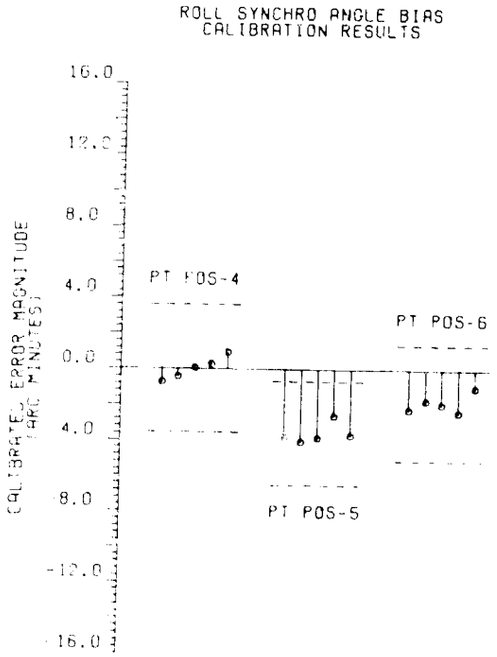

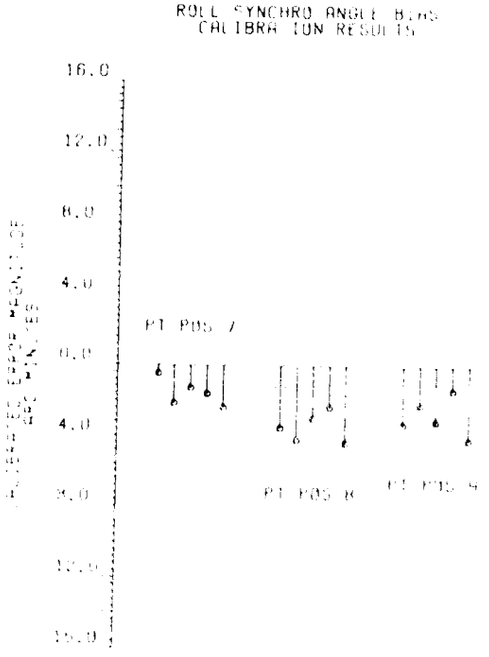

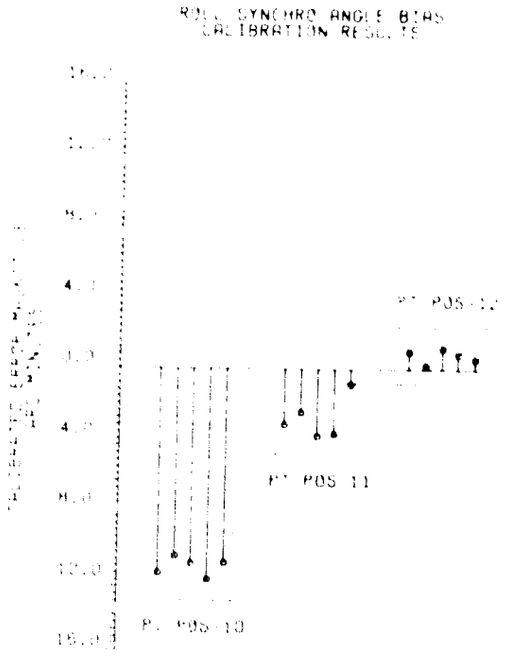

Figure 4-31. Roll Synchro Angle Bias Magnitude Estimates

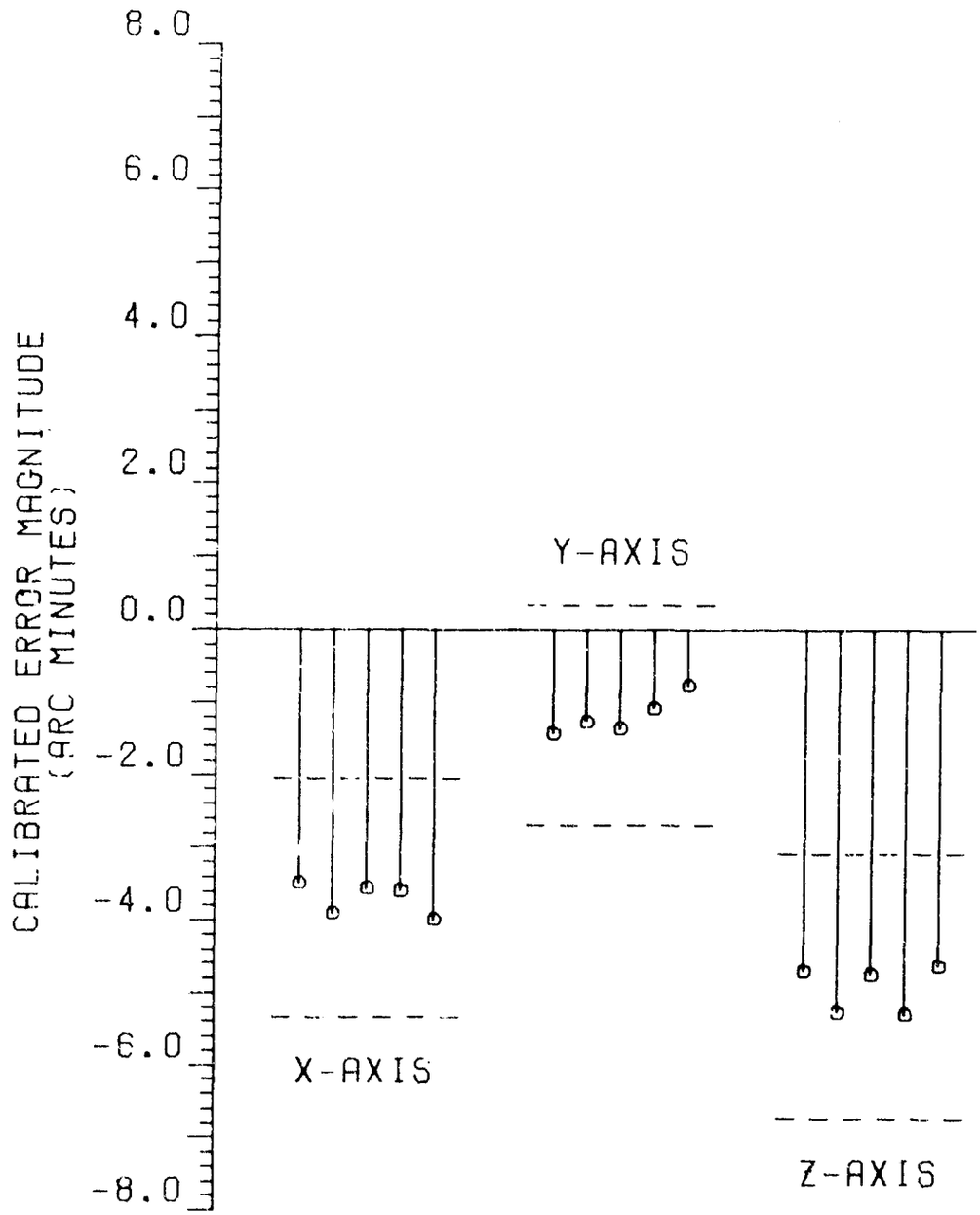

Figure 9-32. IMU Case-to-Navigation Frame Mis-Alignment Angle Error Magnitude Estimates

tilt table and Kalman Filter methods were consistent to the estimation accuracy predicted by the filter. As an example, the roll synchro angle bias for the tenth test sequence was determined as -10.2 arc minutes using the rotary tilt table.

SECTION X

CONCLUSIONS AND RECOMMENDATIONS

The objective of this study has been the design, development, analysis and laboratory demonstration of a system-level IMU calibration technique. In addition to the calibration function, it was desirable that the formulated methodology afford some capability for conducting IMU error model development and validation efforts. Major study ground rules were that: only system-level IMU measurements be used such that the IMU would not have to be disassembled, no AGE other than available laboratory equipment be required, and the solution be implementable on a general purpose digital computer.

A calibration methodology was formulated on the basis of the essential functions an IMU performs: realization of a reference platform coordinate frame and measurement of the instantaneous specific force vector. Physical vector equations were derived which embodied the methodology premises. The physical vector equations were manipulated to yield a system of 68 simultaneous stochastic differential equations. A 68-state Kalman Filter was implemented for the solution of this system of equations and optimal estimation of the IMU calibration parameters. A computer simulation of the IMU, Kalman Filter, and laboratory test procedure indicated the approach to be sound.

Technical feasibility of the methodology was demonstrated through laboratory testing and the actual calibration of a KT-73 IMU, using an off-line data processing computer program. The suitability of the methodology and associated large dimensional Kalman Filter for conducting IMU error model development and validation efforts was demonstrated by the detection, isolation, and identification of previously unmodeled IMU error sources. The experimental calibration results show complete consistency with the statistical ensemble averages predicted by the Kalman Filter's covariance matrix and previous calibration parameter values obtained via the ASM-375 test set.

It is concluded that the developed IMU calibration technique is ideally suited to aid the Reference Systems Software Group in the development of aided-inertial navigation real-time software. Periodic calibration of the IMU will provide a high degree of confidence that the hardware is operating properly. Software compensation for the static IMU error sources in the operation flight computer program will enhance the navigational accuracy of the system while effectively removing many of these error sources from consideration in the design of the suboptimal navigation Kalman Filter. And finally, refinement and validation of the IMU's error model by use of the calibration Kalman Filter and associated methodology will provide assurance that the "to be developed" navigation Kalman Filter solves the real problem at hand.

DOD agencies have observed that advanced avionics research projects sometimes reveal techniques that could result in significant operational improvements and cost reductions. Based on the results of the IMU calibration tests conducted, it is concluded that the developed technique falls into this category. Major areas of potential usefulness to the services are thought to be in the areas of quality assurance and IMU cost-of-ownership reductions.

Increased quality assurance could be achieved by incorporating the developed calibration technique into the services IMU acceptance tests. The technique is well suited to acceptance testing because it requires a minimal amount of age and test time and is accurate and comprehensive. Pure inertial navigational accuracy projections could be made by covariance analysis simulations using the results of the IMU error model development effort and calibration test results.

As a result of contract F33615-73-C-1146 with AFAL, The Analytic Sciences Corporation have identified the need for improved diagnostic methods and more comprehensive IMU tests in the field of service maintenance. The performance, test and repair history of the A-7D AN/ASN-90(V) IMS, using the KT-73 IMU, was studied and the results are highlighted in Reference 5. The problems are thought to be an

inadequate intermediate level maintenance ability to identify out-of-spec IMUs, inconsistencies between and the failure of depot level tests to verify the results obtained at the intermediate level, and iterative depot testing resulting in a minimum of thirty plus hours test time on an IMU to gain confidence that it is operating properly. AGE acquisition and ownership costs also contribute significantly to IMU cost-of-ownership. It is anticipated that adoption of the developed calibration technique at both the intermediate and depot level will ameliorate these problems while resulting in significantly lower IMU ownership costs.

Based on the above, it is recommended that a test program be undertaken at the Aerospace Guidance and Metrology Center (AGMC), Heath AFB to demonstrate the advantages of the large dimensional Kalman Filter calibration technique as opposed to the contemporary approaches presently being employed. A study portion of the program would attempt to quantify the advantages of employing the technique for IMU acceptance tests and at the intermediate maintenance level.

APPENDIX A: COMPUTER PROGRAM LISTING

APPENDIX A

IMU CALIBRATION CDC-6600 FORTRAN IV COMPUTER PROGRAM LISTING

This appendix contains a complete listing of the computer program used to calibrate the KT-73 IMU off-line by using recorded measurement data. The program is entered on a CDC-6600 computer and requires 900 seconds and 221,000 octal words memory for execution. A "production" version of this computer program would reduce both the execution time and memory requirements to a small fraction of those above by eliminating the covariance matrix computations and associated large dimensional matrices. This would be accomplished by storing the time-dependent Kalman gain matrices on a magnetic tape.

The objective of depicting this listing is to provide a reference for those attempting to develop a Kalman Filter algorithm for a similar application. There is a multitude of data, algorithms, and logic associated with the initialization, resetting, and execution of the IMU calibration Kalman Filter that could not be adequately portrayed in the text of the report. This listing provides an accurate definition and description of these details.

IMU calibration results are shown at the end of the program listing. These results are the filter's estimate of the error sources and its predicted estimation accuracy immediately before and after a measurement is used to update the filter. Data is shown for the start of the test, at the end of each platform test sequence, and for the instances in the third and tenth test sequences, where the accelerometer modes are switched. Units for the output data are consistent with the estimation results figures given in Section IX in degrees per hour, arc minutes, micro g, feet per second, and numeric values.

```
      PROGRAM MAIN       /4/74   OPT=1                    FTN 4.5+414        02/07/77  17.43.02        PAGE     1

 1                PROGRAM MAIN(INPUT,OUTPUT,TAPE5=INPUT,TAPE6=OUTPUT,PUNCH,TAPE7)
                  DIMENSION PP(68,68),PU(68,68),XD(68),XS(68),
                 1D(68,12),E(12,12),DP(68,68),F(64,68),
                 2H(6,68),P(6,6),GT(12,68),Q(12,68)
 5                DIMENSION CHP(3,3),
                 1TPP(20),TPR(20),TAP(20),
                 2TPP(3,3),CPA(3,3),SUM1(3,3),GPA GT(6),
                 3GN(3),WIN(3),CGNR(3,3),WIC(3),PRF(3),
                 4VN(3)
10                DIMENSION CAPPI(3),SDD(3),PDU(3),PDP(3),
                 1K(68,6),TILTD(3),PTU(3),PTP(3)
                  DIMENSION C(68,64)
                  DIMENSION PDD(3),PPP(3),PPU(3),TAD(6),
                 1TX(4,4),TY(4,4),TZ(4,4),
15               2TAPP(6),TAPU(6)
                  DIMENSION PDTP(3),
                 1PDTR(3),PDTU(3)
                  DIMENSION DPX(2),DPY(2)
                  DIMENSION WIP(20,3),GRA TP(20,3),PRF TP(20,3),WDP(20,3),DUM(20,3)
20                DIMENSION CAP(12,60,3),CAPD(3)
                  REAL KFT
                  REAL K8T(3)
                  REAL K1(3)
                  DATA TAU A/0.0016/,SIG A/2.0E-05/
25                DATA TAU GL/3600./,TAU GS/1.0/
                  DATA GRAV/980.0781D/,FF/7.2921E-05/
                  DATA PY/3.1415926535/
                  DATA KFT/1.94E-06/
                  ACC PRF=1.0E+03
30                GRAV=GRAV/(2.54*12.0*6076.0)
                  SIG A=SIG A*GRAV
                  TLAT=(39.+(47.+.1458/60.)/60.)*PY/180.
          COMPUTE DEGREES TO RADIANS CONVERSION FACTOR
                  FDTR=PY/180.0
35        COMPUTE DEGREES/HOUR TO RADIANS/SECOND CONVERSION FACTOR
                  FDTRS=FDTR/3600.0
                  CALL FIL INT(PU,FDTR,FDTRS,GRAV,H,P,G,Q)
          COMPUTE IMU MEASUREMENT ATTITUDE REFERENCE SYNCHRO ANGLES
                  DO 50 I=1,14
40                TRR(I)=PY/2.0
                  TPR(I)=0.0
               50 TAR(I)=0.0
                  TRR(1)=0.0
                  TRR(2)=0.
45                TRR(3)=PY/36.0
                  TRR(4)=PY/4.
                  TRR(10)=PY+PY/36.0
                  TRR(11)=PY
                  TRR(12)=2.0*PY/2.0
50                TRR(13)=-PY/36.0
                  TRR(14)=PY/36.0
                  TRR(2)=-PY/4.0
                  TRR(5)=-PY/36.0
                  TRR(6)=PY/4.0
55                TRR(10)=PY/36.0
                  TRR(13)=-PY/36.0
                  TRR(14)=PY/36.0
```

```
      TAR(3)=-PY/2.0                                                    <      59
      TAR(7)=PY/4.0                                                     <      60
60    TAR(8)=PY/2.0                                                     K      61
      TAR(9)=-PY/2.0                                                    <      62
      TAR(10)=-PY/2.0                                                   <      63
      COMPUTE THE ANGULAR VELOCITY OF THE NAVIGATION FRAME RELATIVE TO INERTIA K      64
C     SPACE IN NAVIGATION FRAME COORDINATES  WIN                        <      65
65    WIN(1)=ER*COS(TLAT)                                               K      66
      WIN(2)=0.                                                         <      67
      WIN(3)=ER*SIN(TLAT)                                               <      68
      COMPUTE GRAVITY REFERENCE IN THE GYRO REFERENCE FRAME             <      69
      GN(1)=0.                                                          <      70
70    GN(2)=0.                                                          K      71
      GN(3)=-GRAV                                                       K      72
      DO 46 J=1,3                                                       K      73
   46 KAT(J)=GRAV/ACC_PRE                                               <      74
      KA(1)=KAT(1)                                                      <      75
75    KA(2)=KAT(2)                                                      K      76
      KA(3)=KAT(3)                                                      <      77
      *S=1                                                              <      78
      DO 1003 MN=1,12                                                   <      79
      COMPUTE GIMBAL ROLL ANGLE COORDINATE TRANSFORMATION MATRIX CHR    <      80
80    CHR(1,1)=1.                                                       K      81
      CHR(1,2)=0.                                                       K      82
      CHR(1,3)=0.                                                       <      83
      CHR(2,1)=0.                                                       <      84
      CHR(2,2)=COS(TRR(MN))                                             K      85
85    CHR(2,3)=SIN(TRR(MN))                                             K      86
      CHR(3,1)=0.                                                       <      87
      CHR(3,2)=-CHR(2,3)                                                <      88
      CHR(3,3)=CHR(2,2)                                                 K      89
      COMPUTE GIMBAL PITCH ANGLE COORDINATE TRANSFORMATION MATRIX CRP   <      90
90    CRP(1,1)=COS(TPR(MN))                                             <      91
      CRP(1,2)=0.                                                       K      92
      CRP(1,3)=-SIN(TPR(MN))                                            <      93
      CRP(2,1)=0.                                                       <      94
      CRP(2,2)=1.                                                       K      95
95    CRP(2,3)=0.                                                       K      96
      CRP(3,1)=-CRP(1,3)                                                K      97
      CRP(3,2)=0.                                                       <      98
      CRP(3,3)=CRP(1,1)                                                 <      99
      COMPUTE GIMBAL AZIMUTH ANGLE COORDINATE TRANSFORMATION MATRIX CRA  K      100
100   CRA(1,1)=COS(TAR(MN))                                             K      101
      CRA(1,2)=SIN(TAR(MN))                                             <      102
      CRA(1,3)=0.                                                       <      103
      CRA(2,1)=-CRA(1,2)                                                K      104
      CRA(2,2)=CRA(1,1)                                                 <      105
105   CRA(2,3)=0.                                                       K      106
      CRA(3,1)=0.                                                       K      107
      CRA(3,2)=0.                                                       K      108
      CRA(3,3)=1.                                                       <      109
      COMPUTE THE GIMBAL NEUTRAL TO GIMBAL REFERENCE FRAME              K      110
110   COORDINATE TRANSFORMATION MATRIX  CGNR                            K      111
      CALL MAT MUL(CRP,3,3,CHR,3,DUM1)                                  K      112
      CALL MAT MUL(CRA,3,3,DUM1,3,CGNR)                                 <      113
      COMPUTE THE NOMINAL COMMANDED GYRO ANGULAR VELOCITY RELATIVE TO INERTIAL <    114
C     SPACE IN GYRO REFERENCE FRAME COORDINATES  WIC                    K      115
```

```
      CALL VEC MUL(CGNR,3,3,WIN,WIC)                                    <     116
C     COMPUTE NAVIGATION TO GIMBAL REFERENCE FRAME MEASUREMENT ATTITUDE REFERE K     117
C     COORDINATE TRANSFORMATION MATRIX CNRR                             <     118
      CALL VEC MUL(CGNR,3,3,GN,GRA GR)                                  <     119
C     COMPUTE THE NOMINAL GYRO TORQUING PULSE REPETITION FREQUENCY  PRF <     120
      DO 7 J=1,3                                                        <     121
    7 PRF(J)=WIC(J)/KFT                                                 <     122
      DO 270 I=1,3                                                      <     123
      WFR(MN,I)=WIC(I)                                                  <     124
      GRA TR(MN,I)=GRA GR(I)                                            <     125
      PRF TR(MN,I)=PRF(I)                                               <     126
  270 CONTINUE                                                          <     127
C     COMPUTE STATE EQUATION SYSTEM MATRIX  F(I)                        <     128
      CALL SYS MAT(F,SPAV,TLAT,MN,TR3,TPR,IAD,                          <     129
     1GRA GR,ER,TAU GS,TAU GL,TAU A,PRF,WIC)                            <     130
      DO 976 I=1,3                                                      <     131
      I=I+48                                                            <     132
      G(J,12)=2.0*10.0**(GRA GR(I)**2.0E-14)**2                         <     133
  976 CONTINUE                                                          <     134
      CALL TRANS(G,68,12,GT)                                            <     135
      CALL MAT MUL(G,12,12,GT,68,Q)                                     <     136
      CALL MAT MUL(G,68,12,Q,68,PP)                                     <     137
      DO 41 I=1,68                                                      <     138
      PU(I,31)=0.                                                       <     139
      PU(I,32)=0.                                                       <     140
      PU(I,33)=0.                                                       <     141
      PU(I,49)=0.                                                       <     142
      PU(I,50)=0.                                                       <     143
      PU(I,51)=0.                                                       <     144
      PU(I,52)=0.0                                                      <     145
      PU(I,53)=0.0                                                      <     146
      PU(I,54)=0.0                                                      <     147
      PU(I,55)=0.0                                                      <     148
      PU(I,56)=0.0                                                      <     149
      PU(I,57)=0.0                                                      <     150
      PU(31,I)=0.                                                       <     151
      PU(32,I)=0.                                                       <     152
      PU(33,I)=0.                                                       <     153
      PU(49,I)=0.                                                       <     154
      PU(50,I)=0.                                                       <     155
      PU(51,I)=0.                                                       <     156
      PU(52,I)=0.0                                                      <     157
      PU(53,I)=0.0                                                      <     158
      PU(54,I)=0.0                                                      <     159
      PU(55,I)=0.0                                                      <     160
      PU(56,I)=0.0                                                      <     161
      PU(57,I)=0.0                                                      <     162
      PU(65,I)=0.0                                                      <     163
      PU(66,I)=0.0                                                      <     164
      PU(67,I)=0.0                                                      <     165
      PU(68,I)=0.0                                                      <     166
      PU(I,65)=0.0                                                      <     167
      PU(I,66)=0.0                                                      <     168
      PU(I,67)=0.0                                                      <     169
      PU(I,68)=0.0                                                      <     170
    41 CONTINUE                                                         <     171
      PU(65,65)=(0.1*PRF)**2                                            <     172
```

```
                PU(55,65)=PU(65,55)                                     K          172
                PU(65,65)=PU(65,65)                                     K          173
                PU(65,65)=PU(65,65)+1.E-6                               K          174
      175       IF(MN.GT.1) PU(55,55)=1.E-6*SCALE**2                    K          175
                PU(57,57)=PU(57,57)                                     K          176
                PU(64,64)=PU(64,64)                                     K          177
                PU(65,65)=(1.E-3)**2                                    K          178
                PU(66,66)=PU(65,65)                                     K          179
      180       PU(67,67)=(3.E-05)**2                                   K          180
                PU(68,68)=(1.E-06)**2                                   K          181
             47 CONTINUE                                                K          182
          COMPUTE INITIAL KALMAN FILTER STATE VECTOR OPTIMAL ESTIMATES X0  K          183
                DO 24 J=1,68                                            K          184
      185       X0(J)=0.                                                K          185
                IF(MN.EQ.1.AND.ITEST.EQ.1) X0(J)=0.                     K          186
                DO 24 I=1,68                                            K          187
             24 P0(I,J)=PU(I,J)                                         K          188
             42 CONTINUE                                                K          189
      190       X0(31)=0.                                               K          190
                X0(32)=0.                                               K          191
                X0(33)=0.                                               K          192
                X0(49)=0.                                               K          193
                X0(50)=0.                                               K          194
      195       X0(51)=0.                                               K          195
                X0(52)=0.0                                              K          196
                X0(53)=0.0                                              K          197
                X0(54)=0.0                                              K          198
                X0(55)=0.0                                              K          199
      200       X0(56)=0.0                                              K          200
                X0(57)=0.0                                              K          201
                X0(65)=0.0                                              K          202
                X0(66)=0.0                                              K          203
                X0(67)=0.0                                              K          204
      205       X0(68)=0.0                                              K          205
             47 CONTINUE                                                K          206
                NM=11                                                   K          207
                IF(MN.EQ.1) NM=61                                       K          208
                IOZ=0                                                   K          209
      210       IF(MN.EQ.3) NM=14                                       K          210
                IF(MN.EQ.10) NM=14                                      K          211
                DO 1200 IM=1,NM                                         K          212
                IF(MN.NE.1) GO TO 1[illegible]                          K          213
                IOZ=IOZ+1                                               K          214
      215       IF(IOZ.NE.2) GO TO 1206                                 K          215
                IOZ=0                                                   K          216
                DO 1207 I=1,68                                          K          217
                PU(1,53)=0.0                                            K          218
                PU(I,53)=0.0                                            K          219
      220       PU(I,54)=0.0                                            K          220
                PU(52,I)=0.0                                            K          221
                PU(53,I)=0.0                                            K          222
                PU(54,I)=0.0                                            K          223
      225       PU(52,52)=(1.E-[illegible])**2                          K          224
                PU(53,53)=PU(1,53)                                      K          225
                PU(54,54)=PU(1,53)                                      K          226
                X0(52)=0.                                               K          227
```

```
                  X0(63)=1.                                                  K      230
230               X0(64)=1.                                                  K      231
              100 CONTINUE                                                   K      232
                  P(4,4)=1.6E-21/((7.54*12.0*6.626.01**2)                    K      233
                  P(5,5)=P(4,4)                                              K      234
                  IF(MN.EQ.3.OR.MN.EQ.1) GO TO 133                           K      235
235               IF(MN.EQ.1) GO TO 113                                      K      236
                  GO TO 1?                                                   K      237
              113 CONTINUE                                                   K      238
                  IF(MN.EQ.1) P(4,4)=1.E-04*P(4,4)                           K      239
                  IF(MN.EQ.3.AND.IM.GE.12) P(4,4)=1.0E-04*P(4,4)             K      240
240               IF(MN.EQ.12.AND.IM.GE.12) P(4,4)=1.0E-04*P(4,4)            K      241
                  P(5,5)=P(4,4)                                              K      242
                  SWXY=AMAX1(P(49,34),P(49,58))                              K      243
                  SWRY=AMAX1(P(17,35),P(51,59))                              K      244
                  SWKX=AMAX1(P(49,4?),P(49,61))                              K      245
245               SWKY=AMAX1(P(51,41),P(50,61))                              K      246
                  P(49,34)=0.                                                K      247
                  P(49,4?)=0.                                                K      248
                  P(49,58)=0.                                                K      249
                  P(49,60)=0.                                                K      250
250               P(50,35)=0.                                                K      251
                  P(50,61)=0.                                                K      252
                  P(50,59)=0.                                                K      253
                  P(50,61)=0.                                                K      254
                  IF(MN.EQ.3.AND.IM.LE.11) GO TO 111                         K      255
255               IF(MN.EQ.12.AND.IM.LE.11) GO TO 111                        K      256
                  P(49,59)=SWRY                                              K      257
                  P(51,59)=SWRY                                              K      258
                  P(49,61)=SWKY                                              K      259
                  P(50,61)=SWKY                                              K      260
260               GO TO 1?                                                   K      261
              111 CONTINUE                                                   K      262
                  P(49,34)=SWRX                                              K      263
                  P(50,35)=SWRY                                              K      264
                  P(49,4?)=SWKX                                              K      265
265               P(50,41)=SWK                                               K      266
              112 CONTINUE                                                   K      267
                  IF(MN.EQ.1) GO TO 115                                      K      268
                  IF(IM.NE.12) GO TO 115                                     K      269
                  DO 116 I=1,66                                              K      270
270               PH(65,I)=0.                                                K      271
                  PH(66,I)=0.                                                K      272
                  PH(I,65)=0.                                                K      273
                  PH(I,66)=0.                                                K      274
                  PH(I,44)=0.                                                K      275
275               PH(I,59)=0.                                                K      276
                  PH(I,61)=0.                                                K      277
                  PH(49,I)=0.                                                K      278
                  PH(51,I)=0.                                                K      279
                  PH(61,I)=0.                                                K      280
280               CONTINUE                                                   K      281
                  PH(65,65)=(1.0E-30)**3                                     K      282
                  PH(65,66)=PH(65,65)                                        K      283
                  X0(49)=0.                                                  K      284
                  X0(50)=0.                                                  K      285
285               X0(61)=0.                                                  K      286
```

```
400               SUMDY=-SA*CP*DTX+CA*DTY                                <   402
                  SUMDZ=SP*DTX+DTZ                                       <   403
                  SUMDX=SUMDX+XD(62)                                     <   404
                  SUMDY=SUMDY+XD(63)                                     K   405
                  SUMDZ=SUMDZ+XD(64)                                     <   406
405               GDD(1)=SUMDX                                           K   407
                  GDD(2)=SUMDY                                           <   408
                  GDD(3)=SUMDZ                                           <   409
                  DTX=0.0                                                <   410
                  DTY=0.0                                                <   411
410               DTZ=0.0                                                K   412
                  DO 73 I=1,64                                           <   413
                  IF(I.GT.27.AND.I.LT.52) GO TO 73                       <   414
                  IF(I.GT.54.AND.I.LT.62) GO TO 73                       <   415
                  DTX=DTX+F(31,I)*XD(I)                                  <   416
415               DTY=DTY+F(32,I)*XD(I)                                  <   417
                  DTZ=DTZ+F(33,I)*XD(I)                                  <   418
               73 CONTINUE                                               K   419
                  SUMDX=CP*CA*DTX+SA*DTY                                 K   420
                  SUMDY=-SA*CP*DTX+CA*DTY                                <   421
420               SUMDZ=SP*DTX+DTZ                                       K   422
                  PDD(1)=SUMDX                                           K   423
                  PDD(2)=SUMDY                                           K   424
                  PDD(3)=SUMDZ                                           <   425
                  DTX=0.0                                                <   426
425               DTY=0.0                                                <   427
                  DTZ=0.0                                                <   428
                  DO 90 I=1,64                                           K   429
                  IF(I.GT.33.AND.I.LT.52) GO TO 90                       <   430
                  IF(I.GT.57.AND.I.LT.62) GO TO 90                       K   431
430               DTX=DTX+F(31,I)*XD(I)                                  <   432
                  DTY=DTY+F(32,I)*XD(I)                                  <   433
                  DTZ=DTZ+F(33,I)*XD(I)                                  <   434
               90 CONTINUE                                               <   435
                  SUMDX=CP*CA*DTX+SA*DTY                                 <   436
435               SUMDY=-SA*CP*DTX+CA*DTY                                <   437
                  SUMDZ=SP*DTX+DTZ                                       <   438
                  PDTD(1)=SUMDX                                          <   439
                  PDTD(2)=SUMDY                                          <   440
                  PDTD(3)=SUMDZ                                          <   441
                  DO 1004 IC=1,2                                         K   442
                  IF(IC.EQ.2) GO TO 74                                   <   443
                  DO 71 I=1,64                                           <   444
                  DO 71 J=1,64                                           <   445
               71 C(I,J)=PP(I,J)                                         K   446
445               GO TO 75                                               <   447
               74 CONTINUE                                               <   448
                  DO 72 I=1,64                                           K   449
                  DO 72 J=1,64                                           <   450
               72 C(I,J)=PU(I,J)                                         K   451
450            75 CONTINUE                                               <   452
                  CXX=0.0                                                <   453
                  CYY=0.0                                                K   454
                  CZZ=0.0                                                <   455
                  CXY=0.0                                                <   456
455               CYZ=0.0                                                <   457
                  DO 76 I=1,64                                           K   458
```

```
      IF(I.GT.18.AND.I.LT.52) GO TO 76                                  K     459
      IF(I.GT.54.AND.I.LT.62) GO TO 76                                  K     460
      DO 80 J=1,64                                                      K     461
463   IF(J.GT.18.AND.J.LT.52) GO TO 80                                  K     462
      IF(J.GT.54.AND.J.LT.62) GO TO 80                                  K     463
      SXX=SXX+F(71,I)*F(31,J)*C(I,J)                                    K     464
      SYY=SYY+F(72,I)*F(32,J)*C(I,J)                                    K     465
      SZZ=SZZ+F(33,I)*F(33,J)*C(I,J)                                    K     466
465   SXY=SXY+F(31,I)*F(32,J)*C(I,J)                                    K     467
      SXZ=SXZ+F(71,I)*F(33,J)*C(I,J)                                    K     468
   80 CONTINUE                                                          K     469
   76 CONTINUE                                                          K     470
      SQX=B1*SXX+B2*SYY+B3*SXY+2.11E-16                                 K     471
470   SQY=B4*SXX+B5*SYY-B3*SXY+2.11E-16                                 K     472
      SQZ=B6*SXX+SZZ+B7*SXY+2.11E-16                                    K     473
      IF(ID.EQ.2) GO TO 81                                              K     474
      PPP(1)=SQX                                                        K     475
      PPP(2)=SQY                                                        K     476
475   PPP(3)=SQZ                                                        K     477
      GO TO 82                                                          K     478
   81 CONTINUE                                                          K     479
      PPU(1)=SQX                                                        K     480
      PPU(2)=SQY                                                        K     481
480   PPU(3)=SQZ                                                        K     482
   82 CONTINUE                                                          K     483
      SXX=0.0                                                           K     484
      SYY=0.0                                                           K     485
      SZZ=0.0                                                           K     486
485   SXY=0.0                                                           K     487
      SXZ=0.0                                                           K     488
      DO 77 I=1,64                                                      K     489
      IF(I.GT.17.AND.I.LT.52) GO TO 77                                  K     490
      IF(I.GT.54.AND.I.LT.62) GO TO 77                                  K     491
490   DO 78 J=1,64                                                      K     492
      IF(J.GT.17.AND.J.LT.52) GO TO 78                                  K     493
      IF(J.GT.54.AND.J.LT.62) GO TO 78                                  K     494
      SXX=SXX+F(31,I)*F(31,J)*C(I,J)                                    K     495
      SYY=SYY+F(32,I)*F(32,J)*C(I,J)                                    K     496
495   SZZ=SZZ+F(33,I)*F(33,J)*C(I,J)                                    K     497
      SXY=SXY+F(31,I)*F(32,J)*C(I,J)                                    K     498
      SXZ=SXZ+F(31,I)*F(33,J)*C(I,J)                                    K     499
   78 CONTINUE                                                          K     500
   77 CONTINUE                                                          K     501
500   SQX=B1*SXX+B2*SYY+B3*SXY+2.11E-16                                 K     502
      SQY=B4*SXX+B5*SYY-B3*SXY+2.11E-16                                 K     503
      SQZ=B6*SXX+SZZ+B7*SXY+2.11E-16                                    K     504
      IF(ID.EQ.2) GO TO 83                                              K     505
      PPP(1)=SQX                                                        K     506
505   PPP(2)=SQY                                                        K     507
      PPP(3)=SQZ                                                        K     508
      GO TO 84                                                          K     509
   83 CONTINUE                                                          K     510
      PPU(1)=SQX                                                        K     511
510   PPU(2)=SQY                                                        K     512
      PPU(3)=SQZ                                                        K     513
   84 CONTINUE                                                          K     514
      SXX=0.0                                                           K     515
```

```
      PROGRAM MAIN       7477   OPT=1                FTN 4.5+414        77/07/22  17.48.  2          PAGE   10

                  SYY=0.0                                                                          <         516
  515             SZZ=0.0                                                                          <         517
                  SYX=0.0                                                                          <         518
                  SXZ=0.0                                                                          <         519
                  DO 93 I=1,64                                                                     <         520
                  IF(I.GT.23.AND.I.LT.32) GO TO 93                                                 <         521
  520             IF(I.GT.37.AND.I.LT.42) GO TO 93                                                 <         522
                  DO 94 J=1,64                                                                     <         523
                  IF(J.GT.33.AND.J.LT.52) GO TO 94                                                 <         524
                  IF(J.GT.57.AND.J.LT.62) GO TO 94                                                 <         525
                  SXX=SXX+F(31,I)*F(31,J)*C(I,J)                                                   <         526
  525             SYY=SYY+F(32,I)*F(32,J)*C(I,J)                                                   <         527
                  SZZ=SZZ+F(33,I)*F(33,J)*C(I,J)                                                   <         528
                  SXY=SXY+F(31,I)*F(32,J)*C(I,J)                                                   <         529
                  SXZ=SXZ+F(31,I)*F(33,J)*C(I,J)                                                   <         530
                94 CONTINUE                                                                        <         531
  530             97 CONTINUE                                                                      <         532
                  SCX=81*SXX+87*SYY+87*SXY+2.11E-16                                                <         533
                  SCY=84*SXX+86*SYY-23*SXY+2.11E-16                                                <         534
                  SCZ=86*SXX+SZZ+37*SXY+2.11E-16                                                   <         535
                  IF(IC.EQ.2) GO TO 95                                                             <         536
  535             POTP(1)=SCX                                                                      <         537
                  POTP(2)=SCY                                                                      <         538
                  POTP(3)=SCZ                                                                      <         539
                  GO TO 96                                                                         <         540
                95 CONTINUE                                                                        <         541
  540             POTU(1)=SCX                                                                      <         542
                  POTU(2)=SCY                                                                      <         543
                  POTU(3)=SCZ                                                                      <         544
                96 CONTINUE                                                                        <         545
                  TX(1,1)=C(28,28)                                                                 <         546
  545             TY(1,1)=C(29,29)                                                                 <         547
                  TZ(1,1)=C(30,30)                                                                 <         548
                  TX(1,2)=C(28,31)                                                                 <         549
                  TY(1,2)=C(29,32)                                                                 <         550
                  TZ(1,2)=C(30,33)                                                                 <         551
  550             TX(1,3)=C(28,55)                                                                 <         552
                  TY(1,3)=C(29,56)                                                                 <         553
                  TZ(1,3)=C(30,57)                                                                 <         554
                  TX(2,2)=C(31,31)                                                                 <         555
                  TY(2,2)=C(32,32)                                                                 <         556
  555             TZ(2,2)=C(33,33)                                                                 <         557
                  TX(2,3)=C(31,55)                                                                 <         558
                  TY(2,3)=C(32,56)                                                                 <         559
                  TZ(2,3)=C(33,57)                                                                 <         560
                  TX(3,3)=C(55,55)                                                                 <         561
  560             TY(3,3)=C(56,56)                                                                 <         562
                  TZ(3,3)=C(57,57)                                                                 <         563
                  DO 1009 IT=1,3                                                                   <         564
                  GO TO(51,52,53),IT                                                               <         565
                51 TA1=0.0                                                                         <         566
  565             TA2=0.0                                                                          <         567
                  TA3=0.0                                                                          <         568
                  K1=1                                                                             <         569
                  K2=2                                                                             <         570
                  K3=3                                                                             <         571
  570             GO TO 60                                                                         <         572
```

```
                  DO 71=46                                                  <  578
                     CA1=1.0                                                <  574
                     K2=44                                                  <  575
                     CA2=-1.0                                               <  576
  575                K3=43                                                  <  577
                     CA3=1.0                                                <  578
                     GO TO 60                                               <  579
                  59 K1=48                                                  <  580
                     CA1=-1.0                                               <  581
  580                K2=47                                                  <  582
                     CA2=1.0                                                <  583
                     K3=45                                                  <  584
                     CA3=-1.0                                               <  585
                  60 CONTINUE                                               <  586
  585                TX(1,4)=C(28,K1)*FA1                                   <  587
                     TY(1,4)=C(29,K2)*FA2                                   <  588
                     TZ(1,4)=C(30,K3)*FA3                                   <  589
                     TX(2,4)=C(31,K1)*FA1                                   <  590
                     TY(2,4)=C(32,K2)*FA2                                   <  591
  590                TZ(2,4)=C(33,K3)*FA3                                   <  592
                     TX(3,4)=C(55,K1)*FA1                                   <  593
                     TY(3,4)=C(56,K2)*FA2                                   <  594
                     TZ(3,4)=C(57,K2)*FA3                                   <  595
                     TX(4,4)=C(K1,K1)*(FA1**2)                              <  596
  595                TY(4,4)=C(K2,K2)*(FA2**2)                              <  597
                     TZ(4,4)=C(K3,K3)*(FA3**2)                              <  598
                     STX=0.0                                                <  599
                     STY=0.0                                                <  600
                     STZ=0.0                                                <  601
  600                DO 61 I=1,4                                            <  602
                     DO 61 J=I,4                                            <  603
                     IF(I.EQ.J) GO TO 62                                    <  604
                     STX=STX+2.0*TX(I,J)                                    <  605
                     STY=STY+2.0*TY(I,J)                                    <  606
  605                STZ=STZ+2.0*TZ(I,J)                                    <  607
                     GO TO 61                                               <  608
                  62 CONTINUE                                               <  609
                     STX=STX+TX(I,J)                                        <  610
                     STY=STY+TY(I,J)                                        <  611
  610                STZ=STZ+TZ(I,J)                                        <  612
                  61 CONTINUE                                               <  613
                     IF(IT.NE.2) GO TO 63                                   <  614
                     OPX(IC)=STX-(2.0/GRAV)*(C(28,59)+                      <  615
                    C(31,53)+C(55,59)+C(46,53))+                            <  616
  615               C(59,59)/(GRAV**2)                                      <  617
                     OPY(IC)=STY+(2.0/GRAV)*(C(29,58)+                      <  618
                    C(32,58)+C(56,58)-C(44,58))+                            <  619
                    C(58,59)/(GRAV**2)                                      <  620
                  63 CONTINUE                                               <  621
  620                IF(IC.EQ.1.AND.IT.EQ.1) PTP(1)=STX                     <  622
                     IF(IC.EQ.1.AND.IT.EQ.2) PTP(2)=STY                     <  623
                     IF(IC.EQ.1.AND.IT.EQ.3) PTP(3)=STZ                     <  624
                     IF(IC.EQ.2.AND.IT.EQ.1) PTU(1)=STX                     <  625
                     IF(IC.EQ.2.AND.IT.EQ.2) PTU(2)=STY                     <  626
  625                IF(IC.EQ.2.AND.IT.EQ.3) PTU(3)=STZ                     <  627
                     IF(IC.EQ.1.AND.IT.EQ.3) TAPP(4)=STX                    <  628
                     IF(IC.EQ.1.AND.IT.EQ.2) TAPP(2)=STY                    <  629
```

```
      PROGRAM MAIN       7477,   OPT=1                    FTN 4.8+414        02/ 7477  17.44.17        PAGE   12

                  IF(IC.EQ.1.AND.IT.EQ.2) TAPP(1)=STZ                                    K         629
                  IF(IC.EQ.2.AND.IT.EQ.2) TAPU(4)=STY                                    K         630
  630             IF(IC.EQ.2.AND.IT.EQ.2) TAPU(2)=STY                                    K         631
                  IF(IC.EQ.2.AND.IT.EQ.2) TAPU(1)=STZ                                    K         632
                  IF(IC.EQ.1.AND.IT.EQ.3) TAPP(6)=STX                                    K         633
                  IF(IC.EQ.1.AND.IT.EQ.3) TAPP(5)=STY                                    K         634
                  IF(IC.EQ.1.AND.IT.EQ.3) TAPP(3)=STZ                                    K         635
  640             IF(IC.EQ.2.AND.IT.EQ.3) TAPU(6)=STX                                    K         636
                  IF(IC.EQ.2.AND.IT.EQ.3) TAPU(5)=STY                                    K         637
                  IF(IC.EQ.2.AND.IT.EQ.3) TAPU(3)=STZ                                    K         638
             1005 CONTINUE                                                               K         639
             1004 CONTINUE                                                               K         640
  650             TILTO(1)=XO(28)+XO(31)+XO(56)                                          K         641
                  TILTO(2)=XO(29)+XO(32)+XO(56)                                          K         642
                  TILTO(3)=XO(30)+XO(33)+XO(57)                                          K         643
                  TAO(1)=TILTO(3)+XO(43)                                                 K         644
                  TAO(2)=TILTO(2)-XO(44)                                                 K         645
  660             TAO(3)=TILTO(3)-XO(45)                                                 K         646
                  TAO(4)=TILTO(1)+XO(46)                                                 K         647
                  TAO(5)=TILTO(2)+XO(47)                                                 K         648
                  TAO(6)=TILTO(1)-XO(48)                                                 K         649
                  DXO=TAO(4)-XO(59)/GRAV                                                 K         650
  670             DYO=TAO(2)+XO(58)/GRAV                                                 K         651
                  CALL MRT VA(PP,PU,XO,IM,MN,GOO,POU,PPP,                                K         652
                 1TILTO,PTU,PTP,PTO,PPP,PPU,                                             K         653
                 2TAO,TAPP,TAPU,                                                         K         654
                 3PPTO,PDTP,PDTU,                                                        K         655
  680            4DPX,DPY,DXO,DYO)                                                       K         656
             1007 CONTINUE                                                               K         657
             1003 CONTINUE                                                               K         658
                  IF(IS.EQ.2) GO TO 1002                                                 K         659
                  DO 271 MN=1,12                                                         K         660
  690             DO 272 I=1,3                                                           K         661
                  WTC(I)=WTR(MN,I)                                                       K         662
                  GRA GR(I)=GRA TR(MN,I)                                                 K         663
                  PPF(I)=PPF TR(MN,I)                                                    K         664
                272 CONTINUE                                                             K         665
  700             CALL SYS MAT(F,GRAV,TLAT,MN,PPP,PPP,TAO,                               K         666
                 1GRA GR,FF,TAU GS,TAU GL,TAU A,PPF,WTC)                                 K         667
                  DTX=0.                                                                 K         668
                  DTY=0.                                                                 K         669
                  DTZ=0.                                                                 K         670
  710             DO 273 I=1,2                                                           K         671
                  IF(I.GE.2.AND.I.LE.3) GO TO 273                                        K         672
                  DTX=DTX+F(31,I)*XO(I)                                                  K         673
                  DTY=DTY+F(32,I)*XO(I)                                                  K         674
                  DTZ=DTZ+F(33,I)*XO(I)                                                  K         675
  720             273 CONTINUE                                                           K         676
                  WOP(MN,1)=-COS(TPP(MN))*COS(TAP(MN))*DTY                               K         677
                 1-SIN(TAP(MN))*DTY                                                      K         678
                  WOP(MN,2)=SIN(TAP(MN))*COS(TPP(MN))*DTX                                K         679
                 1-COS(TAP(MN))*DTY                                                      K         680
  730             WOP(MN,3)=-SIN(TPP(MN))*DTX-DTZ                                        K         681
                  271 CONTINUE                                                           K         682
                  WRITE(6,274)                                                           K         683
                  274 FORMAT(1H1)                                                        K         684
                  DO 275 MN=1,12                                                         K         685
```

```
685                 WRITE(6,276) (WTR(MN,I),I=1,3),(WOP(MN,J),J=1,3)                <      687
                276 FORMAT(1HO,3(1PE13.3,5X),10X,3(1PE13.3,5X))                     <      688
                275 CONTINUE                                                        K      689
                    DO 333 I=1,12                                                   <      690
                    WRITE(7,331) (WTR(I,J),J=1,3)                                   K      691
695             331 FORMAT(3(1PE13.6,2X))                                           K      692
                333 CONTINUE                                                        K      693
               1000 CONTINUE                                                        K      694
                    WRITE(6,331)                                                    K      695
                331 FORMAT(1H1)                                                     K      696
695                 DO 30 I=1,20                                                    K      697
                    I=-3*(I-1)+60                                                   K      698
                    I=20-(I-1)                                                      <      699
                    DO 30 L=1,3                                                     K      700
                    CAP(2,J,L)=CAP(2,K,L)                                           K      701
700                 CAP(2,K,L)=0.                                                   <      702
                 30 CONTINUE                                                        K      703
                    ITS1=-1                                                         K      704
                    DO 934 MN=1,6                                                   <      705
                    ITS1=ITS1+2                                                     K      706
                715 ITS2=ITS1+1                                                     K      707
                    WRITE(6,932) ITS1,ITS2                                          K      708
                932 FORMAT(1H ,42X,I2,53X,I2)                                       <      709
                    IP=14-1                                                         <      710
                    IF(MN.EQ.1) IP=61-1                                             K      711
                712 DO 934 J=1,IP                                                   K      712
                    TME=30.0*FLOAT(J)                                               K      713
                    IF(MN.EQ.1) TME=TME/3.0                                         K      714
                    WRITE(6,933) TME,(CAP(ITS1,J,I),I=1,3),(CAP(ITS2,J,L),L=1,3)    K      715
                933 FORMAT(1H ,1PE10.3,10X,3(1PE13.6,2X),10X,3(1PE13.6,2X))         K      716
                715 934 CONTINUE                                                    <      717
               2001 CONTINUE                                                        K      718
                    END                                                             K      719
```

CARD NR. SEVERITY DETAILS DIAGNOSIS OF PROBLEM

563 I AN IF STATEMENT MAY BE MORE EFFICIENT THAN A 2 OR 3 BRANCH COMPUTED GO TO STATEMENT.

```
      SUBROUTINE SYSMAT(E,GA,FLAT,MN,TRR,TRI,TAP,
     C F,FF,TAGS,TAGL,TAA,PRF,WG)                                      SYSMAT 2
      DIMENSION E(68,68)                                                SYSMAT 3
      DIMENSION TRR(20),TRI(21),TAP(20)                                 SYSMAT 4
      DIMENSION G(3),PRF(3),WG(3)                                       SYSMAT 5
      DATA TWO/540.0/,THA/180.0/                                        SYSMAT 6
      SZ=SIN(TAP(MN))                                                   SYSMAT 7
      CZ=COS(TAP(MN))                                                   SYSMAT 8
      SX=SIN(TRR(MN))                                                   SYSMAT 9
      CX=COS(TRR(MN))                                                   SYSMAT10
      SY=SIN(TRR(MN))                                                   SYSMAT11
      CY=COS(TRR(MN))                                                   SYSMAT12
      TY=SY/CY                                                          SYSMAT13
      IF(ABS(SZ).LT.1.0E-06) SZ=0.0                                     SYSMAT14
      IF(ABS(CZ).LT.1.0E-06) CZ=0.0                                     SYSMAT15
      IF(ABS(SX).LT.1.0E-06) SX=0.0                                     SYSMAT16
      IF(ABS(CX).LT.1.0E-06) CX=0.0                                     SYSMAT17
      IF(ABS(SY).LT.1.0E-06) SY=0.0                                     SYSMAT18
      IF(ABS(CY).LT.1.0E-06) CY=0.0                                     SYSMAT19
      IF(ABS(TY).LT.1.0E-06) TY=0.0                                     SYSMAT20
      TL=SIN(TLAT)                                                      SYSMAT21
      CL=COS(TLAT)                                                      SYSMAT22
      DO 1 I=1,68                                                       SYSMAT23
      DO 1 J=1,68                                                       SYSMAT24
    1 E(I,J)=0.                                                         SYSMAT25
      DO 2 I=7,9                                                        SYSMAT26
    2 E(I,I)=-1./TAGL                                                   SYSMAT27
      E(31,1)=CZ/CY                                                     SYSMAT28
      E(32,1)=CZ                                                        SYSMAT29
      E(33,1)=-TY*CZ                                                    SYSMAT30
      E(31,2)=-SZ/CY                                                    SYSMAT31
      E(32,2)=CZ                                                        SYSMAT32
      E(33,2)=TY*SZ                                                     SYSMAT33
      E(33,3)=1.                                                        SYSMAT34
      E(31,4)=CZ*G(2)/CY                                                SYSMAT35
      E(32,4)=SZ*G(2)                                                   SYSMAT36
      E(33,4)=-TY*CZ*G(2)                                               SYSMAT37
      E(31,5)=-SZ*G(1)/CY                                               SYSMAT38
      E(32,5)=CZ*G(1)                                                   SYSMAT39
      E(33,5)=TY*SZ*G(1)                                                SYSMAT40
      E(37,6)=G(1)                                                      SYSMAT41
      E(31,7)=CZ/CY                                                     SYSMAT42
      E(32,7)=SZ                                                        SYSMAT43
      E(33,7)=-TY*CZ                                                    SYSMAT44
      E(31,8)=-SZ/CY                                                    SYSMAT45
      E(32,8)=CZ                                                        SYSMAT46
      E(33,8)=TY*SZ                                                     SYSMAT47
      E(33,9)=1.                                                        SYSMAT48
      E(31,10)=-G(1)*CZ/CY                                              SYSMAT49
      E(32,10)=-G(1)*SZ                                                 SYSMAT50
      E(33,10)=G(1)*TY*CZ                                               SYSMAT51
      E(31,11)=G(3)*CZ/CY                                               SYSMAT52
      E(32,11)=G(3)*SZ                                                  SYSMAT53
      E(33,11)=-G(3)*TY*CZ                                              SYSMAT54
      E(31,12)=G(2)*CZ/CY                                               SYSMAT55
      E(32,12)=-G(2)*CZ                                                 SYSMAT56
      E(33,12)=-G(2)*TY*SZ                                              SYSMAT57
```

```
                F(31,13)=-G(3)*SZ/CY                                    K       777
                F(32,13)=G(3)*CZ                                        K       778
     61         F(33,13)=G(3)*TY*CZ                                     K       779
                F(32,14)=G(3)                                           K       780
                F(33,14)=-G(2)                                          K       781
                F(31,15)=G(2)*G(3)*SZ/CY                                K       782
                F(32,15)=G(2)*G(3)*SZ                                   K       783
     65         F(33,15)=-G(2)*G(3)*TY*CZ                               K       784
                F(31,17)=-G(1)*G(3)*SZ/CY                               K       785
                F(32,17)=G(1)*G(3)*CZ                                   K       786
                F(33,17)=G(1)*G(3)*TY*SZ                                K       787
                F(33,18)=G(1)*G(2)                                      K       788
     71         F(31,19)=PRF(1)*CZ/CY                                   K       789
                F(32,19)=PRF(1)*SZ                                      K       790
                F(33,19)=-PRF(1)*TY*CZ                                  K       791
                F(31,20)=-PRF(2)*SZ/CY                                  K       792
                F(32,20)=PRF(2)*CZ                                      K       793
     75         F(33,20)=PRF(2)*TY*SZ                                   K       794
                F(33,21)=PRF(3)                                         K       795
                F(31,22)=-WC(2)*CZ/CY                                   K       796
                F(32,22)=-WC(2)*SZ                                      K       797
                F(33,22)=WC(2)*TY*CZ                                    K       798
     81         F(31,23)=WC(3)*CZ/CY                                    K       799
                F(32,23)=WC(3)*SZ                                       K       800
                F(33,23)=-WC(3)*TY*CZ                                   K       801
                F(31,24)=-WC(1)*SZ/CY                                   K       802
                F(32,24)=WC(1)*CZ                                       K       803
     85         F(33,24)=WC(1)*TY*SZ                                    K       804
                F(31,25)=WC(3)*SZ/CY                                    K       805
                F(32,25)=-WC(3)*CZ                                      K       806
                F(33,25)=-WC(3)*TY*SZ                                   K       807
                F(33,26)=-WC(1)                                         K       808
     91         F(33,27)=WC(2)                                          K       809
                F(31,28)=-ER*TY*SX*CL                                   K       810
                F(32,28)=-ER*CX*SL                                      K       811
                F(33,28)=ER*SX*SL/CY                                    K       812
                F(31,29)=ER*(TY*CX*CL+SL)                               K       813
     95         F(32,29)=-ER*SX*CL                                      K       814
                F(33,29)=-ER*CX*CL/CY                                   K       815
                F(31,30)=ER*TY*SX*CL                                    K       816
                F(32,30)=ER*CX*CL                                       K       817
                F(33,30)=-ER*SX*CL/CY                                   K       818
    101         F(31,31)=-ER*TY*SX*SL                                   K       819
                F(32,31)=-ER*CX*SL                                      K       820
                F(33,31)=ER*SX*SL/CY                                    K       821
                F(31,32)=TY*(CZ*WC(1)-SZ*WC(2))/CY+ER*CX*SL/(CY*CY)     K       822
                F(33,32)=-(CZ*WC(1)-SZ*WC(2))/(CY*CY)-ER*TY*CX*SL/CY    K       823
    105         F(31,33)=-(SZ*WC(1)+CZ*WC(2))/CY                        K       824
                F(32,33)=CZ*WC(1)-SZ*WC(2)                              K       825
                F(33,33)=TY*(SZ*WC(1)+CZ*WC(2))                         K       826
                F(49,28)=-GM*(CZ*SY*SX+SZ*CX)                           K       827
                F(50,28)=GM*(SZ*SY*SX-CZ*CX)                            K       828
    111         F(51,28)=GM*CY*SX                                       K       829
                F(49,29)=GM*CZ*CY                                       K       830
                F(50,29)=-GM*SZ*CY                                      K       831
                F(51,29)=GM*SY                                          K       832
                F(49,31)=-GM*(SZ*CX+CZ*SY*SX)                           K       833
```

```
      SUBROUTINE SYSMAT     74/74   OPT=1                FTN 4.5+414     12/07/77  17.49.??      PAGE  ??
  115                 F(50,31)=GM*(SZ*SY*SX-CZ*CX)                                          K       834
                      F(51,31)=GM*CY*SX                                                     K       835
                      F(49,32)=GM*CZ*CY*CX                                                  K       836
                      F(50,32)=-GM*SZ*CY*CX                                                 K       837
                      F(51,32)=GM*SY*CX                                                     K       838
  120                 F(49,33)=-GM*(SZ*SY*CX+CZ*SX)                                         K       839
                      F(50,33)=GM*(SZ*SX-CZ*SY*CX)                                          K       840
                      F(49,34)=1.                                                           K       841
                      F(50,35)=1.                                                           K       842
                      F(51,36)=1.                                                           K       843
  125                 F(49,40)=GM*(CZ*SY*CX-SZ*SX)                                          K       844
                      F(50,41)=-GM*(CZ*SX+SZ*SY*CX)                                         K       845
                      F(51,42)=-GM*CY*CX                                                    K       846
                      F(49,43)=-GM*(SZ*SY*CX+CZ*SX)                                         K       847
                      F(49,44)=-GM*CY*CX                                                    K       848
  130                 F(50,45)=GM*(CZ*SY*CX-SZ*SX)                                          K       849
                      F(50,46)=-GM*CY*CX                                                    K       850
                      F(51,47)=GM*(CZ*SY*CX-SZ*SX)                                          K       851
                      F(51,48)=-GM*(SZ*SY*CX+CZ*SX)                                         K       852
                      DO 7 I=31,33                                                          K       853
  135                 F(I,52)=F(I,1)                                                        K       854
                      F(I,53)=F(I,2)                                                        K       855
                      F(I,54)=F(I,3)                                                        K       856
                      F(I,55)=F(I,31)                                                       K       857
                      F(I,56)=F(I,32)                                                       K       858
  140               7 F(I,57)=F(I,33)                                                       K       859
                      DO 8 I=49,51                                                          K       860
                      F(I,55)=F(I,31)                                                       K       861
                      F(I,56)=F(I,32)                                                       K       862
                    8 F(I,57)=F(I,33)                                                       K       863
  145                 F(37,37)=-1.0/TWA                                                     K       864
                      F(38,38)=-1.0/TWA                                                     K       865
                      F(39,39)=-1.0/TWA                                                     K       866
                      F(62,62)=-1.0/TWG                                                     K       867
                      F(63,63)=-1.0/TWG                                                     K       868
  150                 F(64,64)=-1.0/TWG                                                     K       869
                      F(49,37)=1.0                                                          K       870
                      F(50,38)=1.0                                                          K       871
                      F(51,39)=1.0                                                          K       872
                      F(31,62)=F(31,1)                                                      K       873
  155                 F(32,62)=F(32,1)                                                      K       874
                      F(33,62)=F(33,1)                                                      K       875
                      F(31,63)=F(31,2)                                                      K       876
                      F(32,63)=F(32,2)                                                      K       877
                      F(33,63)=F(33,2)                                                      K       878
  160                 F(33,64)=1.0                                                          K       879
                      F(68,68)=-1.0/250.0                                                   K       880
                      F(49,68)=F(49,40)                                                     K       881
                      F(50,68)=F(50,41)                                                     K       882
                      F(51,68)=F(51,42)                                                     K       883
  165                 F(49,65)=F(43,40)                                                     K       884
                      F(50,66)=F(50,41)                                                     K       885
                      F(51,67)=F(51,42)                                                     K       886
                      DO 5 I=31,33                                                          K       887
                      DO 5 J=1,68                                                           K       888
  170                 IF(ABS(F(I,J)).LE.1.0E-100) F(I,J)=0.                                 K       889
                    5 CONTINUE                                                              K       890
```

```
      SUBROUTINE SYSMAT     74/74   OPT=1                FTN 4.6+414      02/07/77  17.49.02      PAGE   17

                      DO 6 I=49,61                                                    <      891
                      DO 6 J=1,68                                                     <      892
                      IF(ABS(F(I,J)).LE.1.0E-100) F(I,J)=0.                           <      893
  175             6 CONTINUE                                                        <      894
                      END                                                             <      895
```

```
SUBROUTINE WRTMAT     74/74   OPT=1                    FTN 4.5+414        07/ 7/77  17.43.1     PAGE   1

      1                SUBROUTINE WRT MAT(A,ISTEP)                                                  <        845
                       DIMENSION A(66,69),IC(13)                                                    <        847
                       I=1                                                                          <        848
                       DO 10 K=1,4                                                                  <        849
      5                GO TO (1,2,3,4),ISTEP                                                        <        850
                     1 CONTINUE                                                                     <        851
                       WRITE(6,100)                                                                 <        852
                   100 FORMAT(1H1,47X,40H---STATE EQUATION SYSTEM MATRIX  F(T)---)                  K        853
                       GO TO 5                                                                      <        854
     10              2 CONTINUE                                                                     K        855
                       WRITE(6,106)                                                                 <        856
                   106 FORMAT(1H1,46X,38H---INITIAL COVARIANCE MATRIX P(0/0)---)                    <        857
                       GO TO 5                                                                      <        858
                     3 CONTINUE                                                                     <        859
     15                WRITE(6,107)                                                                 <        860
                   107 FORMAT(1H1,47X,38H---PROPAGATED COVARIANCE MATRIX  PP---)                    K        861
                       GO TO 5                                                                      <        862
                     4 CONTINUE                                                                     <        863
                       WRITE(6,108)                                                                 <        864
     20            108 FORMAT(1H1,47X,36H---UPDATED COVARIANCE MATRIX  PU---)                       <        865
                     5 CONTINUE                                                                     <        866
                       WRITE(6,101)                                                                 <        867
                   101 FORMAT(1H0,174H ROW ----------------------------------------------- <        868
                      1-----------------COLUMN-------------------------------------------------- K        869
     25               2----------------)                                                           <        870
                       DO 6 I=1,13                                                                  <        871
                       IC(I)=L                                                                      K        872
                     6 L=L+1                                                                        K        873
                       IF(K.EQ.4) GO TO 7                                                           <        874
     30                WRITE(6,102) (IC(I),I=1,13)                                                  <        875
                   102 FORMAT(1H ,13(8X,I2))                                                        K        876
                       GO TO 8                                                                      K        877
                     7 CONTINUE                                                                     <        878
                       WRITE(6,103) (IC(I),I=1,12)                                                  <        879
     35            103 FORMAT(1H ,12(8X,I2))                                                        <        880
                     8 CONTINUE                                                                     K        881
                       DO 10 I=1,51                                                                 K        882
                       IF(K.EQ.4) GO TO 9                                                           <        883
                       WRITE(6,104) I,(A(I,IC(M)),M=1,13)                                           <        884
     40            104 FORMAT(1H ,I3,1X,13(1X,G9.3))                                                <        885
                       GO TO 11                                                                     K        886
                     9 CONTINUE                                                                     <        887
                       WRITE(6,105) I,(A(I,IC(M)),M=1,12)                                           <        888
                   105 FORMAT(1H ,I3,1X,12(1X,G9.3))                                                <        889
     45              11 CONTINUE                                                                    <        890
                     10 CONTINUE                                                                    <        891
                       END                                                                          K        892
```

```
SUBROUTINE FILINT     77/76   OPT=1                    FTN 4.6+414        02/02/78  17.48.02        PAGE    19

      1                SUBROUTINE FIL INT(DU,EP,EPS,GM,A,B,C,D)                                    K          943
                       DIMENSION DU(EP,EP),A(E,EP),B(E,*),
                      1(EP,12),DI(*,12)                                                            K          945
                       DIMENSION IDP(9),T(9),TAU(3),SIG(7)                                         K          946
      6                DATA TAU(1)/1.*/,TAU(2)/3600.*/,TAU(3)/.***167                              K          947
                       SIG(1)=E.*03*EPS                                                            K          948
                       SIG(2)=E.*1*EPS                                                             K          949
                       SIG(3)=EP.E-EP*GM                                                           K          950
                       IE7                                                                         K          951
     10                DO 1 I=1,9                                                                  K          952
                       IEU+*                                                                       K          953
                       IF(I.EQ.7) JEU+27                                                           K          954
                       IDP(I)=IJ                                                                   K          955
                       IDP(I)=IJ                                                                   K          956
     15              1 CONTINUE                                                                    K          957
                       WRITE(6,1**)                                                                K          958
                   1** FORMAT(1H1,4*X,*E=---KALMAN FILTER SYSTEM MATRICES---)                      K          959
                     2 FORMAT(1H0,1*2H-DW= ----------------------------------------------         K          96*
                      1----------------DOLMN----------------------------------------------         K          961
     2*               2----------------)                                                          K          962
                   1** FORMAT(1H ,9(1PE*.*))                                                       K          963
                       DO 2 I=1,12                                                                 K          964
                       DO 2 J=1,12                                                                 K          965
                       DI(I,J)=E.                                                                  K          966
     25                IF(I.EQ.J) DI(I,J)=1.                                                       K          967
                     2 CONTINUE                                                                    K          968
                       DO 7 I=1,EP                                                                 K          969
                       DO 7 J=1,12                                                                 K          97*
                       D(I,J)=E.                                                                   K          971
     3*              7 CONTINUE                                                                    K          972
                       IE1                                                                         K          973
                       DO 4 I=1,5                                                                  K          974
                       IF(I.EQ.1) K=2                                                              K          975
                       IF(I.EQ.2) K=7                                                              K          976
     35                T(I)=DT5(K)*SQRT(2.*TAU(K))                                                 K          977
                     4 CONTINUE                                                                    K          978
                       T(6,7)=DT5(7)*SQRT(2.E*TAU(7))                                              K          979
                       D(I,8)=D(49,7)                                                              K          98*
                       D(E1,9)=D(49,7)                                                             K          981
     4*                T(E1,1)=DT5(1)*SQRT(2.E*TAU(1))                                             K          982
                       D(77,2)=D(71,1)                                                             K          983
                       D(33,3)=D(71,1)                                                             K          984
                       D(59,1*)=1.3E-1E*SQRT(2.*/25E.*)                                            K          985
                    *OMPUTE INITIAL COVARIANCE MATRIX DU(D/*)                                      K          986
     45                DO 12 I=1,EP                                                                K          987
                       DO 11 J=1,EP                                                                K          988
                    1* DU(I,J)=E*.                                                                 K          989
                       DU(1,1)=(E.1*EPS)**2                                                        K          99*
                       DU(2,2)=DU(1,1)                                                             K          991
     5*                DU(7,7)=((.5*EPS)**2                                                        K          992
                       DU(4,4)=(E.4*EPS/GM)**2                                                     K          993
                       DU(5,5)=(E.5*EPS/GM)**2                                                     K          994
                       DU(6,6)=(E.3*EPS/GM)**2                                                     K          995
                       DU(7,7)=(1.E*EPS)**2                                                        K          996
     55                DU(8,8)=DU(7,7)                                                             K          997
                       DU(9,9)=DU(7,7)                                                             K          998
                       DU(1*,1*)=(1.E*EPS/GM)**2                                                   K          999
```

```
SUBROUTINE FILIN     74/74   OPT=1                    FTN 4.5+41    12/12/77  17.43.12     PAGE    21

                  PU(11,11)=(0.1*FRS/GM)**2                                    K        1007
                  PU(12,12)=PU(10,10)                                          K        1008
   60             PU(13,13)=PU(11,11)                                          K        1009
                  PU(14,14)=PU(3,3)/(GM*GM)                                    K        1010
                  PU(15,15)=PU(11,11)                                          K        1011
                  PU(10,12)=PU(10,10)*0.5                                      K        1012
                  PU(12,10)=PU(10,12)*0.5                                      K        1013
   65             PU(16,16)=(.01*FRS/(GM*GM))**2                               K        1014
                  PU(17,17)=PU(16,16)                                          K        1015
                  PU(18,18)=PU(16,16)                                          K        1016
                  PU(19,19)=(1.34E-16*7.0E-03)**2                              K        1017
                  PU(20,20)=PU(19,19)                                          K        1018
   70             PU(21,21)=PU(19,19)                                          K        1019
                  PU(22,22)=(2.9E-14)**2                                       K        1020
                  DO 11 I=23,27                                                K        1021
                11 PU(I,I)=PU(22,22)                                           K        1022
                  PU(28,28)=(0.267*FR)**2                                      K        1023
   75             PU(29,29)=PU(28,28)                                          K        1024
                  PU(30,30)=PU(28,28)                                          K        1025
                  PU(34,34)=(2.5E-09*GM)**2                                    K        1026
                  PU(35,35)=PU(34,34)                                          K        1027
                  PU(36,36)=PU(34,34)                                          K        1028
   80             PU(40,40)=(3.0E-12)**2                                       K        1029
                  PU(41,41)=PU(40,40)                                          K        1030
                  PU(42,42)=PU(40,40)                                          K        1031
                  DO 12 I=43,48                                                K        1032
                12 PU(I,I)=PU(22,22)                                           K        1033
   85             PU(55,55)=(0.1*FR)**2                                        K        1034
                  PU(56,56)=PU(55,55)                                          K        1035
                  PU(57,57)=PU(55,55)                                          K        1036
                  PU(52,52)=(0.005*FRS)**2                                     K        1037
                  PU(53,53)=PU(52,52)                                          K        1038
   90             PU(54,54)=PU(52,52)                                          K        1039
                  PU(58,58)=PU(34,34)                                          K        1040
                  PU(59,59)=PU(35,35)                                          K        1041
                  PU(60,60)=PU(40,40)                                          K        1042
                  PU(61,61)=PU(41,41)                                          K        1043
   95             PU(62,62)=(0.114*FRS)**2                                     K        1044
                  PU(63,63)=PU(62,62)                                          K        1045
                  PU(64,64)=(0.024*FRS)**2                                     K        1046
                  PU(37,37)=(5.0E-06*GM)**2                                    K1001    5
                  PU(38,38)=PU(37,37)                                          K        1048
  100             PU(39,39)=(200.0E-06*GM)**2                                  K        1049
                  PU(65,65)=(1.0E-05)**2                                       K        1050
                  PU(66,66)=PU(65,65)                                          K        1051
                  PU(67,67)=(3.0E-05)**2                                       K1001    5
                  PU(68,68)=(1.0E-06)**2                                       K        1053
  105          COMPUTE MEASUREMENT NOISE COVARIANCE MATRIX R                   K        1054
                  DO 14 I=1,6                                                  K        1055
                  DO 14 J=1,6                                                  K        1056
                14 R(I,J)=0.                                                   K        1057
                  R(1,1)=(5.0*FR/3600.0)**2                                    K        1058
  110             R(2,2)=R(1,1)                                                K        1059
                  R(3,3)=R(1,1)                                                K        1060
                  R(4,4)=1.6E-05/((2.54*12.0**5/76.0)**2)                      K        1061
                  R(4,4)=1.3E+04*R(4,4)                                        K        1062
                  R(5,5)=R(4,4)                                                K        1063
```

```
                R(6,6)=R(4,4)                                                   1057
                WRITE(6,105)                                                    1058
            105 FORMAT(1H0)                                                     1059
                WRITE(6,106)                                                    1060
            106 FORMAT(1H0,45X,40HMEASUREMENT NOISE COVARIANCE MATRIX R(I))     1061
    120         WRITE(6,102)                                                    1062
                DO 6 I=1,6                                                      1063
              6 IQC(I)=I                                                        1064
                WRITE(6,107) (IQC(K),K=1,6)                                     1065
            107 FORMAT(1H ,6(12X,I2))                                           1066
    125         DO 7 I=1,6                                                      1067
                WRITE(6,108) I,(R(I,IQC(K)),K=1,6)                              1068
            108 FORMAT(1H ,I3,5X,6(1PE12.3,4X))                                 1069
              7 CONTINUE                                                        1070
            COMPUTE MEASUREMENT MATRIX H                                        1071
    130         DO 13 I=1,8                                                     1072
                DO 13 J=1,68                                                    1073
             13 H(I,J)=0.                                                       1074
                H(4,49)=1.                                                      1075
                H(5,50)=1.                                                      1076
    135         H(6,51)=1.                                                      1077
                WRITE(6,105)                                                    1078
                WRITE(6,109)                                                    1079
            109 FORMAT(1H0,40X,41HNON-ZERO MEASUREMENT MATRIX ELEMENTS H(I))    1080
                WRITE(6,102)                                                    1081
    140         K=30                                                            1082
                DO 8 I=1,6                                                      1083
                K=K+1                                                           1084
                IF(I.EQ.4) K=K+15                                               1085
              8 IQC(I)=K                                                        1086
    145         WRITE(6,107) (IQC(K),K=1,6)                                     1087
                DO 9 I=1,6                                                      1088
                WRITE(6,108) I,(H(I,IQC(K)),K=1,6)                              1089
              9 CONTINUE                                                        1090
                END                                                             1091
```

```
      SUBROUTINE TRANS      74/74    OPT=1
      SUBROUTINE TRANS(A,N,M,AT)
      DIMENSION A(N,M),AT(M,N)
      DO 1 I=1,M
      DO 1 J=1,N
    1 AT(I,J)=A(J,I)
      RETURN
      END
```

FTN 4.0+514

SUBROUTINE MATMUL 74/74 OPT=1 FTN 4.5+414 02/07/77 17.49.03 PAGE 23

```
1                SUBROUTINE MAT_MUL(A,M,N,B,L,AB)                    K      1098
                 DIMENSION A(M,N),B(N,L),AB(M,L)                     K      1099
                 DO 1 I=1,M                                          K      1100
                 DO 1 J=1,L                                          K      1101
5                AB(I,J)=0.0                                         K      1102
                 DO 1 K=1,N                                          K      1103
1                AB(I,J)=A(I,K)*B(K,J)+AB(I,J)                       K      1104
                 END                                                 K      1105
```

```
SUBROUTINE VECMUL  74/74   OPT=1                FTN 4.8+414    12/12/77  17.49.1?     PAGE

      1       SUBROUTINE VEC MUL(A,M,N,X,AX)                                    X        1105
              DIMENSION A(M,N),X(N),AX(M)                                       X        1106
              DO 1 I=1,M                                                        X        1107
              AX(I)=0.0                                                         X        1108
              DO 2 K=1,N                                                        X        1109
      5       2 AX(I)=A(I,K)*X(K)+AX(I)                                         X        1110
              1 CONTINUE                                                        X        1111
                END                                                             X        1112
                                                                                X        1113
```

```
SUBROUTINE VECADD    74/74   OPT=1                FTN 4.5+414      02/07/77  17.49.02      PAGE    25

      1               SUBROUTINE VEC ADD(A,B,N,ADD.SUB,C)                                  K        1114
                      DIMENSION A(N),B(N),C(N)                                             K        1115
                      DO 1 I=1,N                                                           K        1116
                      IF(ADD.EQ.1.0) GO TO 2                                               K        1117
      5               IF(SUB.EQ.1.0) GO TO 3                                               K        1118
                    2 C(I)=A(I)+B(I)                                                       K        1119
                      GO TO 1                                                              K        1120
                    3 C(I)=A(I)-B(I)                                                       K        1121
                    1 CONTINUE                                                             K        1122
     10               END                                                                  K        1123
```

```
SUBROUTINE MINV       74/74   OPT=1                FTN 4.8+414      02/ 4.77  17.49.22      PAGE   2E
```

```
      SUBROUTINE MINV(A,B,N)                                                    1124
C                                                                               1125
C        MATRIX INVERSION SUBROUTINE                                            1126
C     CALLING SEQUENCE...                                                       1127
C                                                                               1128
C     CALL MINV(A,B,N)                                                          1129
C                                                                               1130
C        A IS THE INPUT MATRIX (DIMENSIONED N X N)                              1131
C        B WILL BE THE INVERSE MATRIX (DIMENSIONED N X N)                       1132
C        N IS THE DIMENSION OF A AND B                                          1133
C                                                                               1134
C     NOTE...                                                                   1135
C     CALL MINV(A,A,N)                                                          1136
C        CAUSES THE MATRIX A TO BE REPLACED BY ITS INVERSE.                     1137
C                                                                               1138
C                                                                               1139
      DOUBLE PRECISION A(N,N),B(N,N),TPE,PE,P(100)                              1140
      DIMENSION K(100)                                                          1141
      DATA    NMAX/ 100/                                                        1142
C                                                                               1143
      NN=N                                                                      1144
      IF (NN-NMAX) 10,10,500                                                    1145
   10 IF (NN) 500,500,20                                                        1146
   20 DO 30 I=1,NN                                                              1147
      K(I)=I                                                                    1148
      DO 30 J=1,NN                                                              1149
   30 B(I,J)=A(I,J)                                                             1150
      DO 330 I=1,NN                                                             1151
      IP=NN-I+1                                                                 1152
      PE=0.                                                                     1153
      DO 100 II=I,NN                                                            1154
      TPE=B(II,I)                                                               1155
      IF(DABS(PE)-DABS(TPE)) 100,100,120                                        1156
  100 PE=TPE                                                                    1157
      IP=II                                                                     1158
  120 CONTINUE                                                                  1159
      IF (PE) 160,500,160                                                       1160
  160 DO 170 J=2,NN                                                             1161
  170 P(J-1)=B(IP,J)/PE                                                         1162
      P(NN)=1.0/PE                                                              1163
      IP=K(IP)                                                                  1164
      I2=0                                                                      1165
      DO 310 J=1,NN                                                             1166
      I1=J-I2                                                                   1167
      K(I1)=K(J)                                                                1168
      IF (K(J)-IP) 260,250,260                                                  1169
  250 I2=1                                                                      1170
      GO TO 310                                                                 1171
  260 TPE=-B(J,1)                                                               1172
      DO 300 J1=2,NN                                                            1173
  300 B(I1,J1-1)=B(J,J1)+TPE*P(J1-1)                                            1174
      B(I1,NN)=TPE*P(NN)                                                        1175
  310 CONTINUE                                                                  1176
      DO 320 J=1,NN                                                             1177
  320 B(NN,J)=P(J)                                                              1178
  330 K(NN)=IP                                                                  1179
      DO 410 I=1,NN                                                             1180
```

```
 SUBROUTINE MINV       74/74   OPT=1                FTN 4.6+414       02/17/77  17.49.02       PAGE    22

                      DO 400 J=1,NN                                    K        1181
                      T1=K(J)                                          K        1182
60                400 P(I1)=R(T,J)                                     K        1183
                      DO 410 J=1,NN                                    K        1184
                  410 P(I,J)=P(J)                                      K        1185
                      RETURN                                           K        1186
                  500 PRINT 1000, NN                                   K        1187
65                    RETURN                                           K        1188
                  510 PRINT 1001                                       K        1189
                      RETURN                                           K        1190
                 1000 FORMAT (3HNN=,I12,37H IS INCORRECT FOR SUBROUTINE MINV)  K  1191
                 1001 FORMAT (40H0SUBROUTINE MINV FINDS MATRIX A SINGULAR)     K  1192
70                    END                                              K        1193
```

```
SUBROUTINE-  MATVA      74/74   OPT=1                    FTN 4.5+414        12/07/77  17.49.  2        PAGE    33

      1            SUBROUTINE MAT VA(PP,PU,XO,IM,MN,FOO,POU,POO),                <        1194
                  1TILTO,PTU,PTP,PDO,PPP,PPU,                                    <        1195
                  2TAO,TAPP,TAPU,                                                <        1196
                  3DDTO,PDTP,PDTU,                                               <        1197
      6           4DPX,DPY,DXO,DYO)                                              <        1198
                  DIMENSION                                                      <        1199
                  1TAO(6),TAPP(6),TAPU(6),                                       <        1200
                  2DDO(3),PDP(3),PPU(3),                                         <        1201
                  3TILTO(3),PTU(3),PTP(3),                                       <        1202
      11          4PP(68,68),PU(68,68),XO(68),                                   <        1203
                  5DDO(3),PDU(3),PDP(3),                                         <        1204
                  6DDTO(3),PDTP(3),PDTU(3),                                      <        1205
                  7DPX(2),DPY(2),                                                <        1206
                  8P(68),U(68),X(68),                                            <        1207
      16          9PMP(3),PMU(3),DM(3),M(3,2)                                    <        1208
                  DATA M(1,1)/127,M(1,2)/127,M(2,1)/127                          <        1209
                  DATA M(2,2)/147,M(3,1)/127,M(3,2)/147                          <        1210
                  WRITE(6,1)                                                     <        1211
                1 FORMAT(1H1,13X,82H---STATE VECTOR VARIANCES AND OPTIMAL ESTIMATES K        1212
      22          1CONTRASTED AGAINST IMU SIMULATION RESULTS---)                 <        1213
                  M=IM-1                                                         K        1214
                  WRITE(6,2) MN,N                                                K        1215
                2 FORMAT(1H ,23X,24HPLATFORM TEST ATTITUDE =,I4,                 <        1216
                  1?2H  ,MEASUREMENT NUMBER=,I4)                                 <        1217
      26          WRITE(6,104)                                                   K        1218
                104 FORMAT(1HO,112H----------STATE VECTOR ELEMENT---------   -----STANDA K        1219
                  1RD DEVIATION-----    -OPT FILT--    --SYSTEM---    -EST ERROR-)    <        1220
                  WRITE(6,105)                                                   <        1221
                105 FORMAT(1H ,40X,72H-PROPAGATED-    --UPDATED--    -ESTIMATE--    -S K        1222
      31          1IMULATED-    --STD DEV--)                                     <        1223
                  WRITE(6,19)                                                    <        1224
                 19 FORMAT(1H ,18HGYRO CONSTANT BIAS)                            <        1225
                  FCTP=180.0*3600.0/3.1416                                       K        1226
                  GRAV=980.08/(2.54*12.0*6376)                                   K        1227
      36          FCTA=GRAV*GRAV*FCTP                                            <        1228
                  ERM=180.0*60.0/3.1416                                          <        1229
                  ENMFT=6376.0                                                   <        1230
                  FCTM=1.00E+03                                                  K        1231
                  FCTG=6.76E+00/32.2                                             <        1232
      41          DO 3 I=1,68                                                    <        1233
                  FCT=1.0                                                        <        1234
                  IF(I.LE.3) FCT=FCTP                                            <        1235
                  IF(I.GE.4.AND.I.LE.6) FCT=FCTM                                 <        1236
                  IF(I.GE.7.AND.I.LE.9) FCT=FCTP                                 <        1237
      46          IF(I.GE.10.AND.I.LE.15) FCT=FCTM                               K        1238
                  IF(I.GE.16.AND.I.LE.18) FCT=FCTA                               K        1239
                  IF(I.GE.22.AND.I.LE.33) FCT=FRM                                K        1240
                  IF(I.GE.34.AND.I.LE.36) FCT=FCTG                               K        1241
                  IF(I.GE.37.AND.I.LE.39) FCT=FCTG                               K        1242
      51          IF(I.GE.43.AND.I.LE.48) FCT=FRM                                <        1243
                  IF(I.GE.49.AND.I.LE.51) FCT=FNMFT                              K        1244
                  IF(I.GE.52.AND.I.LE.54) FCT=FCTR                               K        1245
                  IF(I.GE.55.AND.I.LE.57) FCT=FRM                                <        1246
                  IF(I.GE.58.AND.I.LE.59) FCT=FCTG                               <        1247
      56          IF(I.GE.62.AND.I.LE.64) FCT=FCTR                               K        1248
                  X(I)=SQRT(PP(I,I))*FCT                                         <        1249
                  U(I)=SQRT(PU(I,I))*FCT                                         <        1250
```

```
                  Y(I)=X0(I)*FCT                                          K       1251
                3 CONTINUE                                                K       1252
60                WRITE(6,101) P(1),U(1),Y(1)                             K       1253
              101 FORMAT(1H ,10X,6HX-AXIS,20X,3(5X,1PE10.3))              K       1254
                  WRITE(6,102) P(2),U(2),Y(2)                             K       1255
              102 FORMAT(1H ,10X,6HY-AXIS,20X,3(5X,1PE10.3))              K       1256
                  WRITE(6,103) P(3),U(3),Y(3)                             K       1257
65            103 FORMAT(1H ,10X,6HZ-AXIS,20X,3(5X,1PE10.3))              K       1258
                  WRITE(6,40)                                             K       1259
               40 FORMAT(1H ,29HGYRO ATTITUDE DEPENDENT BIAS)             K       1260
                  WRITE(6,101) P(52),U(52),Y(52)                          K       1261
                  WRITE(6,102) P(53),U(53),Y(53)                          K       1262
70                WRITE(6,103) P(54),U(54),Y(54)                          K       1263
                  WRITE(6,501)                                            K       1264
              501 FORMAT(1H ,19HGYRO WARM-UP DRIFT)                       K       1265
                  WRITE(6,101) P(62),U(62),Y(62)                          K       1266
                  WRITE(6,102) P(63),U(63),Y(63)                          K       1267
75                WRITE(6,103) P(64),U(64),Y(64)                          K       1268
                  WRITE(6,20)                                             K       1269
               20 FORMAT(1H ,19HGYRO DA G SENSITIVE)                      K       1270
                  WRITE(6,101) P(4),U(4),Y(4)                             K       1271
                  WRITE(6,102) P(5),U(5),Y(5)                             K       1272
80                WRITE(6,103) P(6),U(6),Y(6)                             K       1273
                  WRITE(6,21)                                             K       1274
               21 FORMAT(1H ,23HGYRO G.S.G. CORRELATED)                   K       1275
                  WRITE(6,101) P(7),U(7),Y(7)                             K       1276
                  WRITE(6,102) P(8),U(8),Y(8)                             K       1277
85                WRITE(6,103) P(9),U(9),Y(9)                             K       1278
                  WRITE(6,3)                                              K       1279
                3 FORMAT(1H ,19HGYRO MASS UNBALANCE)                      K       1280
                  WRITE(6,110) P(10),U(10),Y(10)                          K       1281
              110 FORMAT(1H ,10X,3HMSX,23X,3(5X,1PE10.3))                 K       1282
90                WRITE(6,111) P(11),U(11),Y(11)                          K       1283
              111 FORMAT(1H ,10X,3HMIX,23X,3(5X,1PE10.3))                 K       1284
                  WRITE(6,112) P(12),U(12),Y(12)                          K       1285
              112 FORMAT(1H ,10X,3HMSY,23X,3(5X,1PE10.3))                 K       1286
                  WRITE(6,113) P(13),U(13),Y(13)                          K       1287
95            113 FORMAT(1H ,10X,3HMIY,23X,3(5X,1PE10.3))                 K       1288
                  WRITE(6,114) P(14),U(14),Y(14)                          K       1289
              114 FORMAT(1H ,10X,3HMSZ,23X,3(5X,1PE10.3))                 K       1290
                  WRITE(6,115) P(15),U(15),Y(15)                          K       1291
              115 FORMAT(1H ,10X,3HMIZ,23X,3(5X,1PE10.3))                 K       1292
100               IF(MN.EQ.1) GO TO 5                                     K       1293
                  DO 200 I=1,3                                            K       1294
                  FWC=2.0                                                 K       1295
                  IF(I.EQ.1) FWC=-2.0                                     K       1296
                  PM(I)=X0(M(I,1))+X0(M(I,2))                             K       1297
105               IF(I.NE.1) GO TO 203                                    K       1298
                  PM(I)=X0(M(I,1))-X0(M(I,2))                             K       1299
              203 CONTINUE                                                K       1300
                  PMP(I)=PP(M(I,1),M(I,1))+PP(M(I,2),M(I,2))              K       1301
                  PMU(I)=PU(M(I,1),M(I,1))+PU(M(I,2),M(I,2))              K       1302
110               PMP(I)=PMP(I)+FWC*PP(M(I,1),M(I,2))                     K       1303
                  PMU(I)=PMU(I)+FWC*PU(M(I,1),M(I,2))                     K       1304
              200 CONTINUE                                                K       1305
                  DO 204 I=1,3                                            K       1306
                  PMP(I)=SQRT(PMP(I))*FCTM                                K       1307
```

```
      SUBROUTINE AFIVA      74/74   OPT=1                    FTN 4.5+514        12/27/77  17.49.32        PAGE  12

  115                 PMU(I)=SQRT(PMU(I))*FCTM                                  K       1308
                      PM(I)=PM(I)*FCTM                                          K       1309
                  204 CONTINUE                                                  K       1310
                      WRITE(6,205) PMP(1),PMU(1),PM(1)                          K       1311
                  205 FORMAT(1H ,10X,7HMSX-MSY,10X,3(5X,1PE10.3))               K       1312
  120                 WRITE(6,206) PMP(2),PMU(2),PM(2)                          K       1313
                  206 FORMAT(1H ,10X,7HMSX+MSZ,10X,3(5X,1PE10.3))               K       1314
                      WRITE(6,207) PMP(3),PMU(3),PM(3)                          K       1315
                  207 FORMAT(1H ,10X,7HMSY+MSZ,10X,3(5X,1PE10.3))               K       1316
                    5 CONTINUE                                                  K       1317
  125                 WRITE(6,10)                                               K       1318
                   10 FORMAT(1H ,27HGYRO ANISOELASTIC CONSTANTS)                 K       1319
                  208 CONTINUE                                                  K       1320
                      WRITE(6,101) P(16),J(16),X(16)                            K       1321
                      WRITE(6,102) P(17),J(17),X(17)                            K       1322
  130                 WRITE(6,103) P(18),J(18),X(18)                            K       1323
                      WRITE(6,24)                                               K       1324
                   24 FORMAT(1H ,16HGYRO TOTAL DRIFT)                           K       1325
                      DO 25 I=1,3                                               K       1326
                      PPP(I)=SQRT(PPP(I))*FCTP                                  K       1327
  135                 PPU(I)=SQRT(PPU(I))*FCTP                                  K       1328
                      PPO(I)=PPO(I)*FCTP                                        K       1329
                   25 CONTINUE                                                  K       1330
                      WRITE(6,101) PPP(1),PPU(1),PPO(1)                         K       1331
                      WRITE(6,102) PPP(2),PPU(2),PPO(2)                         K       1332
  140                 WRITE(6,103) PPP(3),PPU(3),PPO(3)                         K       1333
                      WRITE(6,11)                                               K       1334
                   11 FORMAT(1H ,17HGYRO SCALE FACTOR)                          K       1335
                      WRITE(6,101) P(19),J(19),X(19)                            K       1336
                      WRITE(6,102) P(20),J(20),X(20)                            K       1337
  145                 WRITE(6,103) P(21),J(21),X(21)                            K       1338
                      WRITE(6,9)                                                K       1339
                    9 FORMAT(1H ,24HGYRO MISALIGNMENT ANGLES)                   K       1340
                      WRITE(6,122) P(22),J(22),X(22)                            K       1341
                  122 FORMAT(1H ,10X,3HBYZ,23X,3(5X,1PE10.3))                   K       1342
  150                 WRITE(6,123) P(23),J(23),X(23)                            K       1343
                  123 FORMAT(1H ,10X,3HBXY,23X,3(5X,1PE10.3))                   K       1344
                      WRITE(6,124) P(24),J(24),X(24)                            K       1345
                  124 FORMAT(1H ,10X,3HBYZ,23X,3(5X,1PE10.3))                   K       1346
                      WRITE(6,125) P(25),J(25),X(25)                            K       1347
  155             125 FORMAT(1H ,10X,3HBYX,23X,3(5X,1PE10.3))                   K       1348
                      WRITE(6,126) P(26),J(26),X(26)                            K       1349
                  126 FORMAT(1H ,10X,3HBZY,23X,3(5X,1PE10.3))                   K       1350
                      WRITE(6,127) P(27),J(27),X(27)                            K       1351
                  127 FORMAT(1H ,10X,3HBZX,23X,3(5X,1PE10.3))                   K       1352
  160                 IF(MN.EQ.1) GO TO 37                                      K       1353
                      GO TO 38                                                  K       1354
                   37 CONTINUE                                                  K       1355
                      DO 50 I=1,3                                               K       1356
                      PPP(I)=SQRT(PPP(I))*FCTP                                  K       1357
  165                 PPU(I)=SQRT(PPU(I))*FCTP                                  K       1358
                      PPO(I)=PPO(I)*FCTP                                        K       1359
                   50 CONTINUE                                                  K       1360
                      WRITE(6,51)                                               K       1361
                   51 FORMAT(1H ,23HPLATFORM GYRO DEPENDENT DRIFT)              K       1362
  170                 WRITE(6,101) PPP(1),PPU(1),PPO(1)                         K       1363
                      WRITE(6,102) PPP(2),PPU(2),PPO(2)                         K       1364
```

```
      SUBROUTINE WRTV4      74/74   OPT=1                FTN 4.5+414      03/17/77  17.49.10      PAGE   21

                WRITE(6,103) PPP(3),PPU(3),PPO(3)                                    1365
             33 CONTINUE                                                             1366
             22 FORMAT(1H1)                                                          1367
      175       WRITE(6,400)                                                        1368
      400    FORMAT(1H ,29HGYRO NON-ORTHOGONALITY ANGLES)                           1369
                CALL ANG COV(PP,PU,X0,GP,GU,G0,                                     1370
               *24,-1.0,22,1.0)                                                     1371
                WRITE(6,124) GP,GU,G0                                               1372
      180       CALL ANG COV(PP,PU,X0,GP,GU,G0,                                     1373
               *26,1.0,23,-1.0)                                                     1374
                WRITE(6,126) GP,GU,G0                                               1375
                CALL ANG COV(PP,PU,X0,GP,GU,G0,                                     1376
               *27,1.0,25,-1.0)                                                     1377
      185       WRITE(6,127) GP,GU,G0                                               1378
                WRITE(6,12)                                                         1379
             12 FORMAT(1H1,27HHOUSING MISALIGNMENT ANGLES)                          1380
                WRITE(6,101) P(28),J(28),X(28)                                      1381
                WRITE(6,102) P(29),J(29),X(29)                                      1382
      190       WRITE(6,103) P(30),J(30),X(30)                                      1383
                WRITE(6,41)                                                         1384
             41 FORMAT(1H ,25HGIMBAL SYNCHRO ANGLE BIAS)                            1385
                WRITE(6,101) P(55),J(55),X(55)                                      1386
                WRITE(6,102) P(56),J(56),X(56)                                      1387
      195       WRITE(6,103) P(57),J(57),X(57)                                      1388
                WRITE(6,13)                                                         1389
             13 FORMAT(1H ,27HDIFFERENTIAL SYNCHRO ANGLES)                          1390
                WRITE(6,101) P(31),J(31),X(31)                                      1391
                WRITE(6,102) P(32),J(32),X(32)                                      1392
      200       WRITE(6,103) P(33),J(33),X(33)                                      1393
                IF(MN.EQ.1) GO TO 28                                                1394
                DO 1) 29                                                            1395
             24 CONTINUE                                                            1396
                WRITE(6,26)                                                         1397
      205    26 FORMAT(1H ,27HPLATFORM TILT ANGLES)                                 1398
                DO 27 I=1,3                                                         1399
                PTP(I)=SQRT(PTP(I))                                                 1400
                PTU(I)=SQRT(PTU(I))                                                 1401
                PTP(I)=PTP(I)*FRM                                                   1402
      210       PTU(I)=PTU(I)*FRM                                                   1403
                TILTO(I)=TILTO(I)*FRM                                               1404
             27 CONTINUE                                                            1405
                WRITE(6,101) PTP(1),PTU(1),TILTO(1)                                 1406
                WRITE(6,102) PTP(2),PTU(2),TILTO(2)                                 1407
      215       WRITE(6,103) PTP(3),PTU(3),TILTO(3)                                 1408
             28 CONTINUE                                                            1409
                WRITE(6,35)                                                         1410
             35 FORMAT(1H ,22HPLATFORM TOTAL DRIFT)                                 1411
                DO 36 I=1,3                                                         1412
      220       PDTP(I)=SQRT(PDTP(I))*FCTR                                          1413
                PDTU(I)=SQRT(PDTU(I))*FCTR                                          1414
                PDTO(I)=PDTO(I)*FCTR                                                1415
             36 CONTINUE                                                            1416
                WRITE(6,101) PDTP(1),PDTU(1),PDTO(1)                                1417
      225       WRITE(6,102) PDTP(2),PDTU(2),PDTO(2)                                1418
                WRITE(6,103) PDTP(3),PDTU(3),PDTO(3)                                1419
                WRITE(6,14)                                                         1420
             14 FORMAT(1H ,19HACCELEROMETER BIAS)                                   1421
```

```
                WRITE(6,101) P(34),J(34),X(34)                          K       1429
225             WRITE(6,102) P(35),J(35),X(35)                          K       1423
                WRITE(6,103) P(36),J(36),X(36)                          K       1424
                IF(MM.EQ.1) GO TO 4                                     K       1425
                WRITE(6,6)                                              K       1426
              6 FORMAT(1H ,20HACC BIAS (HIGH GAIN))                     K       1427
235             WRITE(6,101) P(58),J(58),X(58)                          K       1428
                WRITE(6,102) P(59),J(59),X(59)                          K       1429
              4 CONTINUE                                                K       1430
                WRITE(6,502)                                            K       1431
            502 FORMAT(1H ,21HACC WARM-UP TRANSIENT)                    K       1432
240             WRITE(6,101) P(37),J(37),X(37)                          K       1433
                WRITE(6,102) P(38),J(38),X(38)                          K       1434
                WRITE(6,103) P(39),J(39),X(39)                          K       1435
                WRITE(6,16)                                             K       1436
             16 FORMAT(1H ,25HACCELEROMETER SCALE FACTOR)               K       1437
245             WRITE(6,101) P(40),J(40),X(40)                          K       1438
                WRITE(6,102) P(41),J(41),X(41)                          K       1439
                WRITE(6,103) P(42),J(42),X(42)                          K       1440
                IF(MM.EQ.1) GO TO 37                                    K       1441
                WRITE(6,39)                                             K       1442
250          39 FORMAT(1H ,28HACC SCALE FACTOR (HIGH GAIN))             K       1443
                WRITE(6,101) P(60),J(60),X(60)                          K       1444
                WRITE(6,102) P(61),J(61),X(61)                          K       1445
                WRITE(6,7)                                              K       1446
              7 FORMAT(1H ,24HACC ATT DEP SCALE FACTOR)                 K       1447
255             WRITE(6,101) P(65),J(65),X(65)                          K       1448
                WRITE(6,102) P(66),J(66),X(66)                          K       1449
                WRITE(6,103) P(67),J(67),X(67)                          K       1450
                WRITE(6,15)                                             K       1451
             15 FORMAT(1H ,15HCLOCK STABILITY)                          K       1452
260             WRITE(6,34) P(68),J(68),X(68)                           K       1453
             34 FORMAT(1H ,3HY,3(5X,1PE10.3))                           K       1454
             38 CONTINUE                                                K       1455
                WRITE(6,17)                                             K       1456
             17 FORMAT(1H ,28HACC/PLATFORM MISALIGN ANGLES)             K       1457
265             WRITE(6,122) P(43),J(43),X(43)                          K       1458
                WRITE(6,123) P(44),J(44),X(44)                          K       1459
                WRITE(6,124) P(45),J(45),X(45)                          K       1460
                WRITE(6,125) P(46),J(46),X(46)                          K       1461
                WRITE(6,126) P(47),J(47),X(47)                          K       1462
270             WRITE(6,127) P(48),J(48),X(48)                          K       1463
                WRITE(6,403)                                            K       1464
            403 FORMAT(1H ,28HACC NON-ORTHOGONALITY ANGLES)             K       1465
                CALL ANG_COV(PP,PU,XD,GP,GU,CO,                         K       1466
               0.5,-1.0,43,-1.0)                                        K       1467
275             WRITE(6,124) GP,GU,CO                                   K       1468
                CALL ANG_COV(PP,PU,XD,GP,GU,CO,                         K       1469
              0.7,1.0,44,1.0)                                           K       1470
                WRITE(6,126) GP,GU,CO                                   K       1471
                CALL ANG_COV(PP,PU,XD,GP,GU,CO,                         K       1472
280           0.9,-1.0,46,-1.0)                                         K       1473
                WRITE(6,127) GP,GU,CO                                   K       1474
                IF(MM.EQ.1) GO TO 402                                   K       1475
                WRITE(6,404)                                            K       1476
            404 FORMAT(1H ,34HACC/GYRO FRAME MISALIGN ANGLES)           K       1477
285             CALL ANG_COV(PP,PU,XD,GP,GU,CO,                         K       1478
```

```
                  2?5,-1. ,46,1.0)                                    <      1479
                   WRITE(6,101) GP,GU,GO                              K      1480
                   CALL ANG CONV(PP,PU,XO,GP,GU,GO,                   K      1481
                  2?4,-1.0,23,-1.0)                                   K      1482
 29?              WRITE(6,102) GP,GU,GO                               K      1483
                  CALL ANG CONV(PP,PU,XO,GP,GU,GO,                    <      1484
                  2?2,-1.0,43,1.0)                                    K      1485
                   WRITE(6,103) GP,GU,GO                              K      1486
               42 CONTINUE                                            K      1487
 295               IF(MN.EQ.1) GO TO 31                               K      1488
                   GO TO 32                                           K      1489
               31 CONTINUE                                            K      1490
                  DO 32 I=1,6                                         <      1491
                  TAPP(I)=SQRT(TAPP(I))                               K      1492
 ?99              TAPU(I)=SQRT(TAPU(I))                               K      1493
                  TAPP(I)=TAPP(I)*FRM                                 <      1494
                  TAPU(I)=TAPU(I)*FRM                                 <      1495
                  TAO(I)=TAO(I)*FRM                                   K      1496
               32 CONTINUE                                            K      1497
 3?5              WRITE(6,33)                                         K      1498
               33 FORMAT(1H ,23H1OB/NAV FRAME MISALIGN ANGLES)        <      1499
                  WRITE(6,120) TAPP(1),TAPU(1),TAO(1)                 K      1500
                  WRITE(6,?23) TAPP(2),TAPU(2),TAO(2)                 K      1501
                  WRITE(6,124) TAPP(3),TAPU(3),TAO(3)                 <      1502
 3?0              WRITE(6,125) TAPP(4),TAPU(4),TAO(4)                 K      1503
                  WRITE(6,126) TAPP(5),TAPU(5),TAO(5)                 K      1504
                  WRITE(6,127) TAPP(6),TAPU(6),TAO(6)                 K      1505
                  WRITE(6,50)                                         <      1506
               5  FORMAT(1H ,23HACC(C)/NAV FRAME MISAL ANGLES)        <      1507
 3?5              DPX(1)=SQRT(DPX(1))                                 K      1508
                  DPX(2)=SQRT(DPX(2))                                 <      1509
                  DPY(1)=SQRT(DPY(1))                                 <      1510
                  DPY(2)=SQRT(DPY(2))                                 K      1511
                  DO 240 I=1,2                                        K      1512
 32?              DPX(I)=DPX(I)*FRM                                   <      1513
                  DPY(I)=DPY(I)*FRM                                   <      1514
              24? CONTINUE                                            K      1515
                  DXO=DXO*FRM                                         <      1516
                  DYO=DYO*FRM                                         <      1517
 3?6              WRITE(6,101) DPX(1),DPX(2),DXO                      <      1518
                  WRITE(6,102) DPY(1),DPY(2),DYO                      K      1519
               31 CONTINUE                                            K      1520
                  WRITE(6,18)                                         <      1521
               18 FORMAT(1H ,19HPLATFORM VELOCITIES)                  K      1522
 33?              WRITE(6,101) P(49),J(49),X(49)                      K      1523
                  WRITE(6,102) P(50),J(50),X(50)                      <      1524
                  WRITE(6,103) P(51),J(51),X(51)                      K      1525
                  END                                                 <      1526
```

```
SUBROUTINE FILKAL      74/74   OPT=1                    FTN 4.5+414        77/12/22 17.43.39        PAGE   44

      1                SUBROUTINE FIL KAL (PP,PU,QP,F,                                  K        1527
                      1Q4,R,XQ,XS,K,Q4,MN)                                              K        1528
                       DOUBLE PRECISION Q2(6,6)                                         K        1529
                       DIMENSION PP(68,68),PU(68,68),Q2(68,68),F(68,68),                K        1530
      5                1Q(6,68),S(6,6),XQ(68),HT(68,6),Q4(68,68),                       K        1531
                      2Q1(68,6),XQ(68),Z(6),HX(6),Q3(68),FYQ(68,68),                    K        1532
                      3FY3(68,68),Q5(68,68),Q6(6,68),XQQT(68)                           K        1533
                       REAL K(68,6),TDEN(68,68)                                         K        1534
                       DATA N/68/,M/6/                                                  K        1535
     10          COMPUTE THE PROPAGATED STATE COVARIANCE MATRIX PP(K/K-1),NXN          K        1536
                      DT=30.0                                                           K        1537
                      IF(MN.EQ.1) DT=10.0                                               K        1538
                      DT3=DT/3.0                                                        K        1539
                      DT6=DT/6.0                                                        K        1540
     15               DT8=DT/8.0                                                        K        1541
                      DT38=3.0*DT/8.0                                                   K        1542
                      DT12=DT/2.0                                                       K        1543
                      DT32=3.0*DT/2.0                                                   K        1544
                      DT2=2.0*DT                                                        K        1545
     20               DT23=2.0*DT/3.0                                                   K        1546
                      DO 100 L=1,1                                                      K        1547
                      CALL PDOT(PU,QP,F,FYQ,PP,IDEN)                                    K        1548
                      DO 5 I=1,N                                                        K        1549
                      DO 5 J=1,N                                                        K        1550
     25             5 Q5(I,J)=PU(I,J)+FYQ(I,J)*DT3                                     K        1551
                      CALL PDOT(Q5,QP,F,Q4,PP,IDEN)                                     K        1552
                      DO 6 I=1,N                                                        K        1553
                      DO 6 J=1,N                                                        K        1554
                    6 Q5(I,J)=PU(I,J)+(FYQ(I,J)+Q4(I,J))*DT6                            K        1555
     30               CALL PDOT(Q5,QP,F,Q4,PP,IDEN)                                     K        1556
                      DO 7 I=1,N                                                        K        1557
                      DO 7 J=1,N                                                        K        1558
                    7 Q5(I,J)=PU(I,J)+FYQ(I,J)*DT8+Q4(I,J)*DT38                         K        1559
                      CALL PDOT(Q5,QP,F,FY3,PP,IDEN)                                    K        1560
     35               DO 8 I=1,N                                                        K        1561
                      DO 8 J=1,N                                                        K        1562
                    8 Q5(I,J)=PU(I,J)+FYQ(I,J)*DT12                                     K        1563
                     Q-Q4(I,J)*DT32+FY3(I,J)*DT2                                        K        1564
                      CALL PDOT(Q5,QP,F,Q4,PP,IDEN)                                     K        1565
     40               DO 9 I=1,N                                                        K        1566
                      DO 9 J=1,N                                                        K        1567
                    9 PU(I,J)=PU(I,J)+(FYQ(I,J)+Q4(I,J))*DT6                            K        1568
                     Q+FY3(I,J)*DT23                                                    K        1569
                  100 CONTINUE                                                          K        1570
     45               DO 10 I=1,N                                                       K        1571
                      DO 10 J=1,N                                                       K        1572
                   10 PP(I,J)=PU(I,J)                                                   K        1573
                 COMPUTE PROPAGATED STATE VECTOR XQ(K/K-1),N                            K        1574
                      IDX=10                                                            K        1575
     50               IF(MN.EQ.1) IDX=10                                                K        1576
                      DO 2 I=1,IDX                                                      K        1577
                      CALL VEC MUL(F,N,N,XQ,XQ)                                         K        1578
                      CALL VEC ADD(XQ,XQ,N,1.,.,.,Q3)                                   K        1579
                      CALL VEC MUL(F,N,N,Q3,XQQT)                                       K        1580
     55               DO 4 J=1,N                                                        K        1581
                    4 XQ(J)=XQ(J)+(XQQT(J)+XQ(J))/2.0                                   K        1582
                    2 CONTINUE                                                          K        1583
```

```
      SUBROUTINE FILKAL      74/74   OPT=1                FTN 4.5+414      77/07/22  17.49.00      PAGE   15
C
C     COMPUTE MEASUREMENT  Z,M
      CALL VEC MUL(H,M,N,XS,Z)
C     COMPUTE THE KALMAN GAIN MATRIX K(K), NXN
      CALL TRANS(H,M,N,HT)
      CALL MAT MUL(PP,N,N,HT,N,D1)
      DO 11 I=1,M
      DO 11 J=1,M
      D2(I,J)=0.0
      DO 12 L=1,N
   12 D2(I,J)=H(I,L)*D1(L,J)+D2(I,J)
   11 D2(I,J)=D2(I,J)+R(I,J)
      CALL MINV(D2,M,D)
      DO 13 I=1,N
      DO 13 J=1,M
      K(I,J)=0.0
      DO 13 L=1,M
   13 K(I,J)=D1(I,L)*D2(L,J)+K(I,J)
C     COMPUTE OPTIMAL FILTERED ESTIMATE XO(K/K), N
      CALL VEC MUL(H,M,N,XO,HX)
      CALL VEC ADD(Z,HX,M,D.,1.,Z)
      CALL VEC MUL(K,N,M,Z,DX)
      CALL VEC ADD(XO,DX,N,1.,D.,XO)
C     COMPUTE UPDATED STATE COVARIANCE MATRIX PU(K/K),NXN
      DO 1 I=1,N
      DO 1 J=1,N
      IDEN(I,J)=0.
    1 IF(I.EQ.J) IDEN(I,J)=1.
      CALL MAT MUL(K,N,M,H,N,D4)
      CALL MAT ADD(IDEN,D4,N,N,D.,1.,D4)
      CALL TRANS(D4,N,N,D5)
      CALL MAT MUL(D4,N,N,PP,N,PU)
      CALL MAT MUL(PU,N,N,D5,N,D4)
      CALL MAT MUL(K,N,M,R,M,D1)
      CALL TRANS(K,N,M,D6)
      CALL MAT MUL(D1,N,M,D6,N,D5)
      CALL MAT ADD(D4,D5,N,N,1.D.,D.D,PU)
      END
```

```
1594
1595
1596
1597
1598
1599
1600
1601
1602
1603
1604
1605
1606
1607
1608
1609
1610
1611
1612
1613
1614
1615
1616
1617
1618
1619
1620
```

CARD NR. SEVERITY DETAILS   DIAGNOSIS OF PROBLEM

21   I   LOWER LIMIT .GE. UPPER LIMIT, ONE TRIP LOOP.

```
SUBROUTINE POOT      7477   OPT=1                FTN  4.5+414      77/12/27  17.43.22      PAGE   75

      SUBROUTINE POOT(P,Q2,E,P1,EP,EPT)                                 K       1621
      DIMENSION P(68,68),E(68,68),EP(68,68),                            K       1622
     1EPT(68,68),Q2(68,68),PD(68,68)                                    K       1623
      DATA N/68/                                                        K       1624
      DO 10 I=1,N                                                       K       1625
      DO 10 J=1,N                                                       K       1626
   10 P2(I,J)=0.0                                                       K       1627
      DO 15 I=7,9                                                       K       1628
      DO 15 J=1,N                                                       K       1629
   15 EP(I,J)=E(I,I)*P(I,J)                                             K       1630
      DO 1 I=37,58                                                      K       1631
      IF(I.GT.54.AND.I.LT.58) GO TO 1                                   K       1632
      IF(I.GT.39.AND.I.LT.42) GO TO 1                                   K       1633
      DO 2 J=1,N                                                        K       1634
    2 EP(I,J)=E(I,I)*P(I,J)                                             K       1635
    1 CONTINUE                                                          K       1636
      DO 17 I=31,37                                                     K       1637
      DO 17 L=1,N                                                       K       1638
      A=0.                                                              K       1639
      DO 18 J=1,N                                                       K       1640
   18 A=A+E(I,J)*P(J,L)                                                 K       1641
   17 EP(I,L)=A                                                         K       1642
      DO 19 I=49,51                                                     K       1643
      DO 19 L=1,N                                                       K       1644
      A=0.                                                              K       1645
      DO 20 J=38,N                                                      K       1646
   20 A=A+E(I,J)*P(J,L)                                                 K       1647
   19 EP(I,L)=A                                                         K       1648
      CALL TRANS(EP,N,N,EPT)                                            K       1649
      DO 21 I=1,N                                                       K       1650
      DO 21 J=1,N                                                       K       1651
      PD(I,J)=EP(I,J)+EPT(I,J)+QP(I,J)                                  K       1652
      PD(J,I)=PD(I,J)                                                   K       1653
   21 CONTINUE                                                          K       1654
      END                                                               K       1655
```

```
SUBROUTINE MATADD    74/74   OPT=1                FTN 4.5+414      02/07/77  17.49.02      PAGE   17

      1              SUBROUTINE MAT ADD(A,B,M,N,ADD,SUB,C)                                  K       1656
                     DIMENSION A(M,N),B(M,N),C(M,N)                                         K       1657
                     DO 1 I=1,M                                                             K       1658
                     DO 1 J=1,N                                                             K       1659
      5              IF(ADD.EQ.1.0) GO TO 2                                                 K       1660
                     IF(SUB.EQ.1.0) GO TO 3                                                 K       1661
                   2 C(I,J)=A(I,J)  (I,J)                                                   K       1662
                     GO TO 1                                                                K       1663
                   3 C(I,J)=A(I,J)-B(I,J)                                                   K       1664
     10            1 CONTINUE                                                             K       1665
                     END                                                                    K       1666
```

```
SUBROUTINE ANS(NP,PU,X,Y,FU,FV,
1 F1,F2,F3)
DIMENSION PP(69,69),PU(69,69),X(69)
PI=3.1415
PP(I1,I1)=PP(I2,I2)+E1*E2*PP(I1,I2)*2.
PP(I1,I2)=PP(I2,I2)+2.0*E1*F2*PU(I1,I2)
PU(I1,I1)=PU(I2,I2)+2.0*E1*F2*PU(I1,I2)
FU=SQRT(FU)*FPM
FV=F1*X(I1)+F3*X(I2)
FPM=FPM
```

---STATE VECTOR VARIANCES AND OPTIMAL ESTIMATES CONTRASTED AGAINST IMU SIMULATION RESULTS---
PLATFORM TEST ATTITUDE = 1 ,MEASUREMENT NUMBER= 0

---------STATE VECTOR ELEMENT---------	-----STANDARD DEVIATION---- -PROPAGATED-	--UPDATED--	-OPT FILT-- -ESTIMATE--	--SYSTEM--- -SIMULATED-	-EST ERROR- --STD DEV--
GYRO CONSTANT BIAS					
X-AXIS	1.000E-01	1.000E-01	0.		
Y-AXIS	1.000E-01	1.000E-01	0.		
Z-AXIS	5.000E-01	5.000E-01	0.		
GYRO ATTITUDE DEPENDENT BIAS					
X-AXIS	5.000E-03	5.000E-03	0.		
Y-AXIS	5.000E-03	5.000E-03	0.		
Z-AXIS	5.000E-03	5.000E-03	0.		
GYRO WARM-UP DRIFT					
X-AXIS	1.400E-02	1.400E-02	0.		
Y-AXIS	1.400E-02	1.400E-02	0.		
Z-AXIS	1.400E-02	1.400E-02	0.		
GYRO G SENSITIVE					
X-AXIS	3.994E-01	3.994E-01	0.		
Y-AXIS	3.994E-01	3.994E-01	0.		
Z-AXIS	4.993E-02	4.993E-02	0.		
GYRO G.Y.G. CORRELATED					
X-AXIS	5.000E-03	5.000E-03	0.		
Y-AXIS	5.000E-03	5.000E-03	0.		
Z-AXIS	5.000E-03	5.000E-03	0.		
GYRO MASS UNBALANCE					
MSX	9.985E-01	9.985E-01	0.		
MIX	9.946E-07	9.946E-07	0.		
MSY	9.996E-01	9.996E-01	0.		
MIY	9.996E-03	9.996E-03	0.		
MSZ	4.993E-01	4.993E-01	0.		
MIZ	9.996E-03	9.996E-03	0.		
GYRO ANISOELASTIC CONSTANTS					
X-AXIS	1.000E-02	1.000E-02	0.		
Y-AXIS	1.000E-02	1.000E-02	0.		
Z-AXIS	1.000E-02	1.000E-02	0.		
GYRO TOTAL DRIFT					
X-AXIS	1.018E-01	1.018E-01	0.		
Y-AXIS	1.018E-01	1.018E-01	0.		
Z-AXIS	7.076E-01	7.076E-01	0.		
GYRO SCALE FACTOR					
X-AXIS	1.358E-08	1.358E-08	0.		
Y-AXIS	1.358E-08	1.358E-08	0.		
Z-AXIS	1.358E-08	1.358E-08	0.		
GYRO MISALIGNMENT ANGLES					
BYZ	9.969E-01	9.969E-01	0.		
BXY	9.969E-01	9.969E-01	0.		
BYZ	9.969E-01	9.969E-01	0.		
BYX	9.969E-01	9.969E-01	0.		
BZY	9.969E-01	9.969E-01	0.		
BZX	9.969E-01	9.969E-01	0.		
PLATFORM GYRO DEPENDENT DRIFT					
X-AXIS	1.300E-01	1.300E-01	0.		
Y-AXIS	1.019E-01	1.019E-01	0.		
Z-AXIS	7.108E-01	7.108E-01	0.		
GYRO NON-ORTHOGONALITY ANGLES					
BYZ	1.410E+00	1.410E+00	0.		
BZY	1.410E+00	1.410E+00	0.		
BZX	1.410E+00	1.410E+00	0.		

HOUSING MISALIGNMENT ANGLES			
X-AXIS	4.020E+00	4.020E+01	0.
Y-AXIS	4.020E+00	4.020E+01	0.
Z-AXIS	4.020E+00	4.020E+01	0.
GIMBAL SYNCHRO ANGLE BIAS			
X-AXIS	6.000E+00	6.000E+01	0.
Y-AXIS	6.000E+00	6.000E+01	0.
Z-AXIS	6.000E+00	6.000E+01	0.
DIFFERENTIAL SYNCHRO ANGLE			
X-AXIS	0.	0.	0.
Y-AXIS	0.	0.	0.
Z-AXIS	0.	0.	0.
PLATFORM TILT ANGLES			
X-AXIS	7.222E+00	7.222E+01	0.
Y-AXIS	7.222E+00	7.222E+01	0.
Z-AXIS	7.222E+00	7.222E+01	0.
PLATFORM TOTAL DRIFT			
X-AXIS	1.316E-01	1.316E-01	0.
Y-AXIS	1.066E-01	1.066E-01	0.
Z-AXIS	7.112E-01	7.112E-01	0.
ACCELEROMETER BIAS			
X-AXIS	2.496E+03	2.496E+03	0.
Y-AXIS	2.496E+03	2.496E+03	0.
Z-AXIS	2.496E+03	2.496E+03	0.
ACC WARM-UP TRANSIENT			
X-AXIS	4.993E+00	4.993E+01	0.
Y-AXIS	4.993E+00	4.993E+01	0.
Z-AXIS	1.997E+07	1.997E+07	0.
ACCELEROMETER SCALE FACTOR			
X-AXIS	3.000E-02	3.000E-02	0.
Y-AXIS	3.000E-02	3.000E-02	0.
Z-AXIS	3.000E-02	3.000E-02	0.
ACC/PLATFORM MISALIGN ANGLES			
BYZ	9.969E-01	9.969E-01	0.
BXY	9.969E-01	9.969E-01	0.
BYZ	9.969E-01	9.969E-01	0.
BYX	9.969E-01	9.969E-01	0.
BZY	9.969E-01	9.969E-01	0.
BZX	9.969E-01	9.969E-01	0.
ACC NON-ORTHOGONALITY ANGLES			
BYZ	1.410E+00	1.410E+01	0.
BZY	1.410E+00	1.410E+01	0.
BZX	1.410E+00	1.410E+00	0.
ACC/NAV FRAME MISALIGN ANGLES			
BYZ	7.291E+00	7.291E+00	0.
BXY	7.291E+00	7.291E+01	0.
BYZ	7.291E+00	7.291E+02	0.
BYX	7.291E+01	7.291E+01	0.
BZY	7.291E+00	7.291E+01	0.
BZX	7.291E+00	7.291E+01	0.
ACCEL/NAV FRAME MIDAL ANGLES			
X-AXIS	1.127E+01	1.127E+01	0.
Y-AXIS	1.127E+01	1.127E+01	0.
PLATFORM VELOCITIES			
X-AXIS	0.	0.	0.
Y-AXIS	0.	0.	0.
Z-AXIS	0.	0.	0.

---STATE VECTOR VARIANCES AND OPTIMAL ESTIMATES CONTRASTED AGAINST IMU SIMULATION RESULTS---
PLATFORM TEST ATTITUDE = 1 ,MEASUREMENT NUMBER= 60

---------STATE VECTOR ELEMENT--------	-----STANDARD DEVIATION---- -PROPAGATED-	--UPDATED--	-OPT FILT-- -ESTIMATE-	--SYSTEM--- -SIMULATED-	-EST ERROR- --STD DEV--
GYRO CONSTANT BIAS					
X-AXIS	6.400E-02	6.400E-02	1.072E-01		
Y-AXIS	3.167E-02	3.005E-02	-5.788E-02		
Z-AXIS	3.823E-01	3.554E-01	5.993E-02		
GYRO ATTITUDE DEPENDENT BIAS					
X-AXIS	4.354E-03	4.586E-03	-7.657E-04		
Y-AXIS	4.355E-03	4.586E-03	-2.004E-03		
Z-AXIS	5.000E-03	5.000E-03	-2.135E-04		
GYRO WARM-UP DRIFT					
X-AXIS	2.786E-03	2.764E-03	-1.684E-03		
Y-AXIS	4.199E-03	2.764E-03	-2.463E-03		
Z-AXIS	7.899E-03	7.898E-03	1.628E-05		
GYRO DA G SENSITIVE					
X-AXIS	3.994E-01	3.994E-01	0.		
Y-AXIS	3.994E-01	3.994E-01	0.		
Z-AXIS	4.993E-02	4.993E-02	0.		
GYRO L.T.D. CORRELATED					
X-AXIS	4.982E-03	4.982E-03	2.745E-04		
Y-AXIS	4.993E-03	4.980E-03	7.390E-05		
Z-AXIS	5.000E-03	5.000E-03	5.522E-06		
GYRO MASS UNBALANCE					
MSX	9.986E-01	9.986E-01	0.		
MIX	9.956E-03	9.956E-03	-1.001E-03		
MSY	9.986E-01	9.986E-01	0.		
MIY	9.941E-03	9.940E-03	5.780E-04		
MSZ	3.517E-01	3.549E-01	-5.984E-02		
MIZ	9.986E-03	9.986E-03	0.		
GYRO ANISOELASTIC CONSTANTS					
X-AXIS	1.000E-02	1.000E-02	0.		
Y-AXIS	1.000E-02	1.000E-02	0.		
Z-AXIS	1.000E-02	1.000E-02	0.		
GYRO TOTAL DRIFT					
X-AXIS	6.404E-02	6.401E-02	9.739E-02		
Y-AXIS	2.958E-02	2.854E-02	-6.532E-02		
Z-AXIS	2.905E-01	7.064E-02	1.199E-01		
GYRO SCALE FACTOR					
X-AXIS	1.064E-08	1.064E-08	1.121E-08		
Y-AXIS	1.358E-08	1.358E-08	0.		
Z-AXIS	1.353E-08	1.352E-08	2.193E-10		
GYRO MISALIGNMENT ANGLES					
BXZ	9.969E-01	9.969E-01	0.		
BXY	9.967E-01	9.967E-01	2.789E-12		
BYZ	9.964E-01	9.964E-01	-1.934E-02		
BYX	9.966E-01	9.965E-01	1.611E-02		
BZY	9.969E-01	9.969E-01	-8.011E-04		
BZX	9.969E-01	9.969E-01	0.		
PLATFORM GYRO DEPENDENT DRIFT					
X-AXIS	1.656E-02	1.639E-02	1.648E-01		
Y-AXIS	2.932E-02	2.826E-02	-6.296E-02		
Z-AXIS	2.852E-01	2.215E-02	1.210E-01		
GYRO NON-ORTHOGONALITY ANGLES					
BYZ	1.410E+00	1.410E+00	1.934E-02		
BZY	1.410E+00	1.410E+00	-2.869E-02		
BZX	1.410E+00	1.410E+00	-1.611E-02		

HOUSING MISALIGNMENT ANGLES			
X-AXIS	3.747E+00	3.747E+00	-8.323E-01
Y-AXIS	3.750E+00	3.750E+00	-1.663E+00
Z-AXIS	3.987E+00	3.986E+00	-3.145E-01
GIMBAL SYNCHRO ANGLE BIAS			
X-AXIS	5.045E+00	5.047E+00	-1.854E+00
Y-AXIS	5.058E+00	5.058E+00	-3.717E+00
Z-AXIS	5.889E+00	5.888E+00	-7.005E-01
DIFFERENTIAL SYNCHRO ANGLES			
X-AXIS	1.341E-02	1.374E-02	1.484E+00
Y-AXIS	1.338E-02	1.338E-02	-5.884E-01
Z-AXIS	8.848E+00	8.830E-02	1.401E+00
PLATFORM TILT ANGLES			
X-AXIS	5.484E+00	5.483E+00	-1.202E+00
Y-AXIS	5.503E+00	5.503E+00	-5.974E+00
Z-AXIS	7.517E+00	7.026E+00	3.859E-01
PLATFORM TOTAL DRIFT			
X-AXIS	6.081E-03	5.591E-03	1.480E-01
Y-AXIS	6.219E-03	5.590E-03	-5.830E-02
Z-AXIS	2.848E-01	1.210E-02	1.411E-01
ACCELEROMETER BIAS			
X-AXIS	2.496E+03	2.496E+03	0.
Y-AXIS	2.496E+03	2.496E+03	0.
Z-AXIS	2.488E+03	2.488E+03	3.110E+02
ACC WARM-UP TRANSIENT			
X-AXIS	7.687E-02	7.373E-02	2.157E-02
Y-AXIS	7.373E-02	7.373E-02	-6.572E-02
Z-AXIS	4.424E-02	4.383E-02	-7.331E+00
ACCELEROMETER SCALE FACTOR			
X-AXIS	3.000E-02	3.000E-02	0.
Y-AXIS	3.000E-02	3.000E-02	0.
Z-AXIS	2.492E-03	2.492E-03	-4.485E-02
ACC/PLATFORM MISALIGN ANGLES			
BXZ	9.969E-01	9.969E-01	0.
BYY	9.930E-01	9.930E-01	1.297E-01
BYZ	9.969E-01	9.969E-01	0.
BYX	9.930E-01	9.930E-01	-6.729E-02
BZY	9.969E-01	9.969E-01	0.
BZX	9.969E-01	9.969E-01	0.
ACC NON-ORTHOGONALITY ANGLES			
BYZ	1.410E+00	1.410E+00	0.
BZY	1.407E+00	1.407E+00	1.237E-01
BZX	1.407E+00	1.407E+00	6.729E-02
ACC/NAV FRAME MISALIGN ANGLES			
BXZ	7.583E+00	7.097E+00	3.859E-01
BYY	5.525E+00	5.519E+00	-5.114E+00
BYZ	7.583E+00	7.097E+00	3.859E-01
BYX	5.501E+00	5.510E+00	-1.279E+00
BZY	5.593E+00	5.593E+00	-5.974E+00
BZX	5.574E+00	5.573E+00	-1.202E+00
ACC(S)/NAV FRAME MISAL ANGLES			
X-AXIS	2.055E-03	1.517E-03	-6.271E+00
Y-AXIS	2.140E-03	1.517E-03	-1.574E+01
PLATFORM VELOCITIES			
X-AXIS	2.515E-04	1.169E-04	-8.677E+01
Y-AXIS	2.559E-04	1.163E-04	3.335E+01
Z-AXIS	4.571E-03	4.717E-03	8.694E+02

---STAT VECTOR VARIANCES AND OPTIMAL ESTIMATES CONTRASTED AGAINST IMU SIMULATION RESULTS---
PLATFORM TEST ATTITUDE # 2 ,MEASUREMENT NUMBER= 10

----------STATE VECTOR ELEMENT----------	-----STANDARD DEVIATION---- -PROPAGATED-	--UPDATED--	-OPT FILT-- -ESTIMATE-	--SYSTEM--- -SIMULATED-	-EST ERROR- --STD DEV--
GYRO CONSTANT BIAS					
X-AXIS	6.396E-02	6.396E-02	9.813E-02		
Y-AXIS	2.991E-02	2.991E-02	-5.750E-02		
Z-AXIS	3.510E-01	3.509E-01	-5.745E-04		
GYRO ATTITUDE DEPENDENT BIAS					
X-AXIS	5.000E-03	5.000E-03	4.167E-05		
Y-AXIS	4.999E-03	4.999E-03	6.891E-05		
Z-AXIS	5.000E-03	5.000E-03	-3.912E-05		
GYRO WARM-UP DRIFT					
X-AXIS	1.586E-03	1.585E-03	-9.514E-04		
Y-AXIS	1.585E-03	1.585E-03	-1.410E-03		
Z-AXIS	4.530E-03	4.528E-03	-1.188E-04		
GYRO DA G SENSITIVT					
X-AXIS	3.990E-01	3.994E-01	0.		
Y-AXIS	5.042E-02	5.015E-02	-3.114E-01		
Z-AXIS	4.987E-02	4.986E-02	2.760E-03		
GYRO G.T.G. CORRELATED					
X-AXIS	4.984E-03	4.984E-03	2.345E-04		
Y-AXIS	4.983E-03	4.983E-03	7.527E-05		
Z-AXIS	5.000E-03	5.000E-03	1.663E-05		
GYRO MASS UNBALANCE					
MSX	1.867E-01	1.864E-01	1.177E+00		
MIX	9.956E-03	9.956E-03	-9.317E-04		
MSY	8.698E-01	8.698E-01	5.884E-01		
MIY	9.940E-03	9.940E-03	6.548E-04		
MSZ	3.516E-01	3.515E-01	-1.138E-01		
MIZ	9.986E-03	9.986E-03	0.		
MSX-MSY	8.698E-01	8.698E-01	5.884E-01		
MSX+MSZ	5.010E-01	5.007E-01	1.063E+00		
MSY+MSZ	9.525E-01	9.524E-01	4.746E-01		
GYRO ANISOELASTIC CONSTANTS					
X-AXIS	1.000E-02	1.000E-02	0.		
Y-AXIS	9.998E-03	9.998E-03	1.378E-04		
Z-AXIS	1.000E-02	1.000E-02	0.		
GYRO TOTAL DRIFT					
X-AXIS	1.524E-01	1.522E-01	9.305E-01		
Y-AXIS	2.951E-02	2.937E-02	1.599E-01		
Z-AXIS	3.051E-01	3.050E-01	7.782E-02		
GYRO SCALE FACTOR					
X-AXIS	1.064E-08	1.063E-08	1.133E-08		
Y-AXIS	1.358E-08	1.358E-08	0.		
Z-AXIS	1.346E-08	1.346E-08	1.633E-09		
GYRO MISALIGNMENT ANGLES					
BXZ	9.969E-01	9.969E-01	0.		
BXY	9.967E-01	9.967E-01	2.202E-02		
BYZ	9.964E-01	9.964E-01	-1.649E-02		
BYX	9.965E-01	9.965E-01	2.476E-02		
BZY	9.969E-01	9.969E-01	1.655E-03		
BZX	9.969E-01	9.969E-01	0.		
GYRO NON-ORTHOGONALITY ANGLES					
BYZ	1.410E+00	1.410E+00	1.649E-02		
BZY	1.410E+00	1.410E+00	-2.047E-02		
BZX	1.410E+00	1.410E+00	-2.476E-02		

HOUSING MISALIGNMENT ANGLES			
X-AXIS	3.560E+00	3.560E+00	-1.562E+00
Y-AXIS	3.309E+00	3.309E+00	-1.211E+00
Z-AXIS	3.986E+00	3.986E+00	-3.124E-01
GIMBAL SYNCHRO ANGLE BIAS			
X-AXIS	5.186E+00	5.186E+00	-2.059E+00
Y-AXIS	3.953E+00	3.953E+00	1.406E+00
Z-AXIS	5.594E+00	5.594E+00	1.692E+00
DIFFERENTIAL SYNCHRO ANGLES			
X-AXIS	9.360E-01	9.047E-01	7.202E+00
Y-AXIS	3.350E-02	2.368E-02	8.954E-01
Z-AXIS	1.279E+00	1.278E+00	5.462E+00
PLATFORM TOTAL DRIFT			
X-AXIS	1.292E-01	1.280E-01	1.013E+00
Y-AXIS	7.177E-02	6.006E-02	1.914E-01
Z-AXIS	2.554E-01	2.852E-01	7.203E-02
ACCELEROMETER BIAS			
X-AXIS	2.479E+03	2.479E+03	2.198E+03
Y-AXIS	1.732E+03	1.732E+03	1.062E+03
Z-AXIS	2.227E+03	2.227E+03	8.446E+01
ACC BIAS (HIGH GAIN)			
X-AXIS	1.566E+03	1.566E+03	-2.423E+03
Y-AXIS	1.579E+03	1.579E+03	1.358E+03
ACC WARM-UP TRANSFER			
X-AXIS	9.978E-03	9.978E-03	3.028E-03
Y-AXIS	9.974E-03	9.974E-03	-8.953E-03
Z-AXIS	5.932E-03	5.932E-03	-9.322E-01
ACCELEROMETER SCALE FACTOR			
X-AXIS	3.645E-03	3.645E-03	-2.242E-02
Y-AXIS	3.000E-02	3.000E-02	0.
Z-AXIS	2.231E-03	2.231E-03	-4.608E-02
ACC SCALE FACTOR (HIGH GAIN)			
X-AXIS	3.000E-02	3.000E-02	0.
Y-AXIS	3.000E-02	3.000E-02	0.
ACC ATT DEP SCALE FACTOR			
X-AXIS	1.000E-05	1.000E-05	-2.481E-03
Y-AXIS	1.000E-05	1.000E-05	0.
Z-AXIS	3.000E-05	3.000E-05	7.942E-04
CLOCK STABILITY			
	9.976E-07	9.957E-07	2.043E-07
ACC/PLATFORM MISALIGN ANGLES			
CAZ	9.959E-01	9.963E-01	0.
AXY	9.928E-01	9.929E-01	1.236E-01
AYZ	9.952E-01	9.952E-01	-3.478E-02
AYX	9.918E-01	9.918E-01	-9.767E-02
AZY	9.891E-01	9.891E-01	2.551E-02
AZX	9.969E-01	9.969E-01	0.
ACC NON-ORTHOGONALITY ANGLES			
BYZ	1.409E+00	1.409E+00	3.478E-02
BZY	1.400E+00	1.400E+00	1.491E-01
BZX	1.406E+00	1.406E+00	9.767E-02
ACC/GYRO FRAME MISALIGN ANGLES			
X-AXIS	1.406E+00	1.406E+00	-1.224E-01
Y-AXIS	1.407E+00	1.407E+00	-1.456E-01
Z-AXIS	1.413E+00	1.413E+00	0.
PLATFORM VELOCITIES			
X-AXIS	1.179E-02	8.430E-03	1.761E+02
Y-AXIS	1.463E-02	9.768E-03	1.936E+01
Z-AXIS	1.179E-02	8.472E-03	3.068E+02

---STATE VECTOR VARIANCES AND OPTI[illegible] MATES CONTRASTED AGAINST IMU SIMULATION RESULTS---
PLATFORM TEST ATTITUDE = [illegible] ,MEASUREMENT NUMBER= 10

----------STATE VECTOR ELEMENT----------	----- TANDARD DEVIATION---- -PROPAGATED-	--UPDATED--	-OPT FILT-- -ESTIMATE--	--SYSTEM--- -SIMULATED-	-EST ERROR- --STD DEV--
GYRO CONSTANT BIAS					
X-AXIS	3.516E-02	3.408E-02	8.659E-02		
Y-AXIS	2.681E-02	2.880E-02	-5.733E-02		
Z-AXIS	3.455E-01	3.455E-01	3.489E-02		
GYRO ATTITUDE DEPENDENT BIAS					
X-AXIS	4.991E-03	4.991E-03	-6.786E-05		
Y-AXIS	4.995E-03	4.995E-03	-2.476E-04		
Z-AXIS	5.000E-03	5.000E-03	-1.557E-05		
GYRO WARM-UP DRIFT					
X-AXIS	9.096E-04	9.095E-04	-5.247E-04		
Y-AXIS	9.096E-04	9.096E-04	-7.822E-04		
Z-AXIS	2.598E-03	2.598E-03	-4.640E-05		
GYRO DA G SENSITIVE					
X-AXIS	3.614E-01	3.613E-01	-3.766E-02		
Y-AXIS	4.703E-02	4.703E-02	-3.153E-01		
Z-AXIS	4.977E-02	4.977E-02	1.042E-03		
GYRO E.T.C. CORRELATED					
X-AXIS	4.985E-03	4.985E-03	1.357E-04		
Y-AXIS	4.985E-03	4.985E-03	2.060E-05		
Z-AXIS	5.000E-03	5.000E-03	1.088E-05		
GYRO MASS UNBALANCE					
MSX	1.449E-01	1.449E-01	1.138E+00		
MIX	9.945E-03	9.945E-03	-8.445E-04		
MSY	6.330E-01	6.327E-01	1.243E+00		
MIY	9.940E-03	9.940E-03	7.109E-04		
MSZ	3.477E-01	3.477E-01	-5.482E-02		
MIZ	9.986E-03	9.986E-03	5.400E-06		
MSX+MSY	6.501E-01	6.498E-01	-4.475E-02		
MSX+MSZ	4.951E-01	4.951E-01	1.113E+00		
MSY+MSZ	7.450E-01	7.447E-01	1.159E+00		
GYRO ANISOELASTIC CONSTANTS					
X-AXIS	9.999E-03	9.999E-03	2.339E-05		
Y-AXIS	9.998E-03	9.998E-03	1.644E-04		
Z-AXIS	1.000E-02	1.000E-02	-4.713E-07		
GYRO TOTAL DRIFT					
X-AXIS	2.511E-02	2.439E-02	-2.141E-02		
Y-AXIS	5.589E-02	5.586E-02	-2.055E-01		
Z-AXIS	7.068E-02	7.067E-02	1.192E-01		
GYRO SCALE FACTOR					
X-AXIS	6.590E-09	6.588E-09	1.296E-08		
Y-AXIS	1.007E-08	1.006E-08	-1.035E-08		
Z-AXIS	1.337E-08	1.337E-08	7.697E-10		
GYRO MISALIGNMENT ANGLES					
BXZ	9.962E-01	9.962E-01	8.381E-03		
BXY	9.966E-01	9.966E-01	2.095E-02		
BYZ	9.960E-01	9.960E-01	1.455E-02		
BYX	9.965E-01	9.965E-01	2.642E-02		
BZY	9.969E-01	9.969E-01	-2.039E-03		
BZX	9.969E-01	9.969E-01	-1.923E-03		
GYRO NON-ORTHOGONALITY ANGLES					
BYZ	1.403E+00	1.403E+00	-6.159E-03		
BZY	1.410E+00	1.410E+00	-2.300E-02		
BZX	1.410E+00	1.410E+00	-2.834E-02		

HOUSING MISALIGNMENT ANGLES			
X-AXIS	3.256E+00	3.256E+00	-2.305E+00
Y-AXIS	3.033E+00	3.039E+00	-5.607E-01
Z-AXIS	3.308E+00	3.307E+00	3.180E-01
GIMBAL SYNCHRO ANGLE BIAS			
X-AXIS	4.223E+00	4.223E+00	-8.240E-01
Y-AXIS	4.362E+00	4.362E+00	1.914E+00
Z-AXIS	5.821E+00	5.821E+00	9.613E-02
DIFFERENTIAL SYNCHRO ANGLES			
X-AXIS	3.302E-02	2.677E-02	-1.285E+00
Y-AXIS	2.391E-02	2.671E-02	1.987E-01
Z-AXIS	1.401E-01	1.401E-01	7.017E-01
PLATFORM TOTAL DRIFT			
X-AXIS	3.452E-03	5.367E-03	-4.250E-02
Y-AXIS	7.368E-03	6.263E-03	-2.535E-01
Z-AXIS	3.855E-02	3.854E-02	1.174E-01
ACCELEROMETER BIAS			
X-AXIS	1.108E+03	1.108E+03	-2.883E+03
Y-AXIS	1.508E+03	1.508E+03	6.793E+02
Z-AXIS	2.196E+03	2.196E+03	2.906E+02
ACC BIAS (HIGH GAIN)			
X-AXIS	1.531E+03	1.531E+03	-2.373E+03
Y-AXIS	1.545E+03	1.545E+03	1.017E+03
ACC WARM-UP TRANSIENT			
X-AXIS	1.350E-03	1.350E-03	4.303E-04
Y-AXIS	1.351E-03	1.350E-03	-1.181E-03
Z-AXIS	8.028E-04	8.028E-04	-1.343E-01
ACCELEROMETER SCALE FACTOR			
X-AXIS	1.843E-07	1.843E-07	-2.640E-02
Y-AXIS	1.861E-07	1.861E-07	-8.872E-03
Z-AXIS	2.203E-03	2.203E-03	-4.487E-02
ACC SCALE FACTOR (HIGH GAIN)			
X-AXIS	3.000E-02	3.000E-02	0.
Y-AXIS	3.000E-02	3.000E-02	0.
ACC ATT DEP SCALE FACTOR			
X-AXIS	1.000E-05	1.000E-05	-3.911E-03
Y-AXIS	1.000E-05	1.000E-05	-9.858E-10
Z-AXIS	2.958E-05	2.959E-05	-4.046E-05
CLOCK STABILITY			
	9.376E-07	9.957E-07	5.935E-07
ACC/PLATFORM MISALIGN ANGLES			
BXZ	9.369E-01	9.969E-01	-1.127E-02
BXY	9.875E-01	9.875E-01	2.632E-01
BYZ	9.943E-01	9.943E-01	-4.872E-02
BYX	9.932E-01	9.932E-01	-6.001E-02
BZY	9.828E-01	9.828E-01	1.405E-01
BZX	9.995E-01	9.995E-01	1.137E-01
ACC NON-ORTHOGONALITY ANGLES			
BYZ	1.408E+00	1.408E+00	5.359E-02
BZY	1.388E+00	1.388E+00	4.097E-01
BZX	1.399E+00	1.399E+00	-5.771E-02
ACC/GYRO FRAME MISALIGN ANGLES			
X-AXIS	1.405E+00	1.405E+00	-8.643E-02
Y-AXIS	1.403E+00	1.403E+00	-2.901E-01
Z-AXIS	1.403E+00	1.403E+00	-1.965E-02
PLATFORM VELOCITIES			
X-AXIS	1.456E-03	3.742E-03	-6.163E+01
Y-AXIS	1.455E-03	3.738E-03	3.294E+00
Z-AXIS	8.143E-03	6.886E-03	4.719E+02

---STATE VECTOR VARIANCES AND OPTIMAL ESTIMATES CONTRASTED AGAINST IMU SIMULATION RESULTS---
PLATFORM TEST ATTITUDE = 3 (MEASUREMENT NUMBER= 13

---------STATE VECTOR ELEMENT---------	-----STANDARD DEVIATION---- -PROPAGATED-	--UPDATED--	-OPT FILT-- -ESTIMATE-	--SYSTEM--- -SIMULATED-	-EST ERROR- --STD DEV--
GYRO CONSTANT BIAS					
X-AXIS	3.799E-02	3.787E-02	7.702E-02		
Y-AXIS	2.826E-02	2.825E-02	-5.882E-02		
Z-AXIS	3.455E-01	3.455E-01	4.614E-02		
GYRO ATTITUDE DEPENDENT BIAS					
X-AXIS	4.990E-03	4.990E-03	-9.197E-05		
Y-AXIS	4.995E-03	4.995E-03	-2.315E-04		
Z-AXIS	5.000E-03	5.000E-03	1.498E-04		
GYRO WARM-UP DRIFT					
X-AXIS	7.699E-04	7.677E-04	-2.663E-04		
Y-AXIS	7.699E-04	7.677E-04	-7.614E-04		
Z-AXIS	2.199E-03	2.199E-03	-1.504E-04		
GYRO DB G SENSITIVE					
X-AXIS	3.607E-01	3.606E-01	-5.103E-02		
Y-AXIS	4.603E-02	4.603E-02	-3.184E-01		
Z-AXIS	4.377E-02	4.377E-02	2.372E-03		
GYRO L.T.G. CORRELATED					
X-AXIS	4.985E-03	4.980E-03	-5.827E-04		
Y-AXIS	4.986E-03	4.981E-03	3.863E-04		
Z-AXIS	5.000E-03	5.000E-03	1.337E-05		
GYRO MASS UNBALANCE					
MSX	1.840E-01	1.840E-01	1.214E+00		
MIX	9.945E-03	9.945E-03	-7.605E-04		
MSY	6.356E-01	6.353E-01	1.233E+00		
MIY	9.939E-03	9.939E-03	7.292E-04		
MSZ	3.476E-01	3.475E-01	-7.942E-02		
MIZ	9.986E-03	9.986E-03	-5.159E-05		
MSX-MSY	6.473E-01	6.471E-01	4.806E-03		
MSX+MSZ	4.351E-01	4.350E-01	1.135E+00		
MSY+MSZ	7.424E-01	7.421E-01	1.130E+00		
GYRO ANISOELASTIC CONSTANTS					
X-AXIS	9.999E-03	9.999E-03	3.170E-05		
Y-AXIS	9.998E-03	9.998E-03	1.540E-04		
Z-AXIS	1.000E-02	1.000E-02	4.503E-06		
GYRO TOTAL DRIFT					
X-AXIS	2.473E-02	2.437E-02	-3.293E-02		
Y-AXIS	5.674E-02	5.669E-02	-2.039E-01		
Z-AXIS	7.023E-02	7.023E-02	1.252E-01		
GYRO SCALE FACTOR					
X-AXIS	6.405E-09	6.395E-09	1.312E-08		
Y-AXIS	1.002E-08	1.001E-08	-3.401E-09		
Z-AXIS	1.337E-08	1.337E-08	1.335E-09		
GYRO MISALIGNMENT ANGLES					
BXZ	9.962E-01	9.962E-01	1.136E-02		
BXY	9.966E-01	9.966E-01	1.847E-02		
BYZ	9.960E-01	9.960E-01	1.195E-02		
BYX	9.965E-01	9.965E-01	2.698E-02		
BZY	9.969E-01	9.969E-01	2.132E-02		
BZX	9.969E-01	9.969E-01	1.437E-02		
GYRO NON-ORTHOGONALITY ANGLES					
GYZ	1.413E+00	1.413E+00	-4.357E-04		
GZY	1.410E+00	1.410E+00	2.844E-03		
GZX	1.410E+00	1.410E+00	-8.618E-03		

HOUSING MISALIGNMENT ANGLES			
X-AXIS	3.214E+00	3.214E+00	-2.666E+00
Y-AXIS	2.314E+00	2.314E+00	-6.233E-02
Z-AXIS	3.906E+00	3.906E+00	2.956E-01
GIMBAL SYNCHRO ANGLE BIAS			
X-AXIS	3.886E+00	3.886E+00	-9.927E-01
Y-AXIS	4.207E+00	4.185E+00	1.619E+00
Z-AXIS	5.906E+00	5.806E+00	1.449E-01
DIFFERENTIAL SYNCHRO ANGLES			
X-AXIS	2.478E-02	2.321E-02	-1.675E+00
Y-AXIS	3.487E-02	2.252E-02	3.437E-01
Z-AXIS	1.792E-01	1.790E-01	9.634E-01
PLATFORM TOTAL DRIFT			
X-AXIS	6.502E-03	4.741E-03	-5.753E-02
Y-AXIS	5.351E-03	4.669E-03	-2.492E-01
Z-AXIS	2.817E-02	2.814E-02	1.256E-01
ACCELEROMETER BIAS			
X-AXIS	9.587E+02	3.885E+02	-2.754E+03
Y-AXIS	1.496E+03	1.496E+03	6.138E+02
Z-AXIS	2.185E+03	2.185E+03	4.500E+02
ACC BIAS (HIGH GAIN)			
X-AXIS	1.336E+03	1.335E+03	-1.638E+03
Y-AXIS	1.391E+03	1.391E+03	7.254E+02
ACC WARM-UP TRANSIENT			
X-AXIS	7.411E-04	7.403E-04	1.777E-04
Y-AXIS	7.412E-04	7.404E-04	-7.818E-04
Z-AXIS	4.406E-04	4.406E-04	-7.759E-02
ACCELEROMETER SCALE FACTOR			
X-AXIS	1.678E-03	1.675E-03	-2.656E-02
Y-AXIS	1.908E-02	1.908E-02	-8.981E-03
Z-AXIS	2.190E-03	2.190E-03	-4.472E-02
ACC SCALE FACTOR (HIGH GAIN)			
X-AXIS	1.828E-02	1.824E-02	-1.478E-02
Y-AXIS	1.694E-02	1.694E-02	-5.604E-03
ACC ATT DCP SCALE FACTOR			
X-AXIS	1.000E-05	1.000E-05	-1.634E-09
Y-AXIS	1.000E-05	1.000E-05	-1.045E-09
Z-AXIS	2.961E-05	2.961E-05	-5.633E-05
CLOCK STABILITY			
	9.973E-07	9.942E-07	7.596E-08
ACC/PLATFORM MISALIGN ANGLES			
BYZ	9.869E-01	9.869E-01	-1.550E-02
BYY	9.874E-01	9.874E-01	2.824E-01
BYZ	9.943E-01	9.943E-01	-4.943E-02
BYY	9.898E-01	9.898E-01	-4.480E-02
BZY	9.810E-01	9.810E-01	1.769E-01
BZX	9.877E-01	9.877E-01	1.535E-01
ACC NON-ORTHOGONALITY ANGLES			
BYZ	1.408E+00	1.408E+00	6.433E-02
BZY	1.386E+00	1.386E+00	4.693E-01
BZX	1.346E+00	1.346E+00	-1.137E-01
ACC/SYRO FRAME MISALIGN ANGLES			
X-AXIS	1.404E+00	1.404E+00	-7.178E-02
Y-AXIS	1.403E+00	1.403E+00	-7.138E-01
Z-AXIS	1.409E+00	1.409E+00	-2.686E-02
PLATFORM VELOCITIES			
X-AXIS	3.032E-04	1.295E-04	-1.244E+01
Y-AXIS	1.042E-04	1.295E-04	8.622E-01
Z-AXIS	2.586E-03	2.307E-03	9.535E+01

---STATE VECTOR VARIANCES AND OPTIMAL ESTIMATES CONTRASTED AGAINST IMU SIMULATION RESULTS---
PLATFORM TEST ATTITUDE = 4 ,MEASUREMENT NUMBER= 12

----------STATE VECTOR ELEMENT---------	-----STANDARD DEVIATION---- -PROPAGATED-	--UPDATED--	-OPT FILT-- -ESTIMATE-	--SYSTEM--- -SIMULATED-	-EST ERROR- --STD DEV--
GYRO CONSTANT BIAS					
X-AXIS	2.861E-02	2.860E-02	5.074E-02		
Y-AXIS	2.740E-02	2.740E-02	-6.873E-02		
Z-AXIS	3.410E-01	3.403E-01	7.853E-02		
GYRO ATTITUDE DEPENDENT BIAS					
X-AXIS	4.999E-03	4.999E-03	-1.024E-04		
Y-AXIS	5.000E-03	5.000E-03	-2.007E-05		
Z-AXIS	5.000E-03	5.000E-03	2.144E-05		
GYRO WARM-UP DRIFT					
X-AXIS	4.404E-04	4.404E-04	-1.460E-04		
Y-AXIS	4.403E-04	4.403E-04	-4.360E-04		
Z-AXIS	1.261E-03	1.261E-03	-8.561E-05		
GYRO DA G SENSITIVE					
X-AXIS	2.464E-02	2.405E-02	3.208E-01		
Y-AXIS	3.971E-02	3.971E-02	-3.715E-01		
Z-AXIS	4.974E-02	4.974E-02	9.339E-04		
GYRO L.T.C. CORRELATED					
X-AXIS	4.982E-03	4.982E-03	-6.015E-04		
Y-AXIS	4.983E-03	4.983E-03	3.552E-04		
Z-AXIS	5.000E-03	5.000E-03	1.461E-05		
GYRO MASS UNBALANCE					
MSX	1.828E-01	1.827E-01	1.225E+00		
MIX	9.945E-03	9.945E-03	-6.360E-04		
MSY	1.401E-01	1.397E-01	1.175E+00		
MIY	9.939E-03	9.939E-03	7.208E-04		
MSZ	3.433E-01	3.432E-01	-5.128E-02		
MIZ	9.984E-03	9.984E-03	-4.129E-05		
MSX-MSY	1.136E-01	1.134E-01	4.906E-02		
MSX+MSZ	4.894E-01	4.892E-01	1.173E+00		
MSY+MSZ	4.738E-01	4.726E-01	1.124E+00		
GYRO ANISOELASTIC CONSTANTS					
X-AXIS	9.998E-03	9.998E-03	-1.166E-04		
Y-AXIS	9.998E-03	9.998E-03	1.692E-04		
Z-AXIS	1.000E-02	1.000E-02	4.134E-06		
GYRO TOTAL DRIFT					
X-AXIS	3.302E-02	3.276E-02	-1.770E-01		
Y-AXIS	1.041E-01	1.038E-01	7.625E-01		
Z-AXIS	1.144E-01	1.143E-01	1.147E-01		
GYRO SCALE FACTOR					
X-AXIS	5.003E-03	5.002E-03	1.761E-08		
Y-AXIS	5.398E-09	5.397E-09	-3.508E-09		
Z-AXIS	.375E-08	1.375E-08	5.930E-10		
GYRO MISALIGNMENT ANGLES					
BXZ	9.959E-01	9.959E-01	3.965E-02		
BXY	9.966E-01	9.966E-01	1.488E-02		
BYZ	9.957E-01	9.957E-01	1.217E-02		
BYX	9.965E-01	9.965E-01	2.727E-02		
BZY	9.969E-01	9.969E-01	1.839E-02		
BZX	9.969E-01	9.969E-01	1.703E-02		
GYRO NON-ORTHOGONALITY ANGLES					
BYZ	1.408E+00	1.408E+00	2.748E-02		
BZY	1.410E+00	1.410E+00	3.506E-03		
BZX	1.413E+00	1.413E+00	-1.024E-02		

HOUSING MISALIGNMENT ANGLES			
X-AXIS	2.849E+00	2.849E+00	-2.029E+00
Y-AXIS	2.591E+00	2.591E+00	-9.395E-01
Z-AXIS	3.885E+00	3.885E+00	6.545E-01
GIMBAL SYNCHRO ANGLE BIAS			
X-AXIS	3.594E+00	3.594E+00	4.538E-02
Y-AXIS	4.973E+00	4.973E+00	-2.939E+00
Z-AXIS	4.967E+00	4.967E+00	2.914E+00
DIFFERENTIAL SYNCHRO ANGLES			
X-AXIS	3.048E-02	2.368E-02	-4.153E-01
Y-AXIS	5.158E-01	5.143E-01	3.742E+00
Z-AXIS	5.128E-01	5.126E-01	5.833E-01
PLATFORM TOTAL DRIFT			
X-AXIS	6.933E-03	5.757E-03	-7.995E-02
Y-AXIS	1.041E-01	1.038E-01	7.499E-01
Z-AXIS	1.018E-01	1.018E-01	1.181E-01
ACCELEROMETER BIAS			
X-AXIS	9.315E+02	9.315E+02	-2.952E+03
Y-AXIS	9.449E+02	9.449E+02	1.461E+03
Z-AXIS	1.983E+03	1.983E+03	2.931E+02
ACC BIAS (HIGH GAIN)			
X-AXIS	1.327E+03	1.327E+03	-3.665E+03
Y-AXIS	1.351E+03	1.351E+03	8.337E+02
ACC WARM-UP TRANSIENT			
X-AXIS	1.002E-04	1.002E-04	2.410E-05
Y-AXIS	1.002E-04	1.002E-04	-1.056E-04
Z-AXIS	5.963E-05	5.963E-05	-9.973E-03
ACCELEROMETER SCALE FACTOR			
X-AXIS	1.448E-03	1.448E-03	-2.639E-02
Y-AXIS	1.361E-03	1.361E-03	-1.726E-02
Z-AXIS	1.987E-03	1.983E-03	-4.448E-02
ACC SCALE FACTOR (HIGH GAIN)			
X-AXIS	1.665E-02	1.665E-02	-1.562E-02
Y-AXIS	1.612E-02	1.612E-02	-9.401E-03
ACC ATT DEP SCALE FACTOR			
X-AXIS	1.000E-05	1.000E-05	0.
Y-AXIS	1.000E-05	1.000E-05	-2.999E-08
Z-AXIS	3.000E-05	3.000E-05	-2.332E-08
CLOCK STABILITY	9.476E-07	9.957E-07	-5.643E-08
ACC/PLATFORM MISALIGN ANGLES			
BXZ	9.933E-01	9.925E-01	5.394E-02
BXY	9.871E-01	9.871E-01	2.776E-01
BYZ	9.925E-01	9.925E-01	-1.361E-02
BYX	9.871E-01	9.871E-01	-9.775E-02
BZY	9.785E-01	9.785E-01	1.356E-01
BZX	9.739E-01	9.739E-01	9.239E-02
ACC NON-ORTHOGONALITY ANGLES			
BYZ	1.402E+00	1.402E+00	-5.863E-02
BZY	1.383E+00	1.383E+00	4.173E-01
BZX	1.373E+00	1.373E+00	4.259E-03
ACC/GYRO FRAME MISALIGN ANGLES			
X-AXIS	1.402E+00	1.402E+00	-1.245E-01
Y-AXIS	1.403E+00	1.403E+00	-2.925E-01
Z-AXIS	1.406E+00	1.406E+00	3.429E-02
PLATFORM VELOCITIES			
X-AXIS	1.464E-02	9.773E-03	-4.032E+01
Y-AXIS	1.178E-02	8.427E-03	1.364E+02
Z-AXIS	1.178E-02	9.427E-03	3.044E+02

---STATE VECTOR VARIANCES AND OPTIMAL ESTIMATES CONTRASTED AGAINST IMU SIMULATION RESULTS---
PLATFORM TEST ATTITUDE = 5 ,MEASUREMENT NUMBER= 10

----------STATE VECTOR ELEMENT--------	-----STANDARD DEVIATION-----PROPAGATED-	--UPDATED--	-OPT FILT--ESTIMATE--	--SYSTEM---SIMULATED-	-EST ERROR--STD DEV--
GYRO CONSTANT BIAS					
X-AXIS	2.633E-02	2.631E-02	3.230E-02		
Y-AXIS	2.728E-02	2.728E-02	-7.190E-02		
Z-AXIS	2.888E-02	2.862E-02	-5.097E-01		
GYRO ATTITUDE DEPENDENT BIAS					
X-AXIS	4.772E-03	4.759E-03	1.998E-04		
Y-AXIS	5.000E-03	5.000E-03	1.922E-06		
Z-AXIS	4.999E-03	4.999E-03	-1.272E-04		
GYRO WARM-UP DRIFT					
X-AXIS	2.522E-04	2.522E-04	-7.934E-05		
Y-AXIS	2.526E-04	2.526E-04	-2.495E-04		
Z-AXIS	7.236E-04	7.236E-04	-2.944E-05		
GYRO DA G SENSITIVE					
X-AXIS	1.925E-02	1.899E-02	3.228E-01		
Y-AXIS	3.879E-02	3.879E-02	-3.411E-01		
Z-AXIS	4.973E-02	4.977E-02	-6.948E-04		
GYRO L.T.G. CORRELATED					
X-AXIS	4.985E-03	4.985E-03	-6.134E-04		
Y-AXIS	4.986E-03	4.985E-03	3.164E-04		
Z-AXIS	5.000E-03	5.000E-03	-6.658E-05		
GYRO MASS UNBALANCE					
MSX	1.054E-01	1.054E-01	9.602E-01		
MIX	9.325E-03	9.289E-03	-3.149E-05		
MSY	4.889E-02	4.886E-02	9.491E-01		
MIY	9.839E-03	9.839E-03	7.464E-04		
MSZ	7.507E-02	7.497E-02	-6.318E-01		
MIZ	9.981E-03	9.981E-03	-5.361E-04		
MSX-MSY	1.116E-01	1.116E-01	2.216E-02		
MSX+MSZ	7.355E-02	7.335E-02	3.975E-01		
MSY+MSZ	8.451E-02	8.437E-02	3.177E-01		
GYRO ANISOELASTIC CONSTANTS					
X-AXIS	9.066E-03	9.012E-03	-6.685E-04		
Y-AXIS	9.998E-03	9.998E-03	1.790E-04		
Z-AXIS	1.000E-02	1.000E-02	3.751E-06		
GYRO TOTAL DRIFT					
X-AXIS	3.087E-02	3.052E-02	-2.915E-01		
Y-AXIS	5.525E-02	5.523E-02	8.784E-01		
Z-AXIS	2.639E-02	2.611E-02	-5.115E-01		
GYRO SCALE FACTOR					
X-AXIS	4.539E-09	4.535E-03	2.074E-09		
Y-AXIS	5.130E-09	5.130E-03	-1.179E-08		
Z-AXIS	1.332E-08	1.332E-03	2.010E-09		
GYRO MISALIGNMENT ANGLES					
BXZ	9.958E-01	9.958E-01	5.500E-02		
BXY	9.919E-01	9.917E-01	-1.330E-03		
BYZ	9.957E-01	9.957E-01	1.905E-02		
BYX	9.965E-01	9.965E-01	2.797E-02		
BZY	9.969E-01	9.969E-01	2.558E-02		
BZX	9.969E-01	9.969E-01	2.797E-03		
GYRO NON-ORTHOGONALITY ANGLES					
BYZ	1.409E+00	1.409E+00	3.696E-02		
BZY	1.406E+00	1.406E+00	2.492E-02		
BZX	1.410E+00	1.410E+00	-2.554E-02		

HOUSING MISALIGNMENT ANGLES			
X-AXIS	2.700E+00	2.700E+00	-2.400E+00
Y-AXIS	2.406E+00	2.406E+00	-1.595E+00
Z-AXIS	3.869E+00	3.869E+00	1.256E+00
GIMBAL SYNCHRO ANGLE BIAS			
X-AXIS	2.917E+00	2.917E+00	-3.873E+00
Y-AXIS	5.399E+00	5.399E+00	5.158E-01
Z-AXIS	3.172E+00	3.171E+00	3.847E+00
DIFFERENTIAL SYNCHRO ANGLES			
X-AXIS	2.840E-02	2.266E-02	-8.978E-01
Y-AXIS	2.638E-01	2.627E-01	4.169E+00
Z-AXIS	3.047E-02	2.369E-02	-2.713E+00
PLATFORM TOTAL DRIFT			
X-AXIS	5.575E-03	5.595E-03	-1.757E-01
Y-AXIS	5.297E-02	5.284E-02	8.294E-01
Z-AXIS	5.931E-03	5.783E-03	-5.639E-01
ACCELEROMETER BIAS			
X-AXIS	7.411E+02	7.412E+02	-3.227E+01
Y-AXIS	7.857E+02	7.856E+02	1.684E+01
Z-AXIS	8.974E+02	8.972E+02	7.213E+01
ACC BIAS (HIGH GAIN)			
X-AXIS	1.268E+03	1.266E+03	-3.737E+01
Y-AXIS	1.340E+03	1.338E+03	7.875E+01
ACC WARM-UP TRANSIENT			
X-AXIS	1.356E-05	1.356E-05	3.784E-06
Y-AXIS	1.356E-05	1.356E-05	-1.465E-06
Z-AXIS	9.071E-06	9.071E-06	-1.360E-07
ACCELEROMETER SCALE FACTO			
X-AXIS	1.262E-03	1.262E-03	-2.736E-03
Y-AXIS	7.863E-04	7.868E-04	-1.698E-02
Z-AXIS	9.051E-04	9.050E-04	-4.619E-02
ACC SCALE FACTOR (HIGH GAIN)			
X-AXIS	1.511E-02	1.514E-02	-1.944E-02
Y-AXIS	1.557E-02	1.557E-02	-5.942E-03
ACC ATT DEP SCALE FACTOR			
X-AXIS	1.000E-05	1.000E-05	0.
Y-AXIS	9.999E-06	9.999E-06	6.536E-08
Z-AXIS	3.000E-05	3.000E-05	0.
CLOCK STABILITY			
	9.976E-07	9.957E-07	-4.783E-10
ACC/PLATFORM MISALIGN ANGLES			
BXZ	9.859E-01	9.859E-01	1.335E-01
BXY	9.761E-01	9.768E-01	1.595E-01
BYZ	9.924E-01	9.924E-01	-6.599E-04
BYX	9.509E-01	9.509E-01	-2.251E-01
BZY	9.722E-01	9.722E-01	1.701E-01
BZX	9.477E-01	9.477E-01	9.942E-03
ACC NON-ORTHOGONALITY ANGLES			
BYZ	1.397E+00	1.397E+00	-1.349E-01
BZY	1.369E+00	1.369E+00	3.595E-01
BZX	1.290E+00	1.290E+00	2.151E-01
ACC/GYRO FRAME MISALIGN ANGLES			
X-AXIS	1.377E+00	1.377E+00	-2.530E-01
Y-AXIS	1.385E+00	1.384E+00	-1.882E-01
Z-AXIS	1.402E+00	1.402E+00	9.464E-02
PLATFORM VELOCITIES			
X-AXIS	1.461E-02	9.768E-03	-4.785E+01
Y-AXIS	8.037E-03	6.837E-03	1.910E+02
Z-AXIS	1.781E-02	9.647E-03	-1.925E+1

---STATE VECTOR VARIANCES AND OPTIMAL ESTIMATES CONTRASTED AGAINST IMU SIMULATION RESULTS---
PLATFORM TEST ATTITUDE = [illegible] ,MEASUREMENT NUMBER= 10

---------STATE VECTOR ELEMENT---------	-----STANDARD DEVIATION----- -PROPAGATED-	--UPDATED--	-OPT FILT-- -ESTIMATE--	--SYSTEM--- -SIMULATED-	-EST ERROR- --STD DEV--
GYRO CONSTANT BIAS					
X-AXIS	2.301E-02	2.292E-02	8.770E-03		
Y-AXIS	2.646E-02	2.644E-02	-6.172E-02		
Z-AXIS	2.563E-02	2.553E-02	-5.194E-01		
GYRO ATTITUDE DEPENDENT BIAS					
X-AXIS	4.877E-03	4.873E-03	-1.680E-03		
Y-AXIS	5.000E-03	5.000E-03	-1.095E-05		
Z-AXIS	4.993E-03	4.993E-03	2.334E-04		
GYRO WARM-UP DRIFT					
X-AXIS	1.446E-04	1.446E-04	-5.230E-05		
Y-AXIS	1.450E-04	1.450E-04	-1.422E-04		
Z-AXIS	4.152E-04	4.152E-04	-1.913E-05		
GYRO DA G SENSITIVE					
X-AXIS	1.799E-02	1.797E-02	3.331E-01		
Y-AXIS	3.859E-02	3.859E-02	-3.467E-01		
Z-AXIS	4.368E-02	4.969E-02	1.950E-03		
GYRO L.F.G. CORRELATED					
X-AXIS	4.987E-03	4.986E-03	-6.769E-04		
Y-AXIS	4.988E-03	4.988E-03	3.743E-04		
Z-AXIS	4.999E-03	4.999E-03	-3.113E-05		
GYRO MASS UNBALANCE					
MSX	7.314E-02	7.900E-02	8.947E-01		
MIX	9.283E-03	9.283E-03	8.555E-05		
MSY	4.856E-02	4.855E-02	9.542E-01		
MIY	9.939E-03	9.939E-03	6.185E-04		
MSZ	3.096E-02	3.060E-02	-5.966E-01		
MIZ	9.981E-03	9.981E-03	-4.821E-04		
MSX-MSY	8.453E-02	8.440E-02	-5.945E-02		
MSX+MSZ	6.352E-02	6.941E-02	2.981E-01		
MSY+MSZ	4.646E-02	4.625E-02	3.576E-01		
GYRO ANISOELASTIC CONSTANTS					
X-AXIS	8.939E-03	8.998E-03	-4.491E-04		
Y-AXIS	9.938E-03	9.998E-03	1.841E-04		
Z-AXIS	1.000E-02	1.000E-02	4.355E-06		
GYRO TOTAL DRIFT					
X-AXIS	2.505E-02	2.486E-02	-3.272E-01		
Y-AXIS	5.427E-02	5.425E-02	8.939E-01		
Z-AXIS	4.262E-02	4.257E-02	-5.201E-01		
GYRO SCALE FACTOR					
X-AXIS	3.874E-09	3.852E-03	2.542E-08		
Y-AXIS	5.019E-09	5.016E-03	-1.289E-08		
Z-AXIS	5.689E-09	5.676E-03	1.030E-05		
GYRO MISALIGNMENT ANGLES					
BXZ	9.953E-01	9.953E-01	1.330E-02		
BXY	9.865E-01	9.863E-01	-1.631E-01		
BYZ	9.957E-01	9.957E-01	2.556E-02		
BYX	9.965E-01	9.965E-01	2.552E-02		
BZY	9.868E-01	9.868E-01	3.710E-02		
BZX	9.869E-01	9.869E-01	5.726E-03		
GYRO NON-ORTHOGONALITY ANGLES					
BYZ	1.408E+00	1.408E+00	-1.296E-02		
BZY	1.402E+00	1.402E+00	2.012E-01		
BZX	1.410E+00	1.410E+00	-1.980E-02		

HOUSING MISALIGNMENT ANGLES			
X-AXIS	2.544E+00	2.544E+00	-2.243E+00
Y-AXIS	2.187E+00	2.187E+00	-2.554E+00
Z-AXIS	3.197E+00	3.176E+00	-1.756E+00
GIMBAL SYNCHRO ANGLE BIAS			
X-AXIS	3.236E+00	3.236E+00	-1.917E+00
Y-AXIS	4.641E+00	4.601E+00	-6.552E+00
Z-AXIS	3.917E+00	3.817E+00	2.719E+00
DIFFERENTIAL SYNCHRO ANGLES			
X-AXIS	4.151E-02	3.273E-02	-1.674E+00
Y-AXIS	2.621E-01	2.621E-01	4.219E+00
Z-AXIS	4.230E-02	3.310E-02	-1.199E+00
PLATFORM TOTAL DRIFT			
X-AXIS	6.737E-03	5.671E-03	-2.284E-01
Y-AXIS	5.252E-02	5.253E-02	8.423E-01
Z-AXIS	1.193E-02	1.022E-02	-4.832E-01
ACCELEROMETER BIAS			
X-AXIS	6.593E+02	6.593E+02	-3.514E+03
Y-AXIS	7.300E+02	7.300E+02	1.998E+03
Z-AXIS	7.596E+02	7.596E+02	-3.578E+03
ACC BIAS (HIGH GAIN)			
X-AXIS	1.240E+03	1.233E+03	-3.368E+03
Y-AXIS	1.327E+03	1.327E+03	8.642E+02
ACC WARM-UP TRANSIENT			
X-AXIS	1.836E-06	1.836E-06	4.516E-07
Y-AXIS	1.834E-06	1.834E-06	-1.929E-06
Z-AXIS	1.928E-06	1.693E-06	-1.827E-04
ACCELEROMETER SCALE FACTOR			
X-AXIS	1.090E-03	1.090E-03	-2.736E-02
Y-AXIS	7.311E-04	7.311E-04	-1.669E-02
Z-AXIS	7.663E-04	7.663E-04	-4.553E-02
ACC SCALE FACTOR (HIGH GAIN)			
X-AXIS	1.421E-02	1.420E-02	-2.756E-02
Y-AXIS	1.537E-02	1.537E-02	-3.243E-02
ACC ATT DEP SCALE FACTOR			
X-AXIS	1.000E-06	1.000E-06	0.
Y-AXIS	7.116E-06	7.113E-06	7.538E-06
Z-AXIS	3.000E-06	3.000E-06	0.
CLOCK STABILITY			
	9.371E-07	9.959E-07	1.879E-07
ACC/PLATFORM MISALIGN ANGLES			
BXZ	9.832E-01	9.832E-01	1.220E-01
BXY	9.736E-01	9.736E-01	1.821E-01
BYZ	9.924E-01	9.924E-01	3.469E-03
BYX	9.270E-01	9.269E-01	-3.898E-01
BZY	9.669E-01	9.669E-01	2.275E-01
BZX	9.436E-01	9.436E-01	-5.853E-02
ACC NON-ORTHOGONALITY ANGLES			
BYZ	1.396E+00	1.396E+00	-1.254E-01
BZY	1.361E+00	1.361E+00	4.096E-01
BZX	1.255E+00	1.255E+00	4.483E-01
ACC/GYRO FRAME MISALIGN ANGLES			
X-AXIS	1.361E+00	1.361E+00	-4.183E-01
Y-AXIS	1.379E+00	1.379E+00	-1.902E-02
Z-AXIS	1.400E+00	1.400E+00	1.087E-01
PLATFORM VELOCITIES			
X-AXIS	1.457E-02	8.750E-03	-3.673E+01
Y-AXIS	7.989E-03	6.824E-03	1.739E+02
Z-AXIS	1.423E-02	9.649E-03	-1.731E+01

---STATE VECTOR VARIANCES AND OPTIMAL ESTIMATES CONTRASTED AGAINST TMO SIMULATION RESULTS---
PLATFORM TEST ATTITUDE = , ,MEASUREMENT NUMBER= 1

---------STATE VECTOR ELEMENT---------	-----STANDARD DEVIATION---- -PROPAGATED-	--UPDATED--	-OPT FILT-- -ESTIMATE-	--SYSTEM--- -SIMULATED-	-EST ERROR- --STD DEV--
GYRO CONSTANT BIAS					
X-AXIS	2.177E-02	2.175E-02	8.421E-03		
Y-AXIS	2.564E-02	2.564E-02	-6.048E-02		
Z-AXIS	2.265E-02	2.263E-02	-5.195E-01		
GYRO ATTITUDE DEPENDENT BIAS					
X-AXIS	4.377E-03	4.377E-03	-8.394E-05		
Y-AXIS	4.377E-03	4.377E-03	9.632E-05		
Z-AXIS	4.358E-03	4.358E-03	1.900E-04		
GYRO WARM-UP DRIFT					
X-AXIS	8.298E-05	8.299E-05	-2.970E-05		
Y-AXIS	8.314E-05	8.314E-05	-8.145E-05		
Z-AXIS	2.374E-04	2.374E-04	-1.529E-05		
GYRO DA G SENSITIVE					
X-AXIS	1.787E-02	1.787E-02	3.335E-01		
Y-AXIS	3.738E-02	3.737E-02	-3.496E-01		
Z-AXIS	3.154E-02	3.142E-02	-5.564E-03		
GYRO L.T.C. CORRELATED					
X-AXIS	4.989E-03	4.988E-03	-6.284E-04		
Y-AXIS	4.988E-03	4.988E-03	2.987E-04		
Z-AXIS	4.998E-03	4.998E-03	-4.298E-05		
GYRO MASS UNBALANCE					
MSX	4.818E-02	4.801E-02	9.020E-01		
MIX	9.278E-03	9.278E-03	1.432E-04		
MSY	4.054E-02	4.042E-02	9.598E-01		
MIY	9.932E-03	9.932E-03	7.913E-04		
MSZ	2.978E-02	2.977E-02	-5.966E-01		
MIZ	9.927E-03	9.926E-03	-4.626E-04		
MSX-MSY	3.352E-02	3.235E-02	-5.793E-02		
MSX+MSZ	3.549E-02	3.527E-02	3.054E-01		
MSY+MSZ	3.450E-02	3.432E-02	3.672E-01		
GYRO ANISOELASTIC CONSTANTS					
X-AXIS	8.932E-03	8.932E-03	-5.195E-04		
Y-AXIS	9.951E-03	9.950E-03	-1.414E-05		
Z-AXIS	9.916E-03	9.915E-03	3.846E-04		
GYRO TOTAL DRIFT					
X-AXIS	4.587E-02	4.574E-02	4.102E-01		
Y-AXIS	3.001E-02	2.990E-02	9.670E-01		
Z-AXIS	1.903E-02	1.885E-02	-5.156E-01		
GYRO SCALE FACTOR					
X-AXIS	3.521E-09	3.619E-09	2.555E-08		
Y-AXIS	4.991E-09	4.991E-09	-1.284E-08		
Z-AXIS	4.848E-09	4.843E-09	1.022E-08		
GYRO MISALIGNMENT ANGLES					
BXZ	9.949E-01	9.949E-01	7.647E-03		
BXY	9.861E-01	9.861E-01	-1.682E-01		
BYZ	9.949E-01	9.947E-01	1.637E-02		
BYX	9.963E-01	9.963E-01	2.124E-02		
BZY	9.964E-01	9.964E-01	3.013E-02		
BZX	9.945E-01	9.945E-01	-1.105E-02		
GYRO NON-ORTHOGONALITY ANGLES					
BYZ	1.408E+00	1.408E+00	-8.723E-03		
BZY	1.402E+00	1.402E+00	1.384E-01		
BZX	1.408E+00	1.408E+00	-3.239E-02		

HOUSING MISALIGNMENT ANGLES			
X-AXIS	2.283E+00	2.283E+00	-2.113E+00
Y-AXIS	2.058E+00	2.059E+00	-2.785E+00
Z-AXIS	2.697E+00	2.695E+00	-2.132E+00
GIMBAL SYNCHRO ANGLE BIAS			
X-AXIS	2.343E+00	2.343E+00	-1.291E+00
Y-AXIS	5.124E+00	5.111E+00	-9.201E-01
Z-AXIS	2.156E+00	2.156E+00	2.334E+00
DIFFERENTIAL SYNCHRO ANGLES			
X-AXIS	3.007E-02	2.349E-02	-1.003E+00
Y-AXIS	2.021E-01	2.017E-01	5.310E+00
Z-AXIS	3.008E-02	2.350E-02	-2.627E+00
PLATFORM TOTAL DRIFT			
X-AXIS	2.898E-02	2.885E-02	6.085E-01
Y-AXIS	2.920E-02	2.898E-02	8.870E-01
Z-AXIS	6.842E-03	5.714E-03	-5.357E-01
ACCELEROMETER BIAS			
X-AXIS	6.464E+02	6.464E+02	-3.518E+03
Y-AXIS	5.360E+02	5.860E+02	2.025E+03
Z-AXIS	6.041E+02	6.041E+02	-4.036E+02
ACC BIAS (HIGH GAIN)			
X-AXIS	1.228E+03	1.228E+03	-3.320E+03
Y-AXIS	1.295E+03	1.295E+03	9.567E+02
ACC WARM-UP TRANSIENT			
X-AXIS	2.484E-07	2.484E-07	6.042E-08
Y-AXIS	2.483E-07	2.483E-07	-2.613E-07
Z-AXIS	1.478E-07	1.478E-07	-2.472E-05
ACCELEROMETER SCALE FACTOR			
X-AXIS	8.711E-04	8.711E-04	-2.801E-02
Y-AXIS	5.870E-04	5.870E-04	-1.663E-02
Z-AXIS	6.109E-04	6.109E-04	-4.557E-02
ACC SCALE FACTOR (HIGH GAIN)			
X-AXIS	1.399E-02	1.399E-02	-2.823E-02
Y-AXIS	1.511E-02	1.511E-02	-2.453E-03
ACC ATT DEP SCALE FACTOR			
X-AXIS	9.999E-06	9.999E-06	-9.215E-09
Y-AXIS	9.999E-06	9.999E-06	-2.619E-08
Z-AXIS	3.000E-06	3.000E-06	0.
CLOCK STABILITY			
	9.976E-07	9.957E-07	-1.333E-07
ACC/PLATFORM MISALIGN ANGLES			
BXZ	8.357E-01	8.957E-01	7.766E-02
BXY	8.889E-01	8.889E-01	2.180E-01
BYZ	9.184E-01	3.184E-01	-8.038E-02
BYX	9.167E-01	9.167E-01	-3.668E-01
BZY	8.803E-01	8.803E-01	3.104E-01
BZX	9.327E-01	9.327E-01	-5.083E-02
ACC NON-ORTHOGONALITY ANGLES			
BYZ	1.162E+00	1.162E+00	3.315E-03
BZY	1.110E+00	1.110E+00	5.284E-01
BZX	1.232E+00	1.232E+00	4.176E-01
ACC/GYRO FRAME MISALIGN ANGLES			
X-AXIS	1.354E+00	1.354E+00	-3.880E-01
Y-AXIS	1.322E+00	1.322E+00	-4.980E-02
Z-AXIS	1.339E+00	1.339E+00	6.942E-02
PLATFORM VELOCITIES			
X-AXIS	1.170E-02	8.403E-03	1.494E+02
Y-AXIS	1.170E-02	8.403E-03	1.407E+02
Z-AXIS	1.448E-02	4.722E-03	-1.538E+01

---STATE VECTOR VARIANCES AND OPTIMAL ESTIMATES CONTRAST D AGAINST IMU SIMULATION RESULTS---
PLATFORM TEST ATTITUDE = 8 ,MEASUREMENT NUMBER= 10

---------STATE VECTOR ELEMENT---------	-----STANDARD DEVIATION---- -PROPAGATED-	--UPDATED--	-OPT FILT-- -ESTIMATE-	--SYSTEM--- -SIMULATED-	-EST ERROR- --STD DEV--
GYRO CONSTANT BIAS					
X-AXIS	2.157E-02	2.157E-02	9.984E-03		
Y-AXIS	1.882E-02	1.870E-02	-6.803E-02		
Z-AXIS	2.227E-02	2.227E-02	-5.173E-01		
GYRO ATTITUDE DEPENDENT BIAS					
X-AXIS	5.000E-03	5.000E-03	-6.915E-06		
Y-AXIS	4.941E-03	4.941E-03	-4.207E-04		
Z-AXIS	4.943E-03	4.942E-03	1.577E-03		
GYRO WARM-UP DRIFT					
X-AXIS	4.760E-05	4.760E-05	-1.742E-05		
Y-AXIS	4.736E-05	4.735E-05	-4.454E-05		
Z-AXIS	1.360E-04	1.360E-04	-2.007E-05		
GYRO DA G SENSITIVE					
X-AXIS	1.738E-02	1.738E-02	3.340E-01		
Y-AXIS	3.635E-02	3.634E-02	-3.594E-01		
Z-AXIS	2.592E-02	2.584E-02	-4.127E-02		
GYRO L.T.C. CORRELATED					
X-AXIS	4.989E-03	4.989E-03	-6.476E-04		
Y-AXIS	4.980E-03	4.980E-03	1.744E-04		
Z-AXIS	4.998E-03	4.997E-03	1.176E-04		
GYRO MASS UNBALANCE					
MSX	4.584E-02	4.583E-02	9.199E-01		
MIX	9.276E-03	9.276E-03	-3.789E-05		
MSY	3.751E-02	3.747E-02	9.813E-01		
MIY	9.801E-03	9.800E-03	5.554E-04		
MSZ	2.896E-02	2.895E-02	-5.864E-01		
MIZ	9.753E-03	9.751E-03	-4.034E-03		
MSX-MSY	2.620E-02	2.611E-02	-6.144E-02		
MSX+MSZ	3.207E-02	3.204E-02	3.735E-01		
MSY+MSZ	2.808E-02	2.799E-02	3.350E-01		
GYRO ANISOELASTIC CONSTANTS					
X-AXIS	8.989E-03	8.989E-03	-3.328E-04		
Y-AXIS	9.792E-03	9.791E-03	3.445E-04		
Z-AXIS	9.826E-03	9.825E-03	-2.233E-03		
GYRO TOTAL DRIFT					
X-AXIS	5.319E-02	5.319E-02	9.325E-01		
Y-AXIS	2.251E-02	2.247E-02	2.916E-01		
Z-AXIS	1.834E-02	1.821E-02	-4.743E-01		
GYRO SCALE FACTOR					
X-AXIS	3.610E-09	3.610E-09	2.572E-08		
Y-AXIS	3.549E-09	3.525E-09	-1.123E-08		
Z-AXIS	4.791E-09	4.790E-09	1.153E-08		
GYRO MISALIGNMENT ANGLES					
BXZ	9.942E-01	9.942E-01	-3.472E-02		
BXY	9.846E-01	9.846E-01	-2.099E-01		
BYZ	9.867E-01	9.865E-01	5.894E-02		
BYX	9.954E-01	9.954E-01	3.172E-02		
BZY	9.954E-01	9.954E-01	1.184E-01		
BZX	9.905E-01	9.905E-01	-1.994E-01		
GYRO NON-ORTHOGONALITY ANGLES					
BYZ	1.398E+00	1.398E+00	-9.366E-02		
BZY	1.400E+00	1.400E+00	3.273E-01		
BZX	1.404E+00	1.404E+00	-2.296E-01		

HOUSING MISALIGNMENT ANGLES			
X-AXIS	2.092E+00	2.092E+00	-2.914E+00
Y-AXIS	1.921E+00	1.921E+00	-2.985E+00
Z-AXIS	2.388E+00	2.384E+00	-2.754E+00
GIMBAL SYNCHRO ANGLE BIAS			
X-AXIS	2.268E+00	2.268E+00	-2.991E+00
Y-AXIS	4.772E+00	4.753E+00	-7.677E+00
Z-AXIS	2.207E+00	2.207E+00	-3.863E+00
DIFFERENTIAL SYNCHRO ANGLES			
X-AXIS	2.995E-02	2.343E-02	-1.762E+00
Y-AXIS	2.032E-01	2.031E-01	5.253E+00
Z-AXIS	2.996E-02	2.344E-02	-2.334E+00
PLATFORM TOTAL DRIFT			
X-AXIS	4.078E-02	4.076E-02	1.047E+00
Y-AXIS	6.839E-03	5.714E-03	3.499E-01
Z-AXIS	6.836E-03	5.716E-03	-4.792E-01
ACCELEROMETER BIAS			
X-AXIS	5.667E+02	5.667E+02	-3.312E+03
Y-AXIS	5.642E+02	5.642E+02	1.879E+03
Z-AXIS	4.465E+02	4.465E+02	-2.693E+02
ACC BIAS (HIGH GAIN)			
X-AXIS	1.202E+03	1.202E+03	-3.067E+03
Y-AXIS	1.252E+03	1.252E+03	5.042E+02
ACC WARM-UP TRANSIENT			
X-AXIS	3.354E-08	3.354E-08	9.122E-09
Y-AXIS	3.360E-08	3.360E-08	-3.528E-08
Z-AXIS	2.001E-08	2.001E-08	-3.346E-06
ACCELEROMETER SCALE FACTOR			
X-AXIS	5.677E-04	5.677E-04	-2.763E-02
Y-AXIS	5.651E-04	5.651E-04	-1.677E-02
Z-AXIS	4.610E-04	4.610E-04	-4.543E-02
ACC SCALE FACTOR (HIGH GAIN)			
X-AXIS	1.358E-02	1.358E-02	-2.839E-02
Y-AXIS	1.457E-02	1.456E-02	-2.293E-04
ACC ATT DEP SCALE FACTOR			
X-AXIS	9.996E-06	9.996E-06	2.000E-07
Y-AXIS	1.000E-05	1.000E-05	0.
Z-AXIS	3.000E-05	3.000E-05	0.
CLOCK STABILITY			
	9.976E-07	9.957E-07	-8.585E-08
ACC/PLATFORM MISALIGN ANGLES			
BXZ	7.904E-01	7.904E-01	-1.991E-01
BXY	8.802E-01	8.802E-01	1.379E-01
BYZ	7.940E-01	7.940E-01	-3.214E-01
BYX	8.806E-01	8.806E-01	-3.233E-01
BZY	8.721E-01	8.721E-01	3.832E-01
BZX	8.666E-01	8.665E-01	-8.449E-02
ACC NON-ORTHOGONALITY ANGLES			
BYZ	7.611E-01	7.611E-01	5.205E-01
BZY	1.093E+00	1.093E+00	4.411E-01
BZX	1.082E+00	1.082E+00	4.078E-01
ACC/GYRO FRAME MISALIGN ANGLES			
X-AXIS	1.330E+00	1.330E+00	-3.545E-01
Y-AXIS	1.315E+00	1.315E+00	7.096E-02
Z-AXIS	1.271E+00	1.271E+00	-1.644E-01
PLATFORM VELOCITIES			
X-AXIS	8.003E-03	6.833E-03	2.348E+02
Y-AXIS	1.444E-02	9.710E-03	1.284E+01
Z-AXIS	1.444E-02	9.710E-03	-2.241E+01

---STATE VECTOR VARIANCES AND OPTIMAL ESTIMATES CONTRASTED AGAINST IMU SIMULATION RESULTS---
PLATFORM TEST ATTITUDE = 3 ,MEASUREMENT NUMBER= 10

----- ---STATE VECTOR ELEMENT--------	-----STANDARD DEVIATION---- -PROPAGATED-	--UPDATED--	-3PT FILT-- -ESTIMATE-	--SYSTEM--- -SIMULATED-	-EST ERROR- --STD DEV--
GYRO CONSTANT BIAS					
X-AXIS	2.132E-02	2.132E-02	7.842E-03		
Y-AXIS	8.091E-03	7.893E-03	-5.962E-02		
Z-AXIS	1.453E-02	1.447E-02	-5.131E-01		
GYRO ATTITUDE DEPENDENT BIAS					
X-AXIS	5.000E-03	5.000E-03	-5.910E-06		
Y-AXIS	4.953E-03	4.953E-03	3.114E-04		
Z-AXIS	4.974E-03	4.974E-03	1.454E-04		
GYRO WARM-UP DRIFT					
X-AXIS	2.731E-05	2.731E-05	-1.003E-05		
Y-AXIS	2.715E-05	2.715E-05	-2.615E-05		
Z-AXIS	7.799E-05	7.799E-05	-1.264E-05		
GYRO DA G SENSITIVE					
X-AXIS	1.712E-02	1.712E-02	3.352E-01		
Y-AXIS	1.534E-02	1.495E-02	-3.477E-01		
Z-AXIS	1.402E-02	1.392E-02	-3.563E-02		
GYRO L.T.C. CORRELATED					
X-AXIS	4.991E-03	4.991E-03	-6.046E-04		
Y-AXIS	4.977E-03	4.977E-03	3.090E-04		
Z-AXIS	4.994E-03	4.994E-03	1.334E-04		
GYRO MASS UNBALANCE					
MSX	4.535E-02	4.535E-02	9.239E-01		
MIX	9.275E-03	9.275E-03	-7.367E-05		
MSY	3.717E-02	3.717E-02	9.829E-01		
MIY	9.218E-03	9.211E-03	2.089E-03		
MSZ	2.873E-02	2.873E-02	-5.889E-01		
MIZ	9.232E-03	9.229E-03	-4.835E-03		
MSX-MSY	2.450E-02	2.443E-02	-5.900E-02		
MSX+MSZ	3.165E-02	3.165E-02	3.350E-01		
MSY+MSZ	2.697E-02	2.697E-02	3.940E-01		
GYRO ANISOELASTIC CONSTANTS					
X-AXIS	8.988E-03	8.988E-03	-3.040E-04		
Y-AXIS	9.557E-03	9.556E-03	1.304E-03		
Z-AXIS	9.824E-03	9.824E-03	-2.207E-03		
GYRO TOTAL DRIFT					
X-AXIS	4.778E-02	4.778E-02	-9.180E-01		
Y-AXIS	1.769E-02	1.686E-02	-4.072E-01		
Z-AXIS	2.174E-02	2.151E-02	-5.485E-01		
GYRO SCALE FACTOR					
X-AXIS	3.599E-09	3.599E-09	2.583E-09		
Y-AXIS	2.345E-09	2.129E-09	-1.215E-08		
Z-AXIS	3.702E-09	3.695E-09	1.060E-08		
GYRO MISALIGNMENT ANGLES					
BXZ	9.941E-01	9.941E-01	-3.708E-02		
BXY	9.845E-01	9.845E-01	-2.113E-01		
BYZ	9.865E-01	9.865E-01	5.378E-02		
BYX	9.773E-01	9.771E-01	1.173E-01		
BZY	9.875E-01	9.875E-01	1.493E-01		
BZX	9.888E-01	9.888E-01	-2.181E-01		
GYRO NON-ORTHOGONALITY ANGLES					
BYZ	1.398E+00	1.398E+00	-9.086E-02		
BZY	1.334E+00	1.334E+00	3.612E-01		
BZX	1.389E+00	1.389E+00	-3.356E-01		

MOUNT TO MISALIGNMENT ANGL			
X-AXIS	1.378E+00	1.977E+00	-2.911E+00
Y-AXIS	1.728E+00	1.728E+00	-2.046E+00
Z-AXIS	2.378E+00	2.378E+00	-2.738E+00
GIMBAL SYNCHRO ANGL BIAS			
X-AXIS	2.330E+00	2.330E+00	-3.149E+00
Y-AXIS	5.465E+00	5.463E+00	-7.038E-01
Z-AXIS	2.495E+00	2.495E+00	-4.085E+00
DIFFERENTIAL SYNCHRO ANGL			
X-AXIS	2.348E-02	2.348E-02	-2.351E+00
Y-AXIS	3.324E-01	3.324E-01	5.173E+00
Z-AXIS	3.357E-02	2.357E-02	-2.832E+00
PLATFORM TOTAL DRIFT			
X-AXIS	4.650E-02	4.650E-02	-1.030E+00
Y-AXIS	5.722E-03	5.722E-03	-4.661E-01
Z-AXIS	3.750E-03	3.750E-03	-5.784E-01
ACCELEROMETER BIAS			
X-AXIS	7.100E+00	7.100E+00	-3.620E+03
Y-AXIS	4.383E+02	4.383E+02	2.100E+03
Z-AXIS	4.286E+02	4.286E+02	-3.506E+02
ACC BIAS (HIGH GAIN)			
X-AXIS	1.148E+03	1.148E+03	-3.288E+03
Y-AXIS	1.182E+03	1.182E+03	7.536E+02
ACC ASYM-UP TRANSIENT			
X-AXIS	4.578E-03	4.578E-03	1.192E-09
Y-AXIS	4.548E-03	4.548E-03	-4.774E-09
Z-AXIS	3.708E-03	3.708E-03	-4.528E-07
ACCELEROMETER SCALE FACTOR			
X-AXIS	7.115E-06	7.113E-06	-2.734E-02
Y-AXIS	4.330E-04	4.330E-04	-1.655E-02
Z-AXIS	4.440E-04	4.440E-04	-4.552E-02
ACC SCALE FACTOR (HIGH GAIN)			
X-AXIS	1.319E-02	1.319E-02	-2.371E-02
Y-AXIS	1.359E-02	1.359E-02	-2.933E-04
ACC ASYMMETRY SCALE FACTOR			
X-AXIS	1.000E-05	1.000E-05	-3.197E-09
Y-AXIS	1.000E-05	1.000E-05	0.
Z-AXIS	3.000E-05	3.000E-05	0.
CLOCK STABILITY			
	8.976E-07	8.957E-07	-1.626E-10
ACC/PLATFORM MISALIGN ANG			
AXZ	7.528E-01	7.528E-01	-3.263E-01
AYY	7.283E-01	7.283E-01	-9.713E-02
AYZ	7.654E-01	7.654E-01	-3.194E-01
AZY	8.336E-01	8.336E-01	-1.913E-01
AZX	7.442E-01	7.442E-01	-2.475E-02
AZY	8.331E-01	8.331E-01	-2.870E-02
ACC NON-ORTHOGONALITY ANG			
BXZ	6.277E-01	6.271E-01	6.456E-01
BZY	5.710E-01	5.710E-01	-1.219E-01
BZX	9.535E-01	9.534E-01	2.193E-01
ACC/GYRO FRAME MISALIGN ANGLES			
X-AXIS	1.273E+00	1.273E+00	-3.086E-01
Y-AXIS	1.220E+00	1.220E+00	3.084E-01
Z-AXIS	1.247E+00	1.247E+00	-2.882E-01
PLATFORM VELOCITIES			
X-AXIS	5.033E-03	5.033E-03	-3.045E+02
Y-AXIS	1.454E-02	9.741E-03	2.906E+01
Z-AXIS	1.447E-02	1.721E-03	-2.377E+01

---STA... ...STATE DEVIATIONS AND ERROR ESTIMATES (CONTRASTED AGAINST IMU SIMULATION RESULTS)---
...ALIGNMENT ATTITUDE ... ..., MEASUREMENT NUMBER= 10

...ERROR SOURCE...	-----STANDARD DEVIATION----		-DRY FILT--	--SYSTEM---	-EST ERROR-
	-PROPAGATED-	--UPDATED--	-ESTIMATES--	-SIMULATED-	--STD DEV--
GYRO CONSTANT BIAS					
X-AXIS	1.530E-02	1.527E-02	-1.615E-02		
Y-AXIS	7.758E-03	7.758E-03	-5.751E-02		
Z-AXIS	1.343E-02	1.333E-02	-5.109E-01		
GYRO RETICLE ... BIAS					
X-AXIS	4.844E-03	4.844E-03	-1.052E-03		
Y-AXIS	4.836E-03	4.834E-03	-1.228E-03		
Z-AXIS	4.831E-03	4.830E-03	-1.877E-04		
GYRO MISALIGNMENTS					
X-AXIS	1.564E-05	1.564E-05	-4.754E-06		
Y-AXIS	1.556E-05	1.556E-05	-1.400E-05		
Z-AXIS	4.471E-05	4.471E-05	-8.753E-06		
GYRO G SENSITIVE					
X-AXIS	1.574E-02	1.574E-02	3.281E-01		
Y-AXIS	3.020E-03	3.013E-03	-3.713E-01		
Z-AXIS	1.388E-02	1.388E-02	-3.563E-02		
GYRO ...Y-D... SQUEEZE					
X-AXIS	4.386E-03	4.386E-03	-9.803E-04		
Y-AXIS	4.386E-03	4.386E-03	-2.754E-04		
Z-AXIS	4.386E-03	4.386E-04	1.550E-04		
GYRO ...R UNBALANCE					
MBX	4.838E-02	4.788E-02	9.075E-01		
MBY	8.763E-03	8.357E-03	-5.928E-03		
MBZ	3.710E-02	3.710E-02	3.730E-01		
MIX	5.787E-03	5.693E-03	-7.133E-03		
MIZ	2.843E-02	2.843E-02	-5.866E-01		
MIZ	3.227E-03	3.227E-03	-4.889E-03		
MBX-MBY	2.266E-02	2.252E-02	-7.164E-02		
MBX+MBZ	3.038E-02	3.009E-02	3.228E-01		
MBY+MBZ	2.767E-02	2.670E-02	3.924E-01		
GYRO ...TOELASTIC SENSITIVE					
X-AXIS	8.823E-03	8.328E-03	-1.871E-03		
Y-AXIS	3.508E-03	3.439E-03	3.614E-03		
Z-AXIS	8.822E-03	8.822E-03	-1.906E-03		
GYRO TOTAL DRIFT					
X-AXIS	1.734E-02	1.730E-02	2.693E-02		
Y-AXIS	8.768E-03	8.643E-03	4.765E-02		
Z-AXIS	3.378E-02	3.378E-02	-1.108E+00		
GYRO SCALE FACTOR					
X-AXIS	3.233E-04	3.233E-04	2.825E-04		
Y-AXIS	1.211E-04	1.177E-04	-1.480E-04		
Z-AXIS	3.456E-04	3.452E-04	1.316E-04		
GYRO MISALIGNMENT ANGLE					
RXZ	9.927E-01	9.927E-01	1.782E-02		
RYY	9.718E-01	9.718E-01	-1.865E-03		
RYZ	9.866E-01	9.856E-01	1.282E-01		
RZY	9.624E-01	9.621E-01	-3.777E-02		
RZY	9.874E-01	9.874E-01	1.595E-01		
RZY	9.886E-01	9.886E-01	-2.511E-01		
GYRO NON-ORTHOGONALITY ANGLE					
RXZ	1.338E+00	1.338E+00	-1.141E-01		
RZY	1.386E+00	1.386E+00	1.714E-01		
RZX	1.341E+00	1.341E+00	-2.163E-01		

HOUSING MISALIGNMENT ANGLES			
X-AXIS	1.736E+00	1.736E+00	-3.335E-02
Y-AXIS	1.662E+00	1.663E+00	-1.451E+00
Z-AXIS	2.216E+00	2.215E+00	-4.775E-02
GIMBAL SYNCHRO ANGLE BIAS			
X-AXIS	1.934E+00	1.933E+00	-1.381E+01
Y-AXIS	2.403E+00	2.403E+00	-5.842E+00
Z-AXIS	4.331E+00	4.335E+00	4.630E+00
DIFFERENTIAL SYNCHRO ANGLE B			
X-AXIS	2.773E-02	2.776E-02	-1.764E-01
Y-AXIS	2.303E-02	2.745E-02	-2.963E-01
Z-AXIS	1.731E-01	1.731E-01	-5.688E+00
PLATFORM TOTAL DRIFT			
X-AXIS	7.534E-03	6.530E-03	6.973E-02
Y-AXIS	7.314E-03	6.454E-03	-3.545E-02
Z-AXIS	3.413E-02	3.412E-02	-1.143E+00
ACCELEROMETER BIAS			
X-AXIS	7.093E+02	7.033E+02	-3.620E+03
Y-AXIS	4.141E+02	4.145E+02	2.262E+03
Z-AXIS	3.746E+01	3.786E+01	-2.457E+02
ACC BIAS (HIGH GAIN)			
X-AXIS	1.134E+03	1.134E+03	-3.469E+03
Y-AXIS	1.150E+03	1.149E+03	3.564E+02
ACC WARM-UP TRANSIENT			
X-AXIS	6.141E-10	6.141E-10	1.859E-10
Y-AXIS	6.153E-10	6.153E-10	-6.663E-10
Z-AXIS	3.663E-10	3.663E-10	-6.125E-08
ACCELEROMETER SCALE FACTOR			
X-AXIS	7.111E-06	7.111E-06	-2.734E-02
Y-AXIS	4.149E-04	4.149E-04	-1.653E-02
Z-AXIS	2.431E-05	2.431E-05	-4.542E-02
ACC SCALE FACTOR (HIGH GAIN)			
X-AXIS	1.733E-02	1.733E-02	-2.733E-02
Y-AXIS	1.332E-02	1.332E-02	-6.447E-04
ACC ATT DEP SCALE FACTOR			
X-AXIS	1.003E-05	1.003E-05	-1.340E-03
Y-AXIS	1.003E-05	1.003E-05	-9.474E-03
Z-AXIS	2.999E-05	2.999E-05	-1.746E-02
CLOCK STABILITY			
	9.976E-07	9.985E-07	1.137E-07
ACC/PLATFORM MISALIGN ANGLES			
BXZ	7.408E-01	7.408E-01	-1.871E-01
BXY	6.773E-01	6.773E-01	1.899E-01
BYZ	7.615E-01	7.615E-01	-2.261E-01
BYX	7.562E-01	7.554E-01	2.740E-01
BZY	6.781E-01	6.781E-01	-1.560E-01
BZX	7.474E-01	7.473E-01	-1.073E-01
ACC NON-ORTHOGONALITY ANGLES			
SXZ	5.831E-01	5.831E-01	4.139E-01
SZY	1.650E-01	1.651E-01	3.365E-02
SZX	5.877E-01	5.877E-01	-1.561E-01
ACC/GYRO FRAME MISALIGN ANGLES			
X-AXIS	1.137E+00	1.135E+00	3.977E-01
Y-AXIS	1.174E+00	1.174E+00	-1.980E-01
Z-AXIS	1.234E+00	1.233E+00	-2.044E-01
PLATFORM VELOCITIES			
X-AXIS	1.425E-02	3.644E-03	6.066E+00
Y-AXIS	1.442E-02	3.693E-03	3.5 8E+01
Z-AXIS	8.135E-03	6.880E-03	-4.735E-02

---STATE VECTOR VARIANCES AND OPTIMAL ESTIMATE CONTRASTED AGAINST THE SIMULATION RESULTS---
PLATFORM T-ST ATTITUDE = 10 ,MEASUREMENT NUMBER= 17

---------STATE VECTOR ELEMENT--------	-----STANDARD DEVIATION---- PROPAGATED-	--UPDATED--	-OPT FILT-- -ESTIMATE-	--SYSTEM--- -SIMULATED-	-ERR ERROR- --STD DEV--
GYRO CONSTANT BIAS					
X-AXIS	1.520E-02	1.507E-02	-2.115E-02		
Y-AXIS	7.767E-03	7.756E-03	-5.763E-02		
Z-AXIS	1.314E-02	1.317E-02	-5.183E-01		
GYRO ATTITUDE DEPENDENT BIAS					
X-AXIS	4.348E-03	4.947E-03	-1.298E-03		
Y-AXIS	4.843E-03	4.886E-03	-8.638E-04		
Z-AXIS	4.998E-03	4.998E-03	-5.113E-05		
GYRO WARM-UP DRIFT					
X-AXIS	1.326E-05	1.324E-05	-2.947E-06		
Y-AXIS	1.315E-05	1.315E-05	-1.042E-05		
Z-AXIS	3.744E-05	3.743E-05	-5.132E-06		
GYRO DA G SENSITIVE					
X-AXIS	1.981E-02	1.983E-02	3.215E-01		
Y-AXIS	8.368E-03	8.783E-03	-3.320E-01		
Z-AXIS	1.837E-02	1.837E-02	-3.517E-02		
GYRO L.F.G. CORRELATED					
X-AXIS	4.386E-03	4.973E-03	-1.633E-03		
Y-AXIS	4.366E-03	4.955E-03	-1.615E-04		
Z-AXIS	4.995E-03	4.995E-03	1.12E-04		
GYRO MASS UNBALANCE					
MSX	3.035E-02	7.091E-03	3.160E-01		
MIX	8.342E-03	8.337E-03	-7.646E-03		
MSY	3.043E-02	3.042E-02	3.952E-01		
MIY	5.571E-03	5.442E-03	-5.844E-03		
MSZ	2.370E-02	2.367E-02	-5.880E-01		
MIZ	9.227E-03	9.225E-03	-5.179E-03		
MSX-MSY	2.533E-02	2.532E-02	-6.316E-02		
MSX+MSZ	2.542E-02	2.680E-02	3.223E-01		
MSY+MSZ	2.611E-02	2.610E-02	3.271E-01		
GYRO ANISOELASTIC CONSTANTS					
X-AXIS	3.750E-03	3.750E-03	-1.714E-03		
Y-AXIS	3.496E-03	3.495E-03	3.071E-03		
Z-AXIS	3.421E-03	3.421E-03	-1.340E-03		
GYRO TOTAL DRIFT					
X-AXIS	1.774E-02	1.744E-02	2.045E-02		
Y-AXIS	9.514E-03	9.496E-03	4.390E-02		
Z-AXIS	2.462E-02	2.462E-02	-1.142E+00		
GYRO SCALE FACTOR					
X-AXIS	2.802E-08	2.733E-08	2.834E-08		
Y-AXIS	1.162E-08	1.120E-08	-1.478E-08		
Z-AXIS	3.449E-08	3.446E-08	1.330E-08		
GYRO MISALIGNMENT ANGLES					
BXZ	9.322E-01	9.023E-01	1.522E-02		
BXY	9.715E-01	9.714E-01	2.276E-02		
BYZ	9.344E-01	9.844E-01	1.967E-01		
BYX	9.613E-01	9.613E-01	-5.142E-02		
BZY	9.874E-01	9.874E-01	1.637E-01		
BZX	9.995E-01	9.995E-01	-2.458E-01		
GYRO NON-ORTHOGONALITY ANGLES					
BYZ	1.396E+00	1.396E+00	-1.815E-01		
BZY	1.395E+00	1.395E+00	1.762E-01		
BZX	1.381E+00	1.381E+0	-1.453E-01		

HOUSING MISALIGNMENT ANGLES			
X-AXIS	1.777E+00	1.777E+00	-3.638E+00
Y-AXIS	1.638E+00	1.638E+00	-1.378E+00
Z-AXIS	2.132E+00	2.131E+00	-4.126E+00
GIMBAL SYNCHRO ANGLE BIAS			
X-AXIS	1.914E+00	1.914E+00	-1.103E+01
Y-AXIS	2.382E+00	2.382E+00	-6.083E+00
Z-AXIS	4.858E+00	4.840E+00	5.771E+00
DIFFERENTIAL SYNCHRO ANGLES			
X-AXIS	3.396E-02	2.396E-02	-2.161E-01
Y-AXIS	3.469E-02	2.270E-02	-3.477E-01
Z-AXIS	1.882E-01	1.880E-01	-7.380E+00
PLATFORM TOTAL DRIFT			
X-AXIS	6.466E-03	4.776E-03	6.635E-02
Y-AXIS	6.227E-03	4.678E-03	-3.332E-02
Z-AXIS	2.112E-02	2.080E-02	-1.138E+00
ACCELEROMETER BIAS			
X-AXIS	7.099E+00	7.099E+00	-3.620E+03
Y-AXIS	4.091E+02	4.090E+02	2.151E+03
Z-AXIS	3.753E+01	3.752E+01	-2.536E+02
ACC BIAS (HIGH GAIN)			
X-AXIS	8.872E+00	7.833E+00	-3.712E+03
Y-AXIS	4.091E+02	4.090E+02	2.329E+03
ACC WARM-UP TRANSIENT			
X-AXIS	3.369E-10	3.369E-10	1.154E-10
Y-AXIS	3.376E-10	3.376E-10	-3.662E-10
Z-AXIS	2.007E-10	2.001E-10	-3.760E-09
ACCELEROMETER SCALE FACTOR			
X-AXIS	7.111E-06	7.111E-06	-2.736E-02
Y-AXIS	4.093E-04	4.097E-04	-1.649E-02
Z-AXIS	2.781E-05	2.791E-05	-4.564E-02
ACC SCALE FACTOR (HIGH GAIN)			
X-AXIS	7.278E-05	5.476E-05	-2.414E-02
Y-AXIS	4.168E-04	4.132E-04	-1.774E-02
ACC ATT DEP SCALE FACTOR			
X-AXIS	1.000E-05	1.000E-05	2.655E-09
Y-AXIS	1.000E-05	1.000E-05	-1.328E-08
Z-AXIS	2.994E-05	2.998E-05	-7.618E-08
CLOCK STABILITY	9.373E-07	9.947E-07	2.034E-07
ACC/PLATFORM MISALIGN ANGLES			
ΘXZ	7.396E-01	7.396E-01	-2.437E-01
ΘXY	6.765E-01	6.765E-01	1.889E-01
ΘYZ	7.594E-01	7.594E-01	-3.122E-01
ΘYX	7.593E-01	7.593E-01	2.116E-01
ΘZY	6.772E-01	6.772E-01	-1.756E-01
ΘZX	7.434E-01	7.433E-01	-2.388E-01
ACC NON-ORTHOGONALITY ANGLES			
ΘXZ	5.861E-01	5.860E-01	5.550E-01
ΘZY	1.644E-01	1.644E-01	1.331E-02
ΘZX	6.799E-01	6.797E-01	-3.569E-03
ACC/GYRO FRAME MISALIGN ANGLES			
X-AXIS	1.196E+00	1.196E+00	2.624E-01
Y-AXIS	1.173E+00	1.173E+00	-2.166E-01
Z-AXIS	1.237E+00	1.237E+00	-2.590E-01
PLATFORM VELOCITIES			
X-AXIS	7.301E-04	1.235E-04	1.178E+00
Y-AXIS	7.368E-04	1.256E-04	7.313E-01
Z-AXIS	2.376E-03	2.304E-03	-8.648E-01

---STATE VECTOR VARIANCES AND OPTIMAL ESTIMATES CONTRASTED AGAINST IMU SIMULATION RESULTS---
PLATFORM TEST ATTITUDE = 11 ,MEASUREMENT NUMBER= 10

----------STATE VECTOR ELEMENT----------	-----STANDARD DEVIATION----- -PROPAGATED-	--UPDATED--	-OPT FILT-- -ESTIMATE--	--SYSTEM--- -SIMULATED-	-EST ERROR- --STD DEV--
GYRO CONSTANT BIAS					
X-AXIS	1.601E-02	1.601E-02	-1.823E-02		
Y-AXIS	6.994E-03	6.992E-03	-4.739E-02		
Z-AXIS	1.234E-02	1.234E-02	-5.229E-01		
GYRO ATTITUDE DEPENDENT BIAS					
X-AXIS	4.835E-03	4.824E-03	2.070E-03		
Y-AXIS	4.934E-03	4.891E-03	1.589E-03		
Z-AXIS	5.000E-03	4.001E-03	2.408E-06		
GYRO WARM-UP DRIFT					
X-AXIS	7.443E-06	7.436E-06	-4.668E-06		
Y-AXIS	7.540E-06	7.540E-06	-5.646E-06		
Z-AXIS	2.170E-05	2.170E-05	-2.115E-05		
GYRO G SENSITIVE					
X-AXIS	8.076E-03	7.959E-03	3.346E-01		
Y-AXIS	8.620E-03	8.615E-03	-3.285E-01		
Z-AXIS	1.386E-02	1.366E-02	-3.483E-02		
GYRO G**2 CORRELATED					
X-AXIS	4.952E-03	4.950E-03	-5.872E-04		
Y-AXIS	4.902E-03	4.962E-03	-1.370E-05		
Z-AXIS	4.996E-03	4.996E-03	8.399E-05		
GYRO MASS UNBALANCE					
MXX	2.891E-02	2.883E-02	5.975E-01		
MIX	5.101E-03	4.974E-03	3.420E-03		
MSY	3.015E-02	3.015E-02	9.714E-01		
MIY	5.331E-03	5.331E-03	-3.606E-03		
MSZ	2.362E-02	2.362E-02	-5.879E-01		
MIZ	9.225E-03	9.225E-03	-5.574E-03		
MSX-MSY	1.800E-02	1.791E-02	-7.397E-02		
MSX+MSY	2.330E-02	2.383E-02	3.036E-01		
MSY+MSZ	2.574E-02	2.574E-02	3.835E-01		
GYRO ANISOELASTIC CONSTANTS					
X-AXIS	9.666E-03	9.662E-03	2.865E-04		
Y-AXIS	9.472E-03	9.471E-03	4.445E-03		
Z-AXIS	9.821E-03	9.821E-03	-2.074E-03		
GYRO TOTAL DRIFT					
X-AXIS	1.562E-02	1.550E-02	-1.283E-02		
Y-AXIS	9.876E-03	9.854E-03	-4.945E-02		
Z-AXIS	2.304E-02	2.904E-02	-1.112E+00		
GYRO SCALE FACTOR					
X-AXIS	2.498E-09	2.485E-09	3.025E-08		
Y-AXIS	1.101E-09	1.100E-09	-1.436E-08		
Z-AXIS	3.402E-09	3.400E-09	1.381E-08		
GYRO MISALIGNMENT ANGLES					
ΘXZ	9.819E-01	9.818E-01	7.139E-02		
ΘXY	9.581E-01	9.576E-01	-2.215E-01		
ΘYZ	9.691E-01	9.687E-01	5.027E-01		
ΘYX	9.600E-01	9.600E-01	9.649E-02		
ΘZY	9.874E-01	9.874E-01	1.717E-01		
ΘZX	9.885E-01	9.885E-01	-2.487E-01		
GYRO NON-ORTHOGONALITY ANGLES					
ΘYZ	1.387E+00	1.386E+00	-4.234E-01		
ΘZY	1.376E+00	1.375E+00	3.333E-01		
ΘZX	1.379E+00	1.379E+00	-3.452E-01		

HOUSING MISALIGNMENT ANGLES			
X-AXIS	1.702E+00	1.702E+00	-3.440E-02
Y-AXIS	1.573E+00	1.573E+00	-1.725E+00
Z-AXIS	1.995E+00	1.991E+00	-5.695E+00
GIMBAL SYNCHRO ANGLE BIAS			
X-AXIS	2.035E+00	2.035E+00	-3.813E+00
Y-AXIS	1.736E+00	1.735E+00	6.019E-01
Z-AXIS	3.376E+00	3.282E+00	7.697E+00
DIFFERENTIAL SYNCHRO ANGLES			
X-AXIS	2.899E-02	2.296E-02	8.079E-01
Y-AXIS	2.952E-02	2.322E-02	-1.583E-01
Z-AXIS	1.479E-01	1.479E-01	-5.341E+00
PLATFORM TOTAL DRIFT			
X-AXIS	6.567E-03	6.636E-03	1.619E-01
Y-AXIS	5.764E-03	5.693E-03	-4.062E-02
Z-AXIS	2.978E-02	2.977E-02	-1.188E+00
ACCELEROMETER BIAS			
X-AXIS	7.030E+00	7.039E+00	-3.620E+03
Y-AXIS	2.517E+02	2.517E+02	3.011E+03
Z-AXIS	1.835E+01	1.835E+01	-1.663E+02
ACC BIAS (HIGH GAIN)			
X-AXIS	7.832E+00	7.832E+00	-3.772E+03
Y-AXIS	2.518E+02	2.517E+02	3.163E+03
ACC WARM-UP TRANSIENT			
X-AXIS	4.558E-11	4.558E-11	1.757E-11
Y-AXIS	4.545E-11	4.545E-11	-4.212E-11
Z-AXIS	2.339E-11	1.885E-11	-4.575E-09
ACCELEROMETER SCALE FACTOR			
X-AXIS	7.111E-06	7.111E-06	-2.794E-02
Y-AXIS	2.523E-04	2.523E-04	-1.565E-02
Z-AXIS	1.498E-05	1.498E-05	-4.536E-02
ACC SCALE FACTOR (HIGH GAIN)			
X-AXIS	5.435E-05	5.435E-05	-2.415E-02
Y-AXIS	2.580E-04	2.580E-04	-1.690E-02
ACC ATT DEP SCALE FACTOR			
X-AXIS	1.000E-05	1.000E-05	0.
Y-AXIS	1.000E-05	1.000E-05	0.
Z-AXIS	2.585E-05	2.585E-05	3.843E-05
CLOCK STABILITY			
	9.976E-07	9.956E-07	-1.233E-07
ACC/PLATFORM MISALIGN ANGLES			
BYZ	7.085E-01	7.085E-01	2.892E-01
BXY	6.645E-01	6.643E-01	1.334E-01
BYZ	7.162E-01	7.162E-01	3.519E-01
BYX	6.974E-01	6.974E-01	9.897E-01
BZY	6.654E-01	6.652E-01	1.040E-01
BZX	6.969E-01	6.969E-01	5.097E-01
ACC NON-ORTHOGONALITY ANGLES			
BYZ	3.635E-01	3.635E-01	-6.410E-01
BZY	1.406E-01	1.406E-01	2.394E-01
BZX	4.109E-01	4.109E-01	-1.419E+00
ACC/GYRO FRAME MISALIGN ANGLES			
X-AXIS	1.163E+00	1.163E+00	8.172E-01
Y-AXIS	1.144E+00	1.142E+00	8.814E-02
Z-AXIS	1.219E+00	1.219E+00	2.178E-01
PLATFORM VELOCITIES			
X-AXIS	1.423E-02	9.666E-03	-4.092E+01
Y-AXIS	1.411E-02	9.684E-03	1.232E+01
Z-AXIS	8.003E-03	6.832E-03	-4.388E+02

---STATE VECTOR VARIANCES AND OPTIMAL ESTIMATES CONTRASTED AGAINST IMU SIMULATION RESULTS---
PLATFORM TEST ATTITUDE = 12 ,MEASUREMENT NUMBER= 10

---------STATE VECTOR ELEMENT---------	-----STANDARD DEVIATION---- -PROPAGATED-	--UPDATED--	-OPT FILT-- -ESTIMATE--	--SYSTEM--- -SIMULATION-	-SOL ERROR- --STD DEV--
GYRO CONSTANT BIAS					
X-AXIS	1.494E-02	1.494E-02	-2.019E-02		
Y-AXIS	6.567E-03	6.567E-03	-5.249E-02		
Z-AXIS	1.074E-02	1.069E-02	-5.130E-01		
GYRO ATTITUDE DEPENDENT BIAS					
X-AXIS	4.610E-03	4.571E-03	-9.187E-04		
Y-AXIS	5.002E-03	5.003E-03	-4.865E-05		
Z-AXIS	4.931E-03	4.930E-03	1.192E-03		
GYRO WARM-UP DRIFT					
X-AXIS	4.049E-06	4.027E-06	-2.137E-06		
Y-AXIS	4.324E-06	4.324E-06	-3.465E-06		
Z-AXIS	1.244E-06	1.243E-06	-2.111E-06		
GYRO DA G SENSITIVE					
X-AXIS	6.076E-03	5.869E-03	3.323E-01		
Y-AXIS	8.37_E-03	8.570E-03	-3.284E-01		
Z-AXIS	1.372E-02	1.371E-02	-3.219E-02		
GYRO L.T.D. CORRELATED					
X-AXIS	4.333E-03	4.940E-03	-8.019E-04		
Y-AXIS	4.360E-03	4.968E-03	-2.620E-05		
Z-AXIS	4.989E-03	4.989E-03	4.308E-04		
GYRO MASS UNBALANCE					
MSX	2.463E-02	2.861E-02	8.987E-01		
MIX	4.907E-03	4.905E-03	3.272E-03		
MSY	2.991E-02	2.994E-02	9.779E-01		
MIY	5.308E-03	5.303E-03	-4.941E-03		
MSZ	2.282E-02	2.280E-02	-5.747E-01		
MIZ	8.317E-03	8.302E-03	-1.118E-02		
MSX-MSY	1.772E-02	1.772E-02	-7.915E-02		
MSX+MSZ	2.331E-02	2.289E-02	3.130E-01		
MSY+MSZ	2.489E-02	2.489E-02	3.912E-01		
GYRO ANISOELASTIC CONSTANTS					
X-AXIS	8.597E-03	8.591E-03	7.796E-05		
Y-AXIS	9.457E-03	9.457E-03	3.545E-03		
Z-AXIS	9.821E-03	9.821E-03	-2.034E-03		
GYRO TOTAL DRIFT					
X-AXIS	1.554E-02	1.531E-02	3.109E-01		
Y-AXIS	3.126E-02	3.124E-02	-1.032E+00		
Z-AXIS	1.410E-02	1.401E-02	-5.012E-01		
GYRO SCALE FACTOR					
X-AXIS	2.456E-09	2.455E-09	3.037E-08		
Y-AXIS	1.093E-08	1.093E-08	-1.521E-08		
Z-AXIS	3.377E-08	3.375E-08	1.363E-08		
GYRO MISALIGNMENT ANGLES					
BXZ	9.814E-01	9.814E-01	2.861E-02		
BXY	9.568E-01	9.567E-01	-2.795E-01		
BYZ	9.685E-01	9.685E-01	4.670E-01		
BYX	9.596E-01	9.596E-01	2.631E-02		
BZY	9.842E-01	9.841E-01	5.733E-02		
BZX	9.804E-01	9.803E-01	-4.287E-01		
GYRO NON-ORTHOGONALITY ANGLES					
BYZ	1.386E+00	1.386E+00	-4.394E-01		
BZY	1.375E+00	1.375E+00	3.328E-01		
BZX	1.375E+00	1.375E+00	-4.566E-01		

HOUSING MISALIGNMENT ANGLES			
X-AXIS	1.545E+00	1.545E+00	-3.558E+00
Y-AXIS	1.513E+00	1.513E+00	-1.365E+00
Z-AXIS	1.835E+00	1.835E+00	-4.736E+00
GIMBAL SYNCHRO ANGLE BIAS			
X-AXIS	1.639E+00	1.639E+00	1.232E+00
Y-AXIS	4.458E+00	4.479E+00	-5.773E+00
Z-AXIS	1.745E+00	1.745E+00	2.543E+00
DIFFERENTIAL SYNCHRO ANGLES			
X-AXIS	2.688E-02	2.187E-02	2.461E+00
Y-AXIS	1.515E-01	1.614E-01	-4.774E+00
Z-AXIS	2.986E-02	2.339E-02	-2.423E+00
PLATFORM TOTAL DRIFT			
X-AXIS	5.312E-03	5.465E-03	4.888E-01
Y-AXIS	3.247E-02	3.245E-02	-9.549E-01
Z-AXIS	5.829E-03	5.714E-03	-4.900E-01
ACCELEROMETER BIAS			
X-AXIS	7.095E+00	7.095E+00	-3.619E+03
Y-AXIS	6.152E+00	6.149E+00	2.404E+03
Z-AXIS	1.488E+01	1.488E+01	-1.412E+02
ACC BIAS (HIGH GAIN)			
X-AXIS	7.828E+00	7.829E+00	-3.771E+03
Y-AXIS	6.999E+00	6.986E+00	2.572E+03
ACC WARM-UP TRANSIENT			
X-AXIS	6.159E-12	6.159E-12	2.295E-12
Y-AXIS	6.069E-12	6.061E-12	-6.072E-12
Z-AXIS	2.547E-12	2.547E-12	-6.197E-10
ACCELEROMETER SCALE FACTOR			
X-AXIS	7.110E-06	7.110E-06	-2.734E-02
Y-AXIS	6.164E-06	6.160E-06	-1.695E-02
Z-AXIS	1.401E-05	1.401E-05	-4.547E-02
ACC SCALE FACTOR (HIGH GAIN)			
X-AXIS	5.436E-06	5.435E-06	-2.414E-02
Y-AXIS	5.451E-06	5.451E-06	-1.750E-02
ACC ATT DEP SCALE FACTOR			
X-AXIS	1.000E-05	1.000E-05	0.
Y-AXIS	9.998E-06	9.998E-06	-4.661E-07
Z-AXIS	3.000E-05	3.000E-05	0.
CLOCK STABILITY			
	9.376E-07	9.957E-07	8.543E-08
ACC/PLATFORM MISALIGN ANGLES			
ΘXZ	6.813E-01	6.813E-01	-4.215E-02
ΘXY	6.641E-01	6.641E-01	1.107E-01
ΘYZ	6.814E-01	6.814E-01	-1.672E-01
ΘYX	6.665E-01	6.665E-01	5.194E-01
ΘZY	6.649E-01	6.649E-01	5.401E-02
ΘZX	6.669E-01	6.669E-01	-2.247E-02
ACC NON-ORTHOGONALITY ANGLES			
ΘYZ	7.153E-02	7.153E-02	2.044E-01
ΘZY	1.370E-01	1.370E-01	1.647E-01
ΘZX	1.340E-01	1.340E-01	-4.959E-01
ACC/SYRO FRAME MISALIGN ANGLES			
X-AXIS	1.146E+00	1.146E+00	4.914E-01
Y-AXIS	1.142E+00	1.142E+00	1.589E-01
Z-AXIS	1.203E+00	1.203E+00	-7.276E-02
PLATFORM VELOCITIES			
X-AXIS	1.443E-02	9.701E-03	-3.477E+01
Y-AXIS	9.033E-03	6.833E-03	-1.335E+02
Z-AXIS	1.341E-02	9.381E-03	1.157E+00

REFERENCES

1. Platform Model for the A-7D/E Inertial Measurement Set, Kearfott Systems Division, Kearfott Group, General Precision Systems, Inc., Wayne, New Jersey, Doc. No. 6K032D025C, 1968.

2. Andrew H. Jazwinski, Stochastic Processes and Filtering Theory, Academic Press, New York, 1970.

3. J. S. Meditch, Stochastic Optimal Linear Estimation and Control, McGraw-Hill, New York, 1969.

4. Development Specification, Operational Computer Program (OCP), Y202A010, 14 May 1973, Singer-General Precision, Inc., Kearfott Division, Little Falls, New Jersey 07424.

5. Robert F. Shipp, System Improvements Through In-Service Test Analysis, The Analytic Sciences Corporation, Reading, Massachusetts. A Paper Prepared for the Holloman Seventh Biennial Guidance Test Symposium.

☆U.S.Government Printing Office: 1977 — 757-001/86